Treatment wetlands for industrial wastewaters: a study of science, policy, and management

by

Alexander M. Cancelli

M.E.T., Simon Fraser University, 2014

B. Eng., Carleton University, 2010

Thesis Submitted in Partial Fulfillment of the
Requirements for the Degree of
Doctor of Philosophy

in the
School of Resource and Environmental Management
Faculty of Environment

SIMON FRASER UNIVERSITY

Summer 2020

Approval

Name:	**Alexander M. Cancelli**
Degree:	**Doctor of Philosophy**
Title:	**Treatment wetlands for industrial wastewaters: a study of science, policy, and management**
Examining Committee:	**Chair:** Jonn Axsen Associate Professor
	Frank Gobas Senior Supervisor Professor
	Sean Markey Supervisor Professor
	William Doucette Supervisor Professor Department of Civil and Environmental Engineering Utah State University
	Jane Fowler Internal Examiner Assistant Professor Department of Biological Sciences
	Upal Ghosh External Examiner Professor Chemical, Biochemical and Environmental Engineering University of Maryland, Baltimore County
Date Defended/Approved:	July 16, 2020

Abstract

Bitumen extraction in Alberta's oil sands region generates large volumes of oil sands process-affected waters (OSPW) that pose environmental and human health risks. Currently, few feasible options for managing these large and growing volumes of polluted waters exist. The primary objective of this research is to investigate the feasibility, effectiveness, and safety of treatment wetlands as a treatment option for the oil sands industry. To do this, a mechanistic model of the fate and toxicity of OSPW contaminants in treatments wetlands was developed and tested in field studies at the Kearl Treatment Wetland – a free water surface flow wetland in northern Alberta. Measuring concentrations of polycyclic aromatic hydrocarbons (PAHs) and naphthenic acids (NAs) in influent and effluent of the Kearl Treatment Wetland showed that the combined total mass of all detected PAHs and NA reduced by 54 to 83% and 7.5 to 69%, respectively, as a result of treatment. Concentrations of PAHs and NAs in the aqueous phase of the wetland were measured using polyethylene (PE) and Polar Organic Chemical Integrative Samplers (POCIS), respectively. The model is shown to be in good agreement with the experimental observations and required only minimal calibration. Application of the model shows that evapotranspiration is not likely to significantly contribute to the removal of OSPW contaminants. Chemical removal relies mainly on transformation in wetland rooting media due to high microbial activity in wetland biofilm. Higher rates of transformation result in greater removal efficiencies for most chemicals. However, highly hydrophobic substances experience low removal efficiencies and appear to be unaffected by changes in transformation rates in the wetland suggesting wetland treatment is not suitable for these substances. Treatment efficiency is sensitive to wetland surface area and flow rate of water through the wetland suggesting intentional wetland design and operation can improve treatment efficiency. Trade-offs in wetland design and operation can be informed by the model.

Keywords: treatment wetlands; oil sands process-affected water; passive sampling; contaminant-fate; environmental modelling

Dedicated to my wonderful wife for her unfaltering support and patience, and for showing me that what you do today, determines your tomorrow. Also dedicated to my loving parents for their endless support and encouragement.

Acknowledgements

I would like to express my very deep appreciation to those who have supported me and my research throughout this entire process. I am particularly grateful for the assistance given by my senior supervisor, Dr. Frank Gobas. His positive attitude, deep understanding of environmental toxicology, and enthusiasm for good science has been a constant source of energy for me. His guidance goes well beyond the scope of this thesis. I would also like to sincerely thank the members of my supervisory committee: Dr. Sean Markey and Dr. William Doucette. You have both been wonderful resources for me throughout this journey. I greatly admire you both professionally and personally.

I would like to thank Asfaw Bekele and Michelle Young at Imperial Oil Resources Limited, whom have helped me develop professionally outside of academia. They have provided many opportunities to grow my network and share my work with other industry associations such as the Canadian Oil Sands Innovation Alliance. Working with them has been a valuable and rewarding experience.

I would also like to give a huge thank you to the Environmental Toxicology Research Group. Dr. Victoria Otton has supported the development of so many students in our research group, and I am no exception. Her presence in the lab has made life as a graduate student much more enjoyable. I would also like to thank Leslie Saunders and Mark Cantu for always lending an open ear. Did they talk too much? Yes. Were they a distraction? Sometimes. Yet, I will always cherish our open dialogue of life and research. I would also like to thank Nina Piggott, Kate Fremlin, Yung-Shan Lee, Talia Cole, and Stephanie Stelmaschuk who were fantastic lab mates throughout this process.

Last, but certainly not least, I would like to thank the REM administrative staff. Laurence Lee, Sue Zillwood, Elissa Cyr, Iris Schischmanow, May Fan, Vanessa Cowley (and Pepper). I'm amazed how you were able to answer my every question. Thank you for always listening, helping, and supporting beyond your departmental duties. A special shout-out to Laurence, who has answered more of my technical questions than I have for my own parents.

Table of Contents

List of Tables

List of Figures

List of Acronyms

AER	Alberta Energy Regulator
AM	Adaptive Management
AOS	Alberta Oil Sands
BE	Biomimetic extraction
Bitumen	A viscous mixture of hydrocarbons
CEPA	Canadian Environmental Protection Act
D	Octanol-water partition coefficient of ionizable organic chemicals
H	Henry's Law constant
K_{AW}	Air-water partition coefficient
K_{OW}	Octanol-water partition coefficient for neutral organic chemicals
LARP	Lower Athabasca Regional Plan
NAs	Naphthenic acids
Oil sands	A natural petroleum deposit
OSPW	Oil Sands Process-Affected Water
PAHs	Polycyclic Aromatic Hydrocarbons
PES	Polyethylene Samplers
POCIS	Polar Organic Chemical Integrative Samplers
SPME	Solid-phase Microextraction
$t_{1/2}$	Half-life time
t_{95}	Time to reach 95% of steady state
TMF	Tailings Management Framework
TW	Treatment Wetland
WQT	Water Quality Target

Chapter 1. Oil sands process-affected water in the Alberta Oil Sands industry

The Alberta oil sands cover an area of 142,200 km^2 in northern Alberta, Canada, and contain proven oil reserves of 165.4 billion barrels – placing Canada third among largest oil reserves in the world (Government of Alberta, 2020a). These oil sands reserves contain crude oil in the form of bitumen – a black viscous mixture of high molecular weight hydrocarbons. Bitumen typically contains more sulphur, metals, and heavy hydrocarbons than conventional crude oil, and needs to be heated or diluted with lighter hydrocarbons to be transported by pipeline (Alberta Energy Regulator, 2020a). In 2018, the average production of raw bitumen in Alberta exceeded 3 million barrels per day (Alberta Energy Regulator, 2020b) with current projections of 4.25 million barrels per day by 2035 (Canadian Association of Petroleum Producers, 2019). The development of industry operations has provided substantial contributions to Canada's economy, amounting to $3.2 billion in provincial royalties in the 2018-19 fiscal year (Government of Alberta, 2020b). While these economic contributions have been considerable, the scale and growth of the industry has exposed major issues in environmental sustainability. One area of environmental concern is the management and treatment of oil sands process-affected water (OSPW), a waste product from bitumen extraction.

1.1. Oil sands process-affected water

Oil sands process-affected water is created from water-based gravity separation where bitumen is stripped from the mined bitumen-rich subsurface materials (Oil Sands Magazine, 2020a). This method of bitumen extraction mixes oil sands, freshwater, recycled wastewater, and caustic agents to produce a wet slurry where bitumen froth is formed, then separated from OSPW. OSPW remains as a complex mixture of solids (sand, silt, and clay), dissolved organic and inorganic chemicals, and unrecovered bitumen (Holowenko et al., 2002).

Bitumen extraction in the oil sands from surface mining operations requires an average of 2.6 barrels of new water for every one barrel of bitumen produced. As a result, over 990 million m^3 of water has been consumed by the industry and deposited in tailings ponds, covering an area greater than 250 km^2 (Alberta Energy Regulator,

2020b). These tailings ponds are a risk to wildlife and create a significant liability for oil sands companies. In 2010, Syncrude was fined $3 million for the deaths of more than 1,600 ducks that landed on an Aurora North oil sands mine tailings ponds (Jones, 2010). In that same year, more than 550 birds died after landing on tailings ponds belonging to Syncrude and Suncor Energy (Wakefield, 2017). And in 2015, Syncrude was fined more than $2.7 million for the deaths of 31 great blue herons after they landed in a tailings pond at the Mildred Lake mine (Thurton, 2017).

The toxicity of OSPW is largely attributed to a group of complex petrogenic chemicals called naphthenic acids (Armstrong et al., 2008; Marentette et al., 2015; Bartlett et al., 2017). Naphthenic acids (NAs) are surfactants consisting of a mixture of saturated aliphatic, cyclic and alkyl-substituted carboxylic acids. The toxicity of OSPW has also been attributed to neutral organic contaminants such as polycyclic aromatic hydrocarbons (PAHs; Collier et al., 2013; Alharbi et al., 2016; Li et al., 2017). NAs and PAHs are nearly ubiquitous in OSPW, and therefore remain a priority in the efforts to treat OSPW. However, this has remained a difficult wastewater challenge for the industry. Effective treatment solutions have not been fully realized, to date. In part, this is because of the considerable volume of OSPW that is generated, which contains concentrations of NAs and PAHs that are known to elicit acute toxicity in wildlife. Effective treatment technologies are needed to better manage this OSPW and mitigate the environmental risks in oil sands resource development. Without these treatment technologies, there are concerns over the industry's long-term sustainability. To move forward, the industry must implement technologies to remediate OSPW, reduce demand on freshwater resources, and contribute to efforts in tailings reclamation.

1.2. Policy framework for OSPW management

OSPW management is organized under a broad multilateral policy framework. Under Canadian federal legislation, chemicals in OSPW were evaluated for their potential to cause harm to human health and the environment. Under Alberta provincial legislation, a set of comprehensive statutory enactments, regulations, directives, regional plans, and management frameworks direct industry operators to develop strategies that continue to improve environmental protections while maintaining economic growth.

1.2.1. Federal legislation

The Canadian Environmental Protection Act offers fundamental legislation in Canada's pursuit of sustainable development (Canadian Environmental Protection Act, 1999). Under CEPA (1999), the federal government aims to prevent pollution, and protect the environment and human health, in part, by regulating toxic substances in Canada. As defined by CEPA (1999, s. 64), a substance is considered "toxic" if it is entering or may enter the environment in a quantity or concentration or under conditions that:

a) have or may have an immediate or long-term harmful effect on the environment or its biological diversity;

b) constitute or may constitute a danger to the environment on which life depends; or

c) constitute or may constitute a danger in Canada to human life or health.

Substances that meet these criteria are referred to as CEPA-toxic. Naphthenic acids (NAs) and polycyclic aromatic hydrocarbons (PAHs) have both been evaluated through a screening level assessment to investigate their potential for CEPA-toxicity. However, these assessments do not properly express the risks of NAs and PAHs in OSPW. The screening level assessment of NAs concluded that commercial NAs did not meet the criteria for CEPA-toxicity. NAs originating from bitumen extraction were not included in this assessment despite being the primary source of NAs in the environment. Therefore, this screening assessment does not reflect the true measure of toxicity for NAs produced in Canada.

The screening level assessment of PAHs concludes that these substances qualify as CEPA-toxic due to their ubiquity in the environment from both natural and anthropogenic sources. PAHs meet the criteria in CEPA (1999) s. 64(a) due their neoplastic, genotoxic, and population-level effects observed at PAH-contaminated sites, and 64(c) because certain PAHs are classified as "probably carcinogenic to humans". However, this screening assessment mainly considers PAHs released into the environment through incidental spills and does not explicitly reference PAHs in OSPW produced during bitumen extraction and detained in tailings ponds. Therefore, this

screening assessment may not truly reflect the toxicity and risk of PAHs produced during regular operations in Alberta's oil sands region.

The overall toxicity of the main organic chemicals of concern in OSPW is therefore not thoroughly nor explicitly assessed under CEPA (1999). However, there are clear indications of the environmental risk of OSPW related to these chemicals. Firstly, the volume of OSPW produced from bitumen extraction presents adverse risks to wildlife including, but not limited to, migratory birds that confuse these areas with safe ecological havens. The toxicity of NAs and PAHs has been demonstrated in several toxicity tests with OSPW for a variety of biota (Li et al., 2017). The level of toxicity of OSPW, and the liability of tailings ponds for industry operators demonstrates the need to treat OSPW as CEPA-toxic. The development and implementation of treatment technologies is critical to mitigate the risks of OSPW and reduce the potential for CEPA-toxicity in Canada. Provincial policies aim to advance new and existing treatment technologies such as treatment wetlands.

1.2.2. Provincial legislation

Energy projects in Alberta are governed by a total of 11 provincial statutory enactments. Among them are the Environmental Protection and Enhancement Act (2000), Water Act (2000), and Oil Sands Conservation Act (2000) which directly govern OSPW management. These legislative provisions are the basis for several policies, management frameworks, and directives that guide oil sands resource development in Alberta.

Table 1-1: Policy framework for the management of OSPW in the Alberta oil sands region.

	Statutes	Policy, action plan	Outcome
Government of Alberta	Water Act	Water withdrawal limits	Restrict the volume of freshwater consumed for bitumen extraction activities.
	Environmental Protection and Enhancement Act	Zero-discharge policy	Prevent the release of OSPW into the environment.
		Tailings Management Framework	Set limits of the volume of tailings for oil sands operators.
	Oil Sands Conservation Act	Tailings Management Framework	Set limits for accumulated volume of tailings for oil sands operators.
		Directive 085	

The primary mechanisms currently in place to regulate the management of OSPW in the Alberta oil sands are: 1) a restriction to freshwater consumption under regulations set forward through the Water Act (2000), 2) a zero-discharge policy implemented under the Environmental Protection and Enhancement Act (2000), and 3) a Tailings Management Framework for the Mineable Athabasca Oil Sands to limit tailings accumulation (Government of Alberta, 2015), implemented mainly under the Oil Sands Conservation Act (2000) and Environmental Protection and Enhancement Act (2000). To restrict freshwater consumption, daily water withdrawal limits are enforced to ensure that industry withdrawals do not exceed 3% of Athabasca River flow, which is the main source of freshwater for the industry (Oil Sands Magazine, 2020b). The zero-discharge policy applies to all OSPW produced throughout the industry to prevent the unwarranted release of OSPW into the environment. The Tailings Management Framework was created as part of the Lower Athabasca Regional Plan (LARP; Government of Alberta, 2012). LARP integrates a series of management frameworks to guide resource development in the Lower Athabasca Region – the epicentre for oil sands development in Alberta. The Tailings Management Framework and subsequent Directive 085 (Fluid Tailings Management for Oil Sands Mining Projects; Alberta Energy Regulator, 2016) sets volume triggers and limits for fluid tailings (i.e. OSPW) production for industry operators.

These policy tools mainly serve to protect the environment but have also helped to drive innovation in OSPW treatment technologies to improve OSPW recycling, reduce freshwater demand, reduce tailings volumes, and mitigate environmental risks of tailings ponds. Therefore, this policy framework supports an increase in oil production as long as OSPW management aligns with the restrictions, policies, and directives outlined above. Therefore, oil sands companies are searching for technologies that may help to remediate OSPW such as treatment wetlands.

1.3. Treatment wetlands for OSPW remediation

Nature based solutions have been defined in European Commission (2015) as actions that aim to help societies address a variety of environmental, social, and economic challenges in sustainable ways. These actions are inspired by, supported by, or copied from nature (European Commission, 2015 p. 5; Nesshöver et al., 2017). Treatment wetlands are nature based solutions for wastewater treatment. They are

constructed, artificial ecosystems that use natural biogeochemistry to remove pollutants from wastewater.

Treatment wetland systems are often grouped into three hydrologic flow regimes: 1) free water surface (FWS) wetlands are artificial streams that have an open surface water column with emergent vegetation planted in saturated rooting media, 2) horizontal and 3) vertical subsurface flow (SSF) wetlands are aquifer-like designs that permit the flow of water (horizontally or vertically) through coarse-grained medium. FWS wetlands often contain a mix of submerged, emergent, and floating vegetation, whereas SSF designs contain emergent vegetation rooted in the coarse-grained media and therefore only the roots are exposed to water flowing through the interstitial space in the wetland substrate. While many variations and combinations of these wetland designs exist, all treatment wetland systems rely on complex biogeochemical mechanisms for pollutant removal. These mechanisms include processes such as sorption, evapotranspiration, and biodegradation by wetland microbes and vegetation. The capacity for wastewater treatment stems from the complex symbiosis between wetland vegetation and microbes, and the resilience of the microbial community to degrade contaminants under a variety of environmental conditions (Kadlec and Wallace, 2009). The application of treatment wetlands attempts to harness this complex biogeochemistry to create a feasible and effective treatment technology for industrial wastewaters.

Treatment wetlands are recognized as a viable treatment technology in a number of different industrial applications including agricultural runoff (e.g. Page et al. 2010), mine wastewater (e.g. Batty and Younger, 2004), municipal and domestic wastewater (e.g. Toscano et al., 2009), leachate (e.g. Sim et al., 2013), and petroleum refinery process water (e.g. Knight et al., 1999). Some prominent treatment wetlands currently in operation: include the Lorong Halus Treatment Wetland and the Nimr Treatment Wetland. The Lorong Halus Treatment Wetland is a HSSF wetland in Singapore that treats landfill leachate (Sim et al., 2013). The Nimr Treatment Wetland is the world's largest FWS wetland that treats wastewater produced from oil extraction in Oman ("Bauer to build biggest wetland.' 2017).

In all treatment wetlands, there are variations in design and operation, but each are constructed as nature based solutions for wastewater treatment. In the Alberta Oil Sands region, treatment wetlands may help to increase water recycling for bitumen

extraction, mitigate the environmental risks of tailings ponds, and permit the safe release of OSPW into the environment. Ultimately, treatment wetlands may help to foster further transition into a greener economy – a necessary direction for the long-term sustainability of the industry.

1.4. Adaptive management of OSPW

The oil sands industry operates under a policy framework that continuously evolves to adapt to growing industry operations, new guidelines, and technological dynamism. Adaptive management has become an attractive strategy for regulatory agencies and industry associations to operate effectively within this complex and dynamic landscape. For example, adaptive management has been integrated into the Lower Athabasca Regional Plan and Tailings Management Framework, and the Canadian Oil Sands Innovation Alliance (COSIA) cites adaptive management practices extensively in their policy documents. In the Kearl Oil Sands Project application to the Alberta Energy and Utility Board, adaptive management was cited as a method to deal with uncertainties, and to monitor, assess, and respond to cumulative effects on the environment from industry operations.

The National Research Council (2004) provides one of the most widely accepted definitions of adaptive management, which states that:

> Adaptive management [is a process that] promotes flexible decision making that can be adjusted in the face of uncertainties as outcomes from management actions and other events become better understood. Careful monitoring of these outcomes both advances scientific understanding and helps adjust policies or operations as part of an iterative learning process.

Many formal definitions of adaptive management are available throughout the literature (e.g. Williams and Johnson, 1995; Allen et al., 2001; Bormann et al., 2007; Williams, 2011); however, all definitions consistently revolve around major themes of reducing uncertainty, iterative learning, learning-while-doing, and monitoring and assessment. While this definition encompasses these major themes, it lacks full recognition of the learning process involved in adaptive management.

In practice, adaptive management follows an iterative learning process that involves monitoring the impacts from an action plan or management decision, then

assessing the outcomes with the goal to develop a stronger knowledge-base for setting new action plans (Figure 1-1). The simplicity of Figure 1-1 reflects the versatility of adaptive management, and its potential for application in many areas of resource and environmental management. The iterative learning process contained therein is fundamental to the success of adaptive management. It is important to stress that adaptive management is not merely a trial and error process for decision-making, but rather a deliberate management strategy with a formalized learning process. For the development of new and emerging technologies such as treatment wetlands and application to OSPW, this learning process often takes a model-oriented approach.

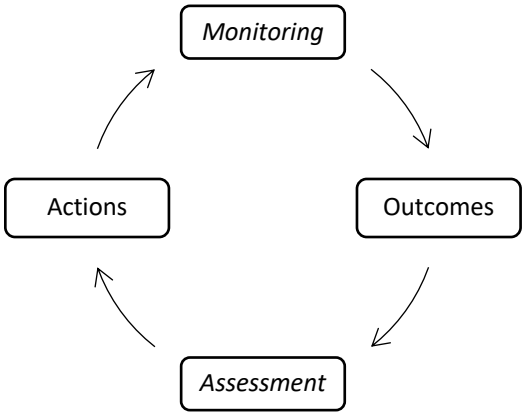

Figure 1-1: Adaptive management cycle

Models are used to synthesize our understanding of an environmental system to explore the impacts from changes in management and environmental factors (Williams, 2011). In this way, a model-oriented approach reduces uncertainty in the outcomes from management actions by providing a tool to simulate various scenarios. This improves decision-making, increases accessibility to new information, and formalizes the learning process. As these informed management actions are implemented, the environmental system is monitored to assess the impacts of these actions, formulate new management actions that reduce undesirable effects, and enhance intended consequences. For treatment wetlands, this involves field studies to collect data on wetland performance. This data is used to inform the model, and new management actions can be evaluated through model simulations, hence completing one full cycle of adaptive management. This science helps inform policy and management while contributing to our understanding of the feasibility, effectiveness, and safety of treatment wetlands for the oil sands industry.

1.5. Research objectives

The research presented here is an investigation into treatment wetlands as a nature-based solution for the remediation and management of OSPW. This research expands on existing science behind treatment wetlands, while offering a unique application to the oil sands industry in Alberta, Canada. Ultimately, this work intends to discover which chemicals treatment wetlands can efficiently remove from OSPW, and which chemicals treatment wetlands cannot. This investigation combines field-based measurements of wetland treatment of OSPW with modelling exercises to understand the fate of contaminants in these environmental systems. This work explores how design, operation, and environmental conditions influence wetland treatment performance. The primary focus of this research is **to investigate whether treatment wetlands are a feasible and effective option for the safe removal of oil sands related contaminants**. The following specific objectives outline the major themes presented in each research chapter:

Chapter 2: Design and develop a modelling approach for the fate of organic chemicals in treatment wetlands that can be used to estimate the efficiency of wetland treatment of organic contaminants under varying wetland designs and environmental conditions using data from the Lorong Halus Treatment Wetland.

Chapter 3: Measure the removal efficiency of polycyclic aromatic hydrocarbons in the Kearl Treatment Wetland.

Chapter 4: Measure the removal efficiency of naphthenic acids in the Kearl Treatment Wetland.

Chapter 5: Apply, test, evaluate, and calibrate the treatment wetland model for neutral and polar organic chemicals in OSPW.

Chapter 6: Assess the application of treatment wetlands for OSPW treatment.

To achieve these objectives, a series of investigations were performed to develop a treatment wetland modelling approach, quantify the removal of organic contaminants in treatment wetlands, and test and evaluate a robust treatment wetland model for both neutral and polar organic chemicals.

Chapter two (published as a peer-reviewed paper in *Water Research*; Cancelli et al., 2019) reports on the development of a modelling approach for assessing the fate of contaminants within treatment wetland environments using data collected from the Lorong Halus Treatment Wetland in Singapore. The contaminant-fate model for hydrophobic organic contaminants in a subsurface flow treatment wetland is presented. This work is based on the modelling approaches described in Mackay et al. (1983) (Quantitative Water-Air-Sediment Interaction (QWASI) model), Mackay (2001) (Level I - IV fugacity models), Gobas (1993) (food-web model), Clark et al. (1995) (Sewage Treatment Plant (STP) model), Arnot and Gobas (2004) (AQUAWEB – Food Web Bioaccumulation model). This chapter was critical to understanding contaminant fate within wetland environments, the roles of wetland biogeochemical processes on chemical removal, and the importance of environmental conditions and design parameters on wetland performance. Data from this chapter were used to inform the operation and experimental design of the Kearl Treatment Wetland studied in the proceeding chapters. Moreover, this work provided an opportunity to develop a model for some of the same contaminants that you find in OSPW.

Chapters three and four present data collected between 2017 and 2019 from the Kearl Treatment Wetland in northern Alberta, Canada. The observations from this constructed wetland provides a unique element to this research, as no other studies have been completed on a full-scale (1 ha) constructed treatment wetland within the Alberta oil sands region. These chapters focus on the quantification of chemical concentrations of polycyclic aromatic hydrocarbons and naphthenic acids in OSPW entering the wetland, and the removal efficiency of those contaminants within the wetland. Data collection occurred through aqueous grab sampling of wetland water and through passive sampling techniques. This data demonstrates the treatment of OSPW under a variety of environmental conditions. The effects of these environmental conditions on treatment efficiency are discussed.

Chapter five builds upon the modelling approach developed in Chapter two, and incorporates new data collected in Chapters three and four to create a robust treatment wetland model for neutral and polar organic chemicals. The model is constructed to help evaluate the application of treatment wetlands for the oil sands industry. The functionality of the model allows for further assessment of the effects of wetland design and operation on chemical removal. The model provides industry operators with a tool to

assess the feasibility of treatment wetlands for their specific wastewater treatment needs.

The final component to this study aims to synthesize the preceding chapters and address broad management questions on how treatment wetlands integrate within the oil sands industry. Chapter six is intended to inform decision-makers on the efficacy of treatment wetlands.

1.6. References

Alberta Energy Regulator (2020a). Oil Sands. Retrieved July 22, 2020, from https://www.aer.ca/providing-information/by-topic/oil-sands.html

Alberta Energy Regulator (2020b). Water Use Performance, August 2019 – AER.ca. Retrieved March 13, 2020, from https://www.aer.ca/protecting-what-matters/holding-industry-accountable/industry-performance/water-use-performance

Alberta Energy Regulator. (2016). *Directive 085, Fluid tailings Management for Oil Sands Mining Projects*. Retrieved from AER website: https://www.aer.ca/documents/directives/Directive085.pdf

Alharbi, H. A., Morandi, G., Giesy, J. P., & Wiseman, S. B. (2016). Effect of oil sands process-affected water on toxicity of retene to early life-stages of Japanese medaka (Oryzias latipes). *Aquatic Toxicology*, *176*, 1–9. https://doi.org/10.1016/j.aquatox.2016.04.009

Allen WJ, Bosch OJH, Kilvington MJ, Harley D, Brown I (2001) Monitoring and adaptive management: addressing social and organisational issues to improve information sharing. *Natural Resources Forum* 25:225–233

Armstrong, S. A., Headley, J. V, Peru, K. M., & Germida, J. J. (2008). Phytotoxicity of oil sands naphthenic acids and dissipation from systems planted with emergent aquatic macrophytes. *Journal of Environmental Science and Health, Part A*, *43*(1), 36–42. https://doi.org/10.1080/10934520701750041

Arnot, J.A. and Gobas, F.A.P.C. (2004). A Food Web Bioaccumulation Model for Organic Chemicals in Aquatic Ecosystems. *Environmental Toxicology and Chemistry* 23, 2343-2355.

Bartlett, A. J., Frank, R. A., Gillis, P. L., Parrott, J. L., Marentette, J. R., Brown, L. R., … Hewitt, L. M. (2017). Toxicity of naphthenic acids to invertebrates: Extracts from oil sands process-affected water versus commercial mixtures. *Environmental Pollution*, *227*, 271–279. https://doi.org/10.1016/j.envpol.2017.04.056

Batty, L. C., & Younger, P. L. (2004). Growth of Phragmites australis (Cav.) Trin ex. Steudel in mine water treatment wetlands: Effects of metal and nutrient uptake. *Environmental Pollution*, 132(1), 85–93. https://doi.org/10.1016/j.envpol.2004.03.022

Bauer to build biggest wetland treatment plant in Oman. (2017, November 6). *TradeArabia*. Retrieved from http://www.tradearabia.com/news/CONS_332605.html

Bormann BT, Haynes RW, Martin JR (2007) Adaptive management of forest ecosystems: did some rubber hit the road? *Bioscience* 57:186–191

Canadian Association of Petroleum Producers (CAPP). (2019). Crude Oil Forecast - Canadian Association of Petroleum Producers. Retrieved March 13, 2020, from https://www.capp.ca/publications-and-statistics/crude-oil-forecast

Canadian Environmental Protection Act, Statutes of Canada (1999, c.33). Retrieved from Justice Laws website: https://laws-lois.justice.gc.ca/eng/acts/C-15.31/

Cancelli, A. M., Gobas, F. A. P. C., Qian, W., Kelly, B. C. (2019). Development and evaluation of a mechanistic model to assess the fate and removal efficiency of hydrophobic organic contaminants in horizontal subsurface flow treatment wetlands. *Water Research*, 151, 183-192. https://doi.org/10.1016/j.watres.2018.12.020

Clark, B., Henry, J.G. and Mackay, D. (1995). Fugacity Analysis and Model of Organic Chemical Fate in a Sewage Treatment Plant. *Environmental Science and Technology*, 29: 1488-1494.

Collier, T. K., Anulacion, B. F., Arkoosh, M. R., Dietrich, J. P., Incardona, J. P., Johnson, L. L., … Myers, M. S. (2013). Effects on Fish of Polycyclic Aromatic Hydrocarbons (PAHs) and Naphthenic Acid Exposures. *Fish Physiology*, *33*, 195–255. https://doi.org/10.1016/B978-0-12-398254-4.00004-2

Environmental Protection and Enhancement Act, Revised Statue of Alberta (2000, c. E-12). Retrieved from Alberta Queen's Printer website: www.qp.alberta.ca/1266.cfm?page=E12.cfm&leg_type=Acts&isbncln=9780779814558

European Commission. 2015. In: Innovation, D.-G.F.R.A. (Ed.), Towards an EU Research and Innovation Policy Agenda for Nature-based Solutions & Renaturing Cities - Final Report of the Horizon 2020 Expert Group. European Commission, Directorate- General for Research and Innovation, Brussels, p. 74.

Gobas F.A.P.C. (1993). A model for predicting the bioaccumulation of hydrophobic organic chemicals in aquatic food-webs: application to Lake Ontario. *Ecological Modelling*. 69:1-17.

Government of Alberta (2020a). Oil sands facts and statistics – Alberta.ca. Retrieved March 13, 2020, from https://www.alberta.ca/oil-sands-facts-and-statistics.aspx

Government of Alberta (2020b). Historical Royalty Data – Alberta.ca. Retrieved March 13, 2020, from https://www.alberta.ca/historical-royalty-revenue-data.aspx

Government of Alberta. (2012). Lower Athabasca Regional Plan: 2012 – 2022. Retrieved from the Government of Alberta website: https://open.alberta.ca/dataset/37eab675-19fe-43fd-afff-001e2c0be67f/resource/a063e2df-f5a6-4bbd-978c-165cc25148a2/download/5866779-2012-08-lower-athabasca-regional-plan-2012-2022.pdf

Government of Alberta. (2015). Lower Athabasca Region: Tailings Management Framework for the Mineable Athabasca Oil Sands. Retrieved from the Government of Alberta website: https://open.alberta.ca/dataset/962bc8f4-3924-46ce-baf8-d6b7a26467ae/resource/7c49eb63-751b-49fd-b746-87d5edee3131/download/2015-larp-tailingsmgtathabascaoilsands.pdf

Government of Canada (1994). Priority Substances List Assessment Report: Polycyclic Aromatic Hydrocarbons. En40-215/42E. Ottawa. Minister of Supply and Services Canada

Holowenko, F. M., Mackinnon, M. D., & Fedorak, P. M. (2002). Characterization of naphthenic acids in oil sands wastewaters by gas chromatography-mass spectrometry. *Water Research*, 36.

Jones, J. (2010, June 25). Syncrude guilty in 1,600 duck deaths in toxic pond. Reuters, Retrieved from www.reuters.com/article/us-syncrude-ducks/syncrude-guilty-in-1600-duck-deaths-in-toxic-pond-idUSTRE65O68520100625

Kadlec, R., and Wallace, S., 2009. Treatment Wetlands (2nd ed.). Boca Raton, FL: Taylor &

Knight, R. L., Kadlec, R. H., & Ohlendorf, H. M. (1999). The use of treatment wetlands for petroleum industry effluents. *Environmental Science and Technology*, 33(7), 973–980. https://doi.org/10.1021/es980740w

Li, C., Fu, L., Stafford, J., Belosevic, M., & Gamal El-Din, M. (2017). The toxicity of oil sands process-affected water (OSPW): A critical review. *Science of the Total Environment*. https://doi.org/10.1016/j.scitotenv.2017.06.024

Mackay D. (2001). Multimedia environmental models: The fugacity approach (2nd ed.). Boca Raton, FL: Taylor & Francis Group.

Mackay, D., Paterson, S., Joy, M. (1983). A Quantitative Water, Air, Sediment Interaction (QWASI) Fugacity Model for Describing the Fate of Chemicals in Rivers. *Chemosphere*. 12: 1193-1208.

Marentette, J. R., Frank, R. A., Bartlett, A. J., Gillis, P. L., Hewitt, L. M., Peru, K. M., … Parrott, J. L. (2015). Toxicity of naphthenic acid fraction components extracted from fresh and aged oil sands process-affected waters, and commercial naphthenic acid mixtures, to fathead minnow (Pimephales promelas) embryos. *Aquatic Toxicology*, 164, 108–117. https://doi.org/10.1016/j.aquatox.2015.04.024

National Research Council (2004) Adaptive management for water resources planning. National Academies Press, Washington, DC

Nesshöver, C., Assmuth, T., Irvine, K. N., Rusch, G. M., Waylen, K. A., Delbaere, B., … Wittmer, H. (2017, February). The science, policy and practice of nature-based solutions: An interdisciplinary perspective. *Science of the Total Environment*, 579(1): 1215-1227, https://doi.org/10.1016/j.scitotenv.2016.11.106

Oil Sands Conservation Act, Revised Statute of Alberta (2000, c. O-7). Retrieved from Alberta Queen's Printer website: www.qp.alberta.ca/1266.cfm?page=O07.cfm&leg_type=Acts&isbncln=9780779772735

Oil Sands Magazine. (2020a). Oil Sands 101: Process Overview. Retrieved March 13, 2020, from https://www.oilsandsmagazine.com/technical/oilsands-101

Oil Sands Magazine. (2020b). Environment: Water Usage. Retrieved March 18, 2020, from https://www.oilsandsmagazine.com/technical/environment/water-usage

Page, D., Dillon, P., Mueller, J., & Bartkow, M. (2010). Quantification of herbicide removal in a constructed wetland using passive samplers and composite water quality monitoring. *Chemosphere*, 81(3), 394–399. https://doi.org/10.1016/j.chemosphere.2010.07.002

Sim, C. H., Quek, B. S., Shutes, R. B. E., & Goh, K. H. (2013). Management and treatment of landfill leachate by a system of constructed wetlands and ponds in Singapore. *Water Science and Technology*, 68(5), 1114–1122. https://doi.org/10.2166/wst.2013.352

Thurton, D. (2017, August 3). Syncrude charged in deaths of 31 great blue herons at oilsands mine. CBC News, Retrieved from https://www.cbc.ca/news/canada/edmonton/syncrude-bird-deaths-2015-oilsands-environment-greenpeace-1.4234472

Toscano, A., Langergraber, G., Consoli, S., & Cirelli, G. L. (2009). Modelling pollutant removal in a pilot-scale two-stage subsurface flow constructed wetlands. *Ecological Engineering*, 35, 281–289. https://doi.org/10.1016/j.ecoleng.2008.07.011

Wakefield, J. (2017, September 19). More than 120 waterfowl, other birds dead at oil sands site north of Fort McMurray. Edmonton Sun, Retrieved from edmontonsun.com/2017/09/19/more-than-120-waterfowl-other-birds-dead-at-oilsands-site-north-of-fort-mcmurray/wcm/bde86404-f092-4b1b-bb58-c2731b0c3ac2

Water Act, Revised Statue of Alberta (2000, c. W-3). Retrieved from Alberta Queen's Printer website: www.qp.alberta.ca/1266.cfm?page=W03.cfm&leg_type=Acts&isbncln=9780779805570

Williams B. K., Johnson F. A. (1995) Adaptive management and the regulation of waterfowl harvests. *Wildlife Society Bulletin*, 23:430–436

Williams, B. K. (2011). Adaptive management of natural resources-framework and issues. *Journal of Environmental Management*, *92*(5), 1346–1353. doi.org/10.1016/j.jenvman.2010.10.041

Chapter 2. Development and evaluation of a mechanistic model to assess the fate and removal efficiency of hydrophobic organic contaminants in horizontal subsurface flow treatment wetlands

Publication reference: Cancelli, A. M., Gobas, F. A. P. C., Qian, W., Kelly, B. C. (2019). Development and evaluation of a mechanistic model to assess the fate and removal efficiency of hydrophobic organic contaminants in horizontal subsurface flow treatment wetlands. Water Research, 151, 183-192. https://doi.org/10.1016/j.watres.2018.12.020

Alexander M. Cancelli constructed, tested, and calibrated the model, wrote modelling code in Microsoft Excel VBA, performed the sensitivity analysis, and wrote the paper.

2.1. Summary

A mechanistic model for assessing the fate and removal efficiency of hydrophobic organic contaminants in horizontal subsurface flow treatment wetlands was developed and evaluated using empirical concentration data from Singapore's Lorong Halus Treatment Wetland. This treatment wetland consists of a series of horizontal subsurface flow reed beds. The model, calibrated for the Lorong Halus Treatment Wetland, provided an adequate description of the concentrations of nine neutral organic substances in water, rhizomes and emergent vegetation in the wetland. The model was applied to investigate the sensitivity of the contaminant removal efficiency to environmental conditions and physicochemical properties of contaminants that enter the wetland. The water-budget of the wetland was found to exhibit an important influence on both the mass-removal efficiency and reduction of contaminant concentrations that can be achieved through wetland treatment. The model illustrated that removal pathways of organic contaminants in the wetland varied as a function of the properties of the contaminants. The mass-removal efficiency of the treatment wetland was greatest for chemicals with a log K_{OW} between 3.0 and 5.0 and log K_{AW} > -1.0. Removal of contaminants through volatilization was found to be greatest for substances with a log K_{OW} between 3 and 5 and log K_{AW} > 0. Transpiration flux in vegetation was found to be most important for substances with a log K_{OW} of 4.5 – 5.5 and log K_{AW} of -5.0 – 0.0. Biotransformation rates of the contaminants in the wetland media play a crucial role in

the removal of contaminants from wastewater. The model provides a tool for assessing the removal capacity of treatment wetlands for neutral organic contaminants and evaluating trade-offs in the design and operation of a horizontal subsurface flow treatment wetland.

2.2. Introduction

Treatment wetlands are constructed, artificial ecosystems designed to harness the natural biogeochemistry of wetlands for reclamation and remediation services. These systems have emerged as a viable solution to various wastewater challenges, including municipal and domestic wastewater (e.g. Toscano et al., 2009), minewater (e.g. Batty and Younger, 2004), agricultural runoff (e.g. Page et al., 2010), industrial wastewater (e.g. Lin et al., 2005), and leachate (e.g. Sim et al., 2013). In these applications, treatment wetland systems have demonstrated their ability to reclaim and remediate soil, groundwater, and surface water with their complex symbiosis between microorganisms, vegetation, and rooting media (U.S. EPA, 2000; Reddy and DeLaune, 2008; Kadlec and Wallace, 2009).

Models have also been developed and applied to entire constructed wetland systems to assess specific criteria such as hydraulic characteristics throughout the system (Chazarenc et al., 2003; Garcia et al., 2004), changes to biochemical oxygen demand or chemical oxygen demand of the wastewater (Chen et al, 1999; Wynn and Liehr, 2001), and nutrient cycling (Mayo and Bigambo, 2005). Many of these models incorporate reactive transport dynamics based on the first-order k-C approach which represents conventional first-order removal (Kadlec and Knight, 1996). The Constructed Wetland 2-D model (Langergraber, 2001) is a well-developed treatment wetland model designed to estimate the biochemical transformation and degradation of organic matter, nitrogen, and phosphorus species in subsurface flow treatment wetlands, using numerical modelling. This multifaceted model performs well for bulk influent and effluent properties but does not provide partitioning and concentration estimates for specific chemicals and does not include vegetation-mediated processes of contaminant removal such as evapotranspiration.

Several models have been developed to describe the biogeochemical mechanisms controlling the fate of pollutants within wetlands. Models that describe the

uptake and fate of non-ionic organic substances in wetland vegetation often use ratios of chemical concentrations in the plant compartment of interest (e.g. shoots, roots, xylem sap) to those in the exposure medium, (soil, pore water, hydroponic solution). These concentration ratios are generally referred to as bioconcentration factors (BCFs) but have also been named for their specific plant tissue compartment such as root concentration factor (RCF; Briggs et al., 1983, Topp et al, 1986), stem concentration factor (SCF; Mackay and Gschwend, 2000; Trapp, 2002), or transpiration-stream (xylem sap) concentration factor (TSCF; Trapp and Mathies, 1995; Rein et al., 2011). Empirical correlations between BCF and certain physicochemical properties such as the octanol-water partition coefficient (K_{OW}) have been used to estimate plant tissue concentrations from concentrations of contaminants dissolved in porewater (Gobas et al., 1991). The BCFs and their correlations with physicochemical properties have been used in support of various chemical management strategies around the world (e.g. Environment Canada, 1995; EUSES, 2012).

Industries that face wastewater challenges need decision tools that can demonstrate the potential for a treatment wetland system to meet water quality objectives (e.g. CCME, 1999; AEP, 1995; ESRD, 2014), while considering trade-offs in their design and operation. There is a current need to develop mechanistic models that can effectively predict the fate and removal efficiency of hydrophobic organic contaminants in treatment wetlands. These models can be useful tools for evaluating the feasibility and design of treatment wetlands for contaminant- and site-specific industrial applications.

The present study involves the development and evaluation of a mechanistic model to assess the fate and removal efficiency of non-ionising hydrophobic organic contaminants in horizontal subsurface flow treatment wetlands. The developed model is designed to estimate contaminant removal efficiencies based on the dynamics of plant uptake, intermedia transport, sorption, and transformation. The ultimate goal of the model is to understand how to safely and effectively implement treatment wetlands under a variety of environmental conditions and treatment scenarios. The model is applied to a large-scale treatment wetland in Singapore, the Lorong Halus Treatment Wetland (LHTW). The model is evaluated using concentration data from a recent field investigation of hydrophobic organic contaminants in different compartments of this treatment wetland (Wang and Kelly, 2017). We further provide an assessment of the

behaviour, merits, and limitations of the model, and the results of a sensitivity analysis to better understand the influence of various model parameters.

2.3. Model Theory

Treatment wetland systems are grouped into three hydrologic flow regimes: i) Free water surface (FWS) wetlands which are artificial streams that have an open surface water column with emergent vegetation planted in saturated rooting media, ii) Horizontal (H-) and iii) Vertical (V-) subsurface flow (SSF) wetlands which are aquifer-like designs that permit the flow of water (horizontally or vertically) through a coarse-grained medium (Kadlec and Knight, 1996; Figure 2-1). Singapore's Lorong Halus Treatment Wetland is a horizontal subsurface flow wetland design. Information from the Lorong Halus Treatment Wetland provides an opportunity to evaluate the performance of this type of treatment wetland.

For the present modelling study of hydrophobic organic contaminants in treatment wetlands, we utilized an environmental modelling approach that has been developed and used by many authors including: Mackay et al. (1983) (Quantitative Water-Air-Sediment Interaction (QWASI) model), Mackay (2001) (Level I - IV fugacity models), Gobas (1993) (food-web model), Clark et al. (1995) (Sewage Treatment Plant (STP) model), Arnot and Gobas (2004) (AQUAWEB – Food Web Bioaccumulation model), and others.

2.3.1. Model Design

The objective of the model is to describe the behavior of hydrophobic organic contaminants in treatment wetlands. The evaluative components of the wetland environment consist of water (W), rhizome vegetation (Rh), and emergent vegetation (EV). Water that enters the treatment wetland environment flows through the pore space of the rooting medium gravel (i.e. horizontal subsurface flow). Chemicals enter the rhizomes through diffusion from water, and xylem transport carries the chemical through to the emergent fraction of the vegetation where transpiration may occur. Figure 2-1 provides a conceptual diagram of the wetland and illustrates these transformation and intermedia transport processes for each of the three modelled wetland compartments.

These processes are described in terms of first-order kinetics in mass balance equations:

$$\frac{dM_W}{dt} = \dot{m}_{in} + k_{Rh\text{-}W} \bullet M_{Rh} - (k_{W\text{-}Rh} + k_V + k_O + k_{Wt}) \bullet M_W \quad \text{Eq. 2-1}$$

$$\frac{dM_{Rh}}{dt} = k_{W\text{-}Rh} \bullet M_W - (k_{Rh\text{-}W} + k_{Rh\text{-}EV} + k_{Rht}) \bullet M_{Rh} \quad \text{Eq. 2-2}$$

$$\frac{dM_{EV}}{dt} = k_{Rh\text{-}EV} \bullet M_{Rh} - (k_{EV\text{-}air} + k_{EVt} + k_{EVg}) \bullet M_{EV} \quad \text{Eq. 2-3}$$

where M is the mass (g) of contaminant, t is time (days), k represents the rate constant (day^{-1}) for each transport and transformation process (Table 2-1). The contaminant loading ($\dot{m}_{in}$, g/day) into the wetland occurs via inflowing wastewater and is the product of the inflow rate (Q_{in}, L/day) and individual chemical concentration (C_{in}, g/L). The model is programmed to run a Euler-type numerical integration to derive the time-course of contaminant concentrations in the compartments of the treatment wetland. This solution is useful to assess the response of the wetland to contaminant loading as it approaches steady-state, and for pulse-loading scenarios to assess the distribution of chemicals over time. The model is also solved for a system at steady-state ($dM_i/dt = 0$). This solution of the model is useful to assess the long-term capacity for reclamation and remediation services.

Table 2-1: Description of parameters in Eqs. 2-1, 2-2, and 2-3.

Symbol	Units	Description
k_O	day^{-1}	Outflow
k_V	day^{-1}	Volatilization
$k_{W\text{-}Rh}$	day^{-1}	Water to rhizome vegetation diffusion
$k_{Rh\text{-}W}$	day^{-1}	Rhizome vegetation to water diffusion
$k_{Rh\text{-}EV}$	day^{-1}	Rhizome vegetation to emergent vegetation transport
$k_{EV\text{-}air}$	day^{-1}	Emergent vegetation to air transport
k_{EVg}	day^{-1}	Growth dilution, emergent vegetation
k_{Wt}	day^{-1}	Transformation in water
k_{Rht}	day^{-1}	Transformation in rhizome vegetation
k_{EVt}	day^{-1}	Transformation in emergent vegetation
M_i	g	Mass of contaminant in media *i*
$\dot{m}_{in}$	g/day	Contaminant loading into the wetland
t	day	Time

Diffusion of contaminants from water to rhizomes is described by a “two-film diffusion model” developed by Whitman (1923). This approach uses mass transfer

coefficients (m/day) that represent the diffusion rates of chemicals between two different media based on the fugacity gradient between those media.

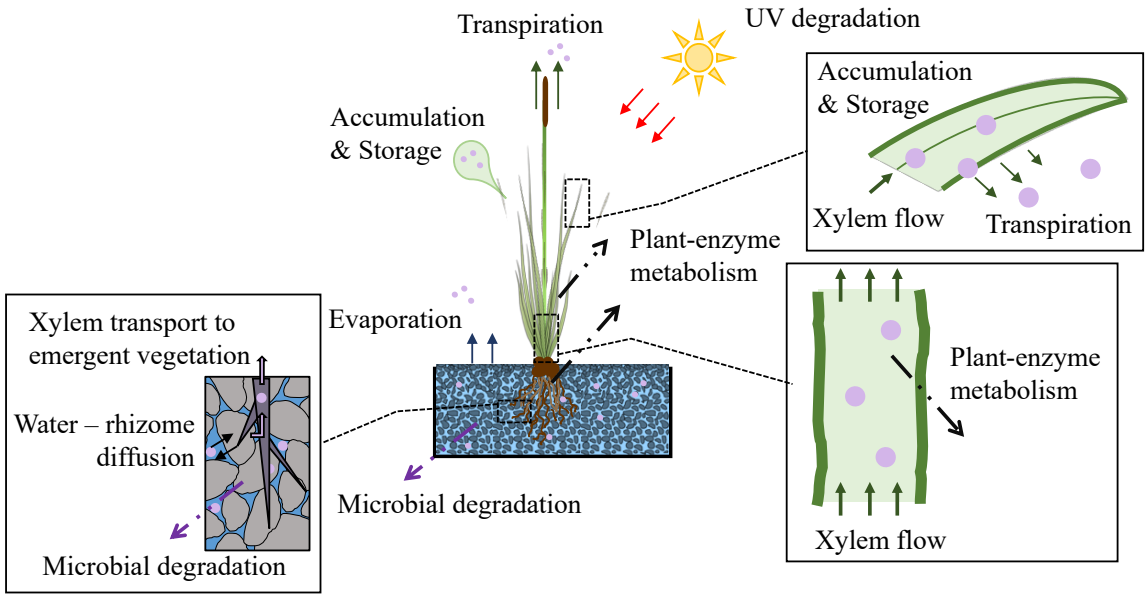

Figure 2-1: Conceptual diagram of the horizontal subsurface flow treatment wetland model. Solid arrows represent transport processes of the chemical in wetland media. Dashed arrows represent transformation processes (chemical, physical, or biological). The effect of vegetation growth on the concentration of the chemical in plants is not shown.

Rhizome to emergent vegetation (Rh→EV) contaminant transport follows the approach outlined in Trapp and Matthies (1995) to derive $k_{Rh\text{-}EV}$ for contaminants with a log K_{OW} greater than 2.5, such that:

$$k_{Rh\rightarrow EV} = \frac{Q_{xylem} \cdot TSCF}{V_W} \cdot \phi_{WD} \quad \text{and;} \qquad \text{Eq. 2-4}$$

$$TSCF = 0.7 \cdot e^{\left[-\frac{(\log K_{OW} - 3.07)^2}{2.78}\right]} \qquad \text{Eq. 2-5}$$

where Q_{wx} (m^3/day) is the xylem flow rate through the vegetation's xylem tubules, TSCF is the transpiration-stream concentrations factor and represents the BCF between the xylem sap and pore water around the rhizomes (i.e. C_{xylem}/C_{water}), V_W (m^3) is the volume of water in the void-space of the substrate, and ϕ_{WD} is the fraction of freely dissolved

contaminant in the porewater. A complete list of model equations is available in the Supplementary Information.

Treatment wetland efficiency is characterized in terms of the mass-loading removal (E_L) and concentration-reduction (E_C). E_L is estimated from the contaminant mass flux entering (influent, $\dot{m}_{in}$) and leaving (effluent, $\dot{m}_{out}$) the wetland:

$$E_L = 1 - (\dot{m}_{out} / \dot{m}_{in}) \quad \text{Eq. 2-6}$$

E_C is estimated from the reduction in the aqueous concentration of the chemical between the influent wastewater and treated effluent:

$$E_C = 1 - (C_{out} / C_{in}) \quad \text{Eq. 2-7}$$

E_L and E_C are functions of all input parameters (N = 42), and therefore respond to changes in the configuration and characteristics of the wetland system. Since $\dot{m}_{out}$ is simply $C_{out} \cdot k_O$, E_L and E_C are equal when there is equal water inflow and outflow, i.e. no net change to the water budget. The relationship between removal efficiency and the configuration and conditions of the wetland is investigated through model demonstrations and a sensitivity analysis.

2.3.2. Model assumptions and limitations

The model assumes that within each compartment, the chemical is homogeneously mixed. The substrate gravel is parameterized to have no inherent sorptive capacity for organics but does offer a surface for suspended sediment deposition which offers sites for sorption of freely dissolved contaminants in the water. Contaminant transport from the rhizomes to the emergent vegetation is assumed to occur principally through xylem flow, while phloem and aerenchyma transport are considered negligible. Thus, the model is not applicable to describe the fate of gases such as methane or oxygen, or essential nutrients such as nitrogen and phosphorus. For our modelling purposes, the atmosphere does not act as a source of contaminant mass, but only as a contaminant sink. No seasonal or diurnal variability is modelled for the climatic variables (e.g. temperature, precipitation, evapotranspiration).

The model accounts for the combined transformation by chemical reactions, physical degradation, and biological transformation. Chemical transformations result from reactions with other chemicals within the wetland environment, and physical transformations may occur from UV-exposure (Fasnacht and Blough, 2002). Biological transformation (biotransformation) occurs from microbial activity, or enzymatic degradation within wetland vegetation (rhizomes and emergent vegetation). All transformation processes are modelled as non-reversible first-order degradation pathways. Transformation is assumed to act upon the freely dissolved contaminant fraction in the environmental media whereas particle-bound contaminant fractions are not subject to transformation (Kickham et al. 2012). Transformation rate constants (k_t) in each medium are first-order rates that can represent both biotic and abiotic transformation processes in water, rhizomes, and emergent vegetation.

2.4. Methods

The model was parameterized and calibrated for a single reed bed (RB3) of Singapore's Lorong Halus Treatment Wetland (LHTW; Table 2-2). The LHTW system was constructed to treat landfill leachate and includes a pre-treatment system (8,000 m^2), five constructed reed beds that run in parallel (total 38,000 m^2), and five polishing ponds (total 13,000 m^2). Data on the LHTW configuration and design, including parameter data for RB3 was obtained from Wang and Kelly (2017) and Sim et al. (2013).

2.4.1. Chemicals

Nine hydrophobic organic contaminants were used for model calibration: galaxolide, tonalide, pentachlorobenzene, hexachlorobenzene, 1,2,3,4-tetrachlorobenzene, musk ketone, methyl triclosan, PCB52, and endosulfan sulfate. These substances were selected from the original data set (86 chemicals) reported by Wang and Kelly (2017) because they were detected in more than two of three grab samples in two sampling events (8th October 2015 and 11th February 2016) and observed concentrations were below each chemical's aqueous solubility limit. Concentrations of hexachlorobenzene, 1,2,3,4-tetrachlorobenzene, and endosulfan sulfate were non-detectable in one of the grab samples and were assumed to equal 50% of the method detection limit reported by Wang and Kelly (2017). The recurrence of

chemicals detected in wetland media indicate that the chemicals have been consistently present in the influent between sampling events, justifying the use of the steady-state version of the model. The concentration measurements of these substances in influent leachate (C_{in}), effluent (C_{out}), vegetation rhizome (C_{Rh}), and (emergent) vegetation leaves (C_{EV}) were averaged over the two sampling events for model calibration.

Table 2-2: Model parameters that describe reed bed #3 at the Lorong Halus Treatment Wetland.

Parameter	Units	Value
Surface Area	m^2	10,000
Depth of rooting medium	m	0.8
Rooting medium porosity (V_{voids}/V_{total})	unitless	0.35
Average grain size of rooting medium	mm	40
Aspect ratio of wetland cell (L:W)	unitless	4:1
Average water depth within the rooting medium	m	0.65
Water inflow	L/day	100,000
Total annual average precipitation	mm/year	2330
Total annual average potential evapotranspiration	mm/year	2,385

Physicochemical properties were obtained from the EPISuite v4.11 program (U.S. EPA, 2013), and half-life times for chemical transformations were derived from the EPISuite v4.11 Biowin model for primary biodegradation (Boethling et al., 1994). Pentachlorobenzene, hexachlorobenzene, PCB 52, and endosulfan sulfate are considered to be recalcitrant, and therefore assigned a $t_{1/2}$ of 10^3 days to represent a negligible rate of transformation in the model. Galaxolide, tonalide, musk ketone, 1,2,3,4-tetrachlorobenzene, and methyl triclosan are considered biodegradable on the order of months and were assigned a $t_{1/2}$ of 250 days in water, and in the absence of information on the biotransformation of the chemicals in wetland vegetation, 2,500 days in rhizomes and emergent vegetation.

2.4.2. Model calibration

To calibrate the model for the LHTW system, the rate constant for contaminant transport from water-to-rhizome ($k_{W\text{-}Rh}$) and rhizome-to-emergent vegetation ($k_{Rh\text{-}EV}$) was multiplied by a calibration coefficient ${\beta_1}^{logKow}$ and ${\beta_2}^{logKow}$ using:

$$k^*_{W-Rh} = k_{W-Rh} \cdot \beta_1^{logKow} \qquad \text{Eq. 2-8}$$

$$k^{*}_{Rh-EV} = k_{Rh-EV} \cdot \beta_2^{logKow} \quad \text{Eq. 2-9}$$

where k^{*} is the calibrated rate constant (day^{-1}), K_{OW} is the octanol-water partition coefficients, and β_1 and β_2 are the calibration coefficients derived by calibrating the model to the empirical data. A calibration coefficient equal to one indicates no calibration of the model. The rationale for the calibration of the rate constants for the transport of the chemical from water to rhizome and from rhizome to emergent vegetation is that there is a lack of information on the uptake and elimination kinetics of the test chemicals in the wetland vegetation. K_{OW} is used in Eq. 2-8 and Eq. 2-9 because it is an important chemical property that controls the environmental fate of organic chemicals.

2.4.3. Model performance analysis

Model performance was evaluated by comparing empirical concentrations ($C_{obs.}$) to the model-estimated concentrations (C_{model}) of the nine contaminants, using the concentration of the contaminants in the influent (C_{in}) as the external variable. The mean model bias (MB_i) was estimated for each medium for which concentration data were available (i = water, rhizome, or emergent vegetation) using:

$$MB_i = e^{\frac{\sum_{j=1}^{n}\left[\ln \frac{C_{model,j}}{C_{obs,j}}\right]}{n}} \quad \text{Eq. 2-10}$$

where j represents the individual contaminants (n = 9) used for model calibration and testing. This method of model performance evaluation assumes that the ratio C_{model} / $C_{obs.}$ has a log-normal distribution. An MB_i greater than one indicates the model systematically over-estimates chemical concentrations in media i by a factor equal to the MB_i value. An MB_i less than one indicates the model systematically under-estimates chemical concentrations in media i by a factor equal to the MB_i value. An MB_i of one indicates that, on average, empirical observation and model calculations are in agreement, i.e. minimal model bias. The 95% confidence intervals of MB_i represents the uncertainty in the model calculations. The MB_i value and the 95% confidence interval reflect the combined sum of error in the model calculations, including model parameterization errors, errors in model structure, and analytical errors and variability in the empirical data used for model performance analysis.

The steady-state assumption of the model was assessed by estimating the time to reach 95% of steady-state (i.e. t_{95}) for each chemical in the three environmental compartments. t_{95} is estimated as $3 \cdot k_{dep.i}$, where $k_{dep.i}$ is the total depuration rate constant for environmental compartment i. These estimates were verified with the dynamic (non-steady-state) version of the model and were used to evaluate whether steady-state conditions were achievable within the timeline of the two sampling events at the LHTW.

2.4.4. Sensitivity analysis

The model uses 42 state variables (N = 42) for the contaminant fate calculations. The sensitivity of each of these parameters was evaluated by the effect of each model parameter on mass removal efficiency (E_L), using a method developed by Morris (1991). This method is useful for determining whether the effect of the input parameter on the mass-removal efficiency is (a) negligible, (b) linear and additive, or (c) non-linear or involved in interactions with other parameters (Campolongo and Saltelli, 1997; Saltelli et al., 2005; Campolongo et al., 2007).

Following the approach outlined in Saltelli et al. (2008), the elementary effects of parameter i (EE_i) were estimated using the mass-removal efficiency as the model output (Y), such that:

$$EE_i = \frac{[Y(X_1, X_2, \dots, X_{i-1}, X_i + \Delta, \dots, X_N) - Y(X_1, X_2, \dots, X_N)]}{\Delta} \qquad \text{Eq. 2-11}$$

The parameter values (X_i) are discretized along a 4-level grid (i.e. Δ = [0, 1/3, 2/3, 1]) such that $X_i = \Delta$ [MAX – MIN] + MIN. Additional details on the calculations for EE_i are available in the Supplementary Information. The mean and standard deviation (μ_i^* and σ_i) of the elementary effects for each parameter were used to analyze the sensitivity of the input parameters and demonstrate their effects on E_L. μ_i^* represents the magnitude of parameter sensitivity to removal efficiency, and σ_i represents the degree of interactions between input parameters.

2.4.5. Model simulations to assess model behaviour

Two applications of the model were used to evaluate horizontal subsurface flow treatment wetlands for the removal of various industrial contaminants from wastewater and to illustrate the merits and limitations of the model. The first application of the model explores the effects of the water budget on the treatment of specific organic pollutants. The second application of the model explores removal efficiency, transpiration, and volatilization of a wide range of contaminants based on their physicochemical properties and demonstrates the significance of biotransformation in contaminant removal. The model was parameterized to the Lorong Halus Treatment Wetland (LHTW).

Simulations to assess the influence of the water balance

Discharge rates for RB3 are not available for the individual treatment wetland cells and therefore the outflow rate was estimated from the steady-state water budget:

$$Q_{out} = Q_{in} + Q_{ext.} - Q_{ET} - Q_{GW} \quad \text{Eq. 2-12}$$

and

$$Q_{ext.} = Q_{P} + Q_{runoff} + Q_{GW} \quad \text{Eq. 2-13}$$

where Q_{out} is the flow rate (m^3/day) of water leaving the wetland cell, Q_{in} is the water flow rate entering the cell from the sedimentation tank, Q_P represents the rate that water enters the wetland via precipitation ($Q_P = P \cdot SA_{RB3}$), Q_{runoff} represents the rate that water enters the wetland via runoff, Q_{ET} is the evapotranspiration rate from the LHTW ($Q_{ET} = ET \cdot SA_{RB3}$), and Q_{GW} is the discharge (-) into groundwater or recharge (+) into the wetland. The sum of Q_P, Q_{runoff}, and Q_{GW} represent the total input of water from external sources (i.e. $Q_{ext.}$). Within the wetland, $Q_{ext.}$ competes with Q_{ET} and Q_{GW} to determine the water balance. This water balance can be represented by the ratio of Q_{out}/Q_{in}. A Q_{out}/Q_{in} ratio greater than one indicates that the input from precipitation, runoff, or groundwater recharge (i.e. $Q_{ext.}$) exceeds the water loss via evapotranspiration and groundwater discharge. A Q_{out}/Q_{in} ratio less than one indicates that the total loss of water exceeds $Q_{ext.}$

At the LHTW system, runoff and groundwater recharge and discharge are considered negligible due to the impermeable liners and physical controls. Q_{in} was estimated from Sim et al. (2013) to be 100,000 L/day of landfill leachate. The LHTW has an average annual precipitation rate of 2,330 mm/year (Meteorological Service Singapore, 2015), an estimated evapotranspiration rate of 2,385 mm/year (Penman-Monteith equation), an estimated outflow rate of 98,500 L/day (Q_{in} = 100,000 L/day) and a mean hydraulic retention time (HRT) of 22.7 days ($HRT = V_{water}/Q_{out}$).

Simulations to assess the influence of physicochemical properties

This application of the model explores which chemical substances are efficiently removed by wetland treatment and which chemical substances are not. A distribution of K_{OW} (octanol-water partition coefficient) and K_{AW} (air-water partition coefficient) was created based on the 3-solubility approach for environmental distribution of organic chemicals between water, air, and organic media (Mackay, 2001). K_{OW} ranged from 3.0 to 7.0, and K_{AW} ranged from -8.0 to 4.0 to reflect various organic contaminants that may enter the treatment wetland. The concentration in the influent was set to 1 ppm. All other physicochemical properties such as Henry's law constant (H; $Pa \cdot m^3/mol$) and the organic carbon-water partition coefficient (K_{OC}) were derived from K_{OW} and K_{AW}.

The roles of K_{OW} and K_{AW} were evaluated using steady-state model outputs: volatilization, transpiration, and mass-loading removal efficiency (E_L). Volatilization and transpiration are shown as a percentage of total removal of contaminant mass from the inflowing wastewater. To highlight the removal via volatilization and transpiration, biotransformation rates in all media were set to 10^{-10} day^{-1} to represent negligible biotransformation within the wetland media. Since biotransformation is not easily estimated based on K_{OW} and K_{AW}, these rates were applied to the entire domain of K_{OW} and K_{AW}. These modelling results represent removal for non-biodegradable (recalcitrant) contaminants. To explore the effects of biotransformation on wetland treatment, this model application was repeated with biotransformation rates of 0.01 day^{-1}, 0.1 day^{-1}, and 0.3 day^{-1}.

2.5. Results and Discussion

2.5.1. Model calibration

Model-estimated concentrations of the test chemicals (n = 9) in water, rhizomes, and emergent vegetation from the LHTW are shown to be within a factor of three to observed concentrations (Figure 2-2). The value of the calibration coefficients β_1 and β_2 (Eq. 2-8 and Eq. 2-9) are 0.60 and 1.56, respectively. β_1 is less than one which indicates an over-prediction of water-to-rhizome mass transport by the uncalibrated model, whereas β_2 is greater than one indicating the rhizome-to-emergent vegetation mass transport is under-predicted by the uncalibrated model. These deviations of the model from the empirical data appear to increase with increasing K_{OW} of the chemical. This calibration approach lowers contaminant concentrations in the rhizomes and elevates contaminant mass within the emergent vegetation to better correlate with the observed data. This suggests that aquatic plants may have a smaller influence on the mass balance than is apparent from plant-water exchange models.

2.5.2. Model behaviour

Model bias

The resulting mean model bias (MB) and its 95% confidence range in the water, rhizome, and emergent vegetation is 0.97 (0.41 – 2.24), 1.03 (0.53 – 2.00), and 1.00 (0.27 – 3.71), respectively. The mean model bias of the calibrated model is close to one for the media investigated, illustrating low systematic bias for the LHTW system based on the nine test chemicals that are poorly biotransformed. The 95% confidence intervals of the overall model bias indicate uncertainty equivalent to a factor of 2.3 for water concentration estimates, 2.0 for rhizome concentration estimates, and 3.7 for emergent vegetation concentration estimates.

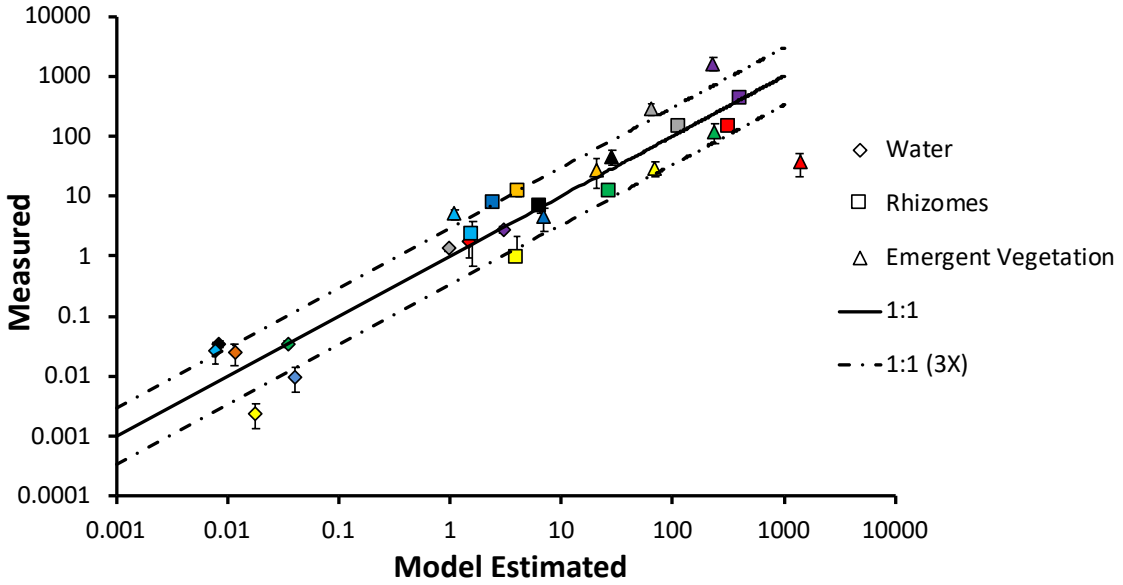

Figure 2-2: Measured and model-estimated concentrations of the nine test chemicals in the water, rhizomes, and emergent vegetation of the Lorong Halus treatment wetland. Error bars represent standard error of the mean observed concentrations. If no error bars are visible, standard error of the mean is equal to or less than the width of the symbol. Endosulfan sulfate = blue; musk ketone = red, 1,2,3,4-tetrachlorobenzene = orange; pentachlorobenzene = green; methyl triclosan = yellow; hexachlorobenzene = black; tonalide = grey; galaxolide = purple; PCB 52 = light blue.

Steady state vs. non-steady state

The time expected to reach 95% of steady state (t_{95}) in water ranges from 40 days (endosulfan sulfate) to 66 days (PCB 52) for the nine test chemicals. Generally, t_{95} of the test chemicals in water increases with increasing log K_{OW} of the chemical. The t_{95} for the rhizome and emergent vegetation compartments range from 75 to 4,200 days and 1.0×10^4 to 4.3×10^4 days (Table B.7). Large estimates of t_{95} for these test chemicals in rhizomes and emergent vegetation result from the slow depuration rates determined by the model. This is in part due to the slow biotransformation rates of these hydrophobic test chemicals. This suggests that the use of the steady-state version of the model is appropriate to estimate chemical concentrations in the water. The t_{95} estimates for rhizomes and emergent vegetation suggests that the concentration of the test chemicals in the vegetation of the LHTW can be expected to continuously increase over time (non-steady state condition). This may explain why the calibration coefficient β_1 for water-to-rhizome exchange is less than one.

2.5.3. Sensitivity analysis

The elementary effects sensitivity metrics (μ_i^* and σ_i) of all 42 parameters (Table A.8) demonstrate significant sensitivity of the mass removal efficiency to a number of parameters. The most sensitive parameters are: log K_{OW} (μ_{logKow}^* = 0.30, σ_{logKow} = 0.86), (water-side) water-rhizome mass transfer coefficient ($\mu_{W\text{-}Rh}^*$ = 0.27, $\sigma_{W\text{-}Rh}$ = 0.29), transformation half-life in water ($\mu_{t1/2,water}^*$ = 0.19, $\sigma_{t1/2,water}$ = 0.24), water temperature ($\mu_{Temp.}^*$ = 0.14, $\sigma_{Temp.}$ = 0.16), and plant stem density, i.e. the number of plants in the wetland (μ_{Np}^* = 0.13, σ_{Np} = 0.14). The log K_{OW} is a central parameter in the treatment wetland model. It is used to calculate the vegetation-water, and suspended sediment-water partition coefficients which are then used to calculate mass transfer coefficients and rate constants. The direct and indirect relationships of log K_{OW} with other variables create many different interactions throughout the model resulting in a large mean (μ_i^*) and standard deviation (σ_i) of its elementary effects on mass-removal efficiency. The (water-side) rhizome-water mass transfer coefficient is used to calculate overall chemical mass transfer from water to rhizome using a two-film diffusion model. This suggests that removal efficiency in the wetland is dependent on characteristics of the vegetation and properties of the chemical that promote diffusion between water and rhizomes.

The sensitivity of mass-removal efficiency to the transformation half-life of the chemical in water demonstrates the importance of biotransformation on the removal of chemicals in wetlands. Chemicals that are more easily biotransformed in wetland media will be more efficiently removed in the wetland. Biotransformation in the water reduces the availability of the chemical for mass transfer into vegetation and therefore affects the contribution of other biogeochemical processes on chemical removal. This is shown by the sensitivity analysis with the large standard deviation of elementary effects suggesting transformation rates in water interacts with other model parameters that affect removal efficiency.

Water temperature and plant density (plants per m^2) are design criteria for the treatment wetland. Their large μ_i^* and σ_i show that mass-removal efficiency is dependent on the wetland design. This suggests that future treatment wetlands can be designed to improve mass-removal efficiency by optimizing these parameters for a site-specific application of a treatment wetland system. However, there are complex interactions between these parameters that influence the performance of the treatment wetland.

These complex interactions provide a rationale for developing a treatment wetland model to aid in future wetland designs.

The analysis also suggests that some parameters may have little to no significant effect on the estimated mass-removal efficiency (E_L) or other outputs from the treatment wetland model. Such parameters include: aspect ratio of the wetland design (i.e. length:width, 1:1 – 8:1) which suggests that many different wetland configurations can be suitable for treatment, and size of emergent vegetation (0.1 – 1.0 kg) which suggests that a variety of plants can be used in treatment wetlands. However, there may be practical implications of these parameters that are not captured by the model. For instance, the aspect ratio of the wetland design may influence mixing of wastewater and erosion of berms and is used by the model to estimate the total surface area of the rooting medium gravel (see Appendix A). Sensitivity to the aspect ratio may occur for model applications that include biofilm as a compartment relevant for the environmental fate of substances within the wetland. The size of emergent vegetation may correlate with the size of the rhizomes which is a more sensitive parameter for removal efficiency or may also correlate with wetland maturity and productivity. Further analysis is required before suggesting these parameters are not influential for treatment wetland design, and to properly assess the influence of these parameters on overall contaminant removal for various treatment wetland systems.

2.5.4. Role of the water balance

Figure 2-3 demonstrates how external inputs such as precipitation, runoff, and groundwater recharge can affect E_L and E_C for hexachlorobenzene (HCB) at the LHTW. If there were no inputs of water into the wetland other than influent (i.e. $Q_{ext.} \rightarrow 0$ L/day), the evapotranspiration is expected to reduce water outflow to 70% of Q_{in} ($Q_{out}/Q_{in} = 0.70$). This water deficit through the wetland results in an E_C for HCB below zero, i.e. concentration of HCB in the effluent exceeds that in the influent despite actual removal of the mass of HCB ($E_L > 0$) from the water by the wetland. If the purpose of the treatment wetland is to reclaim water for discharge into the environment, then the treatment wetland may not be effective as the concentration of HCB in the effluent is greater than that in the influent. If inputs of water into the wetland are able to surpass water losses through evapotranspiration resulting in $Q_{out}/Q_{in} > 1$, then dilution of the HCB occurs causing both E_L and E_C to adopt values greater than zero. The added volume of

water increases flow rates through the LHTW and therefore decreases the hydraulic retention time within the wetland, limiting the exposure of HCB to wetland biogeochemical removal mechanisms.

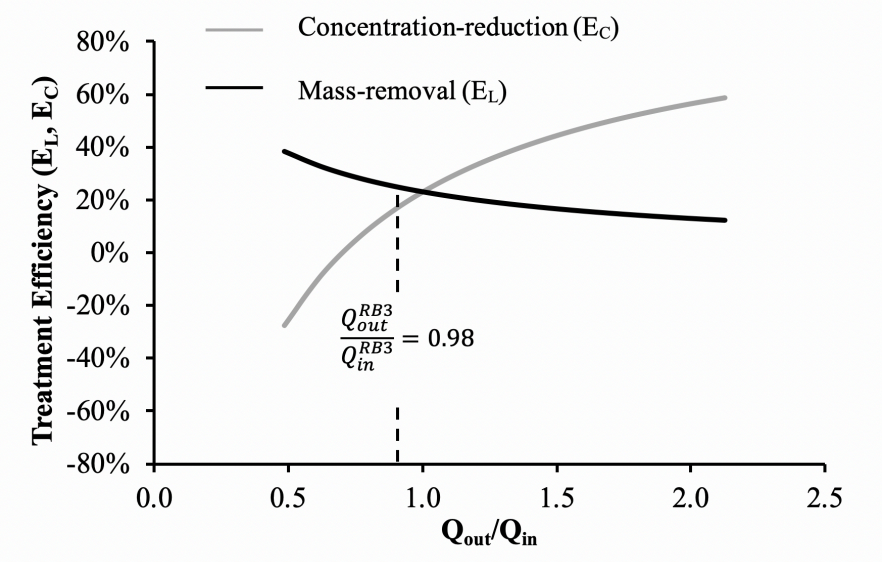

Figure 2-3: Efficiency of mass-removal (E_L) and concentration-reduction (E_C) for hexachlorobenzene (HCB) as a function of the water balance. For reed bed #3 in the LHTW, Q_{out}/Q_{in}= 0.98.

A similar response by E_L and E_C can also be shown for variable conditions of evapotranspiration. With greater evapotranspiration rates there is an increase in E_L for HCB within the wetland resulting from: i) greater xylem flow through vegetation providing a more rapid transport of the chemical from the subsurface water into the vegetation to undergo transpiration, ii) greater volatilization from the subsurface water through the rooting medium, and iii) greater hydraulic retention time within the wetland since the volume of water within the wetland is reduced by evapotranspiration. The hydraulic retention time has been explored in many treatment wetland studies and is a critical design feature for the success of a treatment wetland application (Knight et al., 1999; Hijosa-Valsero et al., 2010; Pavlineri et al, 2017). For substances that are quickly biotransformed, the water balance also affects biotransformation rates since the rate of biotransformation is a function of the concentration of the substance in the water of the wetland. However, water balance has less effect on E_L and E_C for quickly biotransforming substances than for recalcitrant substances. Figure A.1 (Supplementary Information) demonstrates the effect of external water sources on E_L and E_C for pyrene to show the influence of the water budget with a more rapidly biotransformed substance.

2.5.5. Influence of physicochemical properties

Figure 2-4a demonstrates that volatilization of substances is responsible for up to 70% of contaminant removal in absence of biotransformation in the LHTW for substances with a log K_{OW} 3 – 5 and log K_{AW} > 0. Volatilization contributes up to 10% of contaminant removal for persistent substances with a log K_{AW} below -2.0, regardless of its log K_{OW}. The contribution of volatilization to mass removal depends on the wetland design and environmental conditions. At the LHTW, there is little annual variability in air temperature which averages 24.7 deg-C (SD 0.5), with an average daily maximum of 31.5 deg-C (SD 0.7; Meteorological Service Singapore, 2015). Generally, high temperatures at the surface of the wetland will promote volatilization from surface water. However, at the LHTW there is a 15 cm freeboard zone between the water surface and the open air that limits mass transfer of the contaminants from liquid (aqueous phase) to gas (air phase). Reducing the freeboard zone may further improve volatilization of some contaminants.

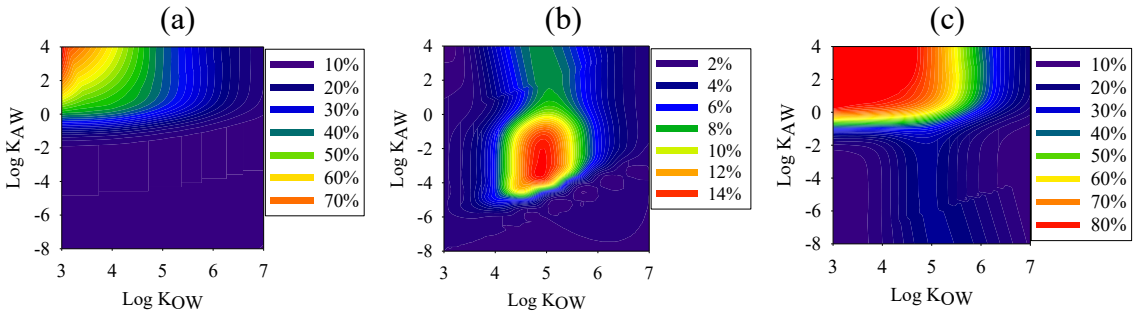

Figure 2-4: Model calculations of (a) % mass removal via volatilization, (b), % mass removal via transpiration, and (c) mass-loading removal efficiency (E_L) for substances of varying K_{OW} and K_{AW} in the Lorong Halus Treatment Wetland.

Figure 2-4b indicates that transpiration through the vegetation at the LHTW is responsible for up to 14% of contaminant removal in absence of biotransformation and is greatest for substances with log K_{OW} of 4.5 – 5.5 and log K_{AW} of -5.0 – 0.0. This range of chemical properties describes chemicals that: (i) do not strongly or irreversibly bind to organic media, and (ii) do not have a high solubility in water. These characteristics of a substance permit diffusion of the contaminant into the rhizomes, and subsequently into the transpiration stream (xylem flow) without strongly binding to the organic carbon or lipid fraction of the vegetation. If the chemical binds too strongly to the organic carbon in the vegetation, only a small fraction of the chemical is left dissolved in the transpiration

stream. Conversely, if a chemical exhibits a high aqueous solubility and low affinity for organic carbon, then there is little partitioning of the chemical from water into the vegetation.

Figure 2-4c suggests that persistent chemicals having a log K_{OW} between 3.0 and 5.0 and log K_{AW} greater than -1.0 are most efficiently removed from wastewater in the LHTW (E_L = 70%). This range of chemical properties closely resembles the optimal range for volatilization, which, in the LHTW, contributes to contaminant removal to a greater degree than transpiration. The lowest mass removal (E_L) in absence of biotransformation was observed for substances with (i) a log $K_{OW} \leq 4$ and log $K_{AW} < 2$, and (ii) a log $K_{OW} \geq 6$ and log $K_{AW} < -1.0$ ($E_L \leq 7\%$). These properties describe substances that are either highly hydrophilic or highly hydrophobic and represent chemicals that are neither prone to volatilization nor transpiration. Hydrophilic substances tend to remain in the water compartment and have lower removal efficiencies because they are mainly subject to removal mechanisms in the water compartment. Transformation in the water is the main mechanism of removal for these substances. Hydrophobic substances bind strongly to organic media, reducing the freely dissolved concentration in the water, which limits the amount of chemical available for volatilization, transpiration, and transformation. Contaminants bound to organic media are initially extracted from the water and the wetland may show high treatment efficiencies that decrease as the system approaches steady-state.

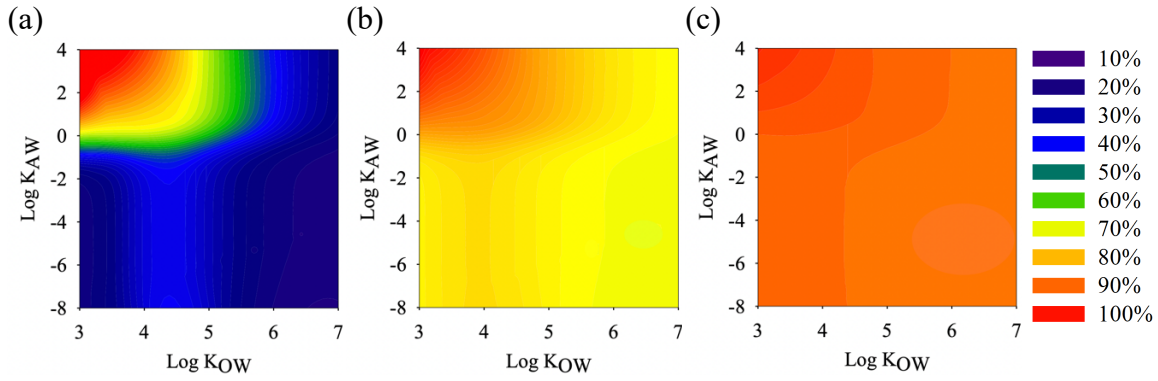

Figure 2-5: Model calculations of mass-loading removal efficiency (E_L) for substances of varying K_{OW} and K_{AW} where biotransformation rates are (a) k = 0.01 day^{-1}, (b) k = 0.1 day^{-1}, and (c) k = 0.3 day^{-1} in the Lorong Halus treatment wetland.

Figure 2-5a, b, and c demonstrate the effects of different biotransformation rates on the mass-removal efficiency (E_L) of contaminants. For biotransformation rates in water of 0.01, 0.1, and 0.3 day^{-1}, the maximum estimated E_L for the LHTW system is 75%, 84%, and 90%, respectively. The greatest E_L values were found for substances having a log K_{OW} between 3.0 and 5.0 and log K_{AW} > -1.0. Improvements to the maximum E_L as biotransformation rates increase are evident, however the effects of biotransformation on mass removal are more profound for substances that are poorly removed by non-biotransformation related removal mechanisms such as volatilization and transpiration. For substances that do not readily undergo volatilization or transpiration, even relatively low rates of biotransformation can significantly contribute to the overall removal from the wetland. As biotransformation rates increase, transpiration and volatilization processes become less significant to the overall mass-removal efficiency. For example, when biotransformation rate is 0.3 day^{-1}, volatilization and transpiration are responsible for < 23% and < 0.1% of contaminant removal, respectively, whereas total biotransformation accounts for > 60% of contaminant removal. Figure 2-5 is useful for interpolating the removal efficiency of various chemicals that occupy regions within the range of K_{OW} and K_{AW} shown in the figures. Biotransformation rates of chemicals are often unknown for certain chemicals within environmental media, but a general range of removal efficiency can still be interpreted from these figures.

Since biotransformation is shown to be significant to the overall removal capacity of contaminants, maintaining a strong community of microorganisms and vegetation that can facilitate various biotransformation processes is important to the performance of these systems (Ibekwe et al., 2003; Button et al., 2016; Mustafa et al., 2017). Characterizing the biotransformation capacity in the wetland through bioassays or other methods is a crucial component to assess treatment efficiencies of remediation wetlands.

2.6. Conclusions

A mechanistic model was developed to assess the fate and removal efficiency of hydrophobic organic contaminants in horizontal subsurface flow wetlands. The model was applied to Singapore's Lorong Halus Treatment Wetland system and evaluated under different modelling scenarios. The calibrated model for the Lorong Halus

Treatment Wetland provided an adequate description of the concentrations of nine neutral organic substances in the water, rhizomes and emergent vegetation of the wetland.

The model demonstrates the influence of the water balance on both mass-removal and contaminant concentration-reduction efficiency for recalcitrant substances in the wetland. Water inputs into the wetland in addition to wastewater influents (e.g., precipitation) will reduce concentrations of contaminants as a result of dilution, but also shorten hydraulic retention times which reduce contaminant-mass removal. Water loss from the wetland through evapotranspiration reduces the concentration-reduction efficiency of the wetland but increases the mass-removal efficiency of contaminants in the wetland. The balance between inputs and losses of water in the wetland has an important effect on the treatment performance.

The model illustrated that removal pathways of organic contaminants in the wetland varied as a function of the properties of the contaminants. The mass-removal efficiency of the treatment wetland was greatest for chemicals with a log K_{OW} between 3.0 and 5.0 and log K_{AW} > -1.0. Removal of persistent contaminants through volatilization was found to be greatest for substances with a log K_{OW} between 3 and 5 and log K_{AW} > 0. Transpiration flux in vegetation was found to be most important for substances with a log K_{OW} of 4.5 – 5.5 and log K_{AW} of -5.0 – 0.0. Biotransformation rates of the contaminants in the wetland media play a crucial role in removal of contaminants from wastewater. The model provides a tool for assessing the organic contaminant removal capacity and evaluating trade-offs in the design and operation of a horizontal subsurface flow treatment wetland.

2.7. References

AEP (Alberta Environmental Protection) (1995). Water Quality Based Effluent Limits Procedure Manual. Source Standards Branch, Environmental Regulatory Services. Alberta Environmental Protection. Edmonton. 78 pp.

Arnot, J.A. and Gobas, F.A.P.C. (2004). A Food Web Bioaccumulation Model for Organic Chemicals in Aquatic Ecosystems. *Environmental Toxicology and Chemistry* 23, 2343-2355.

Batty, L. C. and Younger, P. L. (2004). Growth of Phragmites australis (Cav.) Trin ex. Steudel in mine water treatment wetlands: effects of metal and nutrient uptake. *Environmental Pollution*, 132, 85–93. http://doi.org/10.1016/j.envpol.2004.03.022

Boethling, R. S., Howard, P. H., Meylan, W., Stiteler, W., Beauman, J., and Tirado, N. (1994). Group Contribution Method for Predicting Probability and Rate of Aerobic Biodegradation. *Environmental Science and Technology*, 28, 459–465.

Briggs G.G., Bromilow, R.H., Evans, A.A., and Williams, M. (1983). Relationships between lipophilicity and root uptake and translocation of non-ionized chemicals in barley shoots following uptake by the roots. *Pesticide Science* 14: 492-500.

Button, M., Weber, K., Nivala, J., Aubron, T., and Müller, R. A. (2016). Community-Level Physiological Profiling of Microbial Communities in Constructed Wetlands: Effects of Sample Preparation. *Applied Biochemistry and Biotechnology*, 178, 960–973. http://doi.org/10.1007/s12010-015-1921-7

Campolongo, F., and Saltelli, A. (1997). Sensitivity analysis of an environmental model: an application of different analysis methods. *Reliability Engineering & System Safety*, 57(1), 49–69. http://doi.org/10.1016/S0951-8320(97)00021-5

Campolongo, F., Cariboni, J., and Saltelli, A. (2007). An effective screening design for sensitivity analysis of large models, *Environmental Modelling and Software*, 22(10), 1509-1518.

CCME (Canadian Council of Ministers of the Environment) (1999). Canadian water quality guidelines for the protection of aquatic life. In: Canadian environmental quality guidelines, 1999, Canadian Council of Ministers of the Environment, Winnipeg.

Chazarenc, F., Merlin, G., and Gonthier, Y. (2003). Hydrodynamics of horizontal subsurface flow constructed wetlands. *Ecological Engineering*, 21:165–173.

Chen, S., Wang, G.T., and Xue, S.K. (1999). Modeling BOD removal in constructed wetlands with mixing cell method. *Journal of Environmental Engineering* 125:64–71.

Clark, B., Henry, J.G. and Mackay, D. (1995). Fugacity Analysis and Model of Organic Chemical Fate in a Sewage Treatment Plant. *Environmental Science and Technology*, 29: 1488-1494.

Environment Canada (1995). The Toxic Substances Management Policy. ISBN 0-662-61860-2 Cat. no. En40-499/1-1995.

ESRD (Environment & Sustainable Resource Development) (2014). Environmental Quality Guidelines for Alberta Surface Waters. Water Policy Branch, Policy division. Edmonton. 48 pp.

EUSES (European Union System for the Evaluation of Substances, version 2.1.2) (2012). National Institute of Public Health and the Environment (RIVM), the Netherlands. Available via the European Chemicals Bureau, http://ecb.jrc.it

Fasnacht, M. P., and Blough, N. V. (2002). Aqueous Photodegradation of Polycyclic Aromatic Hydrocarbons. *Environmental Science and Technology* 36, 20: 4364–69. doi:10.1021/es025603k

García, J., Chiva, J., Aguirre, P., Alvarez, E., Sierra, J. P., and Mujeriego, R. (2004). Hydraulic behaviour of horizontal subsurface flow constructed wetlands with different aspect ratio and granular medium size. *Ecological Engineering*. 23:177–187

Gobas F.A.P.C. (1993). A model for predicting the bioaccumulation of hydrophobic organic chemicals in aquatic food-webs: application to Lake Ontario. *Ecological Modelling*. 69:1-17.

Gobas, F.A.P.C., McNeil, E. J., Lovett-Doust, L., and Haffner, G. D. (1991). Bioconcentration of Chlorinated Aromatic Hydrocarbons in Aquatic Macrophytes (Myriophyllum spicatum). *Environmental Science and Technology* 25, 924-929.

Hijosa-Valsero, M., Matamoros, V., Sidrach-Cardona, R., Martín-Villacorta, J., Bécares, E., and Bayona, J. M. (2010). Comprehensive assessment of the design configuration of constructed wetlands for the removal of pharmaceuticals and personal care products from urban wastewaters. *Water Research*, 44(12), 3669–3678. http://doi.org/10.1016/j.watres.2010.04.022

Ibekwe, A. M., Grieve, C. M., and Lyon, S. R. (2003). Characterization of Microbial Communities and Composition in Constructed Dairy Wetland Wastewater Effluent. *Applied and Environmental Microbiology*, 69(9), 5060–5069. http://doi.org/10.1128/AEM.69.9.5060–5069.2003

Kadlec R.H., Knight R.L. (1996) *Treatment Wetlands*. First Edition, CRC Press: Boca Raton, Florida.

Kadlec, R., and Wallace, S. (2009). *Treatment Wetlands* (2nd ed.). Boca Raton, FL: Taylor & Francis Group.

Kickham, P., Otton, S.V., Moore, M.M., Ikonomou, M.G., Gobas, F.A.P.C. (2012). Relationship between biodegradation and sorption of phthalate esters and their metabolites in natural sediments. *Environmental Toxicology and Chemistry* 31 (8), 1730–1737.

Knight, R. L., Kadlec, R. H., and Ohlendorf, H. M. (1999). The Use of Treatment Wetlands for Petroleum Industry Effluents. *Environmental Science and Technology*, 33(7), 973–980. doi:10.1021/es980740w

Langergraber, G. (2001). Development of a simulation tool for subsurface flow constructed wetlands. Vienna, Austria: *Wiener Mitteilungen*, 169.

Lin, Y. F., Jing, S. R., Lee, D. Y., Chang, Y. F., Chen, Y. M., and Shih, K. C. (2005). Performance of a constructed wetland treating intensive shrimp aquaculture wastewater under high hydraulic loading rate. *Environmental Pollution*, 134, 411–421. http://doi.org/10.1016/j.envpol.2004.09.015

Mackay D. (2001). *Multimedia environmental models: The fugacity approach* (2nd ed.). Boca Raton, FL: Taylor & Francis Group.

Mackay, A. A., and Gschwend, P. M. (2000). Sorption of monoaromatic hydrocarbons to wood. *Environmental Science and Technology*. 34(5): 839-845.

Mackay, D., Paterson, S., Joy, M. (1983). A Quantitative Water, Air, Sediment Interaction (QWASI) Fugacity Model for Describing the Fate of Chemicals in Rivers. *Chemosphere*. 12: 1193-1208.

Mayo, A.W., and Bigambo, T. (2005). Nitrogen transformation in horizontal subsurface flow constructed wetlands: I. Model development. *Physics and Chemistry of the Earth* 30:658–667.

Meteorological Service Singapore (2015). Annual Climatological Report 2015. Retrieved from: www.weather.gov.sg/wp-content/uploads/2016/03/Annual-Climatological-Report-2015.pdf

Morris, M.D. (1991). Factorial Sampling Plans for Preliminary Computational Experiments. *Technometrics*. **33**: 161–174. doi:10.2307/1269043.

Mustafa, A., Azim, M. K., Raza, Z., Kori, J. A. (2017). BTEX Removal in a Modified Free Water Surface Wetland, *Chemical Engineering Journal*. https://doi.org/10.1016/j.cej.2017.09.168

Page, D., Dillon, P., Mueller, J., and Bartkow, M. (2010). Quantification of herbicide removal in a constructed wetland using passive samplers and composite water quality monitoring. *Chemosphere*, 81(3), 394–399. http://doi.org/10.1016/j.chemosphere.2010.07.002

Pavlineri, N., Skoulikidis, N. T., and Tsihrintzis, V. A. (2017). Constructed Floating Wetlands: A review of research, design, operation and management aspects, and data meta-analysis. *Chemical Engineering Journal*, 308, 1120–1132. http://doi.org/10.1016/j.cej.2016.09.140

Reddy K.R. and DeLaune, R. (2008). *Biogeochemistry of wetlands: Science and applications* (1st ed.). Boca Raton, FL: Taylor & Francis Group.

Rein, A., Legind, C. N., and Trapp, S. (2011). New concepts for dynamic plant uptake models. *SAR and QSAR in Environmental Research*, 22(1–2), 191–215. http://doi.org/10.1080/1062936X.2010.548829

Saltelli, A., Ratto, M., Andres, T., Campolongo, F., Cariboni, J., Gatelli, D., Saisana, M. and Tarantola, S. (2008). *Global Sensitivity Analysis: The Primer*. West Sussex, England. John Wiley & Sons Ltd.

Saltelli, A., Ratto, M., Tarantola, S., and Campolongo, F. (2005). Sensitivity analysis for chemical models. *Chemical Reviews*, 105(7), 2811–2827. http://doi.org/10.1021/cr040659d

Sim, C. H., Quek, B. S., Shutes, R. B., and Goh, K. H. (2013). Management and treatment of landfill leachate by a system of constructed wetlands and ponds in Singapore. *Water Science and Technology*, 68(5), 1114–1122. http://doi.org/10.2166/wst.2013.352

Topp E., Scheunert, I., Attar, A., and Korte, E. (1986). Factors affecting the uptake of C-14-labeled organic-chemicals by plants from soil. *Ecotoxicological Environmental Safety* 11: 219-228.

Toscano, A., Langergraber, G., Consoli, S., and Cirelli, G. L. (2009). Modelling pollutant removal in a pilot-scale two-stage subsurface flow constructed wetlands. *Ecological Engineering*, 35, 281–289. http://doi.org/10.1016/j.ecoleng.2008.07.011

Trapp, S. (2002). Dynamic root uptake model for neutral lipophilic organics. *Environmental Toxicology and Chemistry* 1(1):203-206.

Trapp, S., and Matthies, M. (1995). Generic one-compartment model for uptake of organic chemicals by foliar vegetation. *Environmental Science and Technology* 29: 2333-2338.

U.S. EPA (2000). Guiding principles for constructed treatment wetlands: Providing water quality and wildlife habitat, EPA 843/B-00/003, U.S. EPA Office of Wetlands, Oceans, and Watersheds.

U.S. EPA (2013). Estimation Programs Interface Suite™ for Microsoft® Windows, v4.11. United States Environmental Protection Agency, Washington, DC, USA.

Wang, Q., and Kelly, B. C. (2017). Occurrence, distribution and bioaccumulation behaviour of hydrophobic organic contaminants in a large-scale constructed wetland in Singapore. *Chemosphere*, 183, 257–265. http://doi.org/10.1016/j.chemosphere.2017.05.113

Whitman, W. (1923). Two-film theory of Gas Absorption. *Chemical and Metallurgical Engineering*. 29 (4).

Wynn, M. T., and Liehr, S. K. (2001). Development of a constructed subsurface-flow wetland simulation model. *Ecological Engineering* 16:519–536.

Chapter 3. Treatment of polycyclic aromatic hydrocarbons in oil sands process-affected water with a surface flow treatment wetland.

3.1. Summary

This study applied a passive sampling approach using low-density polyethylene (PE) passive samplers to determine the treatment efficiency of the Kearl surface flow treatment wetland for polycyclic aromatic hydrocarbons in oil sands process-affected waters. The results show that the wetland's ability to remove individual PAHs from the influent varied substantially among the PAHs investigated. Treatment efficiencies of individual PAHs ranged between essentially 0% for some PAHs to 95% for others. Treatment in the Kearl wetland reduced the combined total mass of all detected PAHs by 54 to 83%. This corresponded to a reduction in the concentration of total PAHs in OSPW of 56 to 82% with inflow concentrations of total PAHs ranging from 7.5 to 19.4 ng/L. The concentration of pyrene in water fell below local regulatory water quality criteria values as a result of wetland treatment. The application of the passive samplers for toxicity assessment showed that in this study PAHs in both the influent and effluent were not expected to cause acute toxicity. Passive sampling appeared to be a useful and cost-effective method to monitor contaminants and to determine the treatment efficiency of contaminants in the treatment wetland.

3.2. Introduction

As demand for freshwater conservation grows, there is a need for sustainable solutions to manage and reuse process-affected waters. In Canada, a considerable volume of Oil Sand Process-affected Waters (OSPW) has been and continues to be generated during bitumen extraction. Since OSPW is currently subject to a 'zero discharge' policy and few treatment options are available, OSPW is either recycled for further use in the extraction process or stored in effluent tailings ponds. These effluent tailings ponds are susceptible to leaching and erosion, and present adverse risks to migratory birds and wildlife that confuse these areas for safe ecological havens (Kelly et al., 2009; Remillard, 2011; Jasechko et al., 2012; Ahad et al., 2015). While efforts to develop feasible solutions for OSPW treatment are ongoing, few have been realized to

date. Treatment wetlands have emerged as a potentially feasible option to treat OSPW (Buchberger and Shaw, 1995; Knight et al., 1999; Davis, 2009; Kadlec and Wallace, 2009; Sundaravadivel and Vigneswaran, 2001; U.S. EPA, 1999). Treatment wetlands are constructed, artificial ecosystems that harness the biogeochemistry of natural systems to reclaim and remediate contaminated land and water.

The biogeochemical mechanisms for contaminant removal within a wetland include microbial and plant-mediated biotransformation, chemical transformations, UV–degradation, evapotranspiration, and sorption to sediments (Kadlec and Wallace, 2009). The capability of wetlands to harness these biogeochemical processes for wastewater treatment has been demonstrated for a variety of wastewaters including municipal and domestic wastewaters, agricultural runoff, pulp and paper wastewater, and waters that contain surfactants, solvents, or pesticides (e.g. Knight et al., 2000; Cameron et al., 2003; Abira et al., 2005; Matamoros et al., 2008; Díaz et al., 2009; Wallace and Davis, 2009; Hijosa-Valsero et al., 2010; Wang and Kelly, 2017). While wastewater treatment has been demonstrated for a variety of wastewaters, many studies have reported treatment wetland performance based on general metrics for water quality such as Biochemical Oxygen Demand, Total Nitrogen, Total Phosphorus, or Total Petroleum Hydrocarbons. Although useful as measures of overall water quality, these general metrics do not detail the removal of specific contaminants of concern from wastewaters. Quantifying the removal of individual contaminants by wetland treatment is critical to evaluate the toxicological risk associated to the influent OSPW and effluent water and to identify which contaminants are more easily removed from wetlands and which contaminants are not, i.e. high vs. low treatment efficiency. Information on the treatment efficiency of engineered treatment wetlands is necessary for assessing the feasibility of treatment wetlands for their specific wastewater challenges.

The objective of this study is to investigate the capacity of wetlands to treat PAHs in OSPW. Specifically, we investigate the treatment efficiency of PAHs in terms of reductions in concentrations, mass loadings and associated toxicity of PAHs in OSPW in the Kearl Treatment (KT) wetland.

3.3. Materials and Methods

3.3.1. Site description

The Kearl Treatment (KT) wetland is a free water surface-flow constructed wetland at the Kearl Oil Sands site (approx. 75 km NNE of Fort McMurray, AB, Canada; 57°26’00"N, 111° 8'31"W) managed by Imperial Oil Resources Ltd. The KT wetland operates in warmer summer months, typically from May to September. It was designed as a pilot-scale wetland to investigate the treatment of on-site Oil Sands Process-affected Water (OSPW). Water is pumped into the wetland at 5 L/s (430 m^3/day), resulting in a hydraulic retention time of approximately 14 days.

In 2017, OSPW was collected as runoff from an overburden disposal area. This overburden disposal area contains stockpiles of excavated overburden from the mined areas at the Kearl Oil Sands site and contains residual amounts of organic contaminants. The runoff is first directed and detained in the north overburden disposal pond located next to the KT wetland which acts as an initial settling basin for suspended sediments. Due to the ‘zero-discharge’ policy for all OSPW, the system operates as a closed-circuit and therefore water is recycled from the KT wetland back into the north overburden disposal pond. The outflow was controlled by a submerged pump that was triggered on when water depth reached 1.7 m, and off when water depth receded to 1.0 m in the Final Deep Pool (Figure 3-1). In 2018, OSPW for the KT wetland was sourced from a drainage pond situated next to an effluent tailings area at the Kearl Oil Sands. The OSPW was pumped to the wetland during a single pump event, where it was fully recycled within the wetland (i.e. no external detention pond was used) for the duration of the 2018 study.

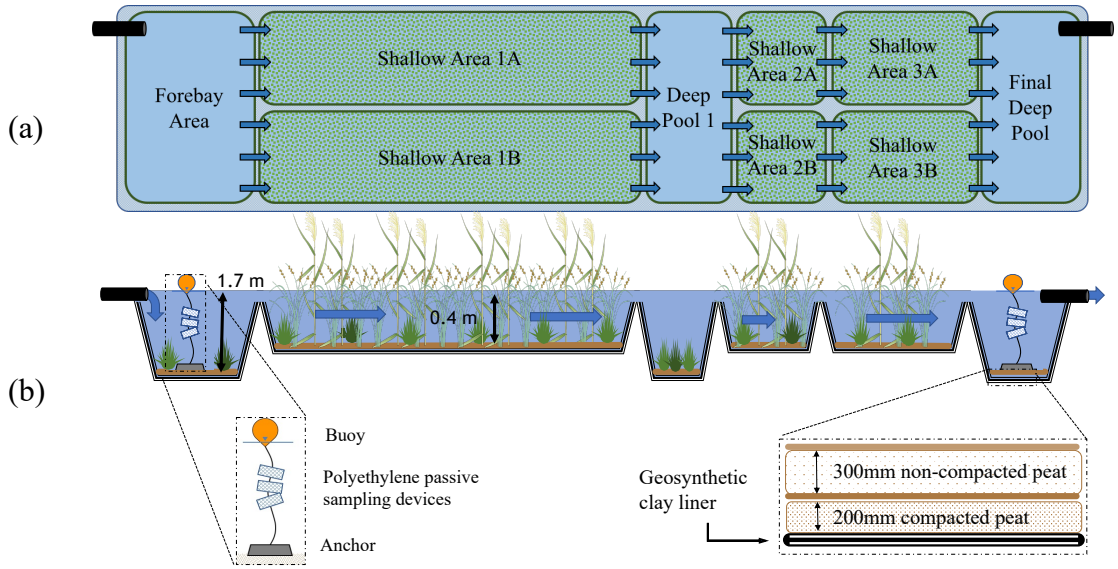

Figure 3-1: Schematic diagram of the Kearl Treatment Wetland (KT wetland) showing (a) planar view, and (b) cross-sectional view with the passive sampling devices and rooting medium.

The wetland consists of six cells in series (3 deep pools, 3 shallow areas) with a longitudinal slope of 0.014%. Water percolates over shallow interior berms that separate each adjacent cell. Shallow berms parallel to water flow in the middle of the shallow pool sections were constructed to improve directional water flow, and provide access for wetland monitoring (e.g. vegetation, erosion, water quality). The KT wetland operates at a total volume of water of approximately 6,000 m^3. The deep pools (forebay, deep pool 1, and final deep pool) operate at a depth of 1.7 m, and are dominated by submerged vegetation, but contain a band of emergent vegetation (approx. 5% of area) along the perimeter of the cells where water depth is shallower. The shallow area cells are densely vegetated with a variety of different species dominated by common cattails (*Typha latifolia*) and water sedge (*Carex aquatilis*).

The rooting medium consists of 200 mm of compacted peat soil underneath 300 mm of non-compacted peat soil from the displaced muskeg originally found on location. The peat was placed over a geosynthetic clay liner that was blanketed with a non-woven geotextile (Figure 3-1).

3.3.2. Water quality monitoring

Total Suspended Solids (TSS), Total Dissolved Solids (TDS), Biochemical Oxygen Demand (BOD), Dissolved Organic Carbon (DOC), Dissolved Inorganic Carbon (DIC), water temperature, conductivity, pH, redox potential, and Dissolved Oxygen (DO) were collected for the OSPW in the wetland to evaluate changes in the quality of OSPW as it passes through the KT wetland. In the 2017 study, samples were obtained from the forebay and final deep pool on July 13th and August 17th, 2017. In the 2018 campaign, OSPW was fully recycled through the wetland, therefore samples were obtained from the forebay on August 26th and September 19th, 2018. Water samples were analyzed by Maxxam Analytics (Calgary, AB, Canada) for Total Suspended Solids (TSS), Total Dissolved Solids (TDS), Biochemical Oxygen Demand (BOD), Dissolved Organic Carbon (DOC), Dissolved Inorganic Carbon (DIC). Field measurements were collected by WorleyParsons Ltd. (Calgary, AB, Canada) for water temperature, conductivity, pH, redox potential, and Dissolved Oxygen (DO) using a YSI® Professional Plus Multiparameter instrument, and turbidity was measured using an Orbeco-Hellige® TB200™ Turbidimeter.

3.3.3. Passive sampling

Low-density polyethylene (PE) passive samplers were deployed in triplicate (n = 3) in the forebay and final deep pool of the KT wetland. The deeper cells were chosen to ensure samplers were deployed within the water column to measure dissolved contaminants in the water. The PE strips (12.70 cm x 15.24 cm, 25μm thickness, 0.5 g) were deployed in stainless steel mesh casings, and attached to an anchor-buoy system to allow for deployment at the centre of the deep cells, and to ensure the PE strips were submerged at approx. 0.3 – 0.5 m depths below the water surface. Three deployments of passive samplers occurred, beginning on 1) July 21st, 2017 (Final Deep Pool) and July 22nd, 2017 (Forebay) for a 37 day and 36 day deployment, respectively, 2) August 28th, 2017 (Forebay and Final Deep Pool) for a 31 day deployment, and 3) August 25th, 2018 (Forebay) and September 8th, 2018 (Final Deep Pool) for 14 day deployments each. Since water was fully recycled through the KT wetland in 2018, the deployments in the forebay and final deep pool were done consecutively, i.e. samplers in the forebay were deployed from days 0 – 14, and samplers in the final deep pool were deployed from days 14 – 28.

The PE samplers were prepared and analyzed by SGS Axys Analytical Services Ltd. (Sidney, BC, Canada). Samplers were stored and shipped in aluminum foil, sealed in a plastic bag, and shipped in a cooler with ice packs to maintain a temperature at < 4 deg-C. The method of analysis of PE sampler devices follows USEPA Methods 1625B and 8270C/D. Instrumental analysis was performed by low-resolution mass spectrometry (LRMS) using an RTX-5 capillary GC column, which operates at a unit mass resolution in the electron impacts (EI) ionization mode using multiple ion detection (MID), acquiring at least one characteristic ion for each target analyte and surrogate standard. Quantification of target analytes was performed using the isotope dilution method, and calculations were carried out using HP EnviroQuant and Prolab MS-Extended for targeting and quantification. Sample detection limits are available in the Supplementary Information.

The reported concentrations provided by the laboratory were issued as units of mass of chemical per gram of polyethylene passive sampler (i.e. C_{PE}, ng/g). The partitioning behaviour of each chemical between the OSPW and the PE sampler was estimated using the calibration equation for PAHs reported by Lohmann (2012):

$$\text{Log } K_{PE\text{-}W} = 1.22\ (\pm 0.046) \cdot \log K_{OW} - 1.22\ (\pm 0.24)\ (R^2 = 0.92;\ \text{SE } 0.27) \qquad \text{Eq. 3-1}$$

This relationship correlates the polyethylene-water partitioning coefficient ($K_{PE\text{-}W}$), with the octanol-water partition coefficient (K_{OW}) for each test chemical. The log K_{OW} for each PAH was obtained from EPISuite v4.11 (U.S. EPA, 2013).

Two field blanks per deployment consisting of clean polyethylene sheets were exposed to ambient air during sampler deployment and collection. Field blanks were wrapped in aluminum foil, sealed in a plastic freezer bag, and refrigerated at < 4 deg-C between use. The average concentration of PAHs in the field blanks ($C_{F.Blank,i}$) were subtracted from the concentrations of PAHs measured in the deployed PE samplers ($C_{PE,i}$) to account for background exposure, i.e. $C^*_{PE,i} = C_{PE,i} - C_{F.Blank,i}$ (Ghosh et al., 2014) Concentrations were assumed to be negligible (i.e. $C^*_{PE,i} = 0$) if the mean concentration of the analyte found in the field blanks exceeded the concentration of that analyte measured in the deployed passive samplers ($C_{F.Blank,i} > C_{PE,i}$).

Two performance reference compounds (PRCs) were impregnated into the polyethylene passive samplers during lab preparation: fluoranthene-d^{10}, and dibenzo(a,h)anthracene-d^{14}. These deuterated PRCs were used to evaluate the state of equilibrium between the water and PE by comparing day zero concentrations ($C_{PRC,0}$) to final concentrations ($C_{PRC,t}$) of the PRCs in the samplers after the deployment period (t, days). The mass transfer coefficients (k_e, d^{-1}) of the two PRCs were determined using:

$$k_e = \ln\left(\frac{C_{PRC,0}}{C_{PRC,t}}\right) \times \frac{1}{t} \qquad \text{Eq. 3-2}$$

To relate the depletion rate constant of the performance reference chemicals to the time to reach 95% equilibrium (i.e., $3/k_e$) between the water and the passive sampler for the target analytes, a linear relationship was developed between log k_e and log K_{OW} of the performance reference chemicals. This relationship was then used to determine $k_{e,i}$ from the log K_{OW} of each target chemical *i* (Burgess et al., 2015). This $k_{e,i}$ was then used to account for the lack of achieving equilibrium within the sampling duration by calculating the dissolved concentration (C_{WD}) of each target chemical *i* in water as:

$$C_{WD,i} = \frac{C^*_{PE,i}}{K_{PE-W,i} \times \left(1 - e^{-k_{e,i}t}\right)} \qquad \text{Eq. 3-3}$$

Standard errors (SE) of C_{WD} were derived through error propagation as:

$$SE_{C_{WD}} = \sqrt{\left(SE_{C^*_{PE,i}} \cdot \frac{\delta C_{WD}}{\delta C^*_{PE}}\right)^2 + \left(SE_{K_{PE-W}} \cdot \frac{\delta C_{WD}}{\delta K_{PE-W}}\right)^2 + \left(SE_{k_e} \cdot \frac{\delta C_{WD}}{\delta k_e}\right)^2} \qquad \text{Eq. 3-4}$$

where the SE of $C^*_{PE,i}$ was determined for each chemical from the measured concentrations of the target analytes in multiple passive samplers; the SE of K_{PE-W} was estimated by applying the delta method to the log-transformed linear regression equation (Eq. 3-1); the SE of $k_{e,i}$ was determined from measurements of PRC concentrations in the PE samplers.

3.3.4. Data analysis

Analytes were included in the data analysis if concentrations in the passive samplers exceeded the method detection limit (DL) in at least two of three replicates. Concentrations of PAHs in water below the DL were assigned a concentration equal to one-half of the chemical's DL (i.e. C_i = DL/2). This was applied to all final deep pool concentration measurements for 7-methylbenzo[a]pyrene in deployment one, one forebay concentration measurement for 2,6-dimethylnaphthalene in deployment two, and two final deep pool concentrations measurements for acenaphthene in deployment three. The great majority of measured concentrations exceeded the DL. For these three substances, a range of average concentrations is provided to reflect the lower estimate (i.e. assumes concentration is zero) and upper estimate (i.e. assumes concentration is equal to the DL). A two-sample t-test assuming unequal variances was performed in JMP®, Version 13.1.0 to detect statistical differences between mean dissolved aqueous concentrations measured in the forebay and final deep pool (α = 0.05). Unequal variances in concentration measurements in the forebay and final deep pool were detected with a two-sided F-test ($p < 0.001$).

3.3.5. Wetland treatment performance evaluation

Concentration-reduction

Changes in the concentration of the test chemicals in the water ($E_{C,i}$) were derived from the concentration of each test chemical *i* in the passive samplers deployed in the influent wastewater (forebay; $C_{PE,i}^{eq.in}$) and treated effluent (final deep pool; $C_{PE,i}^{eq.out}$) as:

$$E_{C,i} = \left(1 - \frac{C_{PE,i}^{eq.out}}{C_{PE,i}^{eq.in}}\right) * 100 \qquad \text{Eq. 3-5}$$

$E_{C,i}$ was estimated directly from the measured concentration of target analyte *i* in the passive sampler ($C_{PE,i}$) to reduce error associated with converting concentrations in passive samplers to those in water. To correct for the different deployment durations of the samplers in forebay and final deep pool, equilibrium concentrations in the PE samplers were estimated using measured $k_{e,i}$ values with:

$$C_{PE,i}^{eq.} = \frac{C_{PE,i}^{*}}{(1 - e^{-k_e t})} \quad \text{Eq. 3-6}$$

Mass removal

Mass removal of PAHs from the wetland was expressed in terms of a mass-loading removal efficiency ($E_{L,i}$) for each chemical *i*. $E_{L,i}$ was determined from the concentrations of freely dissolved analyte *i* in the influent ($C_{WD,i}^{*in}$) and effluent ($C_{WD,i}^{*out}$) water, and the corresponding volumetric flow rates (L/day) of water entering the forebay (Q_{in}) and leaving from the final deep pool (Q_{out}) of the KT wetland:

$$E_{L,i} = \left(1 - \frac{Q_{out} \cdot C_{WD,i}^{*out}}{Q_{in} \cdot C_{WD,i}^{*in}}\right) * 100 \quad \text{Eq. 3-7}$$

Q_{in} in the KT wetland was controlled and maintained at 432,000 L/day (5 L/s) for the duration of the study. Q_{out} was estimated from the water budget: $Q_{out} = Q_{in} + Q_P - Q_{ET}$, where Q_P is the precipitation rate (L/day) and Q_{ET} is the evapotranspiration rate (L/day) in the KT wetland. The mass removal efficiency $E_{L,i}$ expresses the removal of dissolved contaminant mass from OSPW. $E_{L,i}$ differs from $E_{C,i}$ in that it accounts for the effects of changes in the volume of water in the wetland due to precipitation and evapotranspiration on concentration of the target chemical *i* in water. However, it should be stressed that because passive samplers measure only the concentration of dissolved contaminants in the influent and effluent, $E_{L,i}$ may not account for all mass of PAHs removed from the wetland which includes both dissolved and undissolved (sorbed) PAHs.

Precipitation, temperature, and relative humidity data were obtained from historical records of the Fort McMurray, AB, Canada weather station available from Alberta Climate Information Services (2018). Total precipitation (P) was 56.0 mm, 38.9 mm, and 50.3 mm during each of the three deployment periods, respectively. Temperature and relative humidity were used to estimate daily evapotranspiration rates from the KT wetland using the Penman-Monteith equation. Evapotranspiration (ET) at the KT wetland was estimated to be 197 mm, 91.4 mm, and 52.9 mm during each of the three deployment periods, respectively. The volumetric rate of precipitation (Q_P) and evapotranspiration (Q_{ET}) were calculated using the total catchment area and surface

area of wetland cells, respectively (i.e. $Q_P = SA_{catchment} \cdot P$; $Q_{ET} = \Sigma(SA_{cells}) \cdot ET$). The total catchment area ($SA_{catchment}$ = 15,264 m^2) included everything within the external berms of the KT wetland. All precipitation within this area was assumed to enter the wetland as runoff. The total surface area of all wetland cells ($\Sigma(SA_{cells})$ = 7,894.6 m^2) was estimated at the operating water levels, i.e. 1.7 m for deep pools and 0.4 m for shallow cells.

Toxicity

The change in OSPW toxicity was estimated using the chemical activity approach (Lewis, 1907; Gobas et al., 2015; 2018). Chemical activity (*a*; unitless) is a thermodynamic quantity related to fugacity and chemical potential which for dilute solutions can be expressed as the ratio of the chemical's concentration (C; e.g. mol/m^3) to the chemical's solubility in the same media (S; e.g. mol/m^3), i.e. $a = C/S$. The application of chemical activity to assess toxicity for neutral hydrophobic organic chemicals has merit for two main reasons. First, when equilibrated, concentrations of chemicals in different media (e.g. the passive sampler, water and organisms in the water) exhibit similar chemical activities. Hence, when at equilibrium, contaminant concentrations in the passive samplers reveal the chemical activity of contaminants in the water and biota that reside in the wetland, or that may be exposed to the influent or effluent of the wetland. Unless the contaminants are biomagnified in the food-web, the concentration of the contaminants in the organisms exposed to the wetland water will at most approach the chemical activities in the water and the passive samplers. Biotransformation in the organisms can reduce the chemical activities of the parent compound below the chemical activity in the water. Secondly, studies have shown that a combined chemical activity of PAHs between 0.01 and 0.1 causes acute toxic effects through a mode of toxic action referred to as non-polar narcosis (Reichenberg and Mayer, 2006; Schmidt et al., 2013; Thomas et al., 2015). Hence, by converting concentrations of contaminants into chemical activities of contaminants, it is possible to assess whether acute toxic effects can be expected. This makes the chemical activity of PAHs in the water and passive samplers a useful metric for toxicity assessment of individual and mixtures of PAHs.

Chemical activity (a_i) of each of the detected PAHs in water entering and leaving the KT wetland was estimated from the concentration of PAHs in the polyethylene samplers ($C^*_{PE,i}$) and the solubility of each PAH in the polyethylene sheets (SPE,i) as

$a_{\mathrm{i}} = \mathrm{C}_{\mathrm{PE,i}}^{\mathrm{eq.}}/\mathrm{S}_{\mathrm{PE,i}}$. SPE,i was determined as KPE-W,i × Swater,i where Swater,i is the solubility of chemical i in water at 25 deg-C (reported in EPISuite v4.11 using WATERNT™ model; U.S. EPA, 2013). The summation of chemical activities for each individual PAH produces a total chemical activity of all analytes present in the OSPW influent ($\Sigma\, a_{PE,i}^{in}$) and effluent ($\Sigma\, a_{PE,i}^{out}$) of the KT wetland. By comparing the total chemical activities of PAH mixture in the water entering and leaving the KT wetland to the chemical activity threshold value for baseline toxicity (a_0 = 0.01), it is possible to assess whether the influent or effluent has the potential to be toxic to aquatic biota, and to what degree toxicity or toxicological risk has been reduced through wetland treatment. This approach can also be used for substances that exhibit a greater toxicity (or "excess toxicity") than the baseline toxicity as long as the degree of excess toxicity is known from empirical toxicity studies or other methods. For such substances, a_i should be compared to 0.01/γ. where γ is the excess toxicity defined as toxicity greater than baseline toxicity (i.e. γ > 1). For determining the chemical activities of the PAHs in the PE samplers, changes in temperature during the two deployments were ignored and it was assumed that the mean temperature is adequate for determining the chemical activity of the PAHs.

3.4. Results and Discussion

3.4.1. Water quality

Table 3-1 shows that Biochemical Oxygen Demand (BOD), Dissolved Inorganic Carbon (DIC), Dissolved Oxygen (DO), Dissolved Organic Carbon (DOC), pH, Total Dissolved Solids (TDS), Total Suspended Solids (TSS), turbidity, and water temperature of OSPW in the wetland were below the upper limits of the Alberta Environment (2008) water quality targets (WQTs).

DO in water remained constant throughout the wetland during deployment one ($DO_{forebay}$ = 4.57 mg/L; DO_{FDP} = 4.46 mg/L) and increased upon passage through the wetland during deployments two ($DO_{forebay}$ = 5.09 mg/L; DO_{FDP} = 6.39 mg/L) and three ($DO_{forebay}$ = 5.04 mg/L; DO_{FDP} = 9.99 mg/L). The DO concentrations indicate that reoxygenation of the water occurs as it passes over the internal berms between wetland cells.

Table 3-1: Biochemical Oxygen Demand (BOD_5), conductivity, Dissolved Inorganic Carbon (DIC), Dissolved Oxygen (DO), Dissolved Organic Carbon (DOC), pH, Total Dissolved Solids (TDS), Total Suspended Solids (TSS), turbidity, and temperature (T_{water}) of OSPW in the Kearl Treatment Wetland during each deployment period.

		Deployment 1 2017A		Deployment 2 2017B		Deployment 3 2018		
		13-Jul		17-Aug		26-Aug	19-Sep	
Parameter	units	Forebay	FDP	Forebay	FDP	Forebay	Forebay	WQT+
BOD_5	mg/L	< 2.0	< 2.0	< 2.0	< 2.0	---	2	2.4
Conductivity	µS/cm (±0.5%)	811	795	955	919	1700	1700	799
DIC	mg/L	74	75	74	75	46	52	
DO	mg/L (±0.2)	4.57	4.46	5.09	6.39	5.04	9.99[d]	1.44[m]
DOC	mg/L	18	18	18	18	20	20	63.1
pH	pH (±0.2)	7.92	7.77	7.97	7.49	7.40	8.24	6.0 – 10.8
TDS	mg/L	680	680	680	680	860	1200	
TSS	mg/L	< 1.0	< 1.0	< 1.0	< 1.0	12	1.6	82.2
Turbidity	NTU (±2%)	0.84	1.37	0.84	1.11	45	1.5	77
T_{water}	deg-C (SD)	20.7 (2.1)		20.6 (2.1)		10.7 (2.2)		25.3

+ Water Quality Target (peak target), [35]
< – below the reported detection limit
m – minimum value
d – data collected on 22-Sep-18
--- – parameter not analyzed
FDP – Final Deep Pool
(±) – Instrument accuracy

The average recorded water temperature in the KT wetland was 20.7 (SD 2.1) during deployment one, 20.6 (SD 2.1) during deployment two, and 10.7 (SD 2.2) during deployment three. In a study using a surface flow mesocosm wetland, temperature changes from 18.4 deg-C to 11.3 deg-C showed no significant effects on overall heterotrophic activity (Tao et al., 2007), possibly due to the diversity in microbial communities contributing to contaminant removal at different temperatures (Truu, Juhanson, & Truu, 2009). However, the effect on water temperature on heterotrophic activity in wetlands remains an area requiring further investigation.

Warmer air temperatures were recorded during deployment one ($T_{avg.}$ = 17.9 deg-C; SD 2.7) compared to deployments two ($T_{avg.}$ = 12.2 deg-C; SD 4.5) and three ($T_{avg.}$ = 5.8 deg-C; SD 4.3). Modelling work using a modified Penman-Monteith equation

demonstrated that even a 3 deg-C change in air temperature can induce a 14% change in potential evapotranspiration rates (Ramirez and Finnerty, 1996). Therefore, differences in air temperatures among the deployments are expected to have significant effects on evapotranspiration of water from the wetland. Estimated rates of evapotranspiration range between 2.5 to 9.8, 0.6 to 5.8, 1.0 to 3.1 mm/day and total evapotranspiration was 53.7, 24.9, and 14.4 m^3/day in deployments one, two, and three, respectively (Table B.4).

The conductivity of OSPW ranged from 795 to 811 μS/cm in deployment one, 919 and 955 μS/cm in deployment two and was 1700 μS/cm in deployment three and appeared to remain constant throughout the wetland in all 3 deployments. Water quality targets for conductivity (WQT = 799 μS/cm; Alberta Environment, 2008) were exceeded in all deployments. Elevated levels of conductivity are common in OSPW due to naturally occurring high levels of sodium, bicarbonate, chloride, and sulphate found in waters around the Alberta oil sands. Since conductivity showed no significant effects on three floating wetland species at values up to 3,000 μS/cm (Hadad et al., 2006), significant effects on treatment performance as a result of the measured conductivities are not expected in the KT wetland. However, at a conductivity of 4,000 μS/cm, which is much greater than that in the KT wetland, a 44.4 – 67.9% reduction in BOD_5 in a continuous flow constructed wetland system with cattails (*Typha angustifolia*) and Asian crabgrass (*Digitaria bicornis*) was observed (Klomjek and Nitisoravut 2005).

Total dissolved solids (TDS) ranged between 680 mg/L to 1200 mg/L (Table 3-1) and were lower than those typically observed in OSPW (i.e. 2,000 – 2,500 mg/L; Allen, 2008) and within the wide range of concentrations of dissolved solids in surface waters (i.e. 240 mg/L - 279,000 mg/L) of the Alberta oil sands region (Cowie et al., 2015). No WQT has been issued for TDS. Removal efficiencies of organic contaminants in treatment wetlands tend to decrease as salinity increases due to effects on plants, microorganisms, and substrates (Liang et al., 2017). However, an increase in salinity has also been shown to decrease PAH solubility and increase sediment-water partitioning (Means, 1995) which may improve PAH removal the from OSPW.

The pH of OSPW ranged between 7.77 and 7.92 in deployment one, 7.49 and 7.99 in deployment two, and 7.40 and 8.24 in deployment three. Alkaline pH levels ranging from 8.0 – 8.4 have been measured in OSPW from other facilities in the Alberta

oil sands region (Allen, 2008), and are common when alkaline reagents such as sodium hydroxide are added to the process water to improve hydrocarbon extraction efficiency.

TSS concentrations in the OSPW were below detection limits in deployments one and two in 2017. This was due to sedimentation in the overburden disposal pond before water was introduced into the KT wetland. During deployment three in 2018, water was introduced into the wetland during a single rapid pumping event (< 24 hours) at rates of 4.0 – 4.7 m^3/min which caused turbulence and resuspension of sediment in the source water pond. Since no sedimentation pond was used as a preliminary settling basin, OSPW entering the KT wetland in 2018 contained higher concentrations of TSS than in the 2017 deployments. Within the wetland, TSS reduced by 87% after 24 days of recycling demonstrating the capacity for particulate settling in the KT wetland.

3.4.2. Polycyclic aromatic hydrocarbons in influent

During deployments one and two, freely dissolved concentrations of PAHs in water were highest for chrysene (1.28 (SE 0.35) and 0.37 ng/L (SE 0.039)), fluoranthene (0.92 (SE 0.033) and 0.54 ng/L (SE 0.011)), phenanthrene (0.78 (SE 0.075) and 0.88 ng/L (SE 0.047)), and pyrene (5.41 (SE 0.12) and 3.52 ng/L (SE 0.066)), respectively (Figure 3-2 and Figure 3-3). During deployment three freely dissolved PAH concentrations entering the wetland were highest for acenaphthene (2.88 (SE 0.082) ng/L), fluorene (1.34 (SE 0.027) ng/L), phenanthrene (3.83 (SE 0.085) ng/L), pyrene (2.24 (SE 0.13) ng/L), and retene (2.03 (SE 1.4) ng/L) (Figure 3-4).

With the exception of pyrene in the influent of deployment one, concentrations of PAHs in the influent were below the criteria for the protection of aquatic life in Canada (i.e. CCME, 1999) and the water quality targets for the Muskeg River (i.e. Alberta Environment, 2008). Concentrations of PAHs in the influent were similar to concentrations measured by Environment and Climate Change Canada (ECCC) in the Athabasca, Peace, and Slave rivers (Environment and Climate Change Canada, 2015) (Figure B.1). The concentration of pyrene in the influent exceeded the Alberta Environment (2008) water quality target and points to the need to develop remediation strategies to reduce contaminant concentrations to levels that meet environmental quality guidelines and protect wildlife in or visiting the wetland.

3.4.3. Wetland treatment performance

Treatment in the KT wetland resulted in statistically significant reductions in dissolved aqueous concentration for 14 out of 15 PAHs during deployment one, 15 out of 20 PAHs in deployment two, and 19 out of 22 PAHs in deployment three (

Figure 3-2, Figure 3-3, and Figure 3-4). Freely dissolved concentrations of pyrene in OSPW reduced from 5.41 (SE 0.12) ng/L to 0.46 (SE 0.044) ng/L during deployment one, from 3.52 (SE 0.066) ng/L to 0.84 (SE 0.012) ng/L during deployment two, and from 2.24 (SE 0.13) ng/L to 0.58 (SE 0.0087) ng/L during deployment three. This corresponds to an $E_{C,i}$ for pyrene of 91, 76, and 75% and an $E_{L,i}$ for pyrene of 92, 76, and 74% for deployments 1 – 3, respectively. Values of $E_{C,i}$ and $E_{L,i}$ are similar because water inflows and outflows in the wetland were well balanced. Pyrene measured in deployment one reduced to concentrations that did not exceed Alberta Environment‘s (2008) water quality guideline for pyrene.

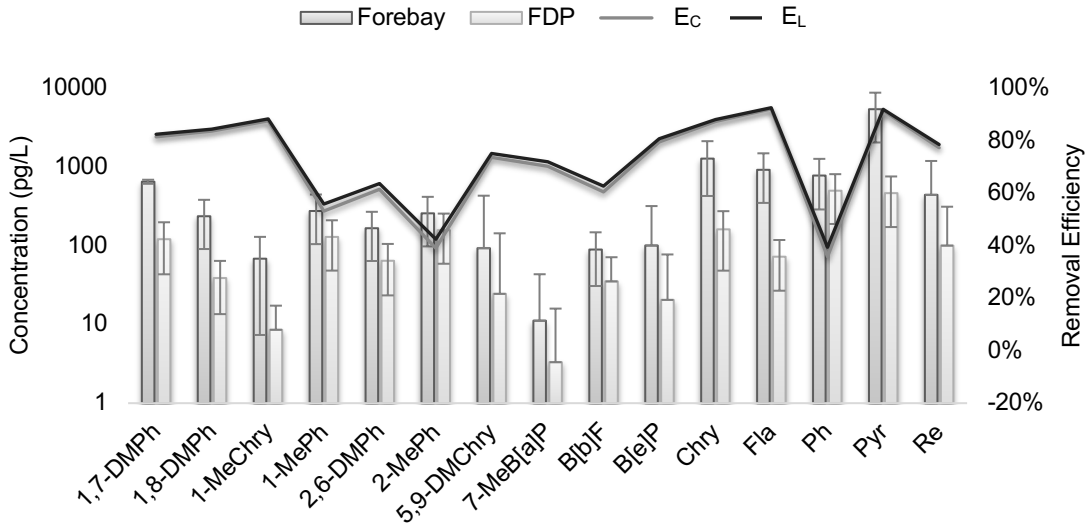

1,7-DMPh = 1,7-Dimethylphenanthrene; 1,8-DMPh = 1,8-Dimethylphenanthrene; 1-MeChry = 1-Methylchrysene; 1-MePh = 1-Methylphenanthrene; 2,6-DMPh = 2,6-Dimethylphenanthrene; 2-MePh = 2-Methylphenanthrene; 5,9-DMChry = 5,9-Dimethylchrysene; 7-MeB[a]P = 7-Methylbenzo[a]pyrene; B[b]F = Benzo[b]fluoranthene; B[e]P = Benzo[e]pyrene; Chry = Chrysene; Fla = Fluoranthene; Ph = Phenanthrene; Pyr = Pyrene; Re = Retene

Figure 3-2: Dissolved aqueous concentrations and removal efficiencies of PAHs in the Kearl Treatment Wetland during deployment one (2017A). Error bars represents standard error of the mean.

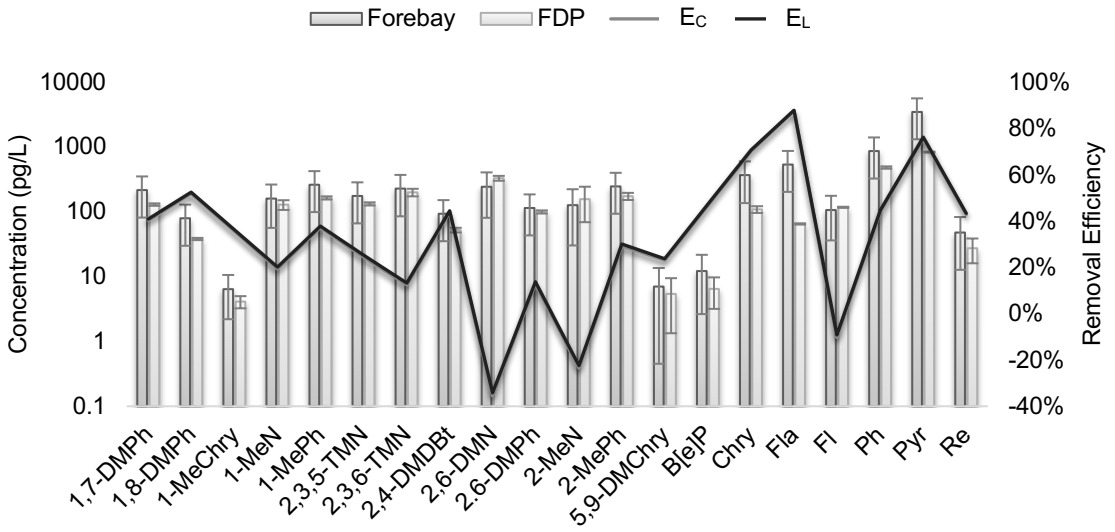

1,7-DMPh = 1,7-Dimethylphenanthrene; 1,8-DMPh = 1,8-Dimethylphenanthrene; 1-MeChry = 1-Methylchrysene; 1-MeN = 1-Methylnaphthalene; 1-MePh = 1-Methylphenanthrene; 2,3,5-TMN = 2,3,5-Trimethylnaphthalene; 2,3,6-TMN = 2,3,6-Trimethylnaphthalene; 2,4-DMDBt = 2,4-Dimethyldibenzothiophene; 2,6-DMN = 2,6-Dimethylnaphthalene; 2,6-DMPh = 2,6-Dimethylphenanthrene; 2-MeN = 2-Methylnaphthalene; 2-MePh = 2-Methylphenanthrene; 5,9-DMChry = 5,9-Dimethylchrysene; B[e]P = Benzo[e]pyrene; Chry = Chrysene; Fla = Fluoranthene; Fl = Fluorene; Ph = Phenanthrene; Pyr = Pyrene; Re = Retene

Figure 3-3: Dissolved aqueous concentrations and removal efficiencies of PAHs in the Kearl Treatment Wetland during deployment two (2017B). Error bars represents standard error of the mean.

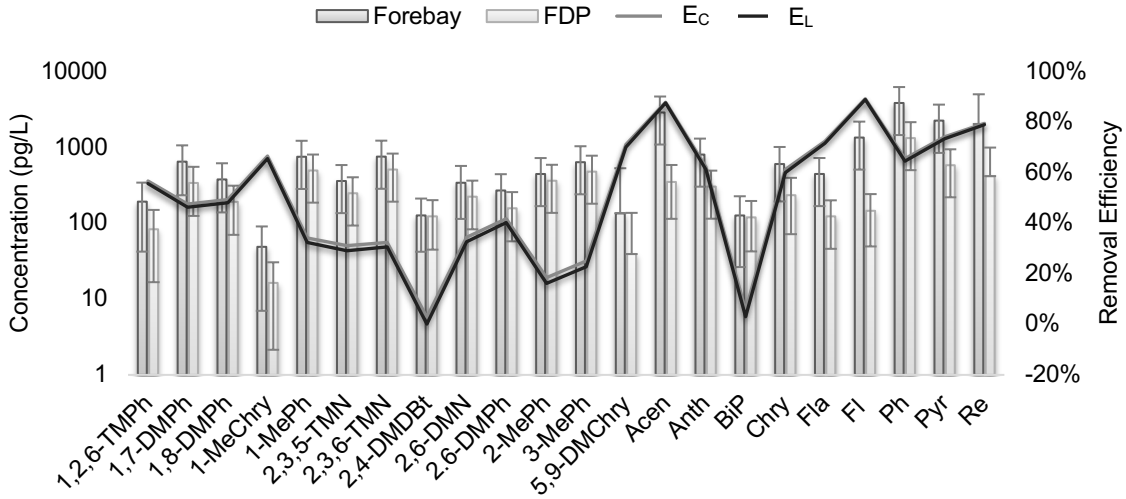

1,2,6-TMPh = 1,2,6-Trimethylphenanthrene; 1,7-DMPh = 1,7-Dimethylphenanthrene; 1,8-DMPh = 1,8-Dimethylphenanthrene; 1-MeChry = 1-Methylchrysene; 1-MePh = 1-Methylphenanthrene; 2,3,5-TMN = 2,3,5-Trimethylnaphthalene; 2,3,6-TMN = 2,3,6-Trimethylnaphthalene; 2,4-DMDBt = 2,4-Dimethyldibenzothiophene; 2,6-DMN = 2,6-Dimethylnaphthalene; 2,6-DMPh = 2,6-Dimethylphenanthrene; 2-MePh = 2-Methylphenanthrene; 3-MePh = 3-Methylphenanthrene; 5,9-DMChry = 5,9-Dimethylchrysene; Acen = Acenaphthene; Anth = Anthracene; BiP = Biphenyl; Chry = Chrysene; Fla = Fluoranthene; Fl = Fluorene; Ph = Phenanthrene; Pyr = Pyrene; Re = Retene

Figure 3-4: Dissolved aqueous concentrations and removal efficiencies of PAHs in the Kearl Treatment Wetland during deployment three (2018). Error bars represents standard error of the mean.

Both $E_{C,i}$ and $E_{L,i}$ for individual PAHs varied substantially, i.e. from 0% (no statistical differences in concentration through the wetland) for certain methylated PAHs to 92% (for $E_{C,i}$) and 93% (for $E_{L,i}$) for fluoranthene during the first deployment. The mean $E_{C,i}$ for all analytes was measured at 72 (SE 4.7)%, 32 (SE 6.9)%, and 50 (SE 5.4)% for each of the three deployments, respectively and closely matched the mean $E_{L,i}$ of 73 (SE 4.4)% for deployment one, 32 (SE 6.9)% for deployment two, and 49 (SE 5.5)% for deployment three. The overall reduction in concentration of all PAHs combined (ΣC_{PAH}) ranged between 56% (deployment two) to 82% (deployment one). The reduction in total mass of all measured PAHs was 83 (SE 37)%, 54 (SE 16)%, and 64 (SE 19)%, in deployments one, two, and three, respectively. The reductions in mass and concentrations of the PAHs, and hence $E_{L,i}$ and $E_{C,i}$ in each deployment were similar because the net change of water in the wetland was close to zero with only small gains and losses of water in the KT wetland. These reductions in concentrations align with those found in other studies. For example, Terzakis et al. (2008) measured an E_C for the combined sum of 16 PAHs of 56% after 24-hours in a pilot-scale surface flow wetland that treated highway runoff in southern Greece. In a pilot-scale vertical flow constructed wetland system in Munich, Germany (Machate et al., 1997), a 99% reduction in the concentration of phenanthrene in artificial wastewater (8 ug/L) was achieved over 14 days. The present study measured a reduction in the concentration of phenanthrene in OSPW influent (i.e. 0.77 ng/L and 3.83 ng/L) in the KT wetland of 36 to 66% over 14 days.

No statistically significant differences between the influent and effluent concentrations were observed for nine PAHs (i.e., benzo[b]fluoranthene (deployment one), 1-methylnaphthalene, 2-methylnaphthalene, 2,3,6-trimethylnaphthalene, 2,6-dimethylnaphthalene, fluorene (deployment two), and 2,4-dimethyldibenzothiophene, 2,6-dimethylnaphthalene, and biphenyl (deployment three). Five of these chemicals are naphthalene-based PAHs with low molecular weights, high aqueous solubilities, and relatively low log K_{OW} (3.86 – 4.73) when compared to the other test chemicals in this study. High water solubility and low log K_{OW} make substances less susceptible to mechanisms of chemical removal in rooting media, biofilm, and vegetation because a higher proportion of the chemical remains in the water phase (Cancelli et al., 2019). Further, their log K_{AW} (< 1.72) is moderately low, suggesting evapotranspiration will not contribute significantly to their removal from OSPW.

Pyrene, fluoranthene, and chrysene consistently exhibited the highest $E_{L,i}$ in all three deployments whereas 2-methylphenanthrene and 2,6-dimethylphenanthrene consistently showed the lowest $E_{L,i}$ among the three deployments (Figure 3-5). This further indicates that chemical make-up and properties play an important role in wetland treatment. The considerable variation in $E_{L,i}$ of individual PAHs shows that environmental conditions also play an important role in wetland treatment.

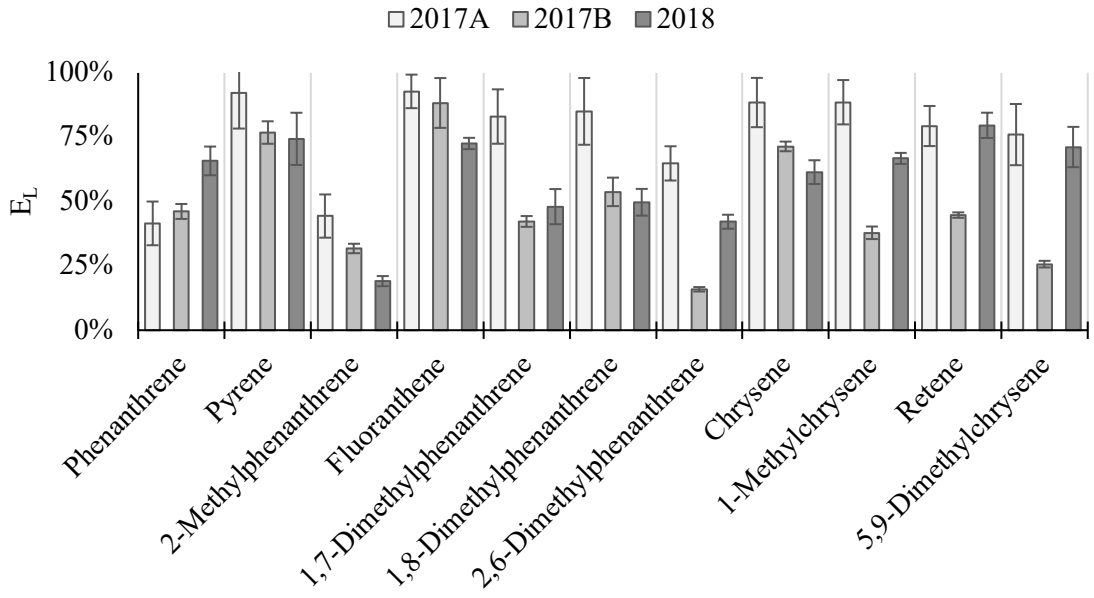

Figure 3-5: Mass-removal efficiency of PAHs measured in all three deployments of PES in the Kearl treatment wetland. Errors bars represent standard error of the mean.

Toxicity

Chemical activities of individual PAHs (Table B.5) were all far below the baseline toxicity value (a_0) of 0.01. This indicates that individual PAHs in both the influent and the effluent of the wetland were below concentrations that cause acute toxic effects in biota. Retene, chrysene, and pyrene exhibited the highest chemical activities in the KT wetland throughout the study. The highest chemical activities for all three of these chemicals were found in the forebay during deployment one, where $a_{retene} = 5.2 \times 10^{-5}$ (SE 1.7×10^{-6}), $a_{chrysene} = 4.8 \times 10^{-5}$ (SE 5.1×10^{-7}), and $a_{pyrene} = 4.0 \times 10^{-5}$ (SE 8.6×10^{-7}). These chemical activities reduced to 1.2×10^{-5} (SE 3.1×10^{-5}) for retene, 6.1×10^{-6} (SE 1.6×10^{-5}) for chrysene, and 3.4×10^{-6} (SE 4.0×10^{-5}) for pyrene in the final deep pool of the wetland, corresponding to reductions in chemical activity of 77, 87, and 91%

respectively. The largest reduction in chemical activity was observed for fluoranthene during deployment one, with a reduction of 92%.

The total chemical activity ($\sum a$) for all analytes included in the analysis was also below the baseline toxicity value (a_0) of 0.01 suggesting concentrations of PAHs in water are below the threshold for acute effects in aquatic biota due to non-polar narcosis. These results are in agreement with the toxicity experiments with the influent OSPW performed by Maxxam Analytics (unpublished data), which showed no acute toxicity of the OSPW to rainbow trout. $\sum a$ was highest during deployment three (n_3 = 22 PAHs) at 3.8×10^{-4} (SE 3.4×10^{-6}) and reduced to 1.0×10^{-4} (SE 6.4×10^{-5}) in the final deep pool (Figure 3-6). Despite more PAHs being detected during deployment two (i.e. 20 PAHs) than during deployment one (i.e. 15 PAHs), $\sum a$ was higher during deployment one largely because average concentrations of PAHs were greater in deployment one than in deployment two. Since the combined chemical activities of the PAHs investigated in this study were far below 0.01, both the influent and effluent are not expected to cause PAH related acute toxicity. Hence, a toxicity reduction as result of wetland treatment cannot be determined. However, if influents with higher concentrations of PAHs are used, treatment may cause a toxicity reduction that can be monitored using a passive sampling approach.

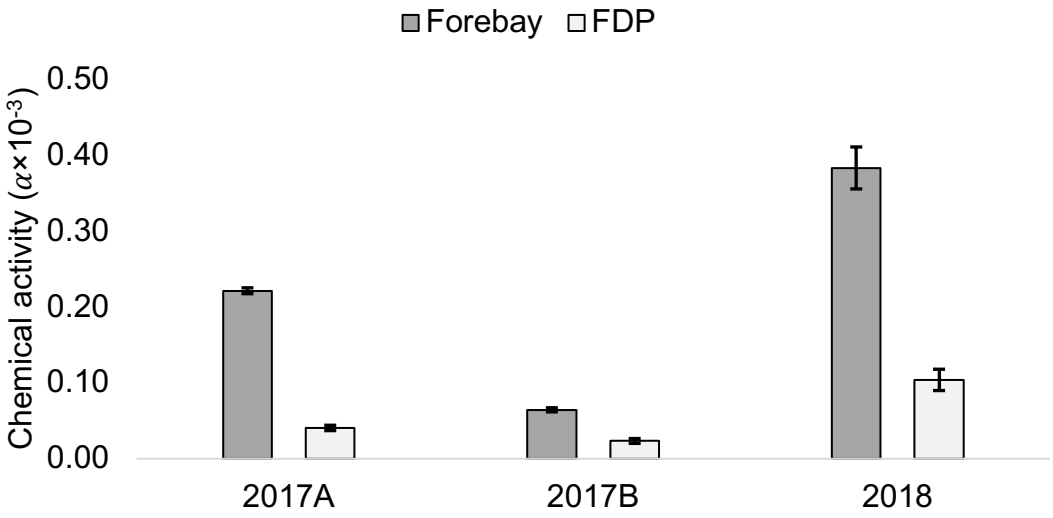

Figure 3-6: Total chemical activity of ∑PAHs in polyethylene samplers the forebay and final deep pool (FDP) during each deployment.

Some limitations of this approach are noteworthy. First, the total chemical activity estimate is limited to contaminants that were analyzed in this study. Other contaminants not quantified in this study are likely to add to the total chemical activity. These contaminants include ionisable and hydrophilic substances such as naphthenic acids which have been recognized as the primary source for aquatic toxicity in OSPW (Bartlett et al., 2017). This means that the total chemical activity of bulk OSPW is likely underestimated in this study. Redman et al. (2018) have addressed this problem by analyzing both neutral organics such as PAHs, and ionisable substances such as naphthenic acids using a non-specific passive sampling technique where the complex mixture of contaminants in OSPW is analyzed as a single contaminant using gas-chromatography with flame-ionization detection. Second, the passive sampling approach applies an equilibrium assumption to equate the chemical activity in the water to that in the organism. This assumption ignores potential biotransformation of PAHs that may occur within wetland biota and therefore chemical activity of PAHs and potential for toxicity in OSPW is likely overestimated. Third, the potential effects of temperature and conductivity were not incorporated into aqueous solubility estimates when calculating chemical activity. Despite these limitations of the passive sampling approach, it is encouraging that the results are consistent with the standard toxicity tests. Further testing of the passive sampling approach outlined in Redman et al. (2018) for toxicity testing may be useful in evaluating the effect of wetland treatment on toxicity in wildlife without undue reliance on animal testing.

3.5. Conclusions

This study shows that a surface treatment wetland is able to substantially reduce concentrations of PAHs in OSPW. Chemical characteristics as well as environmental and climatic conditions and wastewater characteristics appear to be important variables for treatment efficiency in the KT wetland. We aim to use the information of this study as well as a similar study on naphthenic acids to develop and test a model of the treatment efficiency of wetlands that can account for the effect of chemical properties, wetland design characteristics and environmental conditions.

3.6. References

Ahad, J. M. E., Jautzy, J. J., Cumming, B. F., Das, B., Laird, K. R., & Sanei, H. (2015). Sources of polycyclic aromatic hydrocarbons (PAHs) to northwestern Saskatchewan lakes east of the Athabasca oil sands. *Organic Geochemistry*, 80, 35– 45. http://doi.org/10.1016/j.orggeochem.2015.01.001

Alberta Climate Information Services (2018). Current and Historical Alberta Weather Station Data Viewer. Retrieved from the Alberta Agriculture and Forestry website: https://agriculture.alberta.ca/acis/alberta-weather-data-viewer.jsp

Alberta Environment (2008). Muskeg River Interim Management Framework for Water Quantity and Quality Summary Report. Alberta Environment Information Centre, Edmonton, Alberta, Canada. ISBN: 978-0-7785-7631-0.

Allen, E. (2008). Process water treatment in Canada's oil sands industry: I. Target pollutants and treatment objectives, *Journal of Environmental Engineering and Science*, *7*(2), 123–138. http://doi.org/10.1139/S07-038

Buchberger, S. G., and Shaw, G. B. (1995). An approach toward rational design of constructed wetlands for wastewater treatment. *Ecological Engineering*, *4*(4), 249–275. https://doi.org/10.1016/0925-8574(94)00053-8

Burgess, R. M., Lohmann, R., Schubauer-Berigan, J. P., Reitsma, P., Perron, M. M., Lefkovitz, L., & Cantwell, M. G. (2015). Application of passive sampling for measuring dissolved concentrations of organic contaminants in the water column at three marine superfund sites. *Environmental Toxicology and Chemistry*, *34*(8), 1720–1733. https://doi.org/10.1002/etc.2995

Cameron, K., Madramootoo, C., Crolla, A., & Kinsley, C. (2003). Pollutant removal from municipal sewage lagoon effluents with a free-surface wetland. *Water Research*, *37*, 2803–2812. http://doi.org/10.1016/S0043-1354(03)00135-0

Canadian Council of Ministers of the Environment (CCME) (1999). Canadian water quality guidelines for the protection of aquatic life: Introduction. In: Canadian environmental quality guidelines, 1999, Canadian Council of Ministers of the Environment, Winnipeg

Cancelli, A. M., Gobas, F. A. P. C., Qian, W., Kelly, B. C. (2019). Development and evaluation of a mechanistic model to assess the fate and removal efficiency of hydrophobic organic contaminants in horizontal subsurface flow treatment wetlands. *Water Research*, 151, 183-192. https://doi.org/10.1016/j.watres.2018.12.020

Cowie, B. R., James, B., & Mayer, B. (2015). Distribution of total dissolved solids in McMurray Formation water in the Athabasca oil sands region, Alberta, Canada: Implications for regional hydrogeology and resource development. *American Association of Petroleum Geologists Bulletin, 99*(1), 77-90. http://doi.org/10.1306/07081413202

Díaz, F. J., Chow, A. T., O'Geen, A. T., Dahlgren, R. A., & Wong, P.-K. (2009). Effect of constructed wetlands receiving agricultural return flows on disinfection by product precursors. *Water Research*, *43*, 2750–2760. http://doi.org/10.1016/j.watres.2009.03.027

Environment and Climate Change Canada (2015). *Passive Sampling, Oil Sands Region*. Retrieved from the Environment and Climate Change Canada website: http://donnees.ec.gc.ca/data/substances/monitor/surface-water-quality-oil-sands-region/passive-sampling-oil-sands-region/

Ghosh, U., Driscoll, K., Burgess, R. M., Jonker, M. T. O., Reible, D., Gobas, F., … Beegan, C. (2014). Passive Sampling Methods for Contaminated Sediments : Practical Guidance for Selection, Calibration, and Implementation. *Integrated Environmental Assessment and Management*, *10*(2), 210–223. https://doi.org/10.1002/ieam.1507

Gobas F.A.P.C., Otton S.V., Tupper-Ring L.F., Crawford M.A. (2015). Chemical activity calculator for calculating thermodynamic activities of non-polar organic chemicals from concentrations of chemicals in various environ- mental media. Environmental Toxicology Research Group at Simon Fraser University. [cited 2019 December 2]. Available from: http://www.sfu. ca/rem/toxicology/our-models/activity-calculator.html

Gobas, F. A. P. C., Mayer, P., Parkerton, T. F., Burgess, R. M., van de Meent, D., & Gouin, T. (2018). A chemical activity approach to exposure and risk assessment of chemicals: Focus articles are part of a regular series intended to sharpen understanding of current and emerging topics of interest to the scientific community. *Environmental Toxicology and Chemistry*, *37*(5), 1235–1251. https://doi.org/10.1002/etc.4091

Hadad, H. R., Maine, M. A., & Bonetto, C. A. (2006). Macrophyte growth in a pilot-scale constructed wetland for industrial wastewater treatment. *Chemosphere*, *63*(10), 1744–1753. http://doi.org/10.1016/j.chemosphere.2005.09.014

Hijosa-Valsero, M., Matamoros, V., Sidrach-Cardona, R., Martín-Villacorta, J., Bécares, E., & Bayona, J. M. (2010). Comprehensive assessment of the design configuration of constructed wetlands for the removal of pharmaceuticals and personal care products from urban wastewaters. *Water Research*, *44*(12), 3669–3678. http://doi.org/10.1016/j.watres.2010.04.022

Jasechko, S., Gibson, J. J., Jean Birks, S., & Yi, Y. (2012). Quantifying saline groundwater seepage to surface waters in the Athabasca oil sands region. *Applied Geochemistry*, *27*(10), 2068–2076. http://doi.org/10.1016/j.apgeochem.2012.06.007

JMP®, Version 13.1.0. SAS Institute Inc. Cary, NC, 1989-2016.

Kadlec, R., and Wallace, S. (2009). *Treatment Wetlands* (2nd ed.). Boca Raton, FL: Taylor & Francis Group.

Kelly, E. N., Short, J. W., Schindler, D. W., Hodson, P. V, Ma, M., Kwan, A. K., & Fortin, B. L. (2009). Oil sands development contributes polycyclic aromatic compounds to the Athabasca River and its tributaries. *Proceedings of the National Academy of Sciences*, *106*(52), 22346–22351. http://doi.org/10.1073/pnas.0912050106

Klomjek, P., and Nitisoravut, S. (2005). Constructed treatment wetland: A study of eight plant species under saline conditions. *Chemosphere*, *58*(5), 585–593. http://doi.org/10.1016/j.chemosphere.2004.08.073

Knight, R. L., Kadlec, R. H., & Ohlendorf, H. M. (1999). The use of treatment wetlands for petroleum industry effluents. *Environmental Science and Technology*, *33*(7), 973–980. https://doi.org/10.1021/es980740w

Knight, R. L., Payne, V. W. E. B., Borer, R. E., Clarke, R. A. D., & Pries, J. H. (2000). Constructed wetlands for livestock wastewater management. *Ecological Engineering* (Vol. 15). Retrieved from www.elsevier.com/locate/ecoleng

Lewis GN. (1907). Outlines of a new system of thermodynamic chemistry. *Proceedings of the American Academy of Arts and Sciences* 43:259–293.

Liang, Y., Zhu, H., Bañuelos, G., Yan, B., Zhou, Q., Yu, X., & Cheng, X. (2017). Constructed wetlands for saline wastewater treatment: A review. *Ecological Engineering*, *98*, 275–285. http://doi.org/10.1016/j.ecoleng.2016.11.005

Lohmann, R. (2012). Critical review of low-density polyethylene's partitioning and diffusion coefficients for trace organic contaminants and implications for its use as a passive sampler. *Environmental Science and Technology*, *46*(2), 606–618. http://doi.org/10.1021/es202702y

Machate, T., Noll, H., Behrens, H., & Kettrup, A. (1997). Degradation of phenanthrene and hydraulic characteristics in a constructed wetland. *Water Research*, *31*(3), 554–560. https://doi.org/10.1016/S0043-1354(96)00260-6

Matamoros, V., García, J., & Bayona, J. M. (2008). Organic micropollutant removal in a full-scale surface flow constructed wetland fed with secondary effluent. *Water Research*, *42*, 653–660. http://doi.org/10.1016/j.watres.2007.08.016

Means, J. C. (1995). Influence of salinity upon sediment-water partitioning of aromatic hydrocarbons. Marine Chemistry, 51(1), 3–16. https://doi.org/10.1016/0304-4203(95)00043-Q

Ramirez, J., and B. Finnerty. (1996). CO2 and Temperature Effects on Evapotranspiration and Irrigated Agriculture. *Journal of Irrigation and Drainage Engineering*. 22(3) https://doi.org/10.1061/(ASCE)0733-9437(1996)122:3(155)

Redman, A. D., Parkerton, T. F., Butler, J. D., Letinski, D. J., Frank, R. A., Hewitt, L. M., … Giesy, J. P. (2018). Application of the Target Lipid Model and Passive Samplers to Characterize the Toxicity of Bioavailable Organics in Oil Sands Process-Affected Water. *Environmental Science and Technology*, *52*(14), 8039–8049. https://doi.org/10.1021/acs.est.8b00614

Reichenberg F, Mayer P. (2006). Two complementary sides of bioavailability: Accessibility and chemical activity of organic contaminants in sediments and soils. *Environmental Toxicology and Chemistry* 25, 1239–1245.

Remillard, C. (2011). Picturing environmental risk: The Canadian oil sands and the National Geographic. *International Communication Gazette*, 73(1-2), 127–143. http://doi.org/10.1177/1748048510386745

Schmidt S.N., Holmstrup M., Smith K.E.C., Mayer P. (2013). Passive dosing of polycyclic aromatic hydrocarbon (PAH) mixtures to terrestrial spring- tails: Linking mixture toxicity to chemical activities, equilibrium lipid concentrations, and toxic units. *Environmental Science and Technology*, 47(13), 7020-7027.

Sundaravadivel, M., & Vigneswaran, S. (2001). Constructed wetlands for wastewater treatment. *Critical Reviews in Environmental Science and Technology*, *31*(4), 351–409. http://doi.org/10.1080/2001649108925

Tao, W., Hall, K. J., & Ramey, W. (2007). Effects of influent strength on microorganisms in surface flow mesocosm wetlands. *Water Research*, *41*(19), 4557–4565. https://doi.org/10.1016/j.watres.2007.06.031

Terzakis, S., Fountoulakis, M. S., Georgaki, I., Albantakis, D., Sabathianakis, I., Karathanasis, A. D., … Manios, T. (2008). Constructed wetlands treating highway runoff in the central Mediterranean region. *Chemosphere*, *72*(2), 141–149. http://doi.org/10.1016/j.chemosphere.2008.02.044

Thomas, P., Dawick, J., Lampi, M., Lemaire, P., Presow, S., Van Egmond, R., … Galay Burgos, M. (2015). Application of the Activity Framework for Assessing Aquatic Ecotoxicology Data for Organic Chemicals. *Environmental Science and Technology*, *49*(20), 12289–12296. https://doi.org/10.1021/acs.est.5b02873

Truu, M., Juhanson, J., & Truu, J. (2009). Microbial biomass, activity and community composition in constructed wetlands. *Science of the Total Environment*, *407*(13), 3958–3971. http://doi.org/10.1016/j.scitotenv.2008.11.036

U.S. EPA. (1999). *Free Water Surface Wetlands for Wastewater Treatment: A Technology Assessment.* Retrieved from http://water.epa.gov.

U.S. EPA. (2013). Estimation Programs Interface Suite™ for Microsoft® Windows, v4.11. United States Environmental Protection Agency, Washington, DC, USA.

Wallace, S., & Davis, B. (2009). Engineered Wetland Design and Applications for On-Site Bioremediation of PHC Groundwater and Wastewater. *SPE Projects Facilities & Construction*, *4*(March), 1–8. http://doi.org/10.2118/111515-PA

Wang, Q., & Kelly, B. C. (2017). Occurrence, distribution and bioaccumulation behaviour of hydrophobic organic contaminants in a large-scale constructed wetland in Singapore. *Chemosphere*, *183*, 257–265. http://doi.org/10.1016/j.chemosphere.2017.05.113

Chapter 4. Treatment of naphthenic acids in oil sands process-affected waters with a surface flow treatment wetland

4.1. Summary

This study explores the treatment efficiency of naphthenic acids in oil sands process-affected water in the Kearl Treatment Wetland. The study applies a passive sampling approach using Polar Organic Chemical Integrative Samplers (POCIS) and an aqueous sampling program to collect concentration measurements of O_2-naphthenic acids (O_2-NAs). The results show the wetland's capacity to remove naphthenic acids through wetland treatment varied substantially among NAs and between field study periods. The relative abundance of the NAs is greatest for C13 to C15 O_2-NAs with 3 or 4 double bond equivalents. The average concentration-reduction efficiency for each deployment was 13 (2018), 62 (2019A), and 3.2% (2019B), based on the POCIS analysis. The average mass-removal efficiency for each deployment was 7.5% (2018), 68.9% (2019A), and 11.7% (2019B). Removal efficiency for individual naphthenic acids is found to be proportional to the carbon number of the naphthenic acid congener, and inversely proportional to the number of double bond equivalents. This relationship occurs due the partitioning behavior of the NA congeners, characterized by log D (octanol-water distribution coefficient). Using biomimetic extraction techniques with solid phase microextraction fibres, bulk OSPW was correlated with *D. rerio* % deformity (4 d). The estimated toxic response of OSPW show a relative decrease in % deformity of 67.6% ($E_{Tox.}$) through approximately one full cycle of the OSPW, i.e. 14 days. This is an absolute reduction in % deformity of 39.3%.

4.2. Introduction

The oil sands in northeastern Alberta, Canada, contain one of the largest reserves of hydrocarbons in the world with proven reserves of roughly 165 billion barrels (Alberta Energy Regulator, 2019a). In 2018, the average production of raw bitumen in Alberta exceeded 3 million barrels per day (Alberta Energy Regulator, 2019b) from both in-situ (80%) and surface mining (20%) operations. Oil sands surface mining operations requires an average of 2.6 barrels of new water to produce one barrel of bitumen

through water-based gravity separation that strips bitumen from the recovered bitumen-rich subsurface sand (Alberta Energy Regulator, 2018). As a result, over 990 million m^3 of water has been consumed by the industry, and detained in tailings ponds that cover an area greater than 250 km^2. This oil sands process-affected water (OSPW) consists mainly of solids (sand and clay), water, dissolved organic and inorganic chemicals, and unrecovered bitumen (Holowenko et al., 2002; Alberta Energy Regulator, 2018).

Identified as a primary constituent of concern in OSPW are naphthenic acids (NAs) (Toor et al., 2013; Frank et al., 2008) which have shown to elicit toxicological effects on various aquatic plants (e.g. Armstrong et al., 2007), invertebrates (e.g. Bartlett et al., 2017), and fish (e.g. Marentette et al., 2015). NAs are naturally forming compounds commonly found in hydrocarbon deposits, including those found in the Alberta oil sands, that are released from bitumen during the extraction process and dissolve into OSPW (Holowenko et al., 2002). NAs consist of a complex mixture of saturated aliphatic, cyclic and alkyl-substituted carboxylic acids. Classical NAs are represented by the chemical formula: $C_nH_{2n+z}O_2$, where n is the carbon number and *z* is a negative even integer between 0 and -12 that indicates hydrogen deficiency as a result of the formation of rings or double bonds. *z* is often represented in terms of double bond equivalents (DBE) where DBE = 1 – *z*/2. In addition to classical NAs, OSPW contains polyoxygenated NAs (e.g. $C_nH_{2n+z}O_x$), aromatic NAs, and sulfur and nitrogen containing heteroatom NAs which are, along with the classical NAs, collectively referred to as naphthenic acid fraction compounds (NAFC; Hughes et al., 2017a). Concentrations of total NAs in OSPW have been measured up to 120 mg/L (Holowenko et al., 2002).

With an industry primed for continued development, there is a definite need to develop treatment technologies and management strategies for OSPW to permit the safe release of OSPW back into the environment and reduce the land area occupied by tailings ponds. Industry operators recognize this as a major priority and are focused on reducing freshwater demand, increase recycling of OSPW, and the protection of aquatic life (Martin, 2015). Due to their physicochemical properties and recalcitrant nature, NAs in OSPW offer a unique challenge for wastewater treatment technologies. The complex water chemistry and lack of fully developed, feasible, and effective treatment options have forced industry to remain with the status quo, i.e. to detain OSPW in large tailings ponds, which are susceptible to leaching and erosion and present adverse risk to wildlife (Jasechko et al., 2012). Several treatment technologies are currently being developed

that have shown potential in degrading NAs and remediating OSPW but require further research and development to become a feasible solution for this industry. Recently, studies have shown treatment wetlands to be a potential alternative technology to remove NAs from OSPW (Ajaero et al., 2018; Hendrikse et al., 2018).

Treatment wetlands are constructed ecosystems that are designed to harness natural biogeochemistry for remediation and reclamation services. Contaminant removal in treatment wetlands occurs via multiple biogeochemical mechanisms including microbial and plant-mediated biotransformation, chemical transformations, evapotranspiration, and sorption to sediments (Kadlec and Wallace, 2009). Biotransformation mechanisms and sorption to wetland substrate has been shown to be the primary mechanisms of removal for organic contaminants in wetlands (Cancelli et al., 2019; Ajaero et al., 2018). Aliphatic and alicyclic NAs have been shown to primarily undergo β-oxidation in aerobic microorganisms under oxidizing conditions (Quagraine et al., 2005; Han et al., 2008). Ajaero et al. (2018) demonstrates that, due to these oxidative processes for primary NA biotransformation of O_2-NAs to polyoxygenated NAs, the removal of O_2-NAs from OSPW best demonstrates the treatment of OSPW and removal of NAs.

Although NA degradation in wetland-like environments has been investigated (e.g. Ajaero et al., 2018), there are currently no studies investigating NA removal from OSPW in a large-scale surface flow treatment wetland within the Alberta oil sands region. The aim of this study is to investigate the capacity for a free water surface flow treatment wetland to remove O_2-NAs from OSPW with the purpose to inform industry operators about the feasibility of this wastewater treatment alternative. We focus on the Kearl Treatment Wetland (KT wetland) at the Kearl Oil Sands site managed by Imperial Oil Resources Limited.

To investigate wetland treatment for NAs in OSPW, we aim to quantify four metrics that illustrate treatment efficiency: concentration-reduction, mass-removal, first-order rate of removal, and toxicity-reduction. The concentration-reduction efficiency was measured with Polar Organic Chemical Integrated Sampler (POCIS) devices deployed at the inlet and outlet cells of the KT wetland. These passive sampling devices have been used to monitor environmental concentrations of a range of polar organic chemicals including, pesticides, pharmaceuticals, and naphthenic acids (Harman et al.,

2014; Ibrahim et al., 2013). The accumulation of contaminants in POCIS is a reflection of the time-weighted average bioavailable concentration present in the surrounding water. The difference in NA concentrations in the POCIS between the inlet and outlet represents the concentration-reduction efficiency of NAs in OSPW as it passes through the KT wetland. This efficiency metric reflects the capacity of a treatment system to meet specific water quality objectives, although no environmental guidelines yet exist for naphthenic acids. However, the degree to which concentrations change in the wetland can be sensitive to precipitation and evapotranspiration at the wetland (Cancelli et al., 2019). Mass-removal efficiency accounts for changes in water volume due to precipitation and evapotranspiration that may influence OSPW concentrations within the wetland. This metric for mass-removal represents the removal of contaminant mass from the OSPW within the wetland and therefore reflects the removal flux from the various biogeochemical mechanisms that are passively cleansing wetland water of pollutants. The rate at which contaminant concentrations and mass is removed from OSPW mainly follows first-order kinetics. The first-order rate constants for chemical removal from OSPW are provided to illustrate the kinetics of wetland biogeochemistry for the removal of O2-NAs.

Toxicity-reduction efficiency is a useful metric to assess the feasibility of treatment wetlands for the safe release of OSPW into the environment. This measure of treatment efficiency is useful to industry operators who wish to utilize this technology, and to regulators who require evidence that wetland treatment can reduce the risk to a receiving environment. We attempt to demonstrate the reduction in OSPW toxicity using a biomimetic extraction technique for aqueous samples of OSPW collected from the wetland. Biomimetic extraction (BE) was performed by solid phase microextraction to measure the bioavailability of acid-extractable organics in the OSPW, which has shown to correlate bulk OSPW with toxicity (Redman et al., 2018; Parkerton et al., 2017).

The objectives of this study are to 1) profile the suite of O2-NAs present in the OSPW entering the KT wetland, and 2) evaluate the treatment performance for O2-NAs in the KT wetland based on the reduction in concentration, removal of mass, first-order removal rates, and reduction in bulk OSPW toxicity.

4.3. Materials and Methods

4.3.1. The Kearl Treatment Wetland

The Kearl Treatment Wetland (KT wetland; Figure 4-1) is a free water surface-flow constructed wetland at the Kearl Oil Sands site (approx. 75 km NNE of Fort McMurray, AB, Canada; 57°26’00"N, 111° 8'31"W) managed by Imperial Oil Resources Limited. Data on the KT wetland configuration and design is described in Chapter 3.

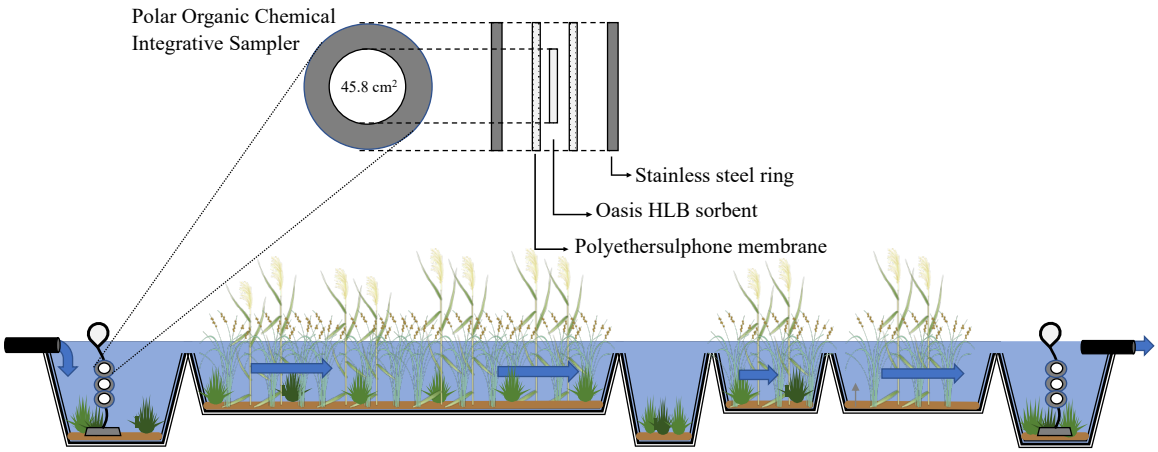

Figure 4-1: Kearl Treatment Wetland with Polar Organic Chemical Integrative Samplers.

OSPW was sourced from a drainage pond situated next to an external tailings area on the Kearl Oil Sands site. The OSPW was pumped to the wetland during a single event and fully recycled within the wetland at 5 L/s (430 m^3/day), resulting in a hydraulic retention time of approximately 14 days. The KT wetland operates at a total volume of water of approximately 6,100 m^3. The wetland consists of six cells in series (3 deep pools, 3 shallow areas) with a longitudinal slope of 0.014%. Water percolates over shallow interior berms that separate each adjacent cell. The deep pools (forebay, deep pool 1, and final deep pool) operate at a depth of 1.7 m, and are dominated by submerged vegetation, but contain a band of emergent vegetation (approx. 5% of area) along the perimeter of the cells where water depth is shallower. The shallow area cells (shallow areas 1, 2, and 3) are densely vegetated with a variety of different species dominated by common cattails (*Typha latifolia*) and water sedge (*Carex aquatilis*). The vegetation is rooted in peat soil from the displaced muskeg originally found on location. The rooting medium consists of 300 mm of non-compacted peat soil placed over 200

mm of compacted peat soil layered on a geosynthetic clay liner that was blanketed with a non-woven geotextile (Chapter 3, Figure 3-1).

4.3.2. Wetland sampling

Passive sampling

Polar Organic Chemical Integrative Samplers (POCIS) were purchased from Environmental Sampling Technologies (St. Joseph, MO, USA). The POCIS disks contained Oasis HLB (hydrophilic-lipophilic balance) sorbent between two polyethersulphone microporous (0.1 µm pore size) membranes. The membranes containing the sorbent are sealed with two stainless steel rings, leaving an exposed area of 45.8 cm^2 for passive diffusion of contaminants from the environmental medium to the Oasis HLB sorbent. The POCIS disks were installed into a stainless-steel holder, and attached to an anchor-buoy system to sample water flowing through the wetland at water depths of 0.3 – 0.5 m. Concentrations of NAs accumulated within the POCIS sorbent after deployment relate to their dissolved aqueous concentrations in the OSPW as shown in several studies describing the uptake kinetics of POCIS (e.g. Morin et al., 2012; Harman et al., 2014; Ibrahim et al., 2013).

Three rounds of deployments were performed at the KT wetland beginning on: 1) August 25, 2018 (2018 deployment), 2) May 12, 2019 (2019A deployment), and 3) June 9, 2019 (2019B deployment). POCIS disks were deployed for five days in triplicate (n = 3) in the forebay (days 0 – 5) and in the final deep pool (days 14 – 19) to correspond with the estimated 14-day hydraulic retention time in the KT wetland. In 2019, two consecutive deployments were performed: 2019A (deployment two), and 2019B (deployment three). The 5-day deployment periods were used to ensure uptake kinetics of the NAs were still within the linear kinetic regime. This may be required in future calculations to calibrate the POCIS concentrations to the freely dissolved concentration of the NAs in the OSPW of the wetland (e.g. Morin et al., 2012).

Prior to deployment, the POCIS disks were stored in a freezer at -20 deg-C. Following deployment, the POCIS disks were wrapped in aluminum foil, sealed in a plastic bag, and shipped to the laboratory in a cooler with wet ice to maintain temperatures < 4 deg-C. Duplicate clean POCIS disks were used as field blanks in the forebay and final deep pool per deployment (n = 4 per deployment). The field blanks

were exposed to ambient air during deployment and collection. Concentrations of NAs measured in the field blanks were subtracted from the concentrations of NAs measured in the deployed POCIS disks.

The POCIS were analyzed by SGS Axys Analytical Services Ltd. (Sidney, BC, Canada). POCIS samples were deconstructed and the sorbent material (Oasis HLB) recovered from within the disks was spiked with internal standard solution, transferred into a glass chromatography column and eluted with methanol. The analysis of extracts was performed by high performance liquid chromatography with triple quadrupole mass spectrometer detection (LC-MS/MS).

NAs concentrations below their detection limit (DL) in all six of the deployed POCIS from both the forebay (n = 3) and final deep pool (n = 3) were not included in further analysis. For the 60 NA congeners analyzed in each deployment ranging from $C_{12}H_{18}O_2$ to $C_{21}H_{40}O_2$, only 11, 9, and 10 of the NAs from deployment one, two, and three, respectively, were not included in further analysis. If at least one NA concentration measurement was above the DL in the POCIS analysis, the remaining sample concentrations for that NA were all assumed to equal one-half of the DL, i.e. DL/2. This assumption was made for a total of 15 out of 180 concentration measurements throughout all three deployments. The large majority of measured concentrations exceeded their DL. For the remaining substances, a range of concentrations is provided in Table C.3 that reflects the lower estimate (i.e. assumes concentration is zero) and upper estimate (i.e. assumes concentration is equal to the DL).

A statistical analysis of the POCIS concentration data was performed by a two-sample t-test in JMP®, Version 13.1.0. This method was used to test for statistical differences between concentrations of NAs in POCIS measured in the forebay and final deep pool ($\alpha = 0.05$).

Aqueous sampling

Samples were collected in 1L amber glass jars from the forebay of the KT wetland on days 0, 2, 3, 5, 7, 9, 12, 15, and 20 of the 2018 field study and days 0, 4, 5, 10, 14, and 19 of the 2019 field study, where day 0 is 1) August 25, 2018, and 2) May 12, 2019. Samples were shipped to SGS Axys Analytical Services Ltd. (Sidney, BC, Canada) for chemical analysis. Samples were homogenized, filtered using Ahlstrom 161

grade 1.1 µm filters, spiked with internal standard solution and cleaned up by solid phase extraction. The analysis of extracts is performed by high performance liquid chromatography with triple quadrupole mass spectrometer detection (LC-MS/MS).

The concentration of 13 NA congeners were below the MDL for all aqueous samples in both the 2018 and 2019 data and were not included in the assessment of total naphthenic acids. For 10 NA congeners in 2018 and 7 NA congeners in 2019, at least one concentration measurement was above the MDL, and the remaining non-detectable concentration measurements were assumed to equal one-half of the MDL, i.e. MDL/2.

During sample collection, water quality data were collected on-site for water temperature, conductivity, pH, oxidation-reduction potential, and Dissolved Oxygen (DO) using a YSI® Professional Plus Multiparameter instrument, and turbidity using an Orbeco-Hellige® TB200™ Turbidimeter by WorleyParsons Ltd. (Calgary, AB, Canada).

4.3.3. Wetland treatment performance evaluation

Concentration-reduction

Changes in the concentration (E_C) of the test chemicals passing through the wetland were derived from the concentration of the test chemical (i) in the POCIS sorbent ($C_{s,i}$) measured in the influent wastewater (forebay; $C_{s,i}^{in}$) and treated wetland effluent (final deep pool; $C_{s,i}^{out}$):

$$E_{C,i} = \left(1 - \frac{C_{s,i}^{out}}{C_{s,i}^{in}}\right) \quad \text{Eq. 4-1}$$

POCIS in the forebay and final deep pool measured time-weighted average concentrations of NAs in OSPW from days 0 – 5 and days 14 – 19, respectively, corresponding with the estimated hydraulic retention time of 14 days. The same deployment durations allow the difference in NA concentration in POCIS between the forebay and final deep pool to demonstrate the treatment after approximately one full cycle of OSPW through the wetland.

Changes to the water budget at the wetland can influence $E_{C,i}$. For example, precipitation may cause a net increase in water volume within the wetland causing dilution of contaminants, whereas evapotranspiration may result in a net decrease in water volume within the wetland causing contaminant concentrations to increase. This may be significant to wetland operators depending on treatment objectives. If the objective is to reduce contaminant concentration, then dilution may be helpful. However, dilution is not viewed as treatment within the wetland. To better characterize the capacity of treatment wetlands to remediate wastewater, we quantify the removal of contaminant mass from OSPW in the wetland in terms of the mass removal efficiency, $E_{M,i}$.

Mass-removal

The removal of contaminant mass ($E_{M,i}$) normalizes $E_{C,i}$ to the change in the volume of water in the wetland caused by external inputs such as precipitation and outputs such as evapotranspiration. $E_{M,i}$ represents the efficiency to remove mass of chemical *i* from OSPW as it passes through the KT wetland. $E_{M,i}$ is a good representation of the cumulative biogeochemical processes within the wetland that contribute to contaminant removal from OSPW, i.e. wetland treatment. $E_{M,i}$ was derived from POCIS measurements corrected to the initial volume of water in the wetland at t = 0, such that:

$$\mathrm{E_{M,i}} = \left(1 - \frac{V_{19} \cdot \mathrm{C_{s,i}^{out}}}{V_5 \cdot \mathrm{C_{s,i}^{in}}}\right) \qquad \text{Eq. 4-2}$$

where V_5 and V_{19} is the volume of water within the wetland on days 5 and 19, respectively, which correspond with POCIS collection and the end of the POCIS deployment periods. V_5 and V_{19} were estimated based on $V_t = V_0 + V_{P(t)} – V_{ET(t)}$ where $V_{P(t)}$ and $V_{ET(t)}$ are the volume of water added by precipitation (P) and by evapotranspiration (ET), from day 0 to t in the wetland. V_0 is approximately 6100 m^3 based on the recorded volume of water added to the wetland at the start of the study. Precipitation (mm) data was obtained from the Kearl Lake weather station. Evapotranspiration (mm) was estimated with the Penman-Monteith equation using temperature, relative humidity, and wind speed data obtained from the Kearl Lake weather station (calculations demonstrated in Appendix D). The volumetric contribution of precipitation (V_P) and evapotranspiration (V_{ET}) were calculated using the total

catchment area and surface area of wetland cells, respectively (i.e. $V_P = SA_{catchment} \cdot P$; $V_{ET} = \Sigma SA_{cells} \cdot ET$). Total catchment area ($SA_{catchment}$ = 15,264 m^2) includes all area within the external berms where precipitation runoff can enter the KT wetland. Total surface area of all wetland cells (ΣSA_{cells} = 7,895 m^2) represents the wetland surface area available for evapotranspiration and was estimated as the sum of surface areas at the operating water levels, i.e. 1.7 m for deep pools and 0.4 m for shallow cells.

Rate of chemical removal

Aqueous grab sample data were used to calculate the first-order removal rate (k) of O2-NAs within the wetland as the slope of a least squares best fit linear regression line for the natural log of the concentration of naphthenic acid i ($C_{eq.i}$) against time t, where

$$C_{eq,i}(t) = C_i(t) \cdot \left(\frac{V_t}{V_0}\right) \qquad \text{Eq. 4-3}$$

$C_{eq.i}$ represents the equivalent aqueous concentration of NA i in OSPW, corrected to the change in water volume (V) in the KT wetland. $C_i(t)$ is the concentration of the naphthenic acids i in the OSPW at time t.

Half-life values were calculated as $t_{1/2,i} = \ln 2/k_i$. NAs that are more readily removed from OSPW by passive wetland treatment will have a lower half-life, whereas more recalcitrant NAs will have a longer half-life. NAs were grouped by carbon number and DBE to determine removal characteristics for similar compounds.

OSPW toxicity-reduction using biomimetic extraction

Biomimetic extraction (BE) by solid-phase microextraction (SPME) of acid-extractable organics followed methods described in Redman et al. (2018). In summary, aqueous samples were collected from the KT wetland in triplicate 100 mL clear glass jars, shipped on ice at < 4 deg-C, and wrapped in aluminum foil upon arrival to minimize UV-degradation of organics in the samples. The samples were transferred to triplicate 20 mL vials and sealed with Teflon-faced septum caps. 50 uL of phosphoric acid was added to each vial to acidify the samples to a pH of ~2.5. Prior to injection into the OSPW samples, SPME fibres were thermally cleaned in the injection port at 280 deg-C until a

clean chromatographic baseline was observed for ≥ 3 minutes. The SPME fibres were then manually injected into the OSPW samples containing a Teflon stir bar rotating at 200-300 rpm for 100 minutes at room temperature (22 deg-C). The GC inlet and FID was set at 280 and 300 deg-C, respectively. Helium carrier gas was set at a constant flow rate of 17 mL/min. The GC oven temperature was programmed at 40 deg-C for 3 minutes, then up to 300 deg-C at 45 deg-C/min.

The FID response was normalized against 2,3-dimethylnaphthalene dissolved in dichloromethane injected at concentrations of 20, 100, and 200 ug/mL. The BE results were normalized to the polydimethylsiloxane (PDMS) volume (0.132 uL) on the SPME fibre and reported as mmol/L_{PDMS}. Measurements were manually blank corrected using SPME fibres exposed to deionized water containing 50 uL of phosphoric acid.

The accumulation of freely dissolved hydrocarbons on the SPME fibre acts as a surrogate measurement for the bioconcentration of contaminants in an organism, whereby lipids are the presumed site of toxic action. BE measurements do not compare directly to bioconcentration factors (Redman et al., 2018) because these measurements do not account for other biological processes such as biotransformation, and due to differences between lipid-water partitioning of contaminants for biota, and PDMS-water partition for SPME fibres. However, these BE measurements do correlate with toxic effects as demonstrated in Redman et al. (2018). The detection of these contaminants with BE-SPME measurements illustrates the bioavailability of total hydrocarbons in bulk OSPW samples and shows the potential for these hydrocarbons to accumulate in the lipids of organisms and cause toxicity.

The reduction in bulk OSPW toxicity ($E_{Tox.}$) represents the change in the toxic effect on biota from exposure to the raw (inflow) and treated (outflow) OSPW. This was determined from the BE measurements of OSPW samples collected from the wetland on day 0 and 14. It is estimated by:

$$E_{Tox.} = \left(1 - \frac{\text{Toxic Effect}_{t=14}}{\text{Toxic Effect}_{t=0}}\right) \quad \text{Eq. 4-4}$$

Using dose-response data from Redman et al. (2018), toxic effects on zebrafish (*D. rerio*) embryos and the water flea (*C. dubia*) can be estimated based on the BE

measurements of bulk OSPW samples from the KT wetland. To do this we fit a two-parameter Weibull cumulative distribution function using the Solver function in Microsoft Excel® using the sum of least squares with the dose-response data points obtained from Redman et al. (2018) for zebrafish (4d deformity) and embryos (4d survival), and water flea (7d reproduction; 4d survival).

4.4. Results and Discussion

4.4.1. Naphthenic acids in influent

Figure 4-2 illustrates the relative abundance of O2-species of naphthenic acids in OSPW entering the wetland organized by carbon number and double bond equivalents (DBE). The relative abundance of the NAs is greatest for C13 to C15 O_2-NAs where DBE = 3 or 4 (Z = -4 or -6), in all three deployments. This profile of O2-NAs is similar to those found in Leshuk et al. (2016) and Ajaero et al. (2018) for OSPW from different industry sources. Leshuk et al. (2016) detected NAs with carbon numbers ranging from 7 – 21, and DBE from approximately 2 to 7, with the highest relative abundance for C15 (DBE = 4) and C17 (DBE = 7) for two industry sources of OSPW. Ajaero et al. (2018) found the highest relative abundance for C13 (DBE = 3) but high relative abundance for C12 – C15 (DBE = 3 – 4), similar to the profile of O2-NAs found in this study.

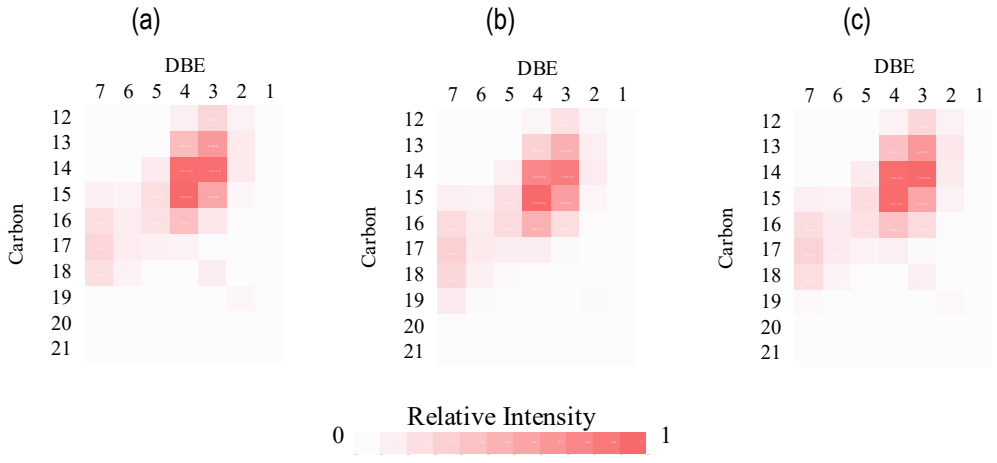

Figure 4-2: Relative distribution of NAs in OSPW entering the Kearl treatment wetland on day 0 of deployments one (a), two (b), and three (c).

Total O2-NA concentration in OSPW entering the wetland for each deployment was measured at 19.7, 20.7, and 13.3 mg/L, respectively. The concentration of individual O2-NAs in OSPW entering the wetland ranged from 208 ng/L ($C_{20}H_{34}O_2$) to 2.68 mg/L

($C_{15}H_{24}O_2$). Concentrations of O2-NA congeners in OSPW generally decreased with increasing carbon number. This is expected due to the lower aqueous solubility of these higher molecular weight compounds. The concentration of total NAs in OSPW has been shown to range from 20 to 120 mg/L with large variability between tailing ponds (Allen, 2008; Leshuk et al., 2016). The OSPW used in our study was collected from a drainage pond adjacent to an external tailings area which explains why lower concentrations were measured compared to other industry sources of OSPW.

4.4.2. Concentration-reduction efficiency (E_C)

The concentration-reduction efficiency (E_C) of each O2-NA measured in the Kearl treatment wetland is presented in Figure 4-3 for all three deployments. The average E_C for each deployment was 13, 62, and 3.2%, respectively based on the POCIS analysis. Using the fit model function in JMP®, both carbon number and DBE are found to be strong predictors of E_C in each deployment ($p < 0.01$; $\alpha = 0.05$; E_C (n, DBE)). This correlation of E_C with carbon number (n) and DBE give Figure 4-3 a distinctive pattern where, within each carbon group, E_C tends to increase with: i) increasing carbon number and, ii) decreasing DBE.

This relationship occurs due the partitioning behavior of the NA congeners, characterized by log D (octanol-water distribution coefficient). Log D represents the pH-dependent solubility of all species (ionized and non-ionized) of a substance between water and organic media. Within the wetland, NAs with higher log D can more rapidly partition from OSPW into adjacent media for sequestration such as in sediment, or transformation such as in biofilm and vegetation. Log D values were estimated from SPARC (Automated Reasoning in Chemistry; ARChem, Danielsville, GA, USA; Hilal et al., 2004) and compared to carbon number and DBE (log D values available in SI). As with E_C, as carbon number increases and DBE decreases, log D increases. This increase represents a chemical that is more hydrophobic, and that has an increasing tendency to partition out of the OSPW and into wetland media.

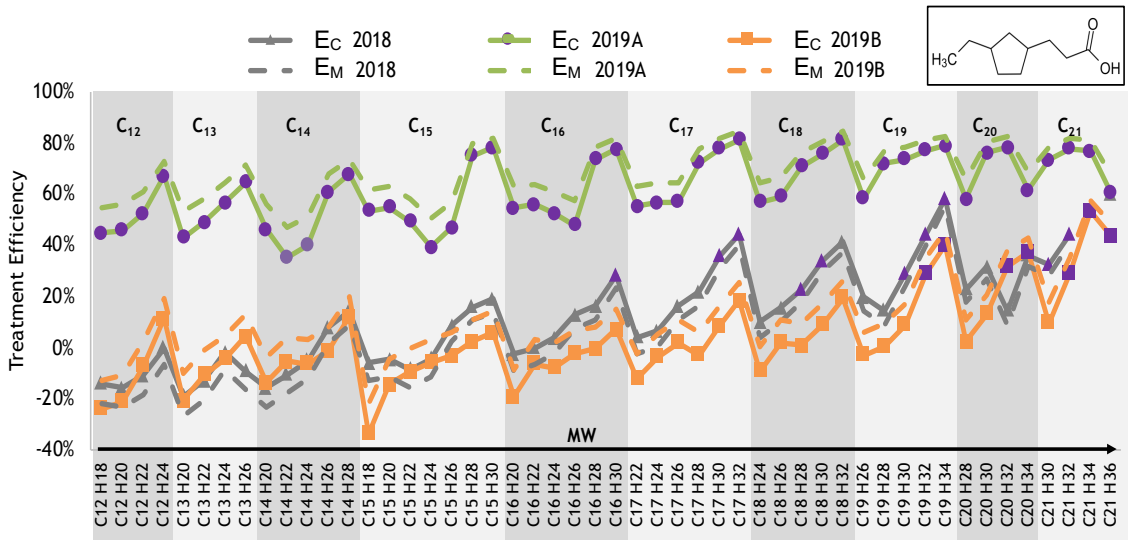

Figure 4-3: Concentration-reduction (E_C) and mass-removal (E_M) efficiency for O2 naphthenic acids measured with POCIS in the Kearl Treatment Wetland. Purple data points represent statistically significant E_C ($p<0.05$).

The highest average E_C over the three deployments in this study was found for the C21 group of NA congeners. Similar results were demonstrated in Ajaero et al. (2018) where O2-NAs with the same DBE showed greater E_C at higher carbon numbers, which they attributed to variability in transformation rates. However, Huang et al. (2015) show that NAs with n > 16 experience higher resistance to biodegradation, and Han et al. (2008) find that carbon number had little effect on the rate of biodegradation suggesting that sorption to organic media is the primary mechanism of removal from wastewater for larger O2-NA congeners with higher log D.

Within each carbon group, the highest E_C generally occurs with the lower DBE congener. DBE represents the level of unsaturation of the O2-NA molecule and indicates the number of H_2 molecules that are needed to convert all molecular bonds to single bonds, and all rings to acyclic structures. Therefore, the greater the DBE, the greater the number of total pi bonds and cyclic structures within the molecule. For O2-NAs, this means greater polarity for the molecule and hence greater aqueous solubility and lower log D. The resulting decrease in log D limits partitioning from water into wetland media making them less susceptible to biogeochemical removal within the wetland. In this study, an increase in DBE within a single carbon group lowers E_C by an average of 5%. Several other studies have shown that biotransformation occurs with lower ring structures (Biryukova et al., 2007; Han et al., 2008; Huang et al., 2013; McKenzie et al.,

2014), whereas more recalcitrant behavior occurs with higher ring structures where DBE $\geq$ 4 (Han et al., 2009; Wang et al., 2013a; Wang et al., 2013b).

In the 2018 deployment, 11 NAs (n = 49) demonstrated a statistically significant ($p < 0.05$; $\alpha = 0.05$) reduction in POCIS concentration between the forebay and final deep pool. The 2019A and 2019B deployments showed a statistically significant reduction in POCIS concentration for 49 NAs (n = 51), and 8 NAs (n = 50; $p < 0.05$; $\alpha = 0.05$), respectively. Differences between forebay and final deep pool POCIS concentrations were primarily observed at higher carbon numbers with lower DBE. The highest reductions were for C21 (DBE = 4), C18 (DBE = 3), and C21 (DBE = 5) for deployments one, two, and three, respectively, with an E_C of 60, 81, and 54%. There were no cases where NAs showed a statistically significant increase in concentration (i.e. negative E_C) through the wetland. These results demonstrate that more recalcitrant NAs (i.e. DBE $\geq$ 4) can be removed from OSPW via wetland treatment supporting continued research in the design and application of treatment wetlands for industrial wastewater. Several lower molecular weight NAs in 2018 and 2019B deployments suggest an E_C of 0, i.e. no statistically significant change in concentration through the wetland. These lower E_C measurements may be a result of the formation of lower molecular weight O2-NAs from bioconversion of higher molecular weight NAs (Quesnel et al., 2011; Islam et al., 2016; Xue et al., 2016). NAs where DBE = 1 are possibly fatty acids produced from biological sources such as plants and microbes (Sun et al., 2017). This would mean that our E_C measurements for lower molecular weight NAs are under-estimated because the final effluent concentration measurements would reflect the residual NA concentrations in the treated OSPW plus the NAs formed in the wetland during operation. E_C would therefore not reflect the actual reduction in concentration for NAs present in the OSPW.

This study is the first to investigate the removal of O2-NAs in a full-scale constructed wetland within the Alberta oil sands region. Our results demonstrate significant removal for a variety of O2-NAs present in OSPW. Other studies have demonstrated the removal of naphthenic acids from small-scale wetland-like environments. For example, Toor et al. (2013) used bench-scale microcosms with a 40-day HRT to demonstrate a decrease in NA concentration of 40% and observe a complete removal of acute (96-hr) mortality for rainbow trout. Ajaero et al. (2018) demonstrated removal of 57-80% for NAs ranging from C11 to C19 in non-aerated

horizontal subsurface flow mesocosms after 27 days of treatment. McQueen et al. (2017) designed a hybrid pilot-scale treatment wetland system with free water surface wetland cells and a solar photocatalytic reactor. The treatment wetland cells showed no significant reduction in NA concentrations, but the photocatalytic reactor provided reductions between 47 – 93 %. Their results suggest hybridization or engineering of treatment wetlands may be a useful method to optimize the removal of more recalcitrant naphthenic acids. Some designs include aeration and ozonation (Wang et al., 2013b), bioaugmentation with bacteria, biostimulation with nutrients and cofactors for microbial degradation, and the addition of materials such as clays to promote flocculation of contaminants with bacteria (Quagraine et al., 2005).

4.4.3. Mass-removal efficiency (E_M)

Mass-removal efficiency (E_M) shown in Figure 4-3 represents the degree to which contaminant mass has been removed from the OSPW between the forebay and final deep pool. The average E_M for each deployment was 7.5% (2018), 68.9% (2019A), and 11.7% (2019B) for NAs in the POCIS samples.

E_M accounts for changes to the water budget by normalizing E_C to the initial volume of water in the wetland on day zero. Dilution of NAs occur in the wetland from precipitation which increases E_C. Conversely, water loss by evapotranspiration will decrease E_C (Cancelli et al., 2019). Figure 4-4 illustrates the net change in water volume within the wetland during each of these deployment periods. The degree to which the change in water volume from precipitation and evapotranspiration affect E_C is examined by comparing E_C with E_M.

E_M is less than E_C for all naphthenic acids in 2018, and E_M is greater than E_C for all naphthenic acids in 2019A and 2019B deployments. In 2018, there was a net gain (ΔV) of 429 m^3 in water volume within the wetland due to high precipitation (771 m^3) coupled with relatively little evapotranspiration (342 m^3). The chemical dilution in the OSPW flowing through the wetland results in lower final effluent concentrations by a factor of V_t/V_0. Since V_t/V_0 is greater than 1, E_C is greater than E_M. In the 2018 deployment, the average effect of the water budget on E_C is 5.7 (SD 1.3)% meaning that, on average, E_C is 5.7% higher than E_M during this deployment.

The warmer, drier conditions in 2019 resulted in a net water loss (ΔV) of 1,232 m^3 and 822 m^3 from the wetland during the 2019A and B deployments, respectively. Under these environmental conditions effluent concentrations of NAs are concentrated, and E_C is reduced. In the 2019 deployments, the average effect of the water budget on E_C is -6.9 (SD 2.3)% and -8.4 (SD 1.5)% for 2019A and B, respectively. These negative E_C values indicate that, on average, E_C is lower than E_L.

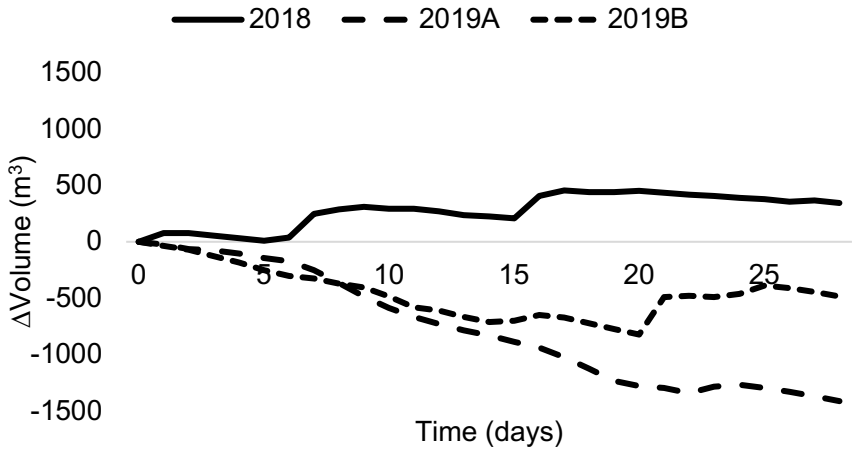

Figure 4-4: The water balance at the Kearl Treatment Wetland during each of the three deployment periods. $\Delta V = V_P - V_{ET}$ where V_P = volume of water added by precipitation (m^3) and V_{ET} = volume of water removed by evapotranspiration (m^3).

E_M provides a good representation of OSPW treatment caused by endogenous biogeochemical mechanisms within the wetland acting to remove contaminants from wastewater. Figure 4-3 illustrates differences in E_M between deployments. With flow rate and wetland design consistent, these differences can be mainly attributed to variability in OSPW chemistry and environmental conditions and their effects on wetland biogeochemistry.

Figure 4-5 provides field measurements of water quality criteria during each deployment. A statistical analysis of these water quality criteria shows that the turbidity of OSPW is significantly correlated ($p < 0.05$; $\alpha = 0.05$) with the concentration of naphthenic acids in OSPW. Higher turbidity is accompanied with higher NA concentration suggesting that a substantial fraction of NAs in water is particulate bound and a main mechanism of removal for NAs is through sorption to suspended particulates and settling. This is especially true for higher molecular weight NAs due to their

physicochemical properties, namely their octanol-water distribution coefficient (log D). The low turbidity in the OSPW at the start of the 2019B deployment indicates that sorption and settling was not likely to substantially contribute to NA removal and explains why treatment efficiencies during this deployment period are low compared to 2018 and 2019A where turbidity was much greater. Differences in E_M despite similar turbidity in the 2018 and 2019A deployments indicate that contributions from other biogeochemical mechanisms are also important for chemical removal.

Naphthenic acids are weak acids with pKa-values around 3.3 for O2 species (Huang et al., 2017). Under more alkaline conditions, a greater proportion of ionized acids compared to non-ionized acids will exist in the water. The ionized species have higher aqueous solubilities and lower log D than their non-ionized counterparts suggesting a greater fraction of the NA will remain in the water, less will partition into adjacent media, and removal efficiency will decrease. In addition, a decrease in log D would suggest a decrease in chemical partitioning from water to lipids, the presumed site of toxic action for these contaminants. Therefore, the toxic effects of NAs are expected to decrease under more alkaline conditions. In this study, pH ranges from 6.8 to 8.0. However, differences between deployments are small so despite the acidic nature of these contaminants, it is not a significant factor to explain the differences in treatment efficiency between deployments. Similarly, conductivity and DO are relatively high throughout the study, and only small differences are observed between deployments. Conductivity of OSPW is naturally high due to the presence of dissolved solids found in natural waters around the Alberta oil sands region (Allen, 2008; Jasechko et al, 2012). Oxygen levels within the OSPW remain high because of the interior berms within the wetland that work to reaerate the OSPW as it percolates into subsequent wetland cells. Figure 4-5 illustrates that pH, conductivity, and DO are similar between deployments, suggesting that, while these criteria may be important for NA removal from OSPW, they do not explain differences in E_M between deployments.

Based on the water quality monitoring data presented in Figure 4-5, differences in treatment efficiency may be attributed to differences in temperature and oxidation-reduction potential. Water temperature has effects on reaction rates where colder temperatures generally slow biochemical reaction kinetics and reduce biological activity responsible for the biodegradation of NAs. Lower water temperatures are shown for the 2018 deployment which occurred in August through September. At the northern latitude

of the KT wetland, seasonal changes during these months correspond with relatively low temperatures and caused seasonal suppression of phytogenic removal mechanisms such as evapotranspiration or plant-mediated biotransformation of contaminants. Warmer temperatures in the 2019A deployment are accompanied by higher treatment efficiencies suggesting that temperature is an important environmental parameter for wastewater treatment. Lower treatment efficiencies observed in 2019B compared to 2019A, despite experiencing similar temperatures, can be explained from the lower turbidity and sorption of NAs during the 2019B deployment.

Oxidation-reduction potential (ORP) describes the oxidative or reductive state of the OSPW within the wetland. More positive ORP describes a system that has a high capacity to oxidize substances in the wastewater. During the 2019 deployments, ORP in the wetland water remains positive suggesting transformation and degradation of O2-NAs occurs through β-oxidation in aerobic microorganisms (Ajaero et al., 2018). This aerobic environment is maintained throughout all deployments as demonstrated with high DO concentrations shown in Figure 4-5. In 2018, however, treatment efficiency may be affected by the negative ORP observed after day 10. In this reductive state, the biotransformation rate of NAs is limited, and treatment efficiency is reduced. ORP is known to fluctuate diurnally due to nightly oxygen consumption by vegetation (Nikolausz et al., 2008). These natural fluctuations explain the coexistence of aerobic and anaerobic microbes in wetlands (Küsel et al., 1999; Nikolausz et al., 2005). The diversity of the microbial community means that even when ORP is negative, biodegradation still occurs through anaerobic pathways. It is important to note that the actual effects of ORP are difficult to interpret since DO concentrations remain high even when ORP is negative.

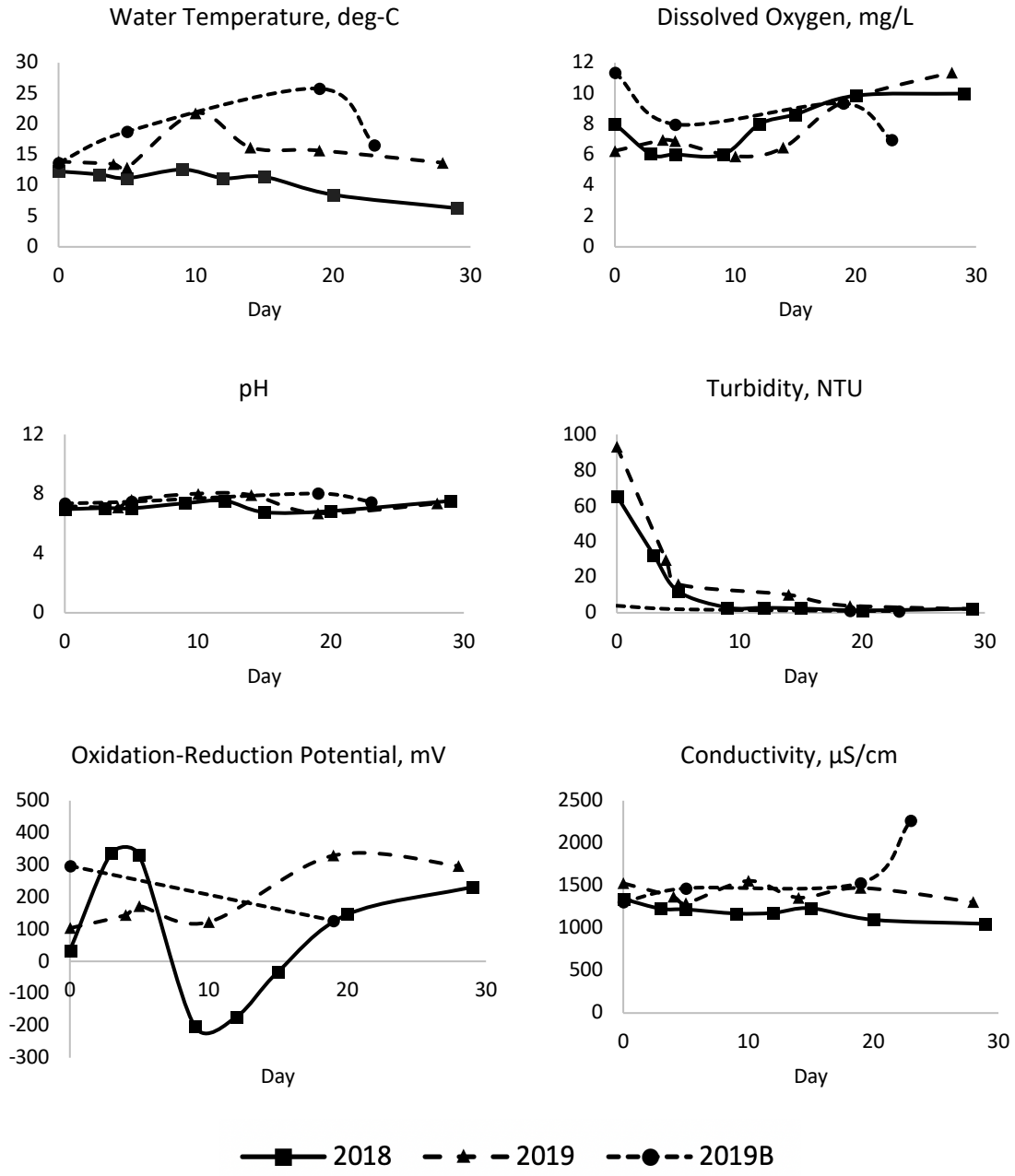

Figure 4-5: Water temperature, dissolved oxygen, pH, turbidity, oxidation-reduction potential, and conductivity of OSPW measured in the Kearl Treatment Wetland during the three deployment periods (2018, 2019A, and 2019B).

4.4.4. First-order removal rate

Figure 4-6 provides average half-life estimates ($t_{1/2}$) for NAs in the 2018 and 2019 wetland study periods, grouped by carbon number and DBE. $t_{1/2}$ is proportional to carbon

number in 2018 ($p < 0.01$; $\alpha = 0.05$) but no correlation is found in 2019 ($p > 0.05$; $\alpha = 0.05$) for carbon number or DBE.

The half-life of NAs measured in the Kearl Treatment wetland ranges from 11 – 186 days in 2018 and 9 – 76 days in 2019. The differences in $t_{1/2}$ between the two deployments suggest that environmental conditions impact removal kinetics from the wetland. The 2018 deployment occurred in August through September when seasonal changes begin to take effect in the Alberta oil sands region. These seasonal effects are accompanied by natural perennial changes in the biogeochemistry of wetlands, including the dynamics of plant senescence. Through senescence, certain plants have been shown to lose 2.1 mg of fatty acids per leaf each day, corresponding to a decrease in fatty acids of more than 80% within the leaf tissue (Yang and Ohlrogge, 2009). These fatty acid chains (DBE = 1) produced by biological sources often resemble low molecular weight naphthenic acids (Sun et al., 2017). Therefore, it is possible that the longer $t_{1/2}$ measured for lower carbon numbers in 2018 was a result of additional NAs entering the OSPW in the wetland during seasonal senescence of wetland vegetation.

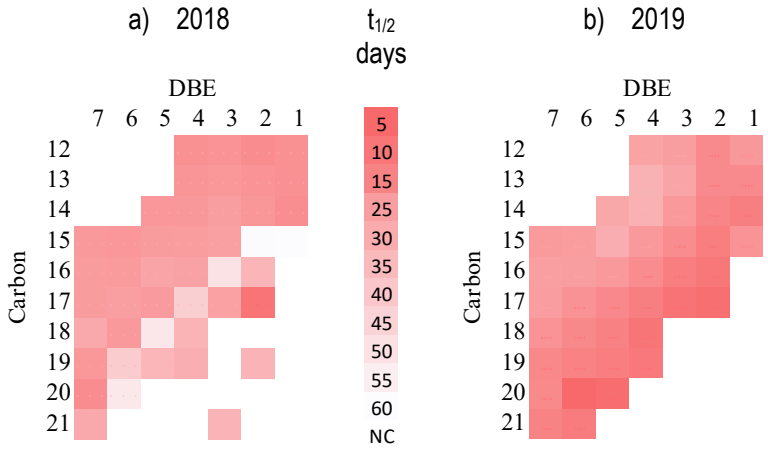

Figure 4-6: Observed half-life (days) for naphthenic acids present in OSPW passing through the Kearl Treatment Wetland in a) 2018 and b) 2019 field studies. NC – not calculated.

Ajaero et al. (2018) show $t_{1/2}$ of O2-NAs to decrease with increasing carbon number, and little effect of DBE on overall rates of removal in a wetland mesocosms. The longer $t_{1/2}$ measured in this study suggest slower removal kinetics may occur in a full-scale treatment wetland compared to small-scale mesocosms. In tailings ponds, $t_{1/2}$ of NAs has been measured on the order of 12.9 to 13.6 years, demonstrating slow biodegradation kinetics compared to those in the KT wetland (Han et al., 2009). Under

conditions with aerobic biodegradation these $t_{1/2}$ estimates were found to decrease to 44 – 240 days for industry OSPW containing a mixture of NAs, and even shorter for commercial NAs (Han et al., 2008; Mahdavi et al., 2015). Ozonation of OSPW has been shown to further increase rates of biodegradation of NAs and shorten $t_{1/2}$ from 83 days in untreated OSPW to 55 days in ozonated OSPW (Wang et al., 2013b). This enforces the concept that the treatment efficiency of NAs in wetlands is sensitive to DO and oxidation potential.

4.4.5. Toxicity-reduction efficiency ($E_{Tox.}$)

Figure 4-7 provides the model estimated *D. rerio* % deformity (4 d) based on the BE concentration measurements of OSPW collected from the wetland. The results show a relative decrease in % deformity of 67.6% ($E_{Tox.}$) through approximately one full cycle of the OSPW, i.e. 14 days. This is an absolute reduction in % deformity of 39.3%. Chemical analysis of the OSPW samples indicate a reduction in total naphthenic acid concentration (i.e. ΣC_{NA}) over the same 14-day period of 35.4% from 20.6 to 13.3 mg/L. The reduction in toxicity is promising and demonstrates the capacity for treatment wetlands as a realistic treatment option for OSPW.

Figure 4-7 shows the reduction of total naphthenic acid concentrations in OSPW from wetland treatment, as well as the estimated *D. rerio* (4d deformity) toxic effect used to calculate $E_{Tox.}$. Total naphthenic acids were found to decrease at a rate (k) of 0.015 day^{-1} through the wetland. In addition to *D. rerio* deformity, several other toxicity data sets from Redman et al. (2018) were also considered for evaluation. However, our BE measurements were, in comparison, relatively low and were showing a less than 1% toxic response for *D. rerio* fish embryos (4d) survival, *C. dubia* (4d) survival, and *C. dubia* (7d) reproduction.

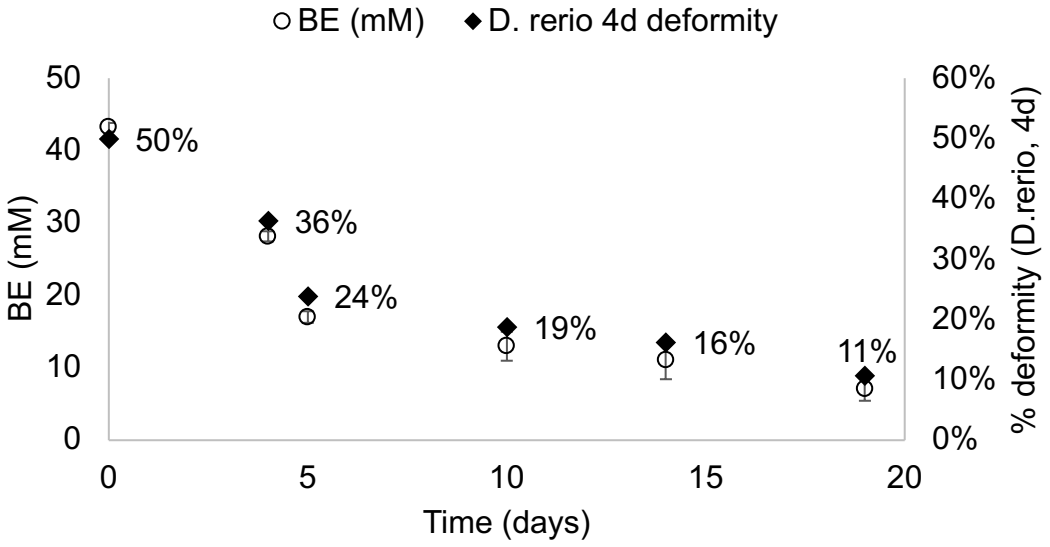

Figure 4-7: Biomimetic extraction measurements ($mmol_{2,3\text{-dimethylnaphthalene}}/L_{PDMS}$) for total acid extractable organics and estimated toxic effect (% D. rerio 4d deformity) of OSPW over time in the KT wetland.

This demonstration for toxicity reduction is based on bulk OSPW acid-extractable organics. Therefore, this representation of $E_{Tox.}$ includes all hydrocarbons measured by BE using solid phase microextraction and may not explicitly describe O2-NAs in the OSPW. Additional work is needed to quantify the presence of polyoxygenated naphthenic acids and other naphthenic acid fraction compounds, and neutral hydrocarbons. In an attempt to quantify the abundance of neutral organics such as polycyclic aromatic hydrocarbons in our OSPW, we performed BE measurements for non-acidified OSPW samples alongside the acidified OSPW samples. Chemical analysis found non-detectable concentrations of neutral organics by day 4 using the methods described here without acidification. Therefore, neutral organics likely only contribute minimally to overall bulk hydrocarbon measurements, and levels from previous work shows concentrations are in the ng/L range (Chapter 3) confirming naphthenic acids as the main constituents of concern based on abundance and toxicity.

The toxicity of NAs has been shown to correlate with carbon number (Frank et al., 2010; Hughes et al., 2017b). Low molecular weight NAs elicit a lower toxic response compared to higher molecular weight NAs because of their higher aqueous solubility and slower rates of diffusion into organic media such as biota lipids, the presumed site of toxic action for NAs. High molecular weight NAs elicit greater toxic effects due to their partitioning behaviour between OSPW and biota lipids. This phenomenon is depicted by

log D (octanol-water distribution coefficient) and is captured with our BE-SPME measurements since SPME fibre-OSPW partitioning is a surrogate measurement for lipid-water partitioning and chemical bioconcentration in biota. A promising result of this study shows that NAs with higher carbon numbers and molecular weight have greater treatment efficiencies (Figure 4-3) and experience more rapid rates of removal (Figure 4-6) suggesting treatment wetlands are a viable option to contribute to OSPW remediation.

4.5. Conclusions

Total O2-NA concentration in OSPW entering the wetland for each deployment was 19.7, 20.7, and 13.3 mg/L, respectively. The concentration of individual O2-NAs in OSPW entering the wetland ranged from 208 ng/L ($C_{20}H_{34}O_2$) to 2.68 mg/L ($C_{15}H_{24}O_2$). Concentrations were highest for C_{13} to C_{15} O_2-NAs where DBE = 3 or 4 (Z = -4 or -6), in all three deployments. The average E_C for each deployment was 13, 62, and 3.2%, respectively. The average E_M for each deployment was 7.5%, 68.9%, and 11.7%, respectively. Removal efficiency for individual naphthenic acids is found to be proportional to the carbon number of the naphthenic acid congener, and inversely proportional to the number of double bond equivalents. This relationship occurs due the partitioning behavior of the NA congeners, characterized by log D (octanol-water distribution coefficient). Higher log D for NAs supports partitioning from the water to adjacent organic media in the wetland where mechanisms such as biotransformation may occur. Turbidity is shown to correlate with NA concentration in the wetland indicating that sorption to suspended particulates and settling is also an important mechanism of removal for more hydrophobic substances. Environmental conditions such as temperature, precipitation, evapotranspiration influence chemical fate and treatment efficiency of NAs in the wetland. The half-life of NAs measured in the Kearl Treatment wetland ranges from 11 – 186 days in 2018 and 9 – 76 days in 2019. Using biomimetic extraction techniques with solid phase microextraction fibres, bulk OSPW was correlated with *D. rerio* % deformity (4 d). The estimated toxic response of OSPW show a relative decrease in % deformity of 67.6% ($E_{Tox.}$) after one 14-day cycle through the wetland. This is an absolute reduction in % deformity of 39.3%. The removal of higher molecular weight NAs demonstrates the potential for treatment wetlands to remediate OSPW.

4.6. References

Ajaero, C., Mcmartin, D. W., Peru, K. M., Bailey, J., Haakensen, M., Friesen, V., … Headley, J. V. (2017). Fourier Transform Ion Cyclotron Resonance Mass Spectrometry Characterization of Athabasca Oil Sand Process-Affected Waters Incubated in the Presence of Wetland Plants. *Energy and Fuels*, *31*, 1731–1740. https://doi.org/10.1021/acs.energyfuels.6b02643

Ajaero, C., Peru, K. M., Simair, M., Friesen, V., O'Sullivan, G., Hughes, S. A., … Headley, J. V. (2018). Fate and behavior of oil sands naphthenic acids in a pilot-scale treatment wetland as characterized by negative-ion electrospray ionization Orbitrap mass spectrometry. *Science of The Total Environment*, *631–632*, 829–839. https://doi.org/10.1016/J.SCITOTENV.2018.03.079

Alberta Energy Regulator. (2018). Water Use Performance. Accessed online March 2020: https://www.aer.ca/protecting-what-matters/holding-industry-accountable/industry-performance/oil-sands-mining-water-use

Alberta Energy Regulator. (2019a). Oil sands. Accessed online August 2019: https://www.aer.ca/providing-information/by-topic/oil-sands.

Alberta Energy Regulator. (2019b). Crude bitumen production. [online]. Accessed online August 2019: https://www.aer.ca/providing-information/data-and-reports/statistical-reports/st98/crude-bitumen/production.

Alberta Environment and Parks (2020) Oil Sands Information Portal: Total Area of the Oil Sands Tailings Ponds Over Time, Dec 31, 1985 - Dec 31, 2016 [Data file]. Retrieved from http://osip.alberta.ca/library/Datasets/Details/542

Allen, E. W. (2008). Process water treatment in Canada's oil sands industry: II. A review of emerging technologies. *Journal of Environmental Engineering and Science*, *7*(5), 499–524. https://doi.org/10.1139/S08-020

Anderson, J., Wiseman, S. B., Moustafa, A., Gamal El-Din, M., Liber, K., & Giesy, J. P. (2012). Effects of exposure to oil sands process-affected water from experimental reclamation ponds on Chironomus dilutus. *Water Research*, *46*, 1662–1672. https://doi.org/10.1016/j.watres.2011.12.007

Armstrong, S. A., Headley, J. V, Peru, K. M., & Germida, J. J. (2008). Phytotoxicity of oil sands naphthenic acids and dissipation from systems planted with emergent aquatic macrophytes. *Journal of Environmental Science and Health, Part A*, *43*(1), 36–42. https://doi.org/10.1080/10934520701750041

Bartlett, A. J., Frank, R. A., Gillis, P. L., Parrott, J. L., Marentette, J. R., Brown, L. R., … Hewitt, L. M. (2017). Toxicity of naphthenic acids to invertebrates: Extracts from oil sands process-affected water versus commercial mixtures. *Environmental Pollution*, *227*, 271–279. https://doi.org/10.1016/j.envpol.2017.04.056

Bauer, A. E., Frank, R. A., Headley, J. V., Peru, K. M., Hewitt, L. M., & Dixon, D. G. (2015). Enhanced characterization of oil sands acid-extractable organics fractions using electrospray ionization-high-resolution mass spectrometry and synchronous fluorescence spectroscopy. *Environmental Toxicology and Chemistry*, *34*(5). https://doi.org/10.1002/etc.2896

Bergerson, J., & Keith, D. (2006). Life cycle assessment of oil sands technologies. *Institute for Sustainable Energy, Environment and Economy, Univ. of Calgary*, (February).

Biryukova, O. V, Fedorak, P. M., & Quideau, S. A. (2007). Biodegradation of naphthenic acids by rhizosphere microorganisms. *Chemosphere* 67(10):2058-2064 https://doi.org/10.1016/j.chemosphere.2006.11.063

Brown, L. D., & Ulrich, A. C. (2015). Oil sands naphthenic acids: A review of properties, measurement, and treatment. *Chemosphere*. https://doi.org/10.1016/j.chemosphere.2015.02.003

Cancelli, A. M., Gobas, F. A. P. C., Qian, W., Kelly, B. C. (2019). Development and evaluation of a mechanistic model to assess the fate and removal efficiency of hydrophobic organic contaminants in horizontal subsurface flow treatment wetlands. *Water Research*, 151, 183-192. https://doi.org/10.1016/j.watres.2018.12.020

Division, E. H., & Branch, E. C. (2004). Toxicity of oil sands to early life stages of fathead minnows (pimephales promelas). *Environmental Toxicology*, *23*(7), 1709–1718.

Foote, L. (2012). Threshold considerations and wetland reclamation in Alberta's mineable oil sands. *Ecology and Society*, *17*(1). https://doi.org/10.5751/ES-04673-170135

Frank, R.A., Fischer, K., Kavanagh, R., Burnison, B.K., Arsenault, G., Headley, J.V., Peru, K.M., Kraak, G.V.D., and Solomon, K.R. (2008). Effect of carboxylic acid content on the acute toxicity of oil sands naphthenic acids. *Environmental Science and Technology*. 43(2), 266–271.

Hale, S. E., Oem, A. M. P., Carnelissen, G., Jonker, M. T. O. O., Waarum, I.-K., Eek, E., … Eek, E. (2016). The role of passive sampling in monitoring the environmental impacts of produced water discharges from the Norwegian oil and gas industry. *Marine Pollution Bulletin*, *111*, 33–40. https://doi.org/10.1016/j.marpolbul.2016.07.051

Han, X., Mackinnon, M. D., & Martin, J. W. (2009). Estimating the in-situ biodegradation of naphthenic acids in oil sands process waters by HPLC/HRMS. *Chemosphere* 76(1): 63-70. https://doi.org/10.1016/j.chemosphere.2009.02.026

Han, X., Scott, A. C., Fedorak, P. M., Bataineh, M., & Martin, J. W. (2008). Influence of molecular structure on the biodegradability of naphthenic acids. *Environmental Science and Technology*, *42*(4), 1290–1295. https://doi.org/10.1021/es702220c

Harman, C., Langford, K., Sundt, R. C., & Brooks, S. (2014). Measurement of naphthenic acids in the receiving waters around an offshore oil platform by passive sampling. *Environmental Toxicology and Chemistry*, *33*(9), 1946–1949. https://doi.org/10.1002/etc.2651

Hendrikse, M., Gaspari, D. P., McQueen, A. D., Kinley, C. M., Calomeni, A. J., Geer, T. D., … Castle, J. W. (2018). Treatment of oil sands process-affected waters using a pilot-scale hybrid constructed wetland. *Ecological Engineering*, *115*(February), 45–57. https://doi.org/10.1016/j.ecoleng.2018.02.009

Hilal, S. H., Karickhoff, S. W., & Carreira, L. A. (2004). Prediction of the solubility, activity coefficient and liquid/liquid partition coefficient of organic compounds. *QSAR and Combinatorial Science*, *23*(9), 709–720. https://doi.org/10.1002/qsar.200430866

Huang, R., Chelme-Ayala, P., Zhang, Y., Changalov, M., & Gamal El-Din, M. (2017). Investigation of dissociation constants for individual and total naphthenic acids species using ultra performance liquid chromatography ion mobility time-of-flight mass spectrometry analysis. *Chemosphere*, *184*, 738–746. https://doi.org/10.1016/j.chemosphere.2017.06.067

Huang, R., Chen, Y., Meshref, M. N. A., Chelme-Ayala, P., Dong, S., Ibrahim, M. D., … Gamal El-Din, M. (2018). Characterization and determination of naphthenic acids species in oil sands process-affected water and groundwater from oil sands development area of Alberta, Canada. *Water Research*, *128*. https://doi.org/10.1016/j.watres.2017.10.003

Hughes, S. A., Huang, R., Mahaffey, A., Chelme-Ayala, P., Klamerth, N., Meshref, M. N. A., … Gamal El-Din, M. (2017a). Comparison of methods for determination of total oil sands-derived naphthenic acids in water samples. *Chemosphere*, *187*, 376–384. https://doi.org/10.1016/j.chemosphere.2017.08.123

Hughes, S. A., Mahaffey, A., Shore, B., Baker, J., Kilgour, B., Brown, C., … Bailey, H. C. (2017b). Using ultrahigh-resolution mass spectrometry and toxicity identification techniques to characterize the toxicity of oil sands process-affected water: The case for classical naphthenic acids. *Environmental Toxicology and Chemistry*, *36*(11), 3148–3157. https://doi.org/10.1002/etc.3892

Ibrahim, I., Togola, A., & Gonzalez, C. (2013). In-situ calibration of POCIS for the sampling of polar pesticides and metabolites in surface water. *Talanta*, Nov 15;116:495-500 https://doi.org/10.1016/j.talanta.2013.07.028

Islam, M. S., Zhang, Y., McPhedran, K. N., Liu, Y., & Gamal El-Din, M. (2016). Mechanistic investigation of industrial wastewater naphthenic acids removal using granular activated carbon (GAC) biofilm based processes. *Science of the Total Environment*. https://doi.org/10.1016/j.scitotenv.2015.09.091

Knight, R. L., Kadlec, R. H., & Ohlendorf, H. M. (1999). The use of treatment wetlands for petroleum industry effluents. *Environmental Science and Technology*, *33*(7), 973–980. https://doi.org/10.1021/es980740w

Küsel, K., Pinkart, H. C., Drake, H. L., & Devereux, R. (1999). Acetogenic and sulfate-reducing bacteria inhabiting the rhizoplane and deep cortex cells of the sea grass Halodule wrightii. *Applied and Environmental Microbiology*, *65*(11), 5117–5123. https://doi.org/10.1128/aem.65.11.5117-5123.1999

Leshuk, T., de Oliveira Livera, D., Peru, K. M., Headley, J. V, Vijayaraghavan, S., Wong, T., & Gu, F. (2016). Photocatalytic degradation kinetics of naphthenic acids in oil sands process-affected water: Multifactorial determination of significant factors. *Chemosphere*, *165*, 10–17. https://doi.org/10.1016/j.chemosphere.2016.08.115

Leung, S. S., MacKinnon, M. D., & Smith, R. E. H. (2003). The ecological effects of naphthenic acids and salts on phytoplankton from the Athabasca oil sands region. *Aquatic Toxicology*, *62*(1), 11–26. https://doi.org/10.1016/S0166-445X(02)00057-7

Li, C., Fu, L., Stafford, J., Belosevic, M., & Gamal El-Din, M. (2017). The toxicity of oil sands process-affected water (OSPW): A critical review. *Science of the Total Environment*. https://doi.org/10.1016/j.scitotenv.2017.06.024

Madill, R. E. A., Orzechowski, M. T., Chen, G., Brownlee, B. G., & Bunce, N. J. (2001). Preliminary risk assessment of the wet landscape option for reclamation of oil sands mine tailings: Bioassays with mature fine tailings pore water. *Environmental Toxicology*, *16*(3), 197–208. https://doi.org/10.1002/tox.1025

Mahdavi, H., Prasad, V., Liu, Y., & Ulrich, A. C. (2015). In situ biodegradation of naphthenic acids in oil sands tailings pond water using indigenous algae-bacteria consortium. *Bioresource Technology*, *187*, 97–105. https://doi.org/10.1016/j.biortech.2015.03.091

Marentette, J. R., Frank, R. A., Bartlett, A. J., Gillis, P. L., Hewitt, L. M., Peru, K. M., … Parrott, J. L. (2015). Toxicity of naphthenic acid fraction components extracted from fresh and aged oil sands process-affected waters, and commercial naphthenic acid mixtures, to fathead minnow (Pimephales promelas) embryos. *Aquatic Toxicology*, *164*, 108–117. https://doi.org/10.1016/j.aquatox.2015.04.024

Martin J. (2015). The challenge: Safe release and reintegration of oil sands process-affected water. *Environmental Toxicology and Chemistry*, 34:2682–2686.

McQueen, A. D., Hendrikse, M., Gaspari, D. P., Kinley, C. M., Rodgers, J. H., & Castle, J. W. (2017). Performance of a hybrid pilot-scale constructed wetland system for treating oil sands process-affected water from the Athabasca oil sands. *Ecological Engineering*, *102*, 152–165. https://doi.org/10.1016/j.ecoleng.2017.01.024

McQueen, A. D., Kinley, C. M., Hendrikse, M., Gaspari, D. P., Calomeni, A. J., Iwinski, K. J., … Jr., J. H. R. (2017). A risk-based approach for identifying constituents of concern in oil sands process-affected water from the Athabasca Oil Sands region. *Chemosphere*, *173*, 340–350. https://doi.org/http://dx.doi.org/10.1016/j.chemosphere.2017.01.072

Morandi, G. D., Wiseman, S. B., Pereira, A., Mankidy, R., Gault, I. G. M., Martin, J. W., & Giesy, J. P. (2015). Effects-Directed Analysis of Dissolved Organic Compounds in Oil Sands Process-Affected Water. *Environmental Science and Technology*, *49*(20). https://doi.org/10.1021/acs.est.5b02586

Morin, N., Coquery, M., Randon, J., & Coquery, M. (2012). Chemical calibration, performance, validation and applications of the polar organic chemical integrative sampler (POCIS) in aquatic environments. *Trends in Analytical Chemistry*, *36*, 144–175. https://doi.org/10.1016/j.trac.2012.01.007

Nikolausz, M., Kappelmeyer, U., Székely, A., Rusznyák, A., Márialigeti, K., & Kästner, M. (2008). Diurnal redox fluctuation and microbial activity in the rhizosphere of wetland plants. *European Journal of Soil Biology*, *44*(3), 324–333. https://doi.org/10.1016/j.ejsobi.2008.01.003

Nikolausz, M., Márialigeti, K., & Kovács, G. (2004). Comparison of RNA- and DNA-based species diversity investigations in rhizoplane bacteriology with respect to chloroplast sequence exclusion. *Journal of Microbiological Methods*, *56*(3), 365–373. https://doi.org/10.1016/j.mimet.2003.11.003

Quagraine, E. K., Peterson, H. G., & Headley, J. V. (2005). In situ bioremediation of naphthenic acids contaminated tailing pond waters in the Athabasca oil sands region - Demonstrated field studies and plausible options: A review. *Journal of Environmental Science and Health - Part A Toxic/Hazardous Substances and Environmental Engineering*. https://doi.org/10.1081/ESE-200046649

Quesnel, D. M., Bhaskar, I. M., Gieg, L. M., & Chua, G. (2011). Naphthenic acid biodegradation by the unicellular alga Dunaliella tertiolecta. *Chemosphere*, 24(4): 504-511, https://doi.org/10.1016/j.chemosphere.2011.03.012

Redman, A. D., Parkerton, T. F., Butler, J. D., Letinski, D. J., Frank, R. A., Hewitt, L. M., … Giesy, J. P. (2018). Application of the Target Lipid Model and Passive Samplers to Characterize the Toxicity of Bioavailable Organics in Oil Sands Process-Affected Water. *Environmental Science and Technology*, *52*(14), 8039–8049. https://doi.org/10.1021/acs.est.8b00614

Rogers, V. V, Liber, K., & Mackinnon, M. D. (2002). Isolation and characterization of naphthenic acids from Athabasca oil sands tailings pond water. *Chemosphere*, 48(5):519-27, https://doi.org/10.1016/S0045-6535(02)00133-9

Sun, C., Shotyk, W., Cuss, C. W., Donner, M. W., Fennell, J., Javed, M., … Martin, J. W. (2017). Characterization of Naphthenic Acids and Other Dissolved Organics in Natural Water from the Athabasca Oil Sands Region, Canada, *Environmental Science and Technology*, 51(17): 9524-9532, https://doi.org/10.1021/acs.est.7b02082

Toor, N. S., Franz, E. D., Fedorak, P. M., MacKinnon, M. D., & Liber, K. (2013). Degradation and aquatic toxicity of naphthenic acids in oil sands process-affected waters using simulated wetlands. *Chemosphere*, *90*(2), 449–458. https://doi.org/10.1016/j.chemosphere.2012.07.059

Wang, B., Wan, Y., Gao, Y., Yang, M., & Hu, J. (2013a). Determination and Characterization of Oxy-Naphthenic Acids in Oilfield Wastewater. *Environmental Science and Technology*, 47(16):9545-54, https://doi.org/10.1021/es401850h

Wang, N., Chelme-Ayala, P., Perez-Estrada, L., Garcia-Garcia, E., Pun, J., Martin, J. W., … Gamal El-Din, M. (2013b). Impact of Ozonation on Naphthenic Acids Speciation and Toxicity of Oil Sands Process-Affected Water to Vibrio fischeri and Mammalian Immune System. *Environmental Science and Technology*, 47(12):6518-26, https://doi.org/10.1021/es4008195

Whitby, C. (2010). Chapter 3: Microbial naphthenic acid degradation. *Advances in Applied Microbiology, 70: 93-125*, https://doi.org/10.1016/S0065-2164(10)70003-4

Wilde, M. J., & Rowland, S. J. (2017). Naphthenic acids in oil sands process waters: Identification by conversion of the acids or esters to hydrocarbons. *Organic Geochemistry*, 115: 188-196, https://doi.org/10.1016/j.orggeochem.2017.09.004

Woudneh, M. B., Coreen Hamilton, M., Benskin, J. P., Wang, G., McEachern, P., & Cosgrove, J. R. (2013). A novel derivatization-based liquid chromatography tandem mass spectrometry method for quantitative characterization of naphthenic acid isomer profiles in environmental waters. *Journal of Chromatography A*, *1293*, 36–43. https://doi.org/10.1016/j.chroma.2013.03.040

Xu, X., Pliego, G., Zazo, J. A., Sun, S., García-Muñoz, P., He, L., … Garc Ia-Mu~ Noz, P. (2017). Critical Reviews in Environmental Science and Technology An overview on the application of advanced oxidation processes for the removal of naphthenic acids from water An overview on the application of advanced oxidation processes for the removal of naphth. *Environmental Science and Technology*, *47*, 1337–1370. https://doi.org/10.1080/10643389.2017.1348113

Xue, J., Zhang, Y., Liu, Y., & Gamal El-Din, M. (2016). Treatment of oil sands process-affected water (OSPW) using a membrane bioreactor with a submerged flat-sheet ceramic microfiltration membrane. *Water Research*, 88(1): 1-11, https://doi.org/10.1016/j.watres.2015.09.051

Zhang, L., Zhang, Y., & Gamal El-Din, M. (2018). Degradation of recalcitrant naphthenic acids from raw and ozonated oil sands process-affected waters by a semi-passive biofiltration process. *Water Research*, *133*, 310–318. https://doi.org/10.1016/j.watres.2018.01.001

Chapter 5. Development and testing of a mechanistic model for wetland treatment of contaminants in oil sands process-affected water: application to the Kearl Treatment Wetland in Alberta

5.1. Summary

A mechanistic model of contaminant fate in a free water surface flow wetland was developed to assess the removal efficiency of polycyclic aromatic hydrocarbons and naphthenic acids – chemicals which are ubiquitous in oil sands process-affected water. The model was applied to the Kearl Treatment Wetland on the Kearl Oil Sands site. The model was tested and evaluated using data described in Chapters 3 and 4. Model testing shows low overall systematic bias in model estimates for the calibrated model which applies temperature-correction models to abiotic and biotic rate constants describing intermedia chemical transformation and transport within the wetland.

Model simulations show that total transformation from the wetland is greatest for substances with a log K_{OW} or log D between 3.0 and 5.5. Evapotranspiration is highest for chemicals with a K_{AW} greater 10 and log K_{OW} or log D less than 3.0. However, the OSPW contaminants modelled in this study do not exceed a K_{AW} of 0.02 and therefore evapotranspiration is not expected to significantly contribute to OSPW remediation in wetlands under normal operations. Chemical removal is highly sensitive to biotransformation rates in the wetland for chemicals with a log K_{OW} or log D less than 7. Chemicals with log K_{OW} or log D greater than 7.0 exhibit low removal efficiency even when biotransformation rates are high. These highly hydrophobic substances are therefore not suitable for long-term wetland treatment. The treatment wetland model presented here may be used by industry operators to assess the feasibility of these treatment systems to meet specific water quality objectives for their wastewater. The model can be also be used to assess trade-offs in wetland design and operation to balance treatment performance with design specifications and operational limits.

5.2. Introduction

To better manage large volumes of oil sands process-affected water (OSPW) produced during bitumen extraction, the oil sands mining industry is investigating various wastewater treatment technologies. One of the more promising technologies is wetland treatment. Treatment wetlands are constructed, artificial ecosystems designed to harness the natural biogeochemistry of wetlands for removing pollutants from wastewaters. This water treatment technology has been successfully integrated into a number of different industries for the treatment of agricultural runoff (e.g. Page et al. 2010), mine wastewater (e.g. Batty and Younger, 2004), municipal and domestic wastewater (e.g. Toscano et al., 2009), leachate (e.g. Sim et al., 2013), and petroleum refinery process water (e.g. Knight et al., 1999). Treatment wetlands are continuing to emerge as a technology that may contribute to a more sustainable oil sands industry by reducing the demand for freshwater (i.e. recycling) and reducing the release of polluted waters back into the environment. To further this technology, it is important to better understand the biogeochemical mechanisms within the wetland, and how they contribute to the removal of contaminants from OSPW.

OSPW is a complex mixture organic and inorganic substances. The main organic chemicals in OSPW are polycyclic aromatic hydrocarbons (PAHs) and naphthenic acids (NAs). PAHs are hydrophobic neutral organic contaminants naturally found in bitumen that cause adverse effects in wildlife (Collier et al., 2013; Alharbi et al., 2016; Li et al., 2017). NAs are naturally occurring organic acids in bitumen and widely considered the main toxic component of OSPW (Toor et al., 2013; Frank et al., 2008). The PAHs and NAs in OSPW exhibit widely varying physicochemical properties that affect the fate of these substances in wetlands. It is the purpose of this study to develop and test a mass-balance model of the behaviour of PAHs, NAs, and other hydrophobic organic contaminants in OSPW in surface flow wetlands using the Kearl Treatment Wetland in northern Alberta as the test case.

Several models have been developed for treatment wetlands. These treatment wetland models focus on hydrology and general water quality metrics like biochemical and chemical oxygen demand, nitrogen removal, and phosphorus removal in wetlands (e.g. Chen et al., 1999; Wynn and Liehr, 2001; Mayo and Bigambo, 2005). There are currently no treatment wetland models of the fate of both neutral and ionic organic

contaminants. However, such models are needed to assess the feasibility of treatment wetlands to meet treatment and water quality objectives (e.g. CCME, 1999) based on site-specific conditions and to provide guidance for treatment wetland design and operation.

5.3. Theory

Treatment wetland systems are grouped into three categories based on their hydraulic flow regimes: 1) free water surface-flow wetlands such as the Kearl Treatment Wetland have an open surface water column; 2) Horizontal- and 3) Vertical-subsurface flow (SSF) wetlands represent aquifer-like designs with water flow occurring horizontally or vertically by gravity drainage through course-grained media.

The model is designed for both neutral hydrophobic contaminants such as PAHs, and polar organic contaminants such as NAs, both of which are relevant to the oil sands industry due to their ubiquity in OSPW and potential to cause adverse effects in wildlife. The model follows the environmental modelling approach established by Mackay et al. (1983) (Quantitative Water-Air- Sediment Interaction (QWASI) model), Mackay (2001) (Level I IV fugacity models), Clark et al. (1995) (Sewage Treatment Plant (STP) model), Arnot and Gobas (2004) (AQUAWEB Food Web Bioaccumulation model), and others, including a previous contaminant-fate wetland model designed for horizontal subsurface flow systems (Cancelli et al., 2019; Chapter 2).

The main objective of the model is to estimate effluent concentrations of contaminants that have entered the wetland in OSPW. The model therefore derives the wetland's efficiency of contaminant removal as a function of the physicochemical properties of the contaminants, wetland characteristics, and environmental conditions. The wetland model includes a number of cells, i.e. 6 for the Kearl Treatment Wetland that are arranged in series (Figure 5-1). Each cell consists of water (W), rooting media (RM), submerged vegetation (SV) and emergent vegetation (EV). Each medium in each cell is modelled as a well-stirred tank reactor. Chemicals are introduced into the wetland through advective wastewater flow. In this study, the wastewater input into the wetland only occurred on day zero of each study period. Water may also enter the wetland through precipitation and is subject to evaporation and transpiration. To mimic the operational conditions at the Kearl treatment wetland during our study, the outflow from

the final wetland cell is recycled back into the forebay of the wetland for all time-dependent model simulations. Within each cell, contaminants are subjected to a series of diffusion, advection, and transformation processes.

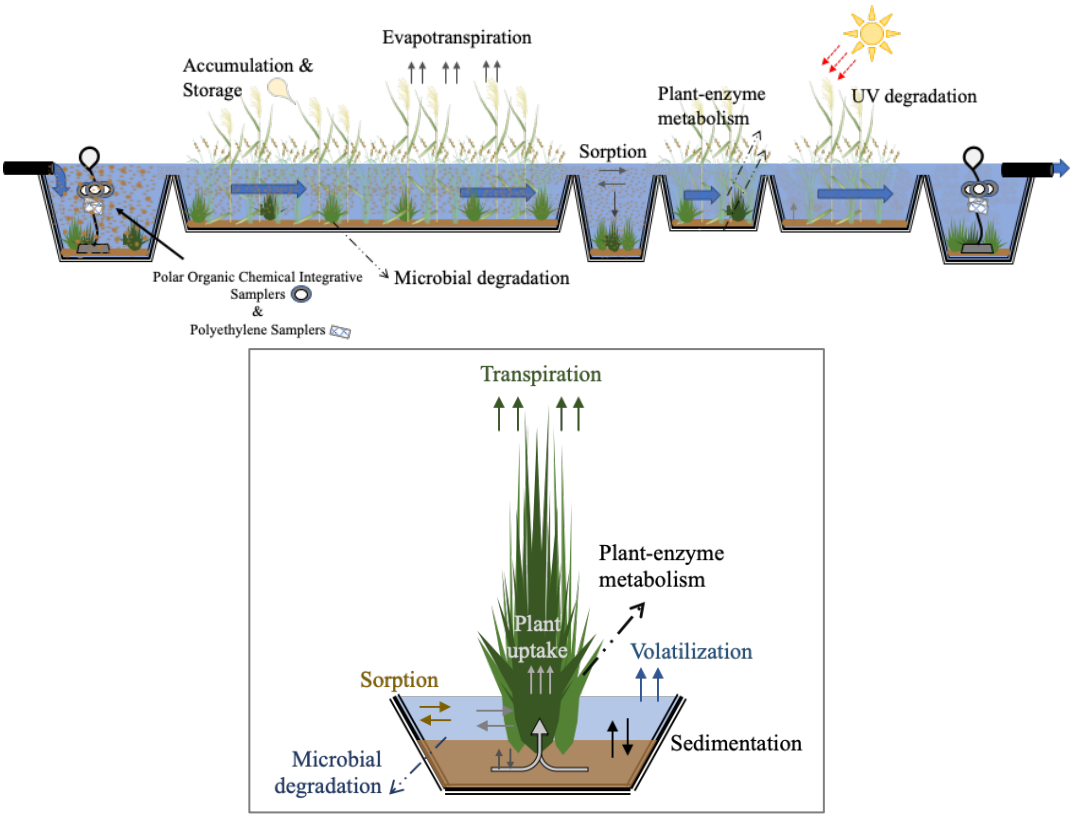

Figure 5-1: Conceptual diagram of the Kearl Treatment Wetland (top) and close-up of wetland chemical fate processes (bottom). Solid arrows represent transport processes of the chemical in wetland media. Dashed arrows represent transformation processes (chemical, physical, or biological). The effect of vegetation growth on the concentration of the chemical in plants is not shown.

Diffusion processes are described by a “two-film diffusion” model first introduced by Whitman (1923). This model uses mass transfer coefficients to derive intermedia transport rates for water-rooting media, water-vegetation, water-air, and vegetation-air based on the fugacity gradient between those media. Diffusion and transformation act upon freely dissolved contaminants in the wetland media. Plant uptake and transpiration processes incorporate the model developed by Trapp and Matthies (1995). Contaminant uptake into plants occurs by diffusion from water into submerged vegetation, and uptake from rooting media into xylem tubules based on the transpiration-stream concentration factor (TSCF) calculated as the larger value between:

$$TSCF = 0.7 \cdot e^{\left[-\frac{(\log K_{OW} - 3.07)^2}{2.78}\right]}, \text{ or} \quad \text{Eq. 5-1}$$

$$TSCF = 0.784 \cdot e^{\left[-\frac{(\log K_{OW} - 1.78)^2}{2.44}\right]} \quad \text{Eq. 5-2}$$

where K_{OW} is the octanol-water partition coefficient (D for ionizable substances; unitless). The concentration of contaminants in rhizome vegetation is the product of the TSCF (unitless) and the freely available concentration of contaminant in the rooting medium (g/kg).

Advective processes include water inflow and outflow, sedimentation and resuspension, and xylem flow from rhizomes to submerged and emergent vegetation. Chemical removal via sedimentation occurs through chemical sorption to suspended sediment, subsequent deposition of these suspended sediments onto rooting media. Burial of these sediments by newly deposited particles may occur, representing a pseudo-loss process where the chemical becomes entrapped in deeper sediments rendering it unavailable for re-introduction into the system. Resuspension of sediment solids that contain sorbed fractions of contaminants can re-introduce contaminants into the wetland water. Contaminant transport from the rooting media to submerged vegetation, and from submerged vegetation to emergent vegetation is assumed to occur principally through xylem flow, while phloem and aerenchymal transport are considered negligible. Thus, the model is not applicable to describe the fate of gases such as methane or oxygen, or essential nutrients such as nitrogen and phosphorus. Advective flow through xylem tubules (Q_{wx}) and into the submerged vegetation is determined as:

$$Q_{wx} = \frac{Q_{ET}}{N_P \cdot SA_W} \quad \text{Eq. 5-3}$$

where Q_T is the evapotranspiration rate (L/day) from the vegetated wetland cells estimated from the Penman-Monteith equation (Appendix D, Table D.5), N_P is the number of plants per m^2 in the vegetation wetland cells, and SA_W is the surface area of the wetland cells. Contaminant flux (g/day) from rhizome to submerged vegetation is determined as the product of Q_{wx} (m^3/day) and the freely available concentration of

contaminants in rhizome vegetation (g/m^3). For our modelling purposes, the atmosphere does not act as a source of contaminant mass, but only as a contaminant sink.

Transformation processes include chemical reactions, physical degradation, and biological transformation. Chemical transformations result from reactions with other chemicals within the wetland environment, and physical transformations may occur from UV-exposure (Fasnacht and Blough, 2002). Biological transformation (biotransformation) occurs from microbial activity (rooting medium), or enzymatic degradation within wetland vegetation (submerged and emergent vegetation). All transformation processes are modelled as non-reversible first-order degradation pathways. Transformation is assumed to act upon the freely dissolved contaminant fraction in the environmental media whereas particle-bound contaminant fractions are not subject to transformation (Kickham et al., 2012). Wetland transport and transformation processes are incorporated into 4 first-order mass-balance equations describing chemical-fate (Table 5-1, Eq. 5-4, Eq. 5-5, Eq. 5-6, and Eq. 5-7).

Table 5-1: Model calculations for chemical fate in free water surface flow treatment wetlands.

Symbol	Description	Calculation
$C_{i,W,c}$	Concentration of contaminant *i* in water, cell c (g/m^3)	$V_{W,c}\frac{dC_{i,W,c}}{dt} = Q_c \cdot C_{c-1} + k_{RM-W} \cdot M_{i,RM,c} - (k_{W-RM} + k_v + k_o + k_{Wt}) \cdot C_{i,W,c} \cdot V_{W,c}$ Eq. 5-4 Q_c = volumetric flow rate (m^3/day) of water entering cell c $Q_c C_{i,w,c-1}$= mass loading of contaminant i into cell c, from the previous cell c – 1 (g/day) $M_{i,RM,c}$ = mass of contaminant i in rooting medium, cell c (g) $V_{W,c}$ = volume of water, cell c (m3) k = rate constant for transport and transformation processes (day^{-1}) t = time (days) c = 1 (forebay) to 6 (final deep pool)
$C_{i,RM.c}$	Concentration of contaminant *i* in rooting medium, cell c (g/m^3)	$V_{RM,c}\frac{dC_{i,RM,c}}{dt} = k_{W-RM} \cdot C_{i,W,c} \cdot V_{W,c} - (k_{RM-W} + k_{RM-SV} + k_b + k_{RMt}) \cdot M_{i,RM,c}$ Eq. 5-5 $C_{i,W,c}$ = concentration of contaminant i in water, cell c (g/m^3) $M_{i,RM,c}$ = mass of contaminant i in rooting medium, cell c (g) $V_{W,c}$ = volume of water, cell c (m3) k = rate constant for transport and transformation processes (day^{-1}) t = time (days) c = 1 (forebay) to 6 (final deep pool)
$C_{i,SV,c}$	Concentration of contaminant *i* in submerged vegetation, cell c (g/m^3)	$V_{SV,c}\frac{dC_{i,SV,c}}{dt} = k_{W-SV} \cdot C_{i,W,c} \cdot V_{W,c} + k_{RM-SV} \cdot M_{i,RM,c} - (k_{SV-W} + k_{SV-EV} + k_{SVt} + k_{gSV}) \cdot M_{i,SV,c}$ Eq. 5-6 $C_{i,W,c}$ = concentration of contaminant i in water, cell c (g/m^3) $M_{i,RM,c}$ = mass of contaminant i in rooting medium, cell c (g) $M_{i,SV,c}$ = mass of contaminant i in submerged vegetation, cell c (g) $V_{W,c}$ = volume of water, cell c (m3) k = rate constant for transport and transformation processes (day^{-1}) t = time (days) c = 1 (forebay) to 6 (final deep pool)
$C_{i,EV,c}$	Concentration of contaminant *i* in emergent vegetation, cell c (g/m^3)	$V_{EV,c}\frac{dC_{i,EV,c}}{dt} = k_{SV-EV} \cdot M_{i,SV,c} - (k_{EV-air} + k_{EVt} + k_{gEV}) \cdot M_{i,EV,c}$ Eq. 5-7 $C_{i,W,c}$ = concentration of contaminant i in water, cell c (g/m^3) $M_{i,SV,c}$ = mass of contaminant i in submerged vegetation, cell c (g) $M_{i,EV,c}$ = mass of contaminant i in emergent vegetation, cell c (g) $V_{W,c}$ = volume of water, cell c (m3) k = rate constant for transport and transformation processes (day^{-1}) t = time (days) c = 1 (forebay) to 6 (final deep pool)

Symbol	Description	Calculation
$V_{W,c}$	Volume of water in cell c (m^3)	$\frac{dV_{W,c}}{dt} = V_c + V_{P,c} - V_{ET,c}$ Eq. 5-8 V_c = initial volume of water in cell c (m^3) $V_{P,c}$ = volume of water added via precipitation to cell c (m^3) $V_{ET,c}$ = volume of water removed via evapotranspiration from cell c (m^3) c = 1 (forebay) to 6 (final deep pool)
k_O	Outflow (day^{-1})	$= \frac{Q_{c,out}}{V_{W,c}}$ Eq. 5-9 $Q_{c,out}$ = Water outflow from wetland cell c (m^3/day) $V_{W,c}$ = Volume of water in wetland cell c (m^3)
k_V	Volatilization (day^{-1})	$= \frac{SA_W \cdot (1 - \Phi_{Veg.}) \cdot f_{DW} \cdot v_e}{V_W} \cdot \varphi$ Eq. 5-10 SA_W = Surface area of water (m^2) $\Phi_{Veg.}$= Fraction of vegetation coverage in wetland (unitless) f_{DW} = Fraction of freely dissolved contaminant in water (unitless) v_e = Volatilization mass transfer coefficient (m/day) V_W = Volume of water in wetland cell (m^3)
k_{W-RM}	Overall water-to-sediment transport (day^{-1}) [sedimentation, diffusion]	$= k_{W-RM1}+k_{W-RM2}$ Eq. 5-11 $k_{W-RM1} = \frac{v_{ss} \cdot f_{DW} \cdot K_{pw}}{\rho_s \cdot 1000 \cdot V_W} \cdot \varphi$ $k_{W-RM2} = \frac{SA_{RM} \cdot v_d \cdot f_{DW}}{V_W} \cdot \varphi$ v_{ss} = Solids settling rate (m/day) f_{DW} = Fraction of freely dissolved contaminant in water (unitless) K_{pw} = Suspended solids–water partition coefficient (L/kg) ρ_s = Density of solids in rooting medium (kg/L) V_W = Volume of water in wetland cell (m^3) SA_{RM} = surface area of rooting medium (m^2) v_d = Water-to-sediment diffusion mass transfer coefficient (m/day)
k_{RM-W}	Overall sediment-to-water transport (day-1) [resuspension, diffusion	$= k_{RM-W1}+k_{RM-W2}$ Eq. 5-12 $k_{RM-W1} = \frac{v_{rs} \cdot f_{ss}}{\rho_s \cdot 1000 \cdot V_{RM}} \cdot \varphi$ $k_{RM-W2} = \frac{SA_{RM} \cdot v_d \cdot f_{DS}}{V_{RM}} \cdot \varphi$ v_{rs} = Solids resuspension rate (kg/day) f_{ss}= fraction of contaminant in solids of rooting medium (unitless) ρ_s= Density of solids in rooting medium (kg/L) V_{RM}= Volume of rooting medium (m^3) SA_{RM} = Surface area of rooting medium (m^2) v_d = water-to-sediment diffusion mass transfer coefficient (m/day) f_{DS}= fraction of freely dissolved contaminant in water of rooting medium (unitless)

Symbol	Description	Calculation
k_B	Burial (day^{-1})	$= \frac{SA_{RM} \cdot v_b \cdot f_{SS}}{\rho_s \cdot 1000 \cdot V_{RM}} \cdot \varphi$ Eq. 5-13 SA_{RM} = Surface area of rooting medium (m^2) v_b = Sediment burial rate (kg/day) f_{ss}= Fraction of contaminant in solids of rooting medium (unitless) ρ_s= Density of solids in rooting medium (kg/L) V_{RM}= Volume of rooting medium (m^3)
k_{RM-SV}	Rhizome vegetation to submerged vegetation (day^{-1})	$= \frac{f_{DS} \cdot Q_{wx} \cdot TSCF}{V_{Rh}} \cdot \varphi$ f_{DS}= Fraction of freely dissolved contaminant in water of rooting medium (unitless) Q_{wx} = Flow rate of water through xylem tubules in wetland vegetation (L/day per plant) TSCF = Transpiration-stream concentration factor (unitless) V_{Rh} = Volume of rhizomes (m^3)
k_{W-SV}	Water-to-submerged vegetation diffusion (day^{-1})	$= \frac{SA_{SV} \cdot v_{waterveg} \cdot f_{DW}}{V_W} \cdot \varphi$ Eq. 5-14 SA_{SV} = Surface area of submerged vegetation (m^2) $v_{waterveg}$ = Water to submerged vegetation diffusion mass transfer coefficient (m/d) f_{DW}= Fraction of freely dissolved contaminant in water (unitless) V_W = Volume of water in wetland cell (m^3)
k_{SV-W}	Submerged vegetation to water diffusion (day^{-1})	$= \frac{k_{W-SV}}{K_{VegWater}} \cdot \varphi$ Eq. 5-15 k_{W-SV} = Water-to-submerged vegetation diffusion (day^{-1}) $K_{VegWater}$ = Vegetation-water partition coefficient (L/kg)
k_{SV-EV}	Submerged vegetation to emergent vegetation transport (day^{-1})	$= \frac{Q_{wx} \cdot f_{WVeg} \cdot \rho_{veg}}{W_{SV}} \cdot \varphi$ Eq. 5-16 Q_{wx} = Flow rate of water through xylem tubules in wetland vegetation (L/day per plant) f_{WVeg}= Contaminant fraction in water of vegetation (unitless) ρ_{veg}= density of vegetation (kg/L) W_{SV} = Weight of submerged vegetation (kg/plant)
k_{EV-air}	Emergent vegetation to air transport (day^{-1})	$= \frac{SA_{EV} \cdot v_T \cdot f_{WVeg}}{V_{EV} \cdot K_{VegAir}} \cdot \varphi$ Eq. 5-17 SA_{EV} = Surface area of emergent vegetation (m^2) v_T = Transpiration mass transfer coefficient (m/day) f_{WVeg}= Contaminant fraction in water of vegetation (unitless) V_{EV} = Volume of emergent vegetation (m^3) K_{VegAir} = Vegetation-air partition coefficient (L/kg)
k_{Wt}	Transformation in water (day^{-1})	$= \frac{\ln(2)}{t_{\frac{1}{2},W}} \cdot \phi$ Eq. 5-18 $t_{\frac{1}{2},W}$= Transformation half-life of chemical in water (days)

Symbol	Description	Calculation
k_{RMt}	Transformation in vegetated rooting medium (day^{-1})	$= \frac{\ln(2)}{t_{\frac{1}{2},RM}} \cdot \phi$ Eq. 5-19 $t_{\frac{1}{2},RM}$= Transformation half-life of chemical in rooting medium (days)
k_{SVt}	Transformation in submerged vegetation (day^{-1})	$= \frac{\ln(2)}{t_{\frac{1}{2},SV}} \cdot \phi$ Eq. 5-20 $t_{\frac{1}{2},SV}$= Transformation half-life of chemical in submerged vegetation (days)
k_{EVt}	Transformation in emergent vegetation (day^{-1})	$= \frac{\ln(2)}{t_{\frac{1}{2},EV}} \cdot \phi$ Eq. 5-21 $t_{\frac{1}{2},EV}$= Transformation half-life of chemical in emergent vegetation (days)
k_{gSV}	Growth dilution in submerged vegetation (day^{-1})	Model input
k_{gEV}	Growth dilution in emergent vegetation (day^{-1})	Model input
φ	Arrhenius equation, temperature correction	$\varphi = \theta^{T_W-5}$ Eq. 5-22 θ = Temperature correction coefficient (unitless) T_W = water temperature (deg-C)
ϕ	Q_5 model, temperature correction	$\phi = Q_5^{\frac{T_W-5}{5}}$ Eq. 5-23 Q_5 = Temperature correction coefficient (unitless) T_W = Water temperature (deg-C)

The model is solved for both steady-state (dC/dt = 0) and time-dependent simulations though a Euler-type numerical simulation for individual contaminants. The model derives contaminant concentrations in water, rooting media, submerged vegetation, and emergent vegetation using the finite differences technique. The steady-state solution of the model is useful for assessing the wetland's removal efficiency for contaminants as a result of a constant wastewater in and outflow in the wetland (i.e. water is not recycled). The time-dependent solution of the model provides a tool to assess the change in concentration of the chemical in the wetland water over time and is useful if operating conditions are not constant over time and, in the case of this study, the wastewater is recycled. The time-dependent model is designed to react to daily precipitation events, and evapotranspiration of water from the wetland making concentration estimates responsive to changes in the water budget.

5.4. Materials and Methods

5.4.1. Application to the Kearl Treatment Wetland

The model was parameterized and calibrated to the Kearl Treatment Wetland (KT wetland), a free water surface-flow constructed wetland on the Kearl Oil Sands site operated by Imperial Oil Resources Limited (approx. 75 km NNE of Fort McMurray, AB, Canada; 57°26’00"N, 111° 8'31"W). The design and operation of the KT wetland is described in Chapters 3 and 4. Model input parameters for the KT wetland are presented in Table 5-2. The KT wetland is approximately 1 ha in total area and consists of six cells-in-series (three deep pool and three shallow areas) whereby water is pumped into the forebay and percolates over interior berms to enter subsequent cells. Wetland investigations were performed between May and September from 2017 to 2019. In 2017, OSPW was pumped into the wetland from a runoff detention pond and was returned back into this detention pond from the final deep pool of the wetland. In 2018 and 2019, OSPW was pumped from a drainage pond situated next to an external tailings area at the Kearl Oil Sands. The OSPW was pumped into the wetland during a single pumping event and fully recycled for the duration of the study (i.e. no external detention pond was used).

Table 5-2: Model parameters that describe the Kearl Treatment Wetland.

Wetland parameter	Symbol	Value
Surface area of wetland cell (water and rooting medium) (m^2)	SA_W & SA_{RM}	[1] 497 [2] 4412 [3] 545 [4] 695 [5] 1001 [6] 455
Vegetation cover (%)	$\Phi_{\mathrm{Veg.}}$	[1] 10% [2] 39% [3] 10% [4] 22% [5] 51% [6] 10%
Surface area of catchment area (m^2)	$SA_{catchment}$	[1] 960 [2] 8528 [3] 1053 [4] 1343 [5] 1935 [6] 880
Average water depth (m)	D_w	[1,3,6] 1.7 [2,4,5] 0.4
Depth of rooting medium (m)	D_{RM}	0.5
Number of emergent plants per m^2	N_P	1
Water content of vegetation (g/g)	Wp	0.8
Weight of rhizomes of one plant (kg/plant)	W_{Rh}	1
Weight of submerged part of one plant (kg/plant)	W_{SV}	1
Weight of emerged part of one plant (kg/plant)	W_{EV}	3
Surface area-volume ratio for submerged vegetation (m^2/m^3)	AV_{SV}	400
Surface area-volume ratio for emergent vegetation (m^2/m^3)	AV_{EV}	800
Density of suspended solids (kg/L)	ρ_{SS}	1.5
Density of rooting medium solids (kg/L)	ρ_s	1.85
Density of vegetation (kg/L)	ρ_{veg}	0.85
Density of organic carbon (kg/L)	ρ_{OC}	1
Organic carbon content of suspended solids (unitless)	OC_{pw}	0.05
Organic carbon content of rooting medium solids (unitless)	OC_{ss}	0.382
Organic carbon content of vegetation (unitless)	OC_v	0.005

[1] – cell 1, forebay
[2] – cell 2, shallow area 1
[3] – cell 3, deep pool 1
[4] – cell 4, shallow area 2
[5] – cell 5, shallow area 3
[6] – cell 6, final deep pool

Daily precipitation, evapotranspiration, and temperature are provided to the model for the duration of the model testing simulations. Precipitation rates during field work was obtained from the Kearl Lake weather station. Evapotranspiration was

estimated with the Penman-Monteith equation using air temperature, relative humidity, and wind speed data obtained from the Kearl Lake weather station (Chapters 3 and 4).

Water temperature measurements from the wetland were collected during field studies using a YSI® Professional Plus Multiparameter instrument. These measurements are incorporated into the model for estimations of temperature-dependent rate constants. For rates of water-sediment partitioning, water-vegetation partitioning, volatilization, and particulate settling (i.e. abiotic processes) the model incorporates the Arrhenius equation: $k_T = k_5 \cdot \theta^{T-5}$ where k_T is the modified rate constant (day^{-1}) at temperature T (deg-C), k_5 is the rate constant at 5 deg-C, θ is the temperature correction coefficient used to calibrate the physical removal mechanisms with changes in temperature. For rates of microbial degradation in the rooting medium or plant-mediated enzymatic transformation in the vegetation (i.e. biotic processes), the model incorporates a Q_5 temperature correction (i.e. a modified Q_{10} model; e.g. Yuste et al., 2004): $k_T = k_5 \cdot Q_5^{(T-5)/5}$ where Q_5 is the temperature correction coefficient used to calibrate the biological processes to temperature. Both an Arrhenius and Q_5 temperature correction methods are used since rates of abiotic processes such as sorption are exothermic processes and therefore inversely proportional to temperature (Hijosa-Valsero et al., 2010) whereas biotransformation rates are proportional to temperature (Kadlec and Wallace, 2009; Tang et al., 2017). Using both temperature-correction methods ensures the model more accurately responds to changes in temperature. θ and Q_5 were determined by trial-and-error during model testing. This method is viewed as a calibration technique to improve model bias.

5.4.2. Test Chemicals

Concentrations of polycyclic aromatic hydrocarbons (PAHs) and naphthenic acids (NAs) in OSPW were collected from the wetland forebay and final deep pool by use of passive sampling devices and water sampling methods. Chapter 3 describes the collection of dissolved PAH concentrations in OSPW using polyethylene passive sampling devices in 2017 and 2018. The passive sampling data from 2017 for PAHs was used for the testing and calibration of the steady-state version of the model. Chapter 4 describes the collection of dissolved NA concentrations in OSPW using Polar Organic Chemical Integrative Samplers (POCIS) in 2018 and 2019. OSPW samples collected from the wetland forebay at specified time points during wetland operation in 2018 and

2019 were analyzed for both PAHs and NAs. The passive sampling data and water samples collected in 2018 and 2019 for PAHs and NAs were used for testing and calibration of the time-dependent version of the model.

A total of 46 PAHs and 60 NAs were used for model calibration. Physicochemical properties required for model input parameters of PAHs were obtained from EPISuite v4.11 program. Due to the ionizing nature of NAs, log D (octanol-water distribution coefficient; unitless) and H (Henry's Law constant; $m^{3}{\cdot}Pa^{-1}{\cdot}mol^{-1}$) were estimated *in-silico* with SPARC (Automated Reasoning in Chemistry; ARChem, Danielsville, GA, USA; Hilal et al., 2004) using SMILES notation generated by the authors for representative NAs based on carbon, hydrogen number, and number of double bond equivalents. Calculations were performed at ionization strength of 0.04 M, calculated from water chemistry data collected from the OSPW (unpublished data). The uncertainties in these estimates of physicochemical properties are not well established, however uncertainty of all model inputs is evaluated in the model bias calculations. The half-life of individual NAs was estimated using data from Ajaero et al. (2018) and Chapter 4. Some modifications were needed to better represent biotransformation, not just overall contaminant half-life within wetland systems as both studies report. Chemical properties are presented in Appendix D, Tables D.1 and D.2 for PAHs and NAs, respectively.

5.4.3. Model output

In each cell (c), the concentration of contaminant (i) in water ($C_{i,W,c}$), rooting media ($C_{i,RM,c}$), submerged vegetation ($C_{i,SV,c}$), and emergent vegetation ($C_{i,EV,c}$) is estimated by the model. Contaminant mass flux terms (g/day) are calculated as $M_j{\cdot}k_{j(-k)}$ where M_j is the mass of contaminant (g) in media j (W, RM, SV, EV) and $k_{j(-k)}$ is the rate constant for contaminant transformation in media j or transport from media j to k. Removal flux terms in the treatment wetland model include: burial, growth dilution of vegetation, volatilization and transpiration (i.e. evapotranspiration), and transformation in rooting media, submerged vegetation, and emergent vegetation.

Treatment removal efficiency is calculated for concentration-reduction ($E_{C,i}$) and mass-removal ($E_{L,i}$) from the wetland water as:

$$\mathrm{E_{C,i}} = \left(1 - \frac{C_{i,w,6}}{C_{i,w,1}}\right) \quad \text{Eq. 5-24}$$

and

$$\mathrm{E_{L,i}} = \left(1 - \frac{Q_6^{out} \cdot C_{i,w,6}}{Q_1 \cdot C_{i,w,1}}\right) \quad \text{Eq. 5-25}$$

where $C_{i,w,6}$ is the concentration of contaminant i in water in the final deep pool (cell 6) of the wetland, $C_{i,w,1}$ is the concentration of contaminant i in water in the wetland forebay (cell 1), and $\mathrm{Q_6^{out}}$ is the flow rate of water leaving cell 6 (out) and Q_1 is the flow rate of water entering cell 1 (in) of the wetland. $E_{C,i}$ is sensitive to all model inputs (n = 52) including chemical properties and wastewater quality (n = 15), environmental conditions (n = 5), wetland design (n = 8), and other wetland parameters concerning chemical fate (n = 24), all of which are programmable in the model. $E_{L,i}$ accounts for changes in the volume of water in the wetland from precipitation and evapotranspiration and therefore a better representation of the chemical removal from wastewater in the wetland.

5.4.4. Model performance analysis

The overall performance of the model was evaluated by comparing model-estimated concentrations ($C_{model,W}$) to empirical concentrations ($C_{obs.,W}$) of the test chemicals. The initial concentration of the test chemical in the OSPW entering the wetland was the external variable. $C_{model,W}$ represents the concentration of the contaminant in water in the final deep pool of the wetland for the steady-state model, and the concentration of contaminant in water in the forebay of the wetland for the time-dependent model to mimic sample collection. The mean model bias (MB) was calculated as:

$$\mathrm{MB} = \mathrm{e}^{\frac{\sum_{n=1}^{N} \ln\left(\frac{C_{model,w,n}}{C_{obs.,w,n}}\right)}{N}} \quad \text{Eq. 5-26}$$

where *N* is the total number of concentration data points (N = 1,419; $N_{PAH(steady\text{-}state)}$ = 42; $N_{PAH(time\text{-}dependent)}$ = 624; $N_{NA(time\text{-}dependent)}$ = 753).

This method of model performance evaluation assumes that the ratio $C_{model,W}/C_{obs.,W}$ has a log-normal distribution. An MB less than one indicates the model systematically under-estimates chemical concentrations by a factor equal to the MB value. An MB greater than one indicates the model systematically over-estimates chemical concentrations by a factor equal to the MB value. An MB equal to one indicates that empirical observation and model calculations are, on average, in agreement, i.e. minimal model bias. The 95% confidence intervals of MB reflect overall model uncertainty and represent the combined sum of error in the model calculations, including model parameterization errors, errors in model structure, and analytical errors and variability in the empirical data used in the model performance analysis.

The steady-state assumption of the model was assessed by estimating the time to reach 95% of steady-state (i.e. t_{95}) for each chemical in the water, rooting medium, submerged vegetation, and emergent vegetation in the wetland. t_{95} is estimated as $3/k_{dep}$, where k_{dep} is the total depuration rate constant for each environmental compartment.

5.4.5. Elementary effects analysis

The model uses 52 state variables for the contaminant fate calculations. The sensitivity of each of these parameters was evaluated by the effect of each model parameter on concentration-reduction efficiency (E_C). Elementary effects of model parameters were determined using the method developed by Morris (1991). This method is useful for determining whether the effect of the input parameter on removal efficiency is (a) negligible, (b) linear and additive, or (c) non-linear or involved in interactions with other parameters (Campolongo and Saltelli, 1997; Saltelli et al., 2005). The elementary effects of parameter i (EE_i) were estimated using:

$$\mathrm{EE_i} = \frac{[\mathrm{Y(X_1,\ X_2, \dots, X_{i-1},\ X_i + \Delta, \dots,\ X_N) - Y(X_1,\ X_2, \dots,\ X_N)}]}{\Delta} \qquad \text{Eq. 5-27}$$

The parameter values (X_i) are discretized along a 4-level grid (i.e. Δ = [0, 1/3, 2/3, 1]) such that $X_i = \Delta$ [MAX - MIN] / MIN. Additional details on the calculations for EE_i are available in Appendix A with the supplementary information for Chapter 2. The mean and standard deviation (μ^*_i and σ_i) of the elementary effects for each parameter were used to analyze the sensitivity of the input parameters and demonstrate their effects on

E_C. μ^*_i represents the magnitude of parameter sensitivity to removal efficiency, and σ_i represents the degree of interactions between other input parameters.

5.4.6. Model simulations to assess chemical behaviour

This model application is useful to explore which chemicals can be efficiently removed from OSPW by wetland treatment, and which chemicals cannot. This was done by simulating a range of chemicals with different physicochemical properties. The model was parameterized to the Kearl Treatment Wetland and chemical removal from OSPW was evaluated for a range of K_{AW} (air-water partition coefficient) and D (octanol-water partition coefficient; K_{OW} for neutral chemicals). The sensitivity of removal efficiency to rates of biotransformation in the wetland are explored by simulating wetland treatment where rates of biotransformation in rooting media are set to 0 day^{-1} (i.e. no transformation), 0.01 day^{-1}, 0.1 day^{-1}, and 0.3 day^{-1}. Rates of biotransformation in vegetation were assumed to be 10 times less than the rate of biotransformation in rooting media for all simulations. Slower rates of transformation were assigned to vegetation due to the lack of understanding of the biotransformation kinetics within these organisms. The contributions from transformation and evapotranspiration on overall chemical removal are demonstrated, and select individual chemicals are used to illustrate which processes contribute to chemical removal for different substances.

5.5. Results and Discussion

5.5.1. Model performance analysis

Uncalibrated model

The overall mean model bias (MB) and 95% confidence intervals for all model estimated contaminant concentrations in OSPW in the wetland is 0.889 (0.852 – 0.927) for the uncalibrated model. MB for the steady-state and time-dependent model calculations is 1.069 (0.795 – 1.436) and 0.884 (0.847 -0.922) for the uncalibrated model, respectively. Overall, model estimates from the uncalibrated model under-estimate chemical concentrations in the wetland. Concentrations are particularly under-estimated for time-dependent simulations of PAHs and NAs when compared to passive sampling data (MB = 0.268 (0.178 – 0.404) for PAHs and 0.510 (0.472 – 0.550) for

NAs). These passive sampling measurements reflect the time-weighted average concentrations of contaminants over the period of deployment, which may not be accurately represented in the treatment wetland model, resulting in poor model performance. PAH concentrations measured by passive sampling also occurred later in the operational season (i.e. August – September), which suggests that lower temperatures during this timeframe may have hindered chemical removal more extensively than the model accounted for with temperature-corrected rate constants. Hence, lower estimated chemical concentrations in the effluent by the uncalibrated model compared to empirical observations (i.e. MB < 1).

Calibration

Table 5-3 presents the values of θ and Q_5 used for temperature-corrections made to rate constants in the treatment wetland model for each model application. For abiotic processes, θ for temperature correction is 1.0 (i.e. no temperature-correction) for all modelling events, except for the modelling of NAs in August 2018 and June 2019 where θ was determined to be 0.4 and 0.5, respectively. These values for August 2018 and June 2019 suggest that temperatures above 5 deg-C cause slower rates for abiotic mechanisms. Biotic processes within the wetland are temperature-corrected using the Q_5 model. Values for Q_5 are shown to be proportional to temperature whereby the lowest Q_5 parameter value (0.800) occurs in August 2018 (coldest average temperatures) and the largest Q_5 parameter value (1.058) occurs in August 2017 (warmest average temperatures). The sensitivity of Q_5 to seasonal temperatures has been demonstrated in other studies (e.g. Yuste et al., 2004; 2005; Chen and Tian, 2005). Spatial variability of Q_5 has also been observed due to natural heterogeneity within a single ecosystem (Zhou et al., 2009), as well as biological factors such as ecosystem diversity (Shi et al., 2012). Further research is required to determine the sensitivity to specific wetland parameters such as plant type and productivity and the composition and activity of microbial communities to be able to estimate Q_5 values for the Kearl Treatment Wetland at different periods of operation.

Table 5-3: θ and Q_5 parameter values for temperature-correction models used in each of the model simulations: Deployments (D) 1 – 3, and aqueous concentrations collected for polycyclic aromatic hydrocarbons (PAHs) and naphthenic acids (NAs).

		Passive sampling					Aqueous sampling	
Study period:		August 2017	September 2017	August 2018	May 2019	June 2019	Aug.–Sept., 2018	May–June, 2019
PAHs	θ	1.00	1.00	1.00	--	--	1.00	1.00
	Q_5	1.058	0.920	0.850	--	--	1.00	1.00
NAs	θ	--	--	0.40	1.00	0.50	1.00	1.00
	Q_5	--	--	0.800	0.997	0.850	0.980	0.960
Temp. Avg. ± SD	deg-C	18.6 ± 2.5	12.0 ± 4.6	†6.0 ± 4.1 ‡8.0 ± 3.3	13.1 ± 5.1	16.3 ± 3.9	6.0 ± 4.1	12.4 ± 4.6

-- Data collection for chemical group not performed.
†Average temperature for days 0 – 28 (PAHs)
‡Average temperature for days 0 – 19 (NAs)

Calibrated model

The overall mean model bias (MB) and 95% confidence intervals for the calibrated model is 1.030 (0.251 – 4.229). MB for the steady-state and time-dependent model calculations is 0.981 (0.198 – 4.858) and 1.031 (0.253 – 4.211) following model calibrations, respectively. MB (95% CI) of time-dependent model estimates of concentrations using passive sampling data improved to 1.005 (0.227 – 4.445) for PAHs and 0.950 (0.613 – 1.472) for NAs after calibration.

The model bias of estimated OSPW concentrations in the wetland indicates low systematic bias for the KT wetland system. Figure 5-2 compares the model-estimated concentrations of PAHs and NAs in OSPW from the calibrated model to the measured concentrations of PAHs and NAs in OSPW. The figure shows low variability in MB for naphthenic acids, particularly with the 2019 time-dependent model where 97.9% of estimates are within a factor of three from the observed values. Larger deviations appear with PAH model simulations, but still 74.2% of model estimates are within a factor of three from the observed values, and 97.6% within a factor of 10.

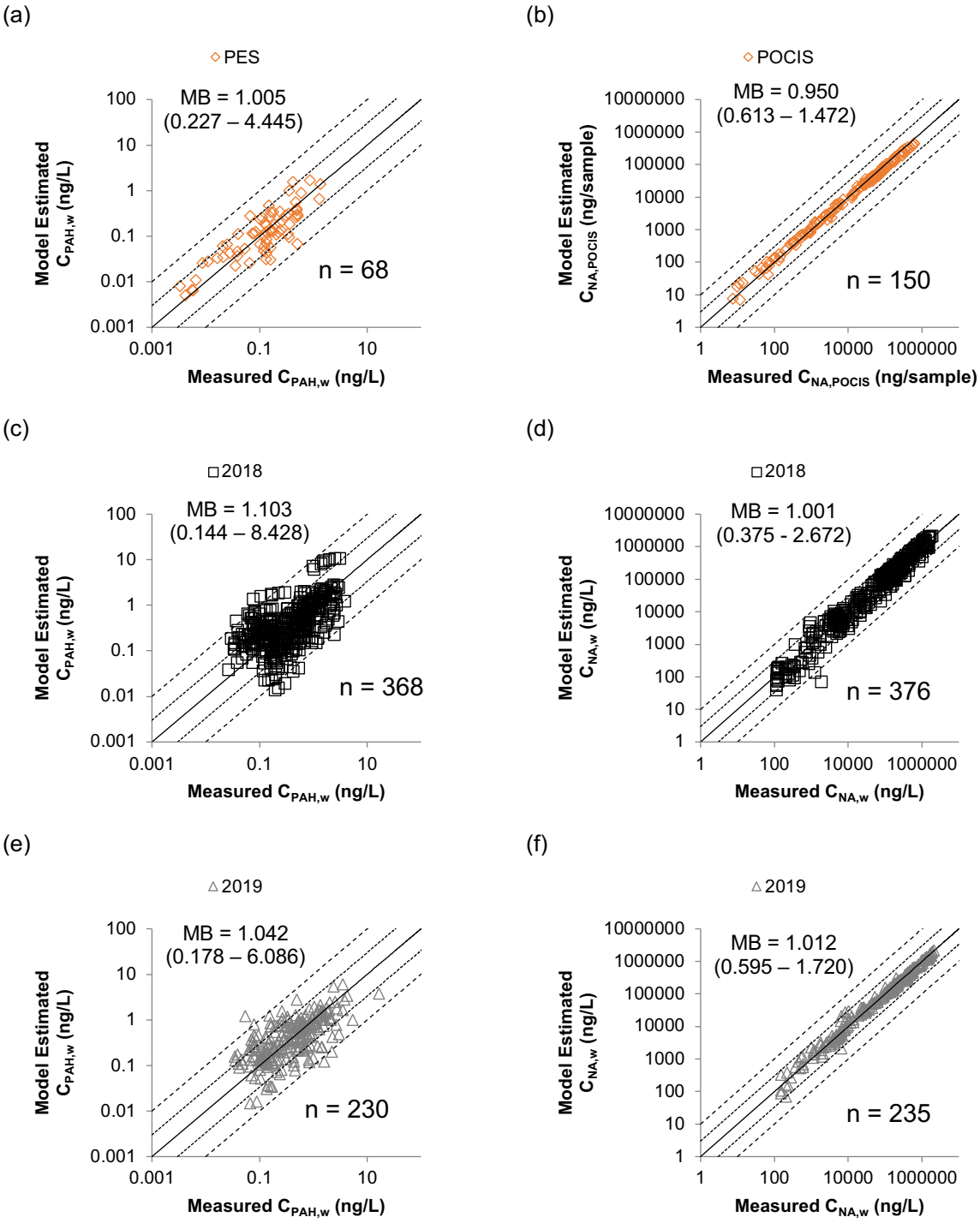

Figure 5-2: Measured and model estimated concentrations of a) PAHs in OSPW in the final deep pool measured with polyethylene samplers, b) NAs in Polar Organic Chemical Integrative Samplers, c) PAHs in OSPW in the forebay (2018, d) NAs in OSPW in the final deep pool (2018), e) PAHs in OSPW in the forebay (2019), and f) NAs in OSPW in the forebay (2019). — represents 1:1 line. ---- represents 1:1 (3x), and – – – – represents 1:1 (10x). Model bias (MB) and 95% confidence intervals are provided.

In general, the calibrated model slightly underestimates concentrations (MB < 1.0) for chemicals with low molecular weight and log K_{OW} (or log D), and slightly overestimates concentrations (MB > 1.0) for chemicals with higher molecular weight and log K_{OW} (or log D). Underestimation of low molecular weight NAs by the model suggests that these contaminants may be forming due to bioconversion from higher molecular weight NAs present in the OSPW (Quesnel et al., 2011; Islam et al., 2016; Xue et al., 2016). The formation of these contaminants was not included in model testing and simulation. Overestimation of the higher molecular weight contaminants may suggest that transformation or sorption rates of these chemicals are faster in the Kearl Treatment wetland than what is parameterized in the model.

The variability in MB is more pronounced for PAHs compared to NAs as indicated by the wider 95% confidence intervals for PAHs in Figure 5-2. This variability may be associated to the relatively low initial concentration of PAHs (average concentration = 1.08 ng/L, SD 1.49 ng/L) compared to NAs (average concentration = 430 ug/L, SD 642 ug/L). There may be greater variability in concentration measurements due to analytical challenges in quantifying low concentrations of PAHs in the wetland water sample with high precision. Another possibility is that the model may not perform well at low concentrations of contaminants in wastewater entering the wetland resulting in poorly fitted model-estimates.

Steady state vs. non-steady state

The t_{95} in water averaged 5.45 days (SD 0.16 days) for all test chemicals (PAHs and NAs) indicating that steady-state for the water compartment is achieved rapidly with small differences between chemicals. The t_{95} for PAHs ranged from 38 to 1,820 days for the rooting media, 104 to 21,660 days for the submerged vegetation, and 209 to 18,250 days in the emergent vegetation. The t_{95} for NAs ranged from 14 to 44 days for the rooting media, 54 to 3,890 days for the submerged vegetation, and 3,030 to 61,810 days in the emergent vegetation. Longer t_{95} in rooting media and vegetation occurs for more recalcitrant chemicals with higher log K_{OW} or log D because they more strongly sorb to the organic media leaving a smaller fraction freely available for biotransformation. t_{95} is extended further if chemicals experience slow depuration rates from the wetland media. For example, the long t_{95} (18,250 days) in emergent vegetation for benzo[e]pyrene is due to its low Henry's Law constant (0.03 $Pa \cdot m^3/mol$; log K_{AW} = -2.44) causing slow

evapotranspiration kinetics in addition to slow biotransformation rates ($t_{EV,1/2}$ = 421 days). The t_{95} for PAHs and NAs show that the steady-state version of the model is appropriate for the evaluation of treatment efficiency which mainly relies on concentrations of chemicals in the water, but is not a useful tool to evaluate concentrations in rooting media, submerged vegetation, and emergent vegetation for PAHs such as pyrene (t_{95} = 260 (rooting medium), 5.6 (water), 820 (submerged veg.), 2,600 (emergent veg.)) or O2-NAs such as $C_{21}H_{40}O_2$ (t_{95} = 32 (rooting medium), 5.7 (water), 3,230 (submerged veg.), 3,460 (emergent veg.)). Concentration estimates in organic wetland media from the steady state model are not accurate representations of chemical fate in normal wetland operations because chemical mass will continue to accumulate in these media for long periods, as suggested by their t_{95}. For simulations where concentration estimates in rooting media and vegetation are desired, the time-dependent version of the model will provide a better representation of chemical fate within the wetland.

5.5.2. Elementary effects analysis

The mean elementary effects (μ^*) and standard deviations (σ) for parameter sensitivity of treatment efficiency are available in Table D.7. The results of this analysis of elementary effects show significant sensitivity of E_C to a number of different model parameters. Among the most sensitive parameters are: hydraulic flow rate (μ^* = 30%, σ = 34%), wetland surface area (μ^* = 25%, σ = 21%), log D (log K_{OW} for neutral chemicals); μ^* = 24%, σ = 35%), vegetation density (μ^* = 21%, σ = 34%), water temperature (μ^* = 19%, σ = 29%), half-life of chemical in submerged vegetation (μ^* = 19%, σ = 40%), weight of submerged vegetation (μ^* = 17%, σ = 39%), and vegetation organic carbon to octanol equivalency factor (μ^* = 16%, σ = 36%).

The sensitivity of these parameters suggest that treatment wetland performance is sensitive to environmental conditions (e.g. temperature), wetland design and operation (e.g. flow rate, wetland surface area, vegetation density, weight of submerged vegetation), and physicochemical properties (e.g. log K_{OW} or log D, transformation half-life in submerged vegetation, vegetation organic carbon to octanol equivalency factor). Therefore, consideration of each of these factors is important in the application of treatment wetland systems for industrial wastewater treatment.

The sensitivity of flow rate and surface area of the wetland demonstrates the most essential criteria to influence chemical removal: time. These parameters directly influence the retention time of wastewater in the wetland. Longer retention times provides more opportunities for chemicals in wastewater to undergo processes of chemical removal. Therefore, E_C increases as i) surface area increases and ii) flow rate decreases, because retention time is longer. Model simulations demonstrate that by increasing retention time of OSPW in the Kearl Treatment Wetland from 14 days to 70 days the removal efficiency of pyrene increases from 63 to 98%. The importance of wetland design parameters such as hydraulic retention time has been explored in many other studies of treatment wetlands (e.g. Chazarenc et al., 2003; Garcia et al., 2004). Therefore, the operating flow rate and wetland design should be determined with site-specific treatment objectives in mind (e.g. CCME, 1999).

Temperature is shown to be an influential parameter for treatment efficiency due to its effects on various wetland biogeochemical processes (see Table 5-1, calculation of rate constants). The model incorporates temperature effects on abiotic and biotic processes within the wetland using temperature-correction models (ϕ and φ). Temperature also effects rates of evapotranspiration from the wetland as shown with the Penman-Monteith equation used to estimate evapotranspiration. Therefore, temperature has several modes of interaction in the model which demonstrates how daily and seasonal fluctuations in temperature can significantly affect wetland performance. The parameterization of site-specific environmental conditions is needed to properly incorporate the effects of temperature on treatment efficiency, and to assess the feasibility of these systems under different environmental conditions.

The weight of submerged vegetation reflects the size of the vegetation compartment in the wetland. Larger vegetation can accumulate greater mass of contaminants, offering storage for extracted chemicals from wastewater. Half-life of the chemical in submerged vegetation represents the rate at which this stored chemical mass can be depurated. Together, these parameters indicate the importance of healthy vegetation for chemical removal. For example, with more chemical mass and shorter half-life in submerged vegetation, greater chemical removal flux from the submerged vegetation will result, leading to greater treatment efficiency in the wetland.

Chemical properties like log K_{OW} or log D have also been shown to be important parameters for contaminant-fate in treatment wetlands (e.g. Cancelli et al., 2019; Chapters 3 and 4). The large standard deviation of the elementary effects of log K_{OW} or log D (σ = 35%) indicates non-linear interactions with other wetland parameters. This means that log K_{OW} or log D also influences the sensitivity of other parameters to treatment efficiency. For example, the removal flux of a chemical from biotransformation in rooting media first requires the chemical to partition from the influent wetland water to the rooting media, which is determined by log D. If log K_{OW} or log D is too low, the chemical will largely remain in the water and will be unavailable for biotransformation in rooting media. If log K_{OW} or log D is too high, the contaminant in the rooting media will not be freely available for biotransformation. Hence, non-linear interactions between log K_{OW} or log D and biotransformation in the rooting media. The sensitivity of E_C and other model parameters to log K_{OW} or log D implies that certain chemicals will be more susceptible to passive wetland treatment than other chemicals. The large standard deviation of the elementary effects from log K_{OW} or log D demonstrate the complex interactions in treatment wetlands responsible for chemical removal.

Certain parameters are shown to have negligible effects on steady-state treatment efficiency. For example, parameters that describe chemical fate in the emergent vegetation such as half-life of transformation in emergent vegetation, growth dilution of emergent vegetation, and plant-side and air-side mass transfer coefficients for chemical transport from vegetation to air have μ^* and σ < 0.001%. The low sensitivity is an artifact of the mass-balance approach employed in this study which involves only one route of influx into the emergent vegetation (xylem flow from submerged vegetation). Therefore, as one mechanism of removal (transpiration, biotransformation, or growth dilution) increases or decreases, the others compensate to solve the mass-balance resulting in little perceived sensitivity to removal efficiency. Regardless of the low measures of sensitivity, these results do not suggest that emergent vegetation are not important for chemical removal. A healthy and productive community of vegetation is important to the symbiosis with microbes within the wetland that create the complex and resilient biogeochemistry capable of wastewater treatment (Kadlec and Wallace, 2009).

To help assess of feasibility for these systems, model parameters were divided into four categories: chemical properties and wastewater quality (n = 15; e.g. log K_{OW} or log D, H, $t_{1/2}$, total suspended solids), environmental conditions (n = 5; e.g. precipitation,

temperature, evapotranspiration), wetland design and operation (n = 8; e.g. surface area, flow rate, vegetation density), and other wetland parameters concerning chemical fate (n = 24; e.g. vegetation organic carbon to octanol equivalency factor, water content in vegetation, growth rate of vegetation, rate of sediment accretion). The average elementary effects (μ^*) for these categories are 6.3%, 6.6%, 12.6%, and 4.2%, respectively. This implies that wetland design and operation are, on average, the most important parameters to treatment efficiency. Treatment efficiency for a free water surface flow wetland can be improved through intentional design and operation. The treatment wetland presented here may be used to assess trade-offs in various wetland designs and operations and to evaluate the feasibility of current and future treatment wetland systems. Chemical properties, wastewater quality, and environmental conditions have similar average effects on wetland treatment efficiency. The treatment wetland model also may be used to evaluate the feasibility for different types of wastewater under a range of environmental conditions.

5.5.3. Model simulations to assess chemical behaviour

Figure 5-3 shows that chemicals with log K_{OW} or log D between 3.0 and 5.5 are most efficiently removed from OSPW in the Kearl Treatment wetland, with K_{AW} having little effect. Removal efficiencies of these chemicals reach 80% when transformation rates in rooting medium are 0.01 day^{-1} and transformation rates in vegetation are 0.001 day^{-1}. As these transformation rates increase, removal efficiency increases for all chemicals with log K_{OW} or log D < 6. Chemicals with log K_{OW} or log D > 6 appear unaffected by changes in transformation rates. These highly hydrophobic substances strongly sorb to organic media and are therefore not freely available for transformation or intermedia transport within the wetland. Chemical removal of these hydrophobic substances is limited to physical removal processes such as sorption which becomes less effective under steady-state conditions. Thus, even when transformations rates are fast, steady-state removal efficiency remains low. Consequently, wetland treatment is not a long-term treatment option for these highly hydrophobic contaminants. Chemicals that were found to be efficiently removed from OSPW under steady state conditions include PAHs such as anthracene, phenanthrene, and pyrene, and NAs such as $C_{16}H_{30}O_2$, $C_{18}H_{32}O_2$, $C_{19}H_{34}O_2$.

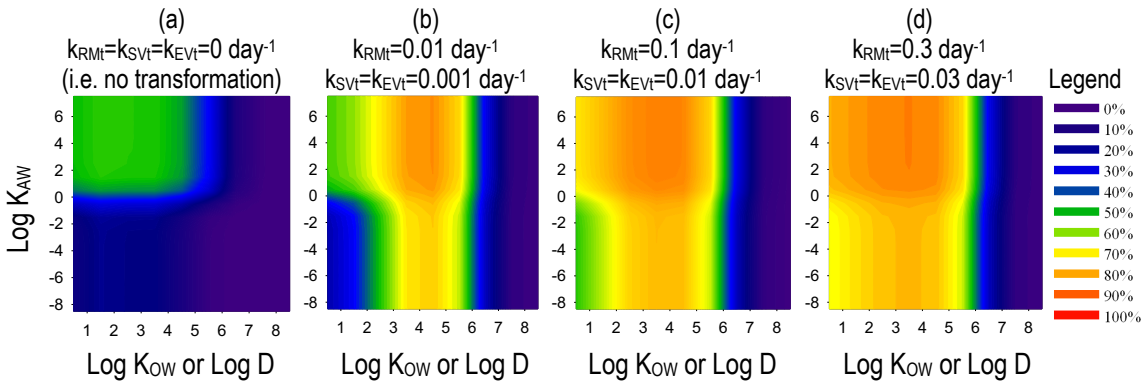

Figure 5-3: Model estimated concentration-reduction efficiency (E_C) for substances of varying D and K_{AW} where biotransformation rates in rooting media (k_{RMt}), submerged vegetation (k_{SVt}), and emergent vegetation (k_{EVt}) are a) zero (i.e. no transformation), b) 0.01 day^{-1}, 0.001 day^{-1}, and 0.001 day^{-1}, c) 0.1 day^{-1}, 0.01 day^{-1}, and 0.01 day^{-1}, d) 0.3 day^{-1}, 0.03 day^{-1}, and 0.03 day^{-1}, respectively.

Despite transformation rates increasing 30-fold from Figure 5-3b to Figure 5-3d, the maximum removal efficiency only increases from 80 to 85% for substances with a log K_{OW} or log D between 3.0 and 5.5 and log K_{AW} above 1.0. This is a product of the Kearl Treatment Wetland design. With water depths of up to 1.7 m, the water compartment contains a portion of the contaminant mass where no transformation is presumed to occur, limiting the maximum removal efficiency that can be achieved. Higher removal efficiencies can be simulated for wetlands with smaller volumes of water if hydraulic retention time stays constant since a smaller portion of contaminant mass will remain in the water. As transformation rates increase, the greatest increase in removal efficiency occurs for substances with log K_{OW} or log D less than 3.0. For example, the removal efficiency of substances with log K_{OW} or log D of 2.0 and log K_{AW} of -6.0 (e.g. $C_{14}H_{24}O_2$) increases from 59 to 80% from Figure 5-3b to Figure 5-3d. Although increases in transformation rates are found to disproportionally improve the removal of these more water-soluble substances, removal efficiency continues to be greatest for substances with log K_{OW} or log D from 3.0 to 5.5.

The overall steady-state removal efficiency illustrated in Figure 5-3 represents the cumulative removal from all biogeochemical processes within the wetland. Figure 5-3 provides a template to assess the removal of different chemicals from wastewater, and to help assess the feasibility of treatment wetlands for different types of wastewaters. Industry operators and decision-makers can determine whether a treatment wetland can offer the level of treatment required to meet specific water quality guidelines. The model

also demonstrates which removal mechanisms contribute to chemical removal from wastewaters which can be used to improve wetland design and operation to optimize these removal mechanisms.

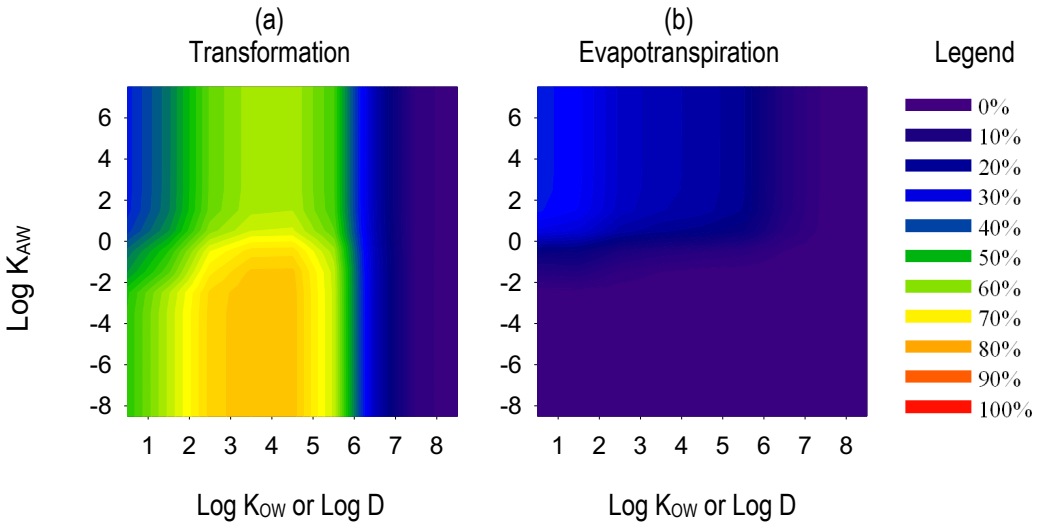

Figure 5-4: Model estimated chemical removal efficiency in the Kearl Treatment Wetland by (a) transformation and (b) evapotranspiration for a range of D and K_{AW} with biotransformation rates of 0.01 day^{-1} in rooting media and 0.001 day^{-1} in vegetation.

Figure 5-4a demonstrates the role of log K_{OW} (or log D) and log K_{AW} on chemical removal from the wetland via transformation which occurs in the rooting media, submerged vegetation, and emergent vegetation. Transformation is shown to be the dominant mechanism of chemical removal in wetlands for contaminants in OSPW, reiterating that a strong microbial community is necessary for the treatment of industrial contaminants by wetlands. For chemicals with biotransformation rates of 0.01 day^{-1} in rooting media and 0.001 day^{-1} in vegetation, total transformation in all media removes up to 80% of chemical mass from the wetland for chemicals with a log K_{OW} or log D between 3.0 and 5.5, and log K_{AW} below -1.0. This makes up essentially all of the chemical removal occurring in the wetland for these substances. For transformation to occur the chemical must partition from water to organic media whilst remaining freely available for biotransformation. When log K_{OW} or log D is below 3.0, not enough of the chemical will partition into organic media to be present for transformation, i.e. the chemical is too water soluble. When log K_{OW} or log D is above 5.5, the chemical will bind strongly to the organic media leaving little contaminant mass freely available for biotransformation (Kickham et al., 2012).

Figure 5-4b demonstrates the role of log K_{OW} (or log D) and log K_{AW} on chemical removal from the wetland via evapotranspiration. Evapotranspiration is not a significant mechanism for removal for a large range of chemicals and is insensitive to log K_{OW} or log D when K_{AW} is less than 10 (log K_{AW} = 1). When K_{AW} is greater than 10 and log K_{OW} or log D is less than 3.0, evapotranspiration contributes up to 40% of total chemical removal from the wetland. However, among the OSPW contaminants included in this study, the highest K_{AW} is approximately 0.02 for PAHs (2-methylnaphthalene), and 0.0002 for NAs ($C_{16}H_{32}O_2$) at a pH of 7. Therefore, evapotranspiration for OSPW contaminants is not expected to significantly contribute to chemical removal in the Kearl Treatment Wetland.

Chemical removal via volatilization exceeds transpiration for 92% of chemicals represented in Figure 5-4, i.e. with log K_{OW} or log D from 0.5 to 8.5 and log K_{AW} from -8.0 to 6.0. Chemical removal via transpiration is greater than volatilization only for chemicals with log K_{OW} or log D less than 4.0 and log K_{AW} between -1.0 and -4.0. These substances are capable of transpiration because a substantial portion remains freely available in the wetland for transport through vegetation. Many NAs meet these criteria for log D and log K_{AW}, suggesting that transpiration outperforms volatilization for many NAs, and further demonstrates the importance of vegetation in treatment wetland systems.

Figure 5-5 illustrates the model-estimated removal via evapotranspiration and transformation in rooting medium, submerged vegetation, and emergent vegetation for two PAHs (pyrene and retene) and two O_2-NAs ($C_{13}H_{20}O_2$ and $C_{15}H_{30}O_2$) in the Kearl Treatment Wetland. The cumulative removal from these processes represent the overall chemical removal from OSPW for these chemicals in the Kearl Treatment Wetland. Contaminants all have different chemical fate within wetlands and are each subject to different combinations of mechanisms for removal from wastewater. For pyrene, retene, and $C_{15}H_{30}O_2$, biotransformation in the rooting media is shown to be the dominant mechanism of removal in wetlands. Rooting media in the wetland includes biofilm where microbial activity is high. Biofilm has been that has been found to play a significant role in chemical fate and degradation for many industrial applications (Nicolella et al., 2000; Kim et al., 2002; Shore et al., 2012; Weber, 2016; Hassani et al., 2014). To properly develop and implement treatment wetlands for industries like oil and gas, continued

research is needed to better understand the dynamics of chemical fate and biodegradation of PAHs and NAs in biofilm.

Transformation in emergent vegetation is shown to occur for $C_{13}H_{20}O_2$. With a log D of 1.089 at a pH of 7. $C_{13}H_{20}O_2$ experiences very little partitioning from water to rooting medium, and instead accumulates in the emergent vegetation. This process of accumulation is slow, with the t_{95} for $C_{13}H_{20}O_2$ in emergent vegetation of 6,180 days. However, once steady state is achieved the accumulated chemical mass in the emergent vegetation results in the removal of 13% of chemical mass via transformation, even when biotransformation rates are low (k_{EVt} = 0.0005 day^{-1}).

These model simulations help to demonstrate the complex fate of contaminants in wetlands. Chemical removal occurs through a series of mechanisms that each contribute to chemical removal from wastewater to remove a wide array of different contaminants. With the help of this model, we can further investigate how we may better design and operate these wetlands to promote important mechanisms of removal in wetlands and adapt to site-specific wastewater challenges.

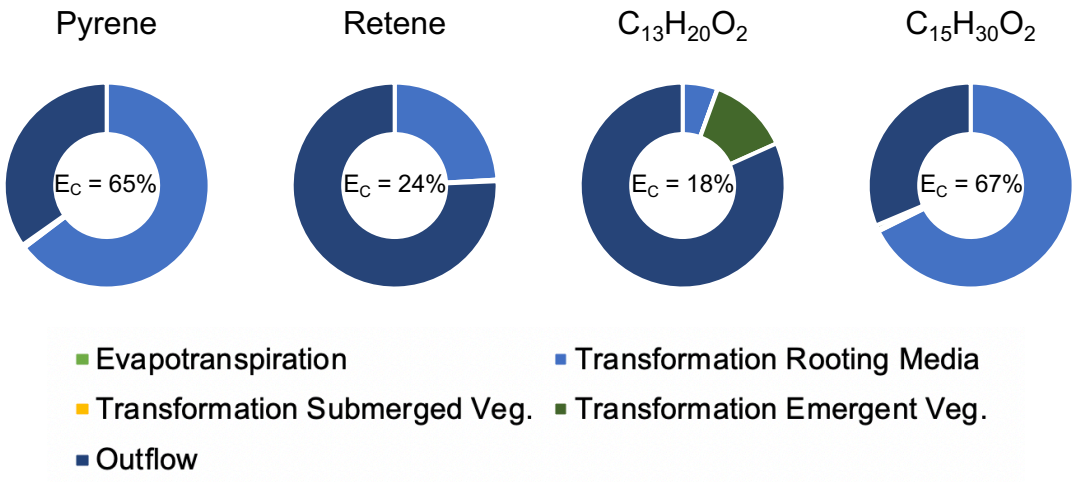

Figure 5-5: Model estimated chemical removal by removal mechanism for two PAHs and two O_2-NAs from the Kearl Treatment Wetland. Outflow represents the fraction remaining in the outflowing wastewater. E_C represents the total reduction in chemical concentration in the wetland from all removal processes.

5.6. Conclusions

A mechanistic model was developed to understand the fate of neutral and polar organic contaminants in treatment wetlands. The model was tested and evaluated with concentration measurements of polycyclic aromatic hydrocarbons (Chapter 3) and naphthenic acids (Chapter 4) in OSPW introduced into the Kearl Treatment Wetland. Model performance evaluation shows low systematic bias in model estimates for the calibrated model which uses Arrhenius and Q_5 temperature-correction models for abiotic (e.g. sorption) and biotic (e.g. microbial degradation) processes, respectively.

Model sensitivity to parameters of wetland design and operation suggests treatment wetlands can be intentionally designed to optimize chemical removal efficiency. Factors that influence hydraulic retention time in the wetland are particularly sensitive for treatment efficiency. The model provides industry operators with a tool to assess trade-offs in wetland design and operation. This will be useful to evaluate the feasibility of treatment wetlands as an alternative treatment technology in various industrial applications.

Total chemical transformation from the wetland was found to be greatest for substances with a log K_{OW} or log D between 3.0 and 5.5, but chemicals with a log K_{OW} or log D > 6.0 are not suitable for wetland treatment. Transformation is shown to play an important role in contaminant removal in wetlands which primarily occurs in rooting media biofilm. Chemical removal via evapotranspiration is highest for chemicals with a log K_{AW} greater than 1.0 and log K_{OW} or log D less than 3.0. However, the OSPW contaminants modelled in this study do not exceed a log K_{AW} of -1.67 and therefore evapotranspiration is not expected to significantly contribute to OSPW remediation.

5.7. References

Ajaero, C., Peru, K. M., Simair, M., Friesen, V., O'Sullivan, G., Hughes, S. A., … Headley, J. V. (2018). Fate and behavior of oil sands naphthenic acids in a pilot-scale treatment wetland as characterized by negative-ion electrospray ionization Orbitrap mass spectrometry. *Science of The Total Environment*, *631–632*, 829–839. https://doi.org/10.1016/J.SCITOTENV.2018.03.079

Alharbi, H. A., Morandi, G., Giesy, J. P., & Wiseman, S. B. (2016). Effect of oil sands process-affected water on toxicity of retene to early life-stages of Japanese medaka (Oryzias latipes). *Aquatic Toxicology*, *176*, 1–9. https://doi.org/10.1016/j.aquatox.2016.04.009

Arnot, J.A., and Gobas, F.A.P.C. (2004). A food web bioaccumulation model for organic chemicals in aquatic ecosystems, *Environmental Toxicology and Chemistry*, *23*, 2343–2355.

Batty, L. C., & Younger, P. L. (2004). Growth of Phragmites australis (Cav.) Trin ex. Steudel in mine water treatment wetlands: Effects of metal and nutrient uptake. *Environmental Pollution*, *132*(1), 85–93. https://doi.org/10.1016/j.envpol.2004.03.022

Campolongo, F., & Saltelli, A. (1997). Sensitivity analysis of an environmental model: an application of different analysis methods. *Reliability Engineering & System Safety*, *57*(1), 49–69. https://doi.org/10.1016/S0951-8320(97)00021-5

Canadian Council of Ministers of the Environment (CCME) (1999). Canadian water quality guidelines for the protection of aquatic life: Introduction. In: Canadian environmental quality guidelines, 1999, Canadian Council of Ministers of the Environment, Winnipeg

Cancelli, A. M., Gobas, F. A. P. C., Qian, W., Kelly, B. C. (2019). Development and evaluation of a mechanistic model to assess the fate and removal efficiency of hydrophobic organic contaminants in horizontal subsurface flow treatment wetlands. *Water Research*, 151, 183-192. https://doi.org/10.1016/j.watres.2018.12.020

Chazarenc, F., Merlin, G., & Gonthier, Y. (2003). Hydrodynamics of horizontal subsurface flow constructed wetlands. *Ecological Engineering*, *21*, 165–173. https://doi.org/10.1016/j.ecoleng.2003.12.001

Chen, H., & Tian, H. Q. (2005). Does a general temperature-dependent Q10 model of soil respiration exist at biome and global scale? *Journal of Integrative Plant Biology*, *47*(11), 1288–1302. https://doi.org/10.1111/j.1744-7909.2005.00211.x

Chen, S., Wang, G.T., and Xue, S.K. (1999). Modeling BOD removal in constructed wetlands with mixing cell method. *Journal of Environmental Engineering* 125:64–71.

Clark, B., Henry, J.G., Mackay, D. (1995). Fugacity Analysis and Model of Organic Chemical Fate in a Sewage Treatment Plant. *Environmental Science and Technology. 29*, 1488-1494.

Collier, T. K., Anulacion, B. F., Arkoosh, M. R., Dietrich, J. P., Incardona, J. P., Johnson, L. L., … Myers, M. S. (2013). Effects on Fish of Polycyclic Aromatic Hydrocarbons (PAHs) and Naphthenic Acid Exposures. *Fish Physiology*, *33*, 195–255. https://doi.org/10.1016/B978-0-12-398254-4.00004-2

Fasnacht, M.P., Blough, N.V. (2002). Aqueous Photodegradation of Polycyclic Aromatic Hydrocarbons. *Environmental Science and Technology*. *36* (20), 4364-4369. https://doi.org/10.1021/es025603k.

Frank, R.A., Kavanagh, R., Kent Burnison, B., Arsenault, G., Headley, J.V., Peru, K.M., Van Der Kraak, G., Solomon, K.R. (2008). Toxicity assessment of collected fractions from an extracted naphthenic acid mixture. *Chemosphere* 72:1309–1314. http://dx.doi.org/10. 1016/j.chemosphere.2008.04.078.

García, J., Chiva, J., Aguirre, P., Alvarez, E., Sierra, J.P., Mujeriego, R. (2004). Hydraulic behaviour of horizontal subsurface flow constructed wetlands with different aspect ratio and granular medium size. *Ecological Engineering, 23*, 177-187.

Hassani, A. H., Borghei, S. M., Samadyar, H., & Ghanbari, B. (2014). Utilization of moving bed biofilm reactor for industrial wastewater treatment containing ethylene glycol: kinetic and performance study. *Environmental Technology*, *35*(4), 499–507. https://doi.org/10.1080/09593330.2013.834947

Hijosa-Valsero, M., Matamoros, V., Sidrach-Cardona, R., Martín-Villacorta, J., Bécares, E., & Bayona, J. M. (2010). Comprehensive assessment of the design configuration of constructed wetlands for the removal of pharmaceuticals and personal care products from urban wastewaters. *Water Research*, *44*(12), 3669–3678. https://doi.org/10.1016/j.watres.2010.04.022

Hilal, S. H., Karickhoff, S. W., & Carreira, L. A. (2004). Prediction of the solubility, activity coefficient and liquid/liquid partition coefficient of organic compounds. *QSAR and Combinatorial Science*, *23*(9), 709–720. https://doi.org/10.1002/qsar.200430866

Huang, R., Chelme-Ayala, P., Zhang, Y., Changalov, M., & Gamal El-Din, M. (2017). Investigation of dissociation constants for individual and total naphthenic acids species using ultra performance liquid chromatography ion mobility time-of-flight mass spectrometry analysis. *Chemosphere*, *184*, 738–746. https://doi.org/10.1016/j.chemosphere.2017.06.067

Islam, M. S., Zhang, Y., McPhedran, K. N., Liu, Y., & Gamal El-Din, M. (2016). Mechanistic investigation of industrial wastewater naphthenic acids removal using granular activated carbon (GAC) biofilm based processes. *Science of the Total Environment*, *541*, 238–246. https://doi.org/10.1016/j.scitotenv.2015.09.091

Kadlec, R., and Wallace, S. (2009). *Treatment Wetlands* (2nd ed.). Boca Raton, FL: Taylor & Francis Group.

Kickham, P., Otton, S.V., Moore, M.M., Ikonomou, M.G., Gobas, F.A.P.C. (2012). Relationship between biodegradation and sorption of phthalate esters and their metabolites in natural sediments. *Environmental Toxicology and Chemistry, 31* (8), 1730e1737.

Kim, T. H., Park, C., Lee, J., Shin, E. B., & Kim, S. (2002). Pilot scale treatment of textile wastewater by combined process (fluidized biofilm process-chemical coagulation-electrochemical oxidation). *Water Research*, *36*(16), 3979–3988. https://doi.org/10.1016/S0043-1354(02)00113-6

Knight, R. L., Kadlec, R. H., & Ohlendorf, H. M. (1999). The use of treatment wetlands for petroleum industry effluents. *Environmental Science and Technology*, *33*(7), 973–980. https://doi.org/10.1021/es980740w

Li, C., Fu, L., Stafford, J., Belosevic, M., & Gamal El-Din, M. (2017). The toxicity of oil sands process-affected water (OSPW): A critical review. *Science of the Total Environment*. https://doi.org/10.1016/j.scitotenv.2017.06.024

Mackay, D. (2001). *Multimedia environmental models: The fugacity approach, second ed*. Taylor & Francis Group, Boca Raton, FL.

Mackay, D., Paterson, S., Joy, M. (1983). A Quantitative Water, Air, Sediment Interaction (QWASI) Fugacity Model for Describing the Fate of Chemicals in Rivers. *Chemosphere 12*, 1193-1208.

Mayo, A.W., and Bigambo, T. (2005). Nitrogen transformation in horizontal subsurface flow constructed wetlands: I. Model development. *Physics and Chemistry of the Earth* 30:658–667.

McQueen, A. D., Hendrikse, M., Gaspari, D. P., Kinley, C. M., Rodgers, J. H., & Castle, J. W. (2017). Performance of a hybrid pilot-scale constructed wetland system for treating oil sands process-affected water from the Athabasca oil sands. *Ecological Engineering*, *102*, 152–165. https://doi.org/10.1016/j.ecoleng.2017.01.024

Morris, M.D. (1991). Factorial Sampling Plans for Preliminary Computational Experiments. *Technometrics 33*, 161-174. https://doi.org/10.2307/1269043.

Nicolella, C., Van Loosdrecht, M. C. M., & Heijnen, J. J. (2000). Wastewater treatment with particulate biofilm reactors. *Journal of Biotechnology*. 80(1): 1-33, https://doi.org/10.1016/S0168-1656(00)00229-7

Page, D., Dillon, P., Mueller, J., & Bartkow, M. (2010). Quantification of herbicide removal in a constructed wetland using passive samplers and composite water quality monitoring. *Chemosphere*, *81*(3), 394–399. https://doi.org/10.1016/j.chemosphere.2010.07.002

Quesnel, D. M., Bhaskar, I. M., Gieg, L. M., & Chua, G. (2011). Naphthenic acid biodegradation by the unicellular alga Dunaliella tertiolecta. *Chemosphere*, *84*(4), 504–511. https://doi.org/10.1016/j.chemosphere.2011.03.012

Saltelli, A., Ratto, M., Tarantola, S., & Campolongo, F. (2005). Sensitivity analysis for chemical models. *Chemical Reviews*, *105*(7), 2811–2827. https://doi.org/10.1021/cr040659d

Saltelli, A., Ratto, M., Tarantola, S., Campolongo, F. (2005). Sensitivity analysis for chemical models. *Chemical Reviews, 105* (7), 2811e2827. http://doi.org/10.1021/cr040659d.

Shi, W. Y., Zhang, J. G., Yan, M. J., Yamanaka, N., & Du, S. (2012). Seasonal and diurnal dynamics of soil respiration fluxes in two typical forests on the semiarid Loess Plateau of China: Temperature sensitivities of autotrophs and heterotrophs and analyses of integrated driving factors. *Soil Biology and Biochemistry*, *52*, 99–107. https://doi.org/10.1016/j.soilbio.2012.04.020

Shore, J. L., M'Coy, W. S., Gunsch, C. K., & Deshusses, M. A. (2012). Application of a moving bed biofilm reactor for tertiary ammonia treatment in high temperature industrial wastewater. *Bioresource Technology*, *112*, 51–60. https://doi.org/10.1016/j.biortech.2012.02.045

Sim, C. H., Quek, B. S., Shutes, R. B. E., & Goh, K. H. (2013). Management and treatment of landfill leachate by a system of constructed wetlands and ponds in Singapore. *Water Science and Technology*, *68*(5), 1114–1122. https://doi.org/10.2166/wst.2013.352

Tang, Z., Sun, X., Luo, Z., He, N., & Sun, O. J. (2018). Effects of temperature, soil substrate, and microbial community on carbon mineralization across three climatically contrasting forest sites. *Ecology and Evolution*, *8*(2), 879–891. https://doi.org/10.1002/ece3.3708

Toor, N. S., Franz, E. D., Fedorak, P. M., MacKinnon, M. D., & Liber, K. (2013). Degradation and aquatic toxicity of naphthenic acids in oil sands process-affected waters using simulated wetlands. *Chemosphere*, *90*(2), 449–458. https://doi.org/10.1016/j.chemosphere.2012.07.059

Toscano, A., Langergraber, G., Consoli, S., & Cirelli, G. L. (2009). Modelling pollutant removal in a pilot-scale two-stage subsurface flow constructed wetlands. *Ecological Engineering*, *35*, 281–289. https://doi.org/10.1016/j.ecoleng.2008.07.011

Trapp, S., & Matthies, M. (1995). Generic One-Compartment Model for Uptake of Organic Chemicals by Foliar Vegetation. *Environmental Science and Technology*, *29*(9), 2333–2338. https://doi.org/10.1021/es00009a027

Weber, K. (2016). Microbial Community Assessment in Wetlands for Water Pollution Control: Past, Present, and Future Outlook. *Water*, *8*(11), 503. https://doi.org/10.3390/w8110503

Whitman, W. (1923). Two-film theory of Gas Absorption. Chem. Metall. Eng. 29 (4).

Wynn, M. T., and Liehr, S. K. (2001). Development of a constructed subsurface-flow wetland simulation model. *Ecological Engineering* 16:519–536

Xue, J., Zhang, Y., Liu, Y., & Gamal El-Din, M. (2016). Treatment of oil sands process-affected water (OSPW) using a membrane bioreactor with a submerged flat-sheet ceramic microfiltration membrane. *Water Research*, *88*, 1–11. https://doi.org/10.1016/j.watres.2015.09.051

Yuste, J.C, Janssens, I. A., & Ceulemans, R. (2005). Calibration and validation of an empirical approach to model soil CO 2 efflux in a deciduous forest. *Biogeochemistry*, *73*(1), 209–230. https://doi.org/10.1007/s10533-004-7201-1

Yuste, J.C, Janssens, I. A., Carrara, A., & Ceulemans, R. (2004). Annual Q10 of soil respiration reflects plant phenological patterns as well as temperature sensitivity. *Global Change Biology*, *10*(2), 161–169. https://doi.org/10.1111/j.1529-8817.2003.00727.x

Zhou, T., Shi, P., Hui, D., & Luo, Y. (2009). Global pattern of temperature sensitivity of soil heterotrophic respiration (Q10) and its implications for carbon-climate feedback. *Journal of Geophysical Research: Biogeosciences*, *114*(2). https://doi.org/10.1029/2008JG000850

Chapter 6. The application of treatment wetlands for OSPW remediation in Alberta's oil sands industry

Alberta's oil sands industry faces a complex wastewater challenge – to manage and remediate oil sands process-affected water (OSPW). The current policy framework supports the innovation, development, and implementation of cost-effective water treatment technologies to manage the large volumes of OSPW produced during bitumen extraction. However, there is widespread agreement among industry operators and regulators that no single "silver-bullet" technology can solve this wastewater challenge. OSPW chemistry is too complex and on such a large scale where substantial variability in treatment needs exists between industry operators. Therefore, the industry is taking a multifaceted approach to manage the wastewater challenges created from bitumen extraction activities, to which treatment wetlands may play an important role.

The aim of this research is to determine if treatment wetlands are feasible, effective, and safe for the removal of organic contaminants in OSPW. The following sections are designed to interpret the findings presented in Chapters 2 – 5 to provide direction for the industry in the application of treatment wetlands for OSPW remediation, with these research foci in mind.

6.1. Are treatment wetlands a feasible option for OSPW remediation?

Treatment wetlands have emerged as a feasible treatment technology for many different wastewater challenges including agricultural runoff (e.g. Page et al. 2010), mine wastewater (e.g. Batty and Younger, 2004), municipal and domestic wastewater (e.g. Toscano et al., 2009), leachate (e.g. Sim et al., 2013), and petroleum refinery process water (e.g. Knight et al., 1999). The research findings presented here suggest that treatment wetlands can also be a feasible treatment option for OSPW remediation in the Alberta oil sands region. However, their feasibility depends on several factors involving: the profile of contaminants in OSPW and their physicochemical properties, wetland design and characteristics, and environmental conditions. Using the treatment wetland models developed in Chapters 2 and 5, the sensitivity of wetland treatment efficiency to these factors are explored. The following sections describe the "fit" of OSPW

contaminants for wetland treatment, optimal treatment wetland designs, and appropriate environmental conditions for their application based on model simulations. Together these demonstrate the feasibility of treatment wetland systems for OSPW remediation.

Wetland treatment of OSPW

Treatment wetland model simulations were performed to illustrate which contaminants are suitable for wetland treatment based on their: i) log K_{OW} for neutral substances or log D for ionizing substances (octanol-water partition coefficient) and ii) log K_{AW} (air-water partition coefficient). The findings suggest that removal efficiency in treatment wetlands are greatest for chemicals with a log K_{OW} or log D between 3.0 and 5.5 and log K_{AW} greater than 1.0 (i.e. $K_{AW} > 10$). Chemicals with a log K_{OW} or log D between 3.0 and 5.5 provide a balance between hydrophobic (high log K_{OW}) and hydrophilic (low log K_{OW}) tendencies. This balance permits chemical partitioning from the wetland water to adjacent organic wetland media but prevents the chemical from binding too strongly which would inhibit biotransformation or further intermedia transport of the chemical. This range of log K_{OW} or log D includes 30% of the PAHs and 42% of the O2-NAs that were detected in this research (Chapters 3 and 4) suggesting many OSPW chemicals may be suitable for wetland treatment. Some examples of these chemicals in OSPW include PAHs like phenanthrene and methylnaphthalene, and NAs like $C_{15}H_{30}O_2$ and $C_{20}H_{34}O_2$. Chemicals with a log K_{OW} (or log D) greater than 6.0 are not suitable for wetland treatment due to their high capacity for sorption to organic media, and small fraction freely available for chemical transformation and transportation within the wetland. Chemicals with a K_{AW} greater than 10 are shown to be susceptible to evapotranspiration from wetlands. However, the organic contaminants in OSPW detected in this research do not exceed a K_{AW} of 0.02 (1-methylnaphthalene) and therefore evapotranspiration is not expected to significantly contribute to OSPW treatment.

Model simulations indicate that biotransformation is the primary mechanism of removal of OSPW contaminants in treatment wetlands. Even biotransformation rates as low as 0.01 day^{-1} in rooting media and 0.001 day^{-1} in vegetation can result in a removal efficiency of 80% in treatment wetlands. However, external sources suggest faster biotransformation rates in wetland media for 61% of the PAHs and 88% of the O2-NAs detected in OSPW in this research (Han et al., 2009; U.S. EPA, 2013 (EPISuite v4.11);

Ajaero et al., 2018). Faster biotransformation rates imply removal efficiencies in the wetland can exceed 80%, suggesting many contaminants in OSPW are susceptible to wetland treatment.

When biotransformation rates are slow, physical removal mechanisms such as sorption to suspended and settled sediment can also contribute to contaminant removal from wastewater in wetlands. Monitoring chemical fate in the Kearl Treatment Wetland shows that turbidity is positively correlated with the total concentration of contaminants in OSPW. As OSPW flows through the wetland turbidity decreases as particulates settle out. The fraction of contaminants sorbed to those particulates are removed from OSPW causing chemical concentrations in OSPW to decrease. For recalcitrant contaminants, this can be an effective mechanism of removal. However, sorption primarily occurs for hydrophobic contaminants (high log K_{OW} or log D), and the net flux of chemical removal through sorption and sedimentation decreases as the system approaches steady-state. For PAHs and NAs, the time needed to reach 95% of steady-state in the water compartment of the Kearl Treatment Wetland is 5.6 (SD 0.11) and 5.4 (SD 0.09) days, respectively, suggesting that the long-term contribution of sorption is not a viable nor consistent mechanism of removal in treatment wetlands. Hydrophobic and recalcitrant substances therefore are not ideal for wetland treatment, although removal may still be rapid until steady-state conditions are achieved.

Chemicals with hydrophilic tendencies remain mostly in the aqueous phase. Therefore, concentrations of these contaminants in the wastewater go relatively unchanged through the wetland, resulting in relatively low removal efficiencies. Many organic acids such as naphthenic acids exhibit this trait. However, the partitioning behaviour of these chemicals can be modified since the log D of these substances is inversely proportional to pH. Meaning that the removal efficiency of naphthenic acids with low log D (i.e. log D < 3.0) may increase if pH is lowered to support greater partitioning of the chemical from water to wetland media. In some cases, this could increase log D to within the optimal range for chemical removal in treatment wetlands (i.e. log D: 3.0 to 5.5). The treatment wetland model can be used to explore the effects of pH on removal efficiency by inputting log D that correspond with different pH levels. This may be useful since OSPW from bitumen extraction tends to be more basic due to the caustic agents often added to the extraction process to improve bitumen recovery (Allen, 2008). If the pH of OSPW remains high and naphthenic acids are highly soluble in water,

wetland treatment may not be feasible for the removal of these chemicals. In some cases, chemical additives might be useful to lower pH, but may not be desirable or feasible in industrial settings. Options to improve the removal of these chemicals may then rely on wetland design and operation.

Factors in wetland design and operation

Flow rate through the wetland, surface area of the wetland, vegetation density, and size of the vegetation were consistently among the most sensitive design and operational parameters affecting pollutant removal efficiency. This suggests that future treatment wetlands can be designed and operated in ways that enhance removal efficiency of organic contaminants by optimizing these parameters for specific applications of treatment wetlands.

The flow rate of water and surface area of the wetland are the primary operational and design parameters to influence chemical removal in wetlands (Knight et al., 1999; Chazarenc et al., 2003; Garcia et al., 2004; Hijosa-Valsero et al., 2010; Pavlineri et al, 2017). The influence from these parameters demonstrates the principle element required for wetland treatment: time. Longer retention times (i.e. slower flow rates or greater surface areas) of water in the wetland allow for greater exposure to wetland removal mechanisms. Model simulations show that by reducing the flow rate of OSPW through the Kearl Treatment Wetland from 5 L/s to 1 L/s the removal efficiency of pyrene increases from 63 to 98%. However, the application of treatment wetlands in an industrial setting requires a balance between treatment efficiency, surface area (land-use), and flow rate (volume of wastewater treated per unit time). The treatment wetland models presented in this research are intended to help industry operators evaluate these trade-offs in design and operation while keeping site-specific treatment objectives in mind (e.g. CCME, 1999).

The sensitivity of removal efficiency to vegetation density and size suggests that a healthy and productive vegetative community in the wetland is vital to treatment. A community of dense and fast-growing vegetation provides a large wetland compartment for chemical accumulation and plant-mediated degradation. Productive wetland vegetation also supports an active microbial community. Macrophytes such as *Phragmites*, *Typha*, *Juncus*, *Spartina* and *Scirpus* have shown to be ideal for treatment

wetlands because they create rhizospheres that support an active and dynamic zone for the microbial degradation (Brix, 1993; Han et al., 2008; Jung et al., 2008; Kadlec and Wallace, 2009; Bhatia and Goyal, 2014; Ajaero et al., 2018). The intimate symbiosis between vegetation and microbes in wetlands is a fundamental interaction in treatment wetlands that should be supported by the design and operation of the wetland.

Other design features may offer ways to enhance chemical removal. For example, aeration can replenish dissolved oxygen in the wetland water and improve the capacity for oxidation of OSPW chemicals – the primary mechanism of biodegradation for naphthenic acids (Quagraine et al., 2005; Han et al., 2008). At the Kearl Treatment Wetland, interior berms were constructed between wetland cells to passively re-aerating the water as it flows through the wetland. Mechanical aerators can also be integrated into wetland designs to increase dissolved oxygen levels if a mechanical solution is required. These intentional designs can promote wetland biotransformation and increase treatment efficiency.

Effects of environmental conditions

Water temperature has been shown to affect wetland biogeochemical processes. In certain instances, abiotic processes such as sorption are shown to be inversely proportional to temperature whereas biotic processes such as biotransformation are found to be proportional to temperature. Therefore, operation throughout different seasons may support different mechanisms of removal. Readily biotransformed substances will be more efficiently removal in warmer conditions, whereas hydrophobic and recalcitrant substances will exhibit greater removal in colder conditions. Since biotransformation is considered the primary mechanism for removal of OSPW contaminants, the feasibility of treatment wetlands is often presumed to be limited to summer operation. Further research on the operation of treatment wetlands under a range of environmental temperatures is needed to assess their feasibility for OSPW remediation in the Alberta oil sands region.

Precipitation and evapotranspiration have also been shown to influence treatment efficiencies. Precipitation will dilute contaminants in the wetland whereas evapotranspiration can concentrate contaminants in the wetland. Dilution from precipitation will reduce chemical concentrations in OSPW which may satisfy specific

water quality guidelines even if little of the contaminant mass has been removed. Conversely, evapotranspiration may remove contaminant mass from the wetland, but little change to concentration may be observed if water loss balances mass removal. This would help to satisfy treatment objectives designed to limit contaminant loading (i.e. mass of chemical per day) on the environment but may not be an effective system for meeting effluent concentration guidelines. Therefore, the water balance at the wetland is an important consideration when assessing wetland treatment performance. Generally, a balanced water budget with high rates of precipitation to reduce chemical concentrations, and high evapotranspiration to offer a mechanism of chemical removal from the wetland is ideal.

6.2. Are treatment wetlands effective and safe on a commercial scale?

Several studies have demonstrated the treatment of OSPW contaminants in wetland environments (e.g. Machate et al., 1997; Terzakis et al. 2008; Toor et al., 2013; Hendrikse et al., 2018; McQueen et al., 2017; Ajaero et al., 2018). The research presented here is the first to investigate a large-scale (1 ha) constructed treatment wetland situated within the Alberta oil sands region. The Kearl Treatment Wetland is a surface flow treatment wetland on the Kearl Oil Sands mining site. Mechanisms of microbial degradation, plant-enzyme mediated reactions, sorption, settling, and evapotranspiration were shown to reduce total PAH and NA concentrations in OSPW from 54 to 83%, and from 7.5 to 69%, respectively (Chapters 3 and 4).

Similar treatment efficiencies have been observed for PAHs and NAs in other treatment wetland studies. For example, Terzakis et al. (2008) report a concentration-reduction of 56% in the combined sum of 16 PAHs after 24-hours in a pilot-scale surface flow wetland (Greece), and Machate et al. (1997) demonstrate a 99% reduction in the concentration of phenanthrene in artificial wastewater after 14 days in a pilot-scale vertical flow constructed wetland (Germany). Toor et al. (2013) measured a 74% reduction in the total NA concentration in a simulated wetland microcosm with a hydraulic retention time of 400 days (University of Saskatchewan). Recently, Hendrikse et al. (2018) measured a 19% reduction in total NA concentration after 16 days retention in a pilot-scale constructed wetland treating Suncor and Syncrude OSPW (Clemson University), and Ajaero et al. (2018) found removal efficiencies of NAs ranging from 57 to

88% after 27 days in constructed wetland microcosms (Saskatchewan, Canada). Similar removal efficiencies between these pilot-scale wetlands and the Kearl Treatment Wetland suggest treatment wetlands can be scaled to commercial-use while maintaining their treatment efficiencies for OSPW contaminants.

When compared to natural attenuation in tailings ponds, the half-life of NAs in wetlands are substantially reduced. In tailings ponds, $t_{1/2}$ of NAs has been measured on the order of 12.9 to 13.6 years (Han et al., 2009). Under laboratory conditions with aerobic biodegradation, $t_{1/2}$ estimates were found to decrease to 44 – 240 days for industry OSPW containing a mixture of NAs (Han et al., 2008; Mahdavi et al., 2015). In the Kearl Treatment wetland, the $t_{1/2}$ of NAs ranged from 11 – 186 days in 2018 and 9 – 76 days in 2019 suggesting that treatment wetland enhance chemical removal compared to tailings ponds and laboratory experiments and offer an effective treatment option for OSPW.

The safe operation of treatment wetlands ensures both endemic and visiting wetland biota are not adversely affected by the OSPW in the wetland. To assess risks to biota, the treatment wetland model can be used to compare estimated concentrations of contaminants in wetland media to thresholds for toxic effects. Understanding these thresholds for toxic effects on endemic wetland biota (e.g. microbes, vegetation) can help identify limits for OSPW contamination and identify wastewaters that are too toxic for wetlands, i.e. cause adverse effects on wetland performance. The treatment wetland model can also be used to assess ecological risk to visiting wetland biota, or biota in an environment receiving wetland discharge (e.g. frogs, fish, birds). This use of the model will help support industry operators in the safe operation of treatments wetland and safe release of treated OSPW. Further research is needed to establish these toxicological thresholds for OSPW contaminants for this model application.

The reduction in toxicity related to PAHs in OSPW entering the Kearl Treatment Wetland can be determined from a chemical activity approach with passive sampling to provide better representation of multiple contaminants (Chapter 3). Acute toxicity was not expected at the concentrations of PAHs measured in OSPW entering the wetland. Hence, a toxicity reduction as result of wetland treatment was not determined in this work. If influents with higher concentrations of PAHs are used, treatment may cause a toxicity reduction that can be monitored using a passive sampling approach and

quantified with chemical activity. Bulk OSPW toxicity was estimated for acid-extractable organics using a biomimetic extraction technique (Chapter 4). Acute lethality related to NAs is not expected from OSPW exposure, however the estimated *D. Rerio* % deformity (96-hr) reduced from 50% for untreated OSPW to 16% for OSPW after 14 days in the wetland. Reductions in wastewater toxicity by wetland treatment have also been demonstrated in Toor et al. (2013) where the (96-hr) LC50 for rainbow trout in untreated OSPW was 67.2% of pure OSPW, and after 40 days in a simulated wetland no more lethality was observed (i.e. LC50 > 100% OSPW).

The toxicity of NAs has been shown to correlate with carbon number (Frank et al., 2010; Hughes et al., 2017). Higher molecular weight NAs elicit a greater toxic response compared to lower molecular weight NAs because of their low aqueous solubility and affinity for biota lipids, the presumed site of toxic action for NAs. The removal efficiency of NAs in the Kearl Treatment Wetland was found to be greatest for these more toxic, higher molecular weight NA congeners. This is a promising discovery that suggests OSPW effluent may become safer to discharge following wetland treatment. This is valuable to industry operators and environmental regulators to demonstrate the feasibility of treatment wetlands and to assess the risk of discharging treated wastewater into the environment.

6.3. What are the next steps towards implementation of this technology into the oil sands industry?

Moving towards implementation of treatment wetlands in the oil sands industry requires further investigation into certain aspects of treatment wetland design and operation. This is needed to better understand the merits and limitations of treatment wetland technology for treating pure fluid tailings water in the Alberta oil sands region.

To reach this level of treatment, the effects of higher PAH and NA concentrations and the presence of non-target pollutants on wetland productivity must be investigated. The quantity and concentration of these pollutants may have a toxic effect on vegetation and microbes that may hinder chemical removal from OSPW. Understanding whether treatment wetlands can be an effective treatment option for higher concentrations of contaminants will determine the full potential of treatment wetlands within the oil sands industry.

The fate of other OSPW pollutants and their effect on wetland biogeochemistry should also be investigated to assess their impacts on treatment efficiency. This extends to dissolved solids such as salts, and naphthenic acid fraction compounds. Dissolved solids such as salts are common in OSPW at variable concentrations and have been found to affect the productivity of plants and microorganisms at higher concentrations (Liang et al., 2017). Naphthenic acid fraction compounds include oxidized NAs (e.g. O_3- and O_4-NAs), hydroxylated species, nitrogen-containing and sulfur-containing species, aromatic and unsaturated compounds (Headley et al., 2013). The composition of naphthenic acid fraction compounds illustrates the complexity of OSPW chemistry. Further investigation into their fate in wetlands will help to better understand OSPW toxicity and toxicity-reduction through treatment wetlands.

The temperature effects on wetland biogeochemistry demonstrated in this work means that the performance of treatment wetlands in the northern Canadian climate is of interest. The Kearl Treatment Wetland has not operated from October through to April, and therefore the operation in low temperatures must be investigated to properly evaluate limitations of wetland treatment for the industry. Results may suggest that treatment be limited to summer to ensure conditions can support biotransformation, and winter be used for wastewater collection only.

It may be possible to improve wetland treatment efficiency of OSPW contaminants by integrating design features that promote mechanisms of removal for recalcitrant contaminants. For example, McQueen et al. (2017) has shown promising results for a photocatalytic reactor integrated with a free water surface wetland to increase removal of NAs by 47 – 93 %. Other wetland systems have integrated mechanisms for aeration and ozonation (Wang et al., 2013), bioaugmentation with bacteria, biostimulation with nutrients and cofactors for microbial degradation, and the addition of materials such as clays to promote flocculation of contaminants with bacteria (Quagraine et al., 2005). These methods may help to improve degradation rates of OSPW contaminants that are difficult to remove through passive wetland treatment. This may be particularly important in the treatment of pure effluent tailings water if chemical removal mechanisms are insufficient at reducing concentrations in highly contaminated wastewater. Research in this area is ongoing but will require continued efforts to determine the commercial viability of these methods for meeting treatment objectives in OSPW remediation.

Continued research into the different treatment technologies for OSPW remediation requires some evolution of the current policy framework to prescribe effluent quality guidelines for pollutant concentrations in treated effluents. Without these guidelines, industry operators lack clear treatment objectives making it difficult to fully assess the feasibility of different treatment solutions. Although deriving these effluent quality guidelines has been a major challenge due to the complex chemistry of OSPW, these guidelines are needed to represent targets for the industry that reflect safe concentrations for effluent discharge. To do this, better methods are needed to translate bulk OSPW concentration to toxicity and risk. One current method uses biomimetic extraction of OSPW contaminants. This method was developed by the ExxonMobil Biomedical Sciences Laboratory (New Jersey, USA; Redman et al., 2018) and also performed in this research (Chapter 4). Through biomimetic extraction, a single bulk OSPW equivalent concentration can be derived that corresponds with toxic effects reported in Redman et al. (2018). Deriving bulk OSPW toxicity eliminates the uncertainties from evaluating each individual contaminant in OSPW. This approach may be useful in developing a single effluent quality guideline for bulk OSPW that permits the safe release of treated OSPW.

As we continue to pursue the application and implementation of treatment wetlands for industrial wastewater, our understanding of these complex ecological systems is likely to improve. An adaptive management approach to investigating treatment wetlands will continue to provide a strong framework for sustained learning of these complex systems and their applications. Model development has shown to play an important role in adaptive management. In this work, adaptive management was applied through model application and testing which created new, informed management actions that work towards optimization of wetland conditions to improve treatment efficiency. This involved a series of field studies to collect data on wetland performance which was used to inform the model. This was completed through a series of sampling events using passive sampling techniques, site surveys of wetland vegetation and hydraulic flow, and weather station reports of environmental conditions. The treatment wetland models for chemical fate and toxicity demonstrate the role of chemical properties, the sensitivity to environmental conditions, and the impacts from changes to wetland design and operation on treatment efficiency. In this way, the model was used to improve our

understanding of the functionality of treatment wetlands and to create new management actions.

In our efforts to further understand the role of treatment wetlands for OSPW remediation, continued monitoring and assessment is needed to support continued learning of these complex systems. In future work, adaptive management will play an important role when learning of the potential effects on wetland performance under various scenarios, including different environmental conditions, and different wastewater sources and constituents of concern. The continuation of this work will undoubtedly require further iterations of the adaptive management cycle. Continued efforts in the science, policy, and management of treatment wetlands may help guide the oil sands industry towards more sustainable operations. The role of adaptive management is, and will continue to be, an important factor in sustainable development.

6.4. References

Ajaero, C., Peru, K. M., Simair, M., Friesen, V., O'Sullivan, G., Hughes, S. A., … Headley, J. V. (2018). Fate and behavior of oil sands naphthenic acids in a pilot-scale treatment wetland as characterized by negative-ion electrospray ionization Orbitrap mass spectrometry. *Science of The Total Environment*, *631–632*, 829–839. https://doi.org/10.1016/J.SCITOTENV.2018.03.079

Allen, E. (2008). Process water treatment in Canada's oil sands industry: I. Target pollutants and treatment objectives, *Journal of Environmental Engineering and Science*, *7*(2), 123–138. http://doi.org/10.1139/S07-038Quagraine et al., 2005;

Bhatia, M., & Goyal, D. (2014). Analyzing remediation potential of wastewater through wetland plants: A review. *Environmental Progress and Sustainable Energy*. https://doi.org/10.1002/ep.11822

Brix H. (1993) Macrophyte-mediated oxygen transfer in wetlands: Transport mechanisms and rates. In: *Constructed Wetlands for Water Quality Improvement*, Moshiri G.A. (ed.) Lewis Publishers: Boca Raton, Florida, pp. 391–398.

Canadian Council of Ministers of the Environment (CCME) (1999). Canadian water quality guidelines for the protection of aquatic life: Introduction. In: Canadian environmental quality guidelines, 1999, Canadian Council of Ministers of the Environment, Winnipeg

Chazarenc, F., Merlin, G., and Gonthier, Y. (2003). Hydrodynamics of horizontal subsurface flow constructed wetlands. *Ecological Engineering*, 21:165–173.

Cowie, B. R., James, B., & Mayer, B. (2015). Distribution of total dissolved solids in McMurray Formation water in the Athabasca oil sands region, Alberta, Canada: Implications for regional hydrogeology and resource development. *American Association of Petroleum Geologists Bulletin, 99*(1), 77-90. http://doi.org/10.1306/07081413202

Frank, R.A., Fischer, K., Kavanagh, R., Burnison, B.K., Arsenault, G., Headley, J.V., Peru, K.M., Kraak, G.V.D., and Solomon, K.R. (2008). Effect of carboxylic acid content on the acute toxicity of oil sands naphthenic acids. *Environmental Science and Technology*. 43(2), 266–271.

García, J., Chiva, J., Aguirre, P., Alvarez, E., Sierra, J. P., and Mujeriego, R. (2004). Hydraulic behaviour of horizontal subsurface flow constructed wetlands with different aspect ratio and granular medium size. *Ecological Engineering*. 23:177–187

Han, X., Mackinnon, M. D., & Martin, J. W. (2009). Estimating the in-situ biodegradation of naphthenic acids in oil sands process waters by HPLC/HRMS. *Chemosphere* 76(1): 63-70. https://doi.org/10.1016/j.chemosphere.2009.02.026

Han, X., Scott, A. C., Fedorak, P. M., Bataineh, M., & Martin, J. W. (2008). Influence of molecular structure on the biodegradability of naphthenic acids. *Environmental Science and Technology*, *42*(4), 1290–1295. https://doi.org/10.1021/es702220c

Headley, J. V, Peru, K. M., Fahlman, B., Colodey, A., & Mcmartin, D. W. (2013). Selective solvent extraction and characterization of the acid extractable fraction of Athabasca oils sands process waters by Orbitrap mass spectrometry. *International Journal of Mass Spectrometry*, *345*, 104–108. https://doi.org/10.1016/j.ijms.2012.08.023

Hendrikse, M., Gaspari, D. P., McQueen, A. D., Kinley, C. M., Calomeni, A. J., Geer, T. D., … Castle, J. W. (2018). Treatment of oil sands process-affected waters using a pilot-scale hybrid constructed wetland. *Ecological Engineering*, *115*(February), 45–57. https://doi.org/10.1016/j.ecoleng.2018.02.009

Hughes, S. A., Mahaffey, A., Shore, B., Baker, J., Kilgour, B., Brown, C., … Bailey, H. C. (2017). Using ultrahigh-resolution mass spectrometry and toxicity identification techniques to characterize the toxicity of oil sands process-affected water: The case for classical naphthenic acids. *Environmental Toxicology and Chemistry*, *36*(11), 3148–3157. https://doi.org/10.1002/etc.3892

Jung, J., Lee, S. C., & Choi, H. K. (2008). Anatomical patterns of aerenchyma in aquatic and wetland plants. *Journal of Plant Biology*, *51*(6), 428–439. https://doi.org/10.1007/BF03036065

Knight, R. L., Kadlec, R. H., & Ohlendorf, H. M. (1999). The use of treatment wetlands for petroleum industry effluents. *Environmental Science and Technology*, *33*(7), 973–980. https://doi.org/10.1021/es980740w

Liang, Y., Zhu, H., Bañuelos, G., Yan, B., Zhou, Q., Yu, X., & Cheng, X. (2017). Constructed wetlands for saline wastewater treatment: A review. *Ecological Engineering*, 98, 275–285. https://doi.org/10.1016/j.ecoleng.2016.11.005

Machate, T., Noll, H., Behrens, H., & Kettrup, A. (1997). Degradation of phenanthrene and hydraulic characteristics in a constructed wetland. *Water Research*, *31*(3), 554–560. https://doi.org/10.1016/S0043-1354(96)00260-6

McQueen, A. D., Hendrikse, M., Gaspari, D. P., Kinley, C. M., Rodgers, J. H., & Castle, J. W. (2017). Performance of a hybrid pilot-scale constructed wetland system for treating oil sands process-affected water from the Athabasca oil sands. *Ecological Engineering*, *102*, 152–165. https://doi.org/10.1016/j.ecoleng.2017.01.024

Quagraine, E. K., Peterson, H. G., & Headley, J. V. (2005). In situ bioremediation of naphthenic acids contaminated tailing pond waters in the Athabasca oil sands region - Demonstrated field studies and plausible options: A review. *Journal of Environmental Science and Health - Part A Toxic/Hazardous Substances and Environmental Engineering*, 40(3): 685-722, https://doi.org/10.1081/ESE-200046649

Redman, A. D., Parkerton, T. F., Butler, J. D., Letinski, D. J., Frank, R. A., Hewitt, L. M., … Giesy, J. P. (2018). Application of the Target Lipid Model and Passive Samplers to Characterize the Toxicity of Bioavailable Organics in Oil Sands Process-Affected Water. *Environmental Science and Technology*, *52*(14), 8039–8049. https://doi.org/10.1021/acs.est.8b00614

Terzakis, S., Fountoulakis, M. S., Georgaki, I., Albantakis, D., Sabathianakis, I., Karathanasis, A. D., … Manios, T. (2008). Constructed wetlands treating highway runoff in the central Mediterranean region. *Chemosphere*, *72*(2), 141–149. http://doi.org/10.1016/j.chemosphere.2008.02.044

Toor, N. S., Franz, E. D., Fedorak, P. M., MacKinnon, M. D., & Liber, K. (2013). Degradation and aquatic toxicity of naphthenic acids in oil sands process-affected waters using simulated wetlands. *Chemosphere*, *90*(2), 449–458. https://doi.org/10.1016/j.chemosphere.2012.07.059

Wang, N., Chelme-Ayala, P., Perez-Estrada, L., Garcia-Garcia, E., Pun, J., Martin, J. W., … Gamal El-Din, M. (2013). Impact of Ozonation on Naphthenic Acids Speciation and Toxicity of Oil Sands Process-Affected Water to Vibrio fischeri and Mammalian Immune System. *Environmental Science and Technology*, 47(12), 6518-6526. https://doi.org/10.1021/es4008195

Zhang, D., Gersberg, R. M., & Keat, T. S. (2009). Constructed wetlands in China. *Ecological Engineering*, 35(10): 1367-1378, https://doi.org/10.1016/j.ecoleng.2009.07.007

Zhi, W., & Ji, G. (2012). Constructed wetlands, 1991-2011: A review of research development, current trends, and future directions. *Science of the Total Environment*, 441: 19-27, https://doi.org/10.1016/j.scitotenv.2012.09.064

Appendix A: Chapter 2 Supplementary Information

Methods

Lorong Halus Treatment Wetland:

The substrate depth is 0.8 m and water depth (D_w) is maintained at 0.65 m in the reed beds leaving a 15 cm freeboard zone. The gravel substrate (30 -50 mm) with 35% porosity (η) acts as the rooting medium for three species of emergent vegetation: cattails (*Typha angustifolia*), vetiver grass (*Chrysopogon zizanioides*), and papyrus (*Cyperus papayrus*) (Sim et al., 2013). Contaminant concentrations the influent, effluent, vegetation roots, and vegetation leaves from RB3 (SA_{RB3} = 10,000 m^2) were obtained from Wang and Kelly (2017) for model evaluation and calibration. The volume of water (V_w) within this reed bed is: $V_w = SA_{RB3} \cdot D_w \cdot \eta = 2.23 \cdot 10^3$ m^3.

Xylem Flow:

Xylem flow rate describes the movement of water through the xylem tubules from rhizomes to the emergent parts of the plant. This process transports water and freely dissolved contaminants through the vegetation to undergo transpiration into air. Using *ET*, the xylem flow rates and transpiration through the vegetation were calculated. The transpiration-to-evaporation ratio (*T/E*) reported by Sanchez-Carillo et al. (2001) for a semi-arid, freshwater wetland in Central Spain was 0.8 for cattails, and 1.5 for reeds. The average *T/E* of 1.15 was used to estimate a total transpiration rate (Q_T) for vegetation at the LHTW of $1.3 \cdot 10^4$ m^3/yr (3.5 mm/day) based on the estimated *ET*. Xylem flow rate (Q_{wx}) is estimated using:

$$Q_{wx} = \frac{Q_T}{N_P \cdot SA_{RB3}}$$

where N_P is the stem-density of vegetation (plants/m^2), and Q_T is the transpiration rate (m^3/day) for the reed bed. Xylem flow rate (Q_{wx}, m^3/day per plant) for the wetland vegetation at the LHTW was estimated to be 0.87 L/day per plant which is similar to the values of 1.0 L/day used in Trapp and Matthies (1995) for xylem flow. The lower xylem flow rate estimated for plants at the LHTW is appropriate since these plants are of a smaller overall biomass (0.5 – 1.0 kg) compared to those described in Trapp and Matthies (1995).

Surface area of rhizomes:

The surface area of the rhizomes was calculated from an estimate of the volume of rhizomes multiplied by the rhizome surface area-to-volume ratio (*SA/V*). The area-to-volume ratio (SA/V) of the rhizomes was estimated using the formulas for SA and V for a cylinder since length and radius were available for similar vegetation. For *Typha latifolia* (broad-leaf cattails), the average radius and length of the rhizomes are approximately $8.9 \cdot 10^{-3}$ m and $6.9 \cdot 10^{-1}$ m, respectively (Rook, 2004). Therefore, *SA/V* is approximately 228 m^2/m^3. The surface area of the rhizome (SA_{Rh}) was calculated as:

$$SA_{Rh} = \left[\frac{W_{Rh} \cdot No.Plants \cdot SA_{RB}}{\rho_{veg.}}\right] \cdot \left({}^{\mathrm{SA}}/_{V_{Rh}}\right)$$

The estimated rhizome surface area available for biofilm growth and activity is $1.13 \cdot 10^4$ m^2.

Surface area of rooting medium:

Surface area of the rooting medium is determined from the capacity of the TW to contain the gravel pieces across its entire length (*l*), width (*w*), and height (*h*) of the LHTW reed bed, respectively. These dimensions are calculated from the length:width aspect ratio (α = 4), which are used to estimate the total surface area of the gravel substrate using:

$$SA_{RM} = \left[4\pi\left(\frac{G}{2}\right)^2\right] \cdot \left[\left(\frac{\sqrt{SA_{RB} \cdot \alpha}}{G}\right) \cdot \left(\frac{\sqrt{{}^{SA_{RB}}/_{\alpha}}}{G}\right) \cdot \left(\frac{D_w}{G}\right)\right]$$

where SA_{RB} is the surface area of the reed bed (10,000 m^2), and D_w is the depth of the water (m) and the depth at which biofilm is active.

Surface area-to-volume ratio of emergent vegetation:

The *SA/V* for the leaves of the vegetation was estimated using the data reported by Roderick et al. (2000) for measurements of SA/V for *Eucalyptus* spp. The *SA/V* ratio was estimated to be approximately 400 m^2/m^3.

Physicochemical properties:

Henry's law constant (*H*; Pa·m^3/mol) was derived from the partition coefficients using:

$$H = \left[\frac{K_{OW}}{K_{OA}}\right] \cdot RT$$

where *R* is the universal gas constant (8.314 m^3·Pa/K·mol) and *T* is temperature (K). The organic carbon-water partition coefficient (K_{OC}) was estimated using the derived relationship with log K_{OW}, from Gerstl (1990) where:

$$logK_{OC} = 0.679 logK_{OW} + 0.663$$

Transformation rates:

The Biowin predictions use a series of different modelling approaches to evaluate the probability of a chemical to be readily biodegradable in the environment. The results of this model are qualitative, and do not provide estimates for half-life times. However, the results describe the potential for biodegradation of the contaminant based on QSAR models programmed into EPISuite (U.S. EPA, 2013)

Evapotranspiration rates:

ET was calculated using the Penman-Monteith equation which derives *ET* using meteorological data. This data was obtained from weather stations in the Changi region of Singapore (the LHTW), and at Fort MacMurray in Alberta, Canada (the CCTW). Table B.6 provides the full parameterization of the meteorological data required for this calculation.

$$ET = \frac{1}{\rho_w \lambda} \cdot \frac{\Delta(R_n - F) + \rho_a c_p (\frac{e_s - e_a}{r_a})}{(\Delta + \gamma \left(1 + \frac{r_s}{r_a}\right))}$$

Sensitivity Analysis:

The sensitivity of 50 parameters (*N* = 50) was evaluated by their individual effects on mass removal efficiency (E_L), using a method developed by Morris (1991). This method is useful to determine whether the effects of the input parameters are (a) negligible, (b) linear and additive, or (c) non-linear or involved in interactions with other parameters (Campolongo and Saltelli, 1997; Saltelli et al., 2005; Campolongo et al.,

2007). To evaluate the elementary effects of N = 50 model parameters, 10 trajectories (r) were created that each contain a 50 x 51 matrix. The matrix is a series of 51 (N + 1) different arrays that contain input values (X_i) for each of the model's input parameters. Moving by column through a trajectory provides a new set of input values into the model. Each new set of values changes randomly for only one parameter value at a time. The completion of a single trajectory means that each input parameter has been changed only once.

The parameter values are discrete, and calculated using a 4-level grid (i.e. Δ = [0, 1/3, 2/3, 1]) such that the discrete values of $X_i = \Delta\,[MAX - MIN] + MIN$. This ensures that parameter estimates are uniformly distributed discrete values, and since each trajectory is randomly generated, the elementary effects for the same parameter in two different trajectories are independent of one another (Saltelli et al., 2008). Using this approach, the elementary effects of parameter i (EE_i) were estimated using removal efficiency (E_L) as the model output (Y), such that:

$$EE_i = \frac{[Y(X_1,\ X_2, \dots, X_{i-1},\ X_i + \Delta, \dots,\ X_N) - Y(X_1,\ X_2, \dots,\ X_N)]}{\Delta}$$

The sensitivity measures, μ_i and σ_i represent the mean and standard deviation of the EE_i for each parameter (i), among the 10 trajectories (r). Since both positive and negative EE_i is possible, Campolongo et al. (2007) suggest calculating the mean of absolute values of the elementary effects, μ_i^*. Therefore, μ_i^* and σ_i are estimated by:

$$\mu_i^* = \frac{1}{r}\sum_{j=1}^{r}\left|EE_i^j\right|$$

$$\sigma_i = \sqrt{\frac{1}{r-1}\sum_{j=1}^{r}\left(EE_i^j - \mu_i\right)^2}$$

The elementary effects sensitivity measures (μ_i^* and σ_i) are used to analyze the sensitivity of the input parameters and demonstrate their effects on removal efficiency (E_L). μ_i^* represents the magnitude of parameter sensitivity to removal efficiency, and σ_i represents the degree of interactions between input parameters.

The sensitivity measures, μ_i and σ_i represent the mean and standard deviation of the EE_i for each parameter (i). Since both positive and negative EE_i is possible, Campolongo et al. (2007) suggest calculating the mean of absolute values of the elementary effects, μ_i^*. Therefore, μ_i^* and σ_i are estimated by:

$$\mu_i^* = \frac{1}{r}\sum_{j=1}^{r}\left|EE_i^j\right|$$

$$\sigma_i = \sqrt{\frac{1}{r-1}\sum_{j=1}^{r}\left(EE_i^j - \mu_i\right)^2}$$

Model Parameterization

Table A.1: Nine contaminants from the LHTW used for the HSSF model calibration. C_{IN} is the measured contaminant concentration entering the HSSF wetland cell. SE = Standard Error of the mean of C_{IN}. K_{OW} = Octanol-to-water partition coefficient; K_{OC} = Organic carbon-to-water partition coefficient; S = Solubility in water at 25 deg-C; H = Henry's Law constant.

Chemical	Mol. Form.	C.A.S. #	C_{IN} ± SE	log K_{ow}	log K_{oc}	S	H
	---	---	*pg/L*	*unitless*	*L/kg*	*mg/L*	*Pa·m³/mol*
Endosulfan Sulfate	C9H6Cl6O4S1	001031-07-8	41.96 ±16.45	3.66	3.55	0.48	$3.29\cdot10^{-2}$
Musk Ketone	C14H18N2O5	000081-14-1	1,838.03 ± 663.90	4.30	3.66	1.90	$2.60\cdot10^{-2}$
1,2,3,4-Tetrachlorobenzene	C6H2Cl4	000634-66-2	16.94 ± 9.14	4.60	3.47	5.92	77.01
Pentachlorobenzene	C6HCl5	608-93-5	43.31 ± 23.41	5.17	3.93	0.55	52.60
Methyl Triclosan	C13H9Cl3O2	4640-01-1	22.19 ± 3.62	5.22	4.07	0.40	7.29
Hexachlorobenzene	C6Cl6	000118-74-1	10.91 ± 2.74	5.73	5.73	0.006	172.25
Tonalide	C18H26O1	1506-02-1	1,106.30 ± 94.66	5.80	4.27	0.24	14.08
Galaxolide	C18H26O1	1222-05-5	3,468.62 ± 339.43	5.90	4.10	1.75	6.73
PCB 52	C12H6Cl4	35693-99-3	8.15 ± 3.05	6.09	4.67	0.046	20.27

Table A.2: Average measured water, leaf, and root concentrations from the LHTW. SE = Standard error of the mean concentration. To average the concentrations, non-detectable concentrations were assumed to be one-half of the method detection limit (MDL) reported in Wang and Kelly (2017).

Chemical	C_{IN}	SE	C_{OUT}	SE	C_{leaf}	SE	C_{root}	SE
	ng/m3	*ng/m3*	*ng/m3*	*ng/m3*	*ng/kg ww*	*ng/kg ww*	*ng/kg ww*	*ng/kg ww*
Endosulfan Sulfate	41.96	16.45	9.62	4.08	28.36	7.74	7.71	0.86
Musk Ketone	1838.03	663.90	1719.04	767.34	36.52	16.16	140.03	3.51
1,2,3,4-Tetrachlorobenzene	16.94	9.14	24.54	9.49	27.70	14.30	115.46	1.61
Pentachlorobenzene	43.314	23.41	34.72	4.43	120.18	45.06	12.22	0.95
Methyl Triclosan	22.194	3.62	2.38	1.05	4.45	1.84	0.95	1.20
Hexachlorobenzene	10.914	2.74	33.41	4.16	44.20	12.35	6.83	1.67
Tonalide	1106.30	94.664	1349.65	115.55	283.32	58.79	140.99	4.43
Galaxolide	3468.62	339.43	2737.95	374.07	1609.36	391.81	417.96	38.52
PCB 52	8.15	3.054	26.31	10.67	5.09	0.95	2.28	1.61

Table A.3: Environmental conditions and operation at the LHTW.

Parameter	LHTW
Total annual average precipitation (mm/year)	2,330
Total annual estimated evapotranspiration (mm/year)	2,385
Water transport through xylem (L/day)	0.874
Average temperature (deg-C)	28.4
Estimated outflow (m^3/day)	98.5
Hydraulic Retention Time (days)	22.7

Table A.4: Model parameterization and input values for the LHTW.

Parameter	Symbol	Value
Rooting medium top surface area (m^2)	SAs	10,000
Depth of rooting medium (m)	Ds	0.8
Rooting medium porosity (Vvoids/Vtotal)	n	0.35
Average grain size of rooting medium (mm)	G	40
Aspect ratio of wetland cell (L:W)	aspect	4
Average water depth within the rooting medium (m)	Dw	0.65
Water inflow (L/day)	F	100,000
Total annual average precipitation (mm/year)	Qp	2,330
Total annual average (theoretical) potential evapotranspiration (mm/year)	PET(Qe)	2,385
Transpiration-to-evaporation ratio	T/E	1.15
Weight (wet) of rhizomes of one plant (kg/plant)	WeightRhizomes	0.7
Surface area-volume ratio for rhizome vegetation (m^2/m^3)	AreaVolRh	250
Weight (wet) of emergent part of one plant (kg/plant)	WeightEmerged	0.3
Surface area-volume ratio for emergent vegetation (m^2/m^3)	AreaVolEV	400
Water content of vegetation (g/g)	Wp	0.8
Organic carbon content of vegetation (unitless)	OCv	0.01
Density of vegetation (kg/L)	dv	1
Correction exponent for vegetation OC to octanol	VOCOW	0.77
Number of plants per m^2 (1/m^2)	NumberofPlants	4
Organic carbon content of suspended solids (unitless)	OCpw	0.01
Concentration of particles in water (kg/L)	Cpw	0.012
Concentration of DOC in water (kg/L)	Cdoc	0.00001
Density of suspended solids (kg/L)	dpw	1.3
Solids settling velocity (m/day)	vsolidsinwater	0
Sediment burial rate (m/day)	vaccretion	0
Water-side evaporation mass transfer coefficient (m/day)	vTew	0.1
Air-side evaporation mass transfer coefficient (m/day)	vTea	0.1
Plant-side transpiration mass transfer coefficient (m/day)	vTplantside	3
Air-side transpiration mass transfer coefficient (m/day)	vTairside	3
Water-side rhizome-water mass transfer coefficient (m/day)	vTwater	0.1
Plant-side rhizome-water mass transfer coefficient (m/day)	vTrh	0.1
Water transport through xylem (L/day)	Qwx	0.874 (calculated)
Growth rate of emergent vegetation (/day)	kgev	0
Atmospheric pressure (atm)	S	1
pH of water	pH	7
Water temperature (avg. - degC)	Tw	30
Temperature correction factor (unitless)	omega	1

Table A.5: Model variables, symbols, and equations. Rate constants for HSSF processes that are illustrated in Fig. 2-1.

Variable	Symbol	Calculation
Octanol-water partition coefficient (unitless)	Kow	=10^logKow
Organic carbon-water partition coefficient (L/Kg)	Koc	=SOCOW*Kow
Air-water partition coefficient (L/L)	Kaw	=H/(8.314*(273+Tw))
Suspended solids-water partition coefficient (L/kg dw)	Kpw	=OCpw*SOCOW*Kow
Dissolved Organic Matter-Water Partition Coefficient	Kdom	=adoc*Kow
Vegetation-air partition coefficient(L/kg)	Kvegair	=Kvegw/Kaw
Plant-water partition coefficient	Kvegw	=((Wp)+(OCv*(Kow^VOCOW)))*(dv/1)
Vegetation organic carbon-water partition coefficient	Kocveg	=Kvegw/OCv
Transpiration stream concentration factor #1	TSCF1	=0.784*EXP((-((logKow-1.78)^2)/2.44))
Transpiration stream concentration factor #2	TSCF2	=0.7*EXP((-((logKow-3.07)^2)/2.78))
Volume of rooting medium, total with voids (m^3)	Vrm	=(Sas*Dw)
Volume of water in rooting medium (m^3)	Vw	=(Sas*Dw*n)-Vrv
Volume of emergent vegetation (m^3)	Vev	=WeightEmerged*NumberofPlants*Sas/(dv*1000)
Volume of rhizomes (m^3)	Vrv	=WeightRhizomes*NumberofPlants*Sas/(dv*1000)
Surface area of rooting medium gravel (m2)	Sarm	=0.9*(4*PI()*((G/1000/2)^2))*((SQRT(Sas*aspect)/(G/1000))*(SQRT(Sas/aspect)/(G/1000))*(Dw/(G/1000)))
Rhizome surface area (m^2)	Srh	=Vrv*AreaVolRh
Surface area of emergent vegetation (m^2)	Sev	=Vev*AreaVolEV
Total external loading (g/day)	L	=(F)*Cin
Water out-flow (L/day)	Fout	=IF((F+((Qp/1000/365.25)*Sas*1000)-(NumberofPlants*Sas*Qwx)-((Qe/1000/365.25)*Sas*1000))<0,0,(F+((Qp/1000/365.25)*Sas*1000)-((Qe/1000/365.25)*Sas*1000)))
Hydraulic retention time (days)	HRT	=Vw/(Fout/1000)
Solids settling rate (kg/day)	vss	=vsolidsinwater
Sediment burial rate (kg/day)	vb	=vaccretion
Solids resuspension rate (kg/day)	vrs	=vss-vb
Volatilization mass transfer coefficient (m/day)	ve	=1/((1/vTew)+1/(Kaw*vTea))

Variable	Symbol	Calculation
Transpiration mass transfer coefficient (m/day)	vT	=1/((1/vTplantside)+1/(vTairside/Kvegair))
Water-to-rhizome vegetation diffusion mass transfer coefficient (m/d)	vWaterVeg	=1/((1/vTwater)+1/(Kvegw*vTrh))
Fraction of freely dissolved contaminant in water (unitless)	fDW	=1/(1+(Cpw*Kpw)+(Cdoc*Kdom))
Fraction of particle bound contaminant in water (unitless)	fPW	=(Kpw*Cpw)/(1+(Kpw*Cpw)+(Kdom*Cdoc))
Fraction of DOC bound contaminant in water (unitless)	fDOCW	=(Kdom*Cdoc)/(1+(Kpw*Cpw)+(Kdom*Cdoc))
Contaminant fraction in water of vegetation	fWVeg	=1/(1+(OCv*Kocveg))
Contaminant fraction in organic carbon of vegetation	fOCVeg	=1-fWVeg
Concentration of particulate organic carbon (kg/L)	Xpoc	=Cpw*OCpw
Outflow (/day)	ko	=Fout/(1000*Vw)
Volatilization (/day)	kv	=((Sas*n)*fDW*ve/Vw)
WATER-to-rhizome vegetation diffusion (/day)	kwrh	=(Srh*fDW*vWaterVeg)/(Vw)*(ß$_1$^(logKow))
Rhizome vegetation-to-WATER diffusion (/day)	krhw	=(kwrh*fWVeg*Vw/((Kvegw)*Vrv))
Rhizome vegetation to emergent vegetation transport (/day)	krhev	=((fDW*Qwx*(TSCF))/Vw*(ß$_2$^(logKow))
Emergent vegetation to air transport (/day)	kevair	=(Sev*fWVeg*vT/(Vev*Kvegair))
Growth dilution, emergent vegetation (/day)	kgev	=kgev
Transformation in water (/day)	kwr	=(0.693/hlw)
Transformation in rhizome vegetation (/day)	ksr	=(0.693/hlrhizome)
Transformation in emergent vegetation (/day)	kevr	=(0.693/hlemerged)
	Solving the Mass Balance	
Rhizome medium depuration (/day)	RMD	=krhw+krhev+ksr
Water medium depuration (/day)	WMD	=ko+kv+kwrh+kwr
Emergent plant depuration (/day)	EPD	=kevair+kgev+kevr
Total mass of contaminant in water (g)	Mw	=(L*RMD)/(RMD*WMD - krhw*kwrh)
Total mass of contaminant in emergent vegetation (g)	Mev	=(L*krhev*kwrh)/(EPD*(RMD*WMD - krhw*kwrh))
Total mass of contaminant in rhizomes (g)	Mrva	=(L*kwrh)/(RMD*WMD - krhw*kwrh)
Concentration of freely dissolved contaminant in water (g/L)	Cwd	=IF (ko=0,"no outflow",Cw*fDW)

Variable	Symbol	Calculation
Concentration of contaminant in water effluent (g/L)	Cw	=IF (ko=0, "no outflow",Mw/(Vw*1000))
Concentration of contaminant in rhizomes vegetated rooting medium (g/kg)	Crh	=Mrva/(Vrv*1000*dv)
Concentration of contaminant in rhizomes of rooting medium normalized to organic carbon (g/kg OC)	Crhoc	=Crh/OCv
Concentration of contaminant in emergent vegetation (g/kg)	Cev	=Mev/(1000*Vev*dv)

Table A.6: Parameterization of the Penman-Monteith equation. Values were derived from meteorological data.

Description	Parameter	Units	LHTW
density of water	ρ_w	kg/m3	998.2
latent heat if vaporization of water	λ	MJ/kg	2.45
gradient of the saturated vapour pressure vs temperature curve	Δ	kPa/C, at T_{avg}	0.225
net radiation	R_n	MJ/m^2d	15.87
soil heat flux	F	=0.04*Rn	0.635
density of moist air	ρ_a	kg/m^3	1.16
specific heat of moist air (1.013)	c_p	MJ/(kg.deg-C)	0.001
saturation vapour pressure	e_s	kPa at T_{avg}	4.03
ambient vapour pressure	e_a	kPa	3.19
aerodynamic resistance to vapour and heat diffusion	r_a	d/m	0.000468
psychrometric constants	γ	kPa/deg-C	0.0675
bulk surface resistance	r_s	d/m	0.000379

Table A.7: Half-life ($t_{1/2}$) and time to steady-state (t_{95}) for each test chemical in each environmental compartment.

	$t_{1/2}$ (days)			t_{95} (days)		
Chemical	**Water**	**Rhizome**	**Emergent Vegetation**	**Water**	**Rhizome**	**Emergent Vegetation**
Endosulfan Sulfate	9.35	17.4	10,000	40.5	75.1	43,300
Musk Ketone	11.1	115	2,500	47.9	499	10,800
1,2,3,4-Tetrachlorobenzene	9.80	147	2,300	42.4	637	9,960
Pentachlorobenzene	12.3	666	9,920	53.3	2,880	42,900
Methyl Triclosan	12.6	228	2,500	54.3	987	10,800
Hexachlorobenzene	12.1	832	9,950	52.4	3,600	43,100
Tonalide	13.6	244	2,500	58.7	1,060	10,800
Galaxolide	13.4	244	2,500	40.5	75.2	43,300
PCB 52	14.9	971	10,000	47.9	499	10,800

Table A.8: Complete list of input parameters (*N* = 42) and sensitivity measures (μ* and σ).

Parameter	μ*	σ
log Kow (unitless)	0.304	0.8592
Water-side rhizome-water mass transfer coeff. (m/day)	0.236	0.2932
Transformation half life time in water (day)	0.187	0.2408
Water temperature (avg. - degC)	0.144	0.1602
Number of plants per m^2 (1/m^2)	0.128	0.1437
Temperature correction factor (unitless)	0.116	0.1178
Rooting medium porosity (Vvoids/Vtotal)	0.086	0.0823
Surface area-volume ratio for rhizome veg. (m^2/m^3)	0.077	0.1106
Weight (wet) of rhizomes of one plant (kg/plant)	0.072	0.0586
Water inflow (L/day)	0.068	0.0119
Concentration of DOC in water (kg/L)	0.061	0.0681
Correction exponent for vegetation OC to octanol	0.059	0.0769
Concentration of particles in water (kg/L)	0.057	0.0942
DOC-octanol proportionality constant (unitless)	0.056	0.0177
Average water depth within the rooting medium (m)	0.050	0.0403
Henry's Law Constant (Pa.m3/mol)	0.049	0.0616
Transformation half-life time in emergent vegetation (day)	0.044	0.0226
Organic carbon content of suspended solids (unitless)	0.043	0.0152
Air-side evaporation mass transfer coefficient (m/day)	0.041	0.0365
Rooting medium top surface area (m^2)	0.039	0.0071
Solids organic carbon to octanol equivalency factor	0.028	0.0173
Total annual average precipitation (mm/year)	0.026	0.0048
Annual average potential evapotranspiration (mm/year)	0.019	0.0049
Density of vegetation (kg/L)	0.007	0.0005
Water-side evaporation mass transfer coefficient (m/day)	0.006	0.0005
Organic carbon content of vegetation (unitless)	0.006	0.0006
Water content of vegetation (g/g)	< 0.001	< 0.0001
Plant-side rhizome-water mass transfer coefficient (m/day)	< 0.001	< 0.0001
Transpiration-to-evaporation ratio	< 0.001	< 0.0001
Concentration in water inflow (g/L)	< 0.001	< 0.0001
Transformation half-life time in emergent vegetation (day)	< 0.001	< 0.0001
Depth of rooting medium (m)	< 0.001	< 0.0001
Average grain size of rooting medium (mm)	< 0.001	< 0.0001
Aspect ratio of wetland cell (L:W)	< 0.001	< 0.0001
Weight (wet) of emergent part of one plant (kg/plant)	< 0.001	< 0.0001
Surface area-volume ratio for emergent veg. (m^2/m^3)	< 0.001	< 0.0001
Density of suspended solids (kg/L)	< 0.001	< 0.0001
Solids settling velocity (m/day)	< 0.001	< 0.0001
Sediment burial rate (m/day)	< 0.001	< 0.0001
Plant-side transpiration mass transfer coefficient (m/day)	< 0.001	< 0.0001
Air-side transpiration mass transfer coefficient (m/day)	< 0.001	< 0.0001
Growth rate of emergent vegetation (/day)	< 0.001	< 0.0001

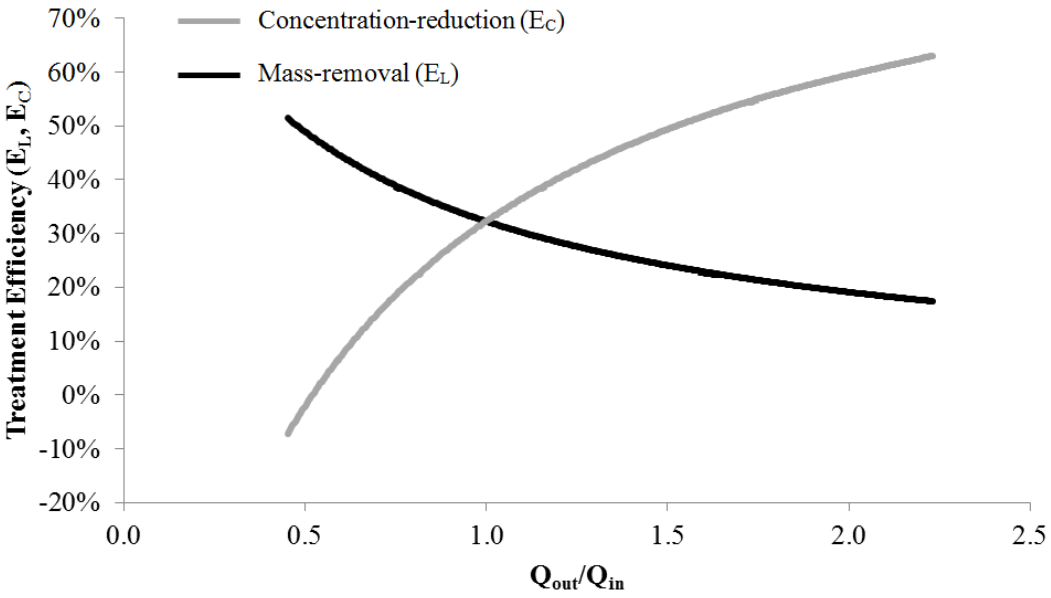

Fig. A.1: **Efficiency of mass-removal (E_L) and concentration-reduction (E_C) for pyrene in the Lorong Halus Treatment Wetland as a function of the water balance.**

Appendix B: Chapter 3 Supplementary Information

Table B.1: Dissolved PAH concentrations in the Forebay and Final Deep Pool for deployment one (July 21 – August 29, 2017)

	Chemical	CAS	Forebay (pg/L)	SE	FDP (pg/L)	SE	E_C (%)	E_L (%)
‡	1-Methylchrysene	3351-28-8	68.4	39.7	8.55	19.1	87.5	88.6
‡	1-Methylphenanthrene	832-69-9	276	15.1	129	7.6	53.1	57.3
†	1,7-Dimethylphenanthrene	483-87-4	649	46.0	121	6.8	81.4	83.1
†	1,8-Dimethylphenanthrene	7372-87-4	237	2.70	38.8	10.1	83.6	85.1
‡	2-Methylphenanthrene	2531-84-2	258	10.3	157	8.8	38.9	44.4
‡	2,6-Dimethylphenanthrene	17980-16-4	167	7.10	64.3	10.3	61.4	64.8
‡	5,9-Dimethylchrysene	139493-40-6	92.9	343	24.5	115	73.7	76.0
*	7-Methylbenzo[a]pyrene	63041-77-0	11.2	32.4	3.32 (0-6.6)	12.1	70.3 (40.6-100)	72.9
	Benzo[b]fluoranthene	205-99-2	89.3	22.4	35.2	28.8	60.6	64.1
‡	Benzo[e]pyrene	192-97-2	101	215	20.5	54.1	79.6	81.4
†	Chrysene	218-01-9	1,276	352	161	51.5	87.4	88.5
‡	Fluoranthene	206-44-0	919	33.5	72.5	7.4	92.1	92.8
*	Phenanthrene	1985-01-08	778	74.6	499	8.0	35.8	41.5
†	Pyrene	129-00-0	5,409	118	465	44.5	91.4	92.2
†	Retene	483-65-8	442	14.2	100	15.3	77.3	79.4

†$p < 0.0001$
‡$p < 0.01$
*$p < 0.05$

Table B.2: Dissolved PAH concentrations in the Forebay and Final Deep Pool for deployment two (August 29 – September 29, 2017)

	Chemical	CAS	Forebay (pg/L)	SE	FDP (pg/L)	SE	E_C (%)	E_L (%)
‡	1-Methylchrysene	3351-28-8	6.45	7.3	4.14	5.2	35.7	37.9
	1-Methylnaphthalene	90-12-0	162	4.9	130	1.4	19.5	22.1
‡	1-Methylphenanthrene	832-69-9	265	1.4	166	0.9	37.4	39.4
‡	1,7-Dimethylphenanthrene	483-87-4	219	30	131	19	40.3	42.3
‡	1,8-Dimethylphenanthrene	7372-87-4	80.3	8.0	38.4	8.0	52.2	53.8
	2-Methylnaphthalene	91-57-6	128	8.2	158	6.3	-23.6	-19.5
*	2-Methylphenanthrene	2531-84-2	249	20	176	23	29.4	31.8
‡	2,3,5-Trimethylnaphthalene	2245-38-7	178	5.0	134	3.8	24.6	27.1
	2,3,6-Trimethylnaphthalene	829-26-5	231	61	202	25	12.5	15.4
‡	2,4-Dimethyldibenzothiophene	31317-18-7	94.3	4.7	52.9	5.0	44.0	45.8
	2,6-Dimethylnaphthalene	581-42-0	246 (205-288)	56	334	75	-35.6 (-62- -16)	-31.1
*	2,6-Dimethylphenanthrene	17980-16-4	116	6.3	101	19	13.0	15.9
*	5,9-Dimethylchrysene	139493-40-6	7.07	4.9	5.4	4.1	23.1	25.7
‡	Benzo[e]pyrene	192-97-2	12.3	5.9	6.5	3.3	47.0	48.8
†	Chrysene	218-01-9	373	39	110	12	70.5	71.4
‡	Fluoranthene	206-44-0	543	11	65.6	1.3	87.9	88.3
	Fluorene	86-73-7	108	24	119	1.9	-10.2	-6.6
‡	Phenanthrene	1985-01-08	877	47	488	17	44.3	46.2
‡	Pyrene	129-00-0	3,524	66	845	12	76.0	76.8
‡	Retene	483-65-8	48.4	19	27.6	11	42.8	44.7

†$p < 0.0001$
‡$p < 0.01$
*$p < 0.05$

Table B.3: Dissolved PAH concentrations in the Forebay and Final Deep Pool for deployment three (August 25 – September 22, 2018)

	COMPOUND	CAS	Forebay (pg/L)	SE	FDP (pg/L)	SE	E_C (%)	E_L (%)
‡	1-Methylchrysene	3351-28-8	48.7	40.9	16.3	18.8	66.5	66.8
‡	1-Methylphenanthrene	832-69-9	750	55.6	494	17.2	34.1	34.6
*	1,2,6-Trimethylphenanthrene	30436-55-6	192	23.8	83	10.2	56.8	57.1
*	1,7-Dimethylphenanthrene	483-87-4	646	12.9	338	4.5	47.6	48.0
*	1,8-Dimethylphenanthrene	7372-87-4	377	31.7	191	11.0	49.3	49.7
*	2-Methylphenanthrene	2531-84-2	444	14.0	362	13.4	18.5	19.1
‡	2,3,5-Trimethylnaphthalene	2245-38-7	359	34.7	248	17.9	31.1	31.6
‡	2,3,6-Trimethylnaphthalene	829-26-5	753	19.6	509	8.60	32.4	33.0
	2,4-Dimethyldibenzothiophene	31317-18-7	126	81.6	123	20.6	2.80	3.5
	2,6-Dimethylnaphthalene	581-42-0	341	23.9	223	8.60	34.5	35.0
*	2,6-Dimethylphenanthrene	17980-16-4	269	10.8	157	5.10	41.7	42.2
‡	3-Methylphenanthrene	832-71-3	636	23.1	477	10.9	24.9	25.5
†	5,9-Dimethylchrysene	139493-40-6	135	203	39.1	42.6	71.0	71.2
†	Acenaphthene	83-32-9	2,875	81.6	349 (175-523)	90.5	87.9 (82-94)	88.0
‡	Anthracene	120-12-7	801	29.4	303	10.7	62.2	62.4
	Biphenyl	92-52-4	126	61.7	133	19.5	-5.0	-4.2
‡	Chrysene	218-01-9	601	84.5	233	32.1	61.2	61.4
‡	Fluoranthene	206-44-0	445	12.4	123	6.00	72.4	72.6
†	Fluorene	86-73-7	1,342	26.6	145	32.6	89.2	89.3
‡	Phenanthrene	1985-01-08	3,832	85.4	1,320	30.3	65.5	65.8
‡	Pyrene	129-00-0	2,245	127	580	8.70	74.2	74.4
‡	Retene	483-65-8	2,027	1,410	416	231.4	79.5	79.6

†$p < 0.0001$
‡$p < 0.01$
*$p < 0.05$

Table B.4: Inflow rate (Q_{in}), precipitation rate (Q_P), evapotranspiration (Q_{ET}), and outflow rate (Q_{out}) of water at the Kearl Treatment Wetland during each deployment period.

Deployment period		Q_{in} L/day	Q_P L/day	Q_{ET} L/day	Q_{out} L/day
2017A	Jul 21 – Aug. 29, 2017	432,000	29,475	53,692	407,783
2017B	Aug. 29 – Sept. 29, 2017	432,000	20,475	24,892	427,583
2018	Aug. 25 – Sept. 22, 2018	432,000	26,475	14,410	444,065

Table B.5: Chemical activity of individual PAHs in polyethylene passive samplers in the forebay and final deep pool (FDP) during each deployment.

		DEPLOYMENT ONE		DEPLOYMENT TWO		DEPLOYMENT THREE	
COMPOUND	CAS_NO	α(forebay)	α(FDP)	α(forebay)	α(FDP)	α(forebay)	α(FDP)
1,2,6-Trimethylphenanthrene	30436-55-6	--	--	--	--	9.4E-06	4.0E-06
1,7-Dimethylphenanthrene	483-87-4	9.1E-06	1.7E-06	3.1E-06	1.8E-06	9.1E-06	4.7E-06
1,8-Dimethylphenanthrene	7372-87-4	3.3E-06	5.4E-07	1.1E-06	5.4E-07	5.3E-06	2.7E-06
1-Methylchrysene	3351-28-8	5.1E-06	6.4E-07	4.8E-07	3.1E-07	3.7E-06	1.2E-06
1-Methylphenanthrene	832-69-9	1.6E-06	7.6E-07	4.0E-09	3.2E-09	--	--
1-Methylphenanthrene	832-69-9	--	--	1.6E-06	9.7E-07	4.4E-06	2.9E-06
2,3,5-Trimethylnaphthalene	2245-38-7	--	--	3.7E-08	2.8E-08	7.5E-08	5.2E-08
2,3,6-Trimethylnaphthalene	829-26-5	--	--	4.1E-08	3.6E-08	4.4E-07	3.0E-07
2,4-Dimethyldibenzothiophene	31317-18-7	--	--	1.3E-07	7.2E-08	7.4E-08	7.2E-08
2,6-Dimethylnaphthalene	581-42-0	--	--	1.7E-08	2.2E-08	1.7E-07	1.1E-07
2,6-Dimethylphenanthrene	17980-16-4	2.3E-06	9.0E-07	1.6E-06	1.4E-06	3.8E-06	2.2E-06
2-Methylphenanthrene	2531-84-2	9.8E-07	6.0E-07	3.1E-09	3.8E-09	1.7E-06	1.4E-06
2-Methylphenanthrene	2531-84-2	--	--	9.5E-07	6.7E-07	--	--
3-Methylphenanthrene	832-71-3	--	--	--	--	2.3E-06	1.7E-06
5,9-Dimethylchrysene	139493-40-6	2.5E-05	6.4E-06	1.9E-06	1.4E-06	3.6E-05	1.0E-05
7-Methylbenzo[a]pyrene	63041-77-0	3.6E-06	1.1E-06	--	--	--	--
Acenaphthene	83-32-9	--	--	--	--	1.1E-06	1.4E-07
Anthracene	120-12-7	--	--	--	--	1.8E-05	7.0E-06
Benzo[b]fluoranthene	205-99-2	4.3E-06	1.7E-06	--	--	--	--
Benzo[e]pyrene	192-97-2	1.8E-05	3.6E-06	2.2E-06	1.2E-06	--	--
Biphenyl	92-52-4	--	--	--	--	1.8E-08	1.7E-08
Chrysene	218-01-9	4.8E-05	6.1E-06	1.4E-05	4.2E-06	2.3E-05	8.9E-06
Fluoranthene	206-44-0	7.1E-06	5.6E-07	4.2E-06	5.1E-07	3.4E-06	9.5E-07
Fluorene	86-73-7	--	--	8.0E-08	8.9E-08	7.9E-07	8.6E-08
Phenanthrene	85-01-8	1.1E-06	7.4E-07	1.3E-06	7.2E-07	5.7E-06	2.0E-06
Pyrene	129-00-0	4.0E-05	3.4E-06	2.6E-05	6.3E-06	1.7E-05	4.3E-06
Retene	483-65-8	5.2E-05	1.2E-05	5.7E-06	3.3E-06	2.4E-04	4.9E-05

-- Chemical not detected. No activity calculated.

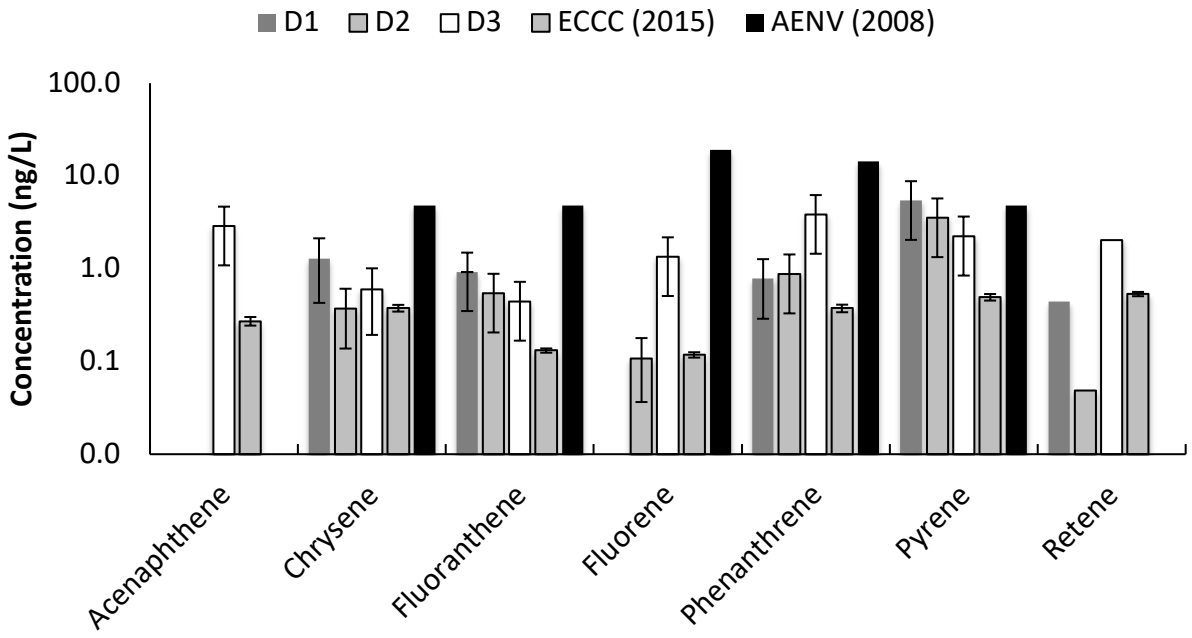

Figure B.1: Comparison of concentrations of select PAHs in Oil Sands Process-Affected Water entering the Kearl Treatment Wetland during deployments one, two, and three to Environment and climate Change Canada (2015) environmental measurements and Alberta Environment (2008) Water Quality Targets.

Appendix C: Chapter 4 Supplementary Information

E_L is estimated with equivalent concentrations ($C_{eq.}$) that account for the effects from precipitation and evapotranspiration, i.e. water gain or loss. This is representative of mass-removal since concentration estimates have been normalized to the initial (day 0) water volume within the wetland, and the wetland operates as a closed-system with 100% recycling of OSPW, i.e. inflow is the same as outflow. Total precipitation (P) was 54.0 mm, 4.3 mm, and 11.1 mm and evapotranspiration (ET) was estimated to be 47.5 mm, 164 mm, and 126 mm from day 0 to 19 during the three deployment periods, respectively.

Table C.1:
Half-life values estimated for each carbon group for naphthenic acids measured in 2018 and 2019. SE = Standard Error of the Mean

	2018		2019	
Carbon	**$t_{1/2}$ (days)**	**SE**	**$t_{1/2}$ (days)**	**SE**
12	34.1	13.3	25.8	2.5
13	33.5	7.0	28.5	4.4
14	34.1	2.0	26.3	4.1
15	50.4	16.0	25.4	3.0
16	65.1	10.6	23.3	3.5
17	48.8	10.0	18.5	3.5
18	59.9	3.3	20.3	3.0
19	68.3	13.7	15.6	2.0
20	116.1	69.9	29.7	15.5
21	40.6	6.4	14.9	5.0

Table C.2:
Half-life values for each double-bond equivalent (DBE) for naphthenic acids measured in 2018 and 2019. SE = Standard Error of the Mean

	2018		2019	
DBE	**$t_{1/2}$ (days)**	**SE**	**$t_{1/2}$ (days)**	**SE**
7	45.4	4.5	25.5	2.0
6	73.3	21.7	20.4	3.3
5	52.3	6.9	22.8	3.7
4	49.1	8.6	30.1	7.1
3	46.4	9.0	23.0	2.6
2	48.8	14.6	15.9	1.9
1	54.8	8.5	19.2	1.3

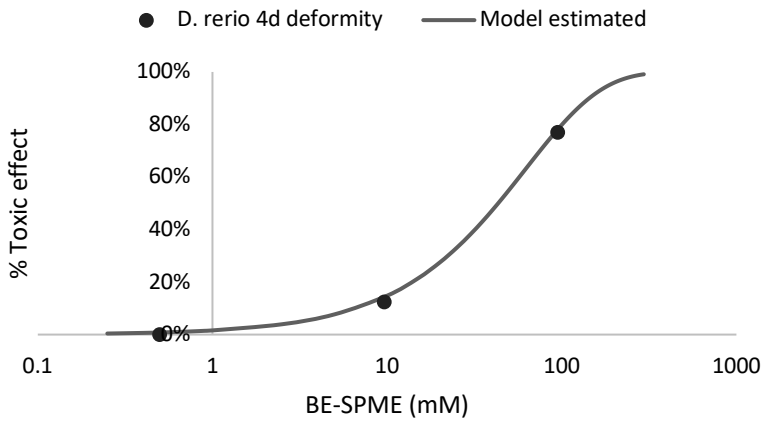

Figure C.1: Estimated 4d-deformity response on *D. rerio* based on BE-SPME measurements of wetland water from Redman et al. (2018).

The toxic effects model for the 4d-deformity of D. rerio based on BE-SPME measurements is derived from a Weibull cumulative distribution function:

$$Toxic\ effect = 1 - e^{-\left(x/\lambda\right)^{\omega}}$$

where *x* is the BE-SPME measurement (mM), λ is the fitted scale parameter to the distribution, and ω is the fitted shape parameter to the distribution. λ and ω were determined using the Solver function in Microsoft Excel®.

Table C.3: Dissolved NA concentrations at the Forebay (FB) and Final Deep Pool (FDP) for 2018, 2019A, and 2019B deployments.

	2018					2019A					2019B				
ng/sample	Forebay	SE	Final Deep Pool	SE	E_C (%)	Forebay	SE	Final Deep Pool	SE	E_C (%)	Forebay	SE	Final Deep Pool	SE	E_C (%)
C12H18O2	4.70E+04	9.09E+03	5.36E+04	5.92E+03	-14.0%	2.58E+04	1.97E+03	1.43E+04	2.09E+03	44.6%	1.01E+04	1.16E+03	1.25E+04	7.54E+02	-23.7%
C12H20O2	1.58E+05	2.91E+04	1.83E+05	1.99E+04	-15.6%	1.06E+05	8.30E+03	5.73E+04	1.01E+04	46.0%	4.55E+04	4.94E+03	5.51E+04	3.50E+03	-21.0%
C12H22O2	4.65E+04	7.78E+03	5.14E+04	5.17E+03	-10.7%	3.29E+04	4.08E+03	1.56E+04	2.89E+03	52.5%	1.31E+04	1.13E+03	1.40E+04	6.89E+02	-6.9%
C12H24O2	2.67E+03	4.42E+02	2.67E+03	1.73E+02	0.1%	1.99E+03	1.92E+02	6.53E+02	1.02E+02	67.1%	6.26E+02	3.69E+01	5.54E+02	4.05E+01	11.4%
C13H20O2	2.43E+05	4.49E+04	2.89E+05	2.87E+04	-18.8%	1.71E+05	1.37E+04	9.73E+04	1.62E+04	43.0%	9.07E+04	9.50E+03	1.09E+05	6.09E+03	-20.4%
C13H22O2	3.83E+05	6.35E+04	4.31E+05	4.27E+04	-12.7%	3.24E+05	2.94E+04	1.66E+05	2.96E+04	48.9%	1.67E+05	1.44E+04	1.84E+05	9.45E+03	-10.4%
C13H24O2	7.60E+04	1.15E+04	7.72E+04	8.83E+03	-1.6%	6.09E+04	5.79E+03	2.65E+04	4.90E+03	56.6%	2.58E+04	2.72E+03	2.69E+04	1.63E+03	-4.1%
C13H26O2	3.25E+03	2.94E+02	3.54E+03	3.06E+02	-8.9%	2.69E+03	2.48E+02	9.50E+02	2.02E+02	64.7%	9.17E+02	9.68E+01	8.75E+02	5.46E+01	4.5%
C14H20O2	6.85E+04	1.17E+04	7.91E+04	7.40E+03	-15.5%	5.50E+04	4.79E+03	2.95E+04	4.91E+03	46.3%	3.03E+04	3.32E+03	3.44E+04	1.19E+03	-13.4%
C14H22O2	5.15E+05	8.95E+04	5.69E+05	6.10E+04	-10.6%	7.60E+05	1.07E+05	4.92E+05	1.02E+05	35.3%	2.79E+05	1.85E+04	2.94E+05	1.64E+04	-5.1%
C14H24O2	5.88E+05	9.47E+04	6.17E+05	6.47E+04	-4.8%	8.07E+05	1.12E+05	4.83E+05	1.04E+05	40.2%	2.68E+05	2.40E+04	2.84E+05	1.54E+04	-6.2%
C14H26O2	8.63E+04	1.33E+04	7.94E+04	7.54E+03	8.0%	7.27E+04	7.13E+03	2.85E+04	5.78E+03	60.9%	2.83E+04	3.14E+03	2.86E+04	1.59E+03	-0.9%
C14H28O2	3.66E+03	5.85E+02	3.14E+03	3.21E+02	14.2%	2.89E+03	2.83E+02	9.37E+02	1.85E+02	67.6%	9.50E+02	7.79E+01	8.34E+02	5.43E+01	12.2%
C15H18O2	8.71E+04	1.54E+04	9.22E+04	1.07E+04	-5.8%	8.33E+04	7.41E+03	3.87E+04	7.78E+03	53.5%	3.41E+04	3.97E+03	4.54E+04	1.97E+03	-33.3%
C15H20O2	6.15E+04	1.07E+04	6.43E+04	6.56E+03	-4.6%	5.61E+04	5.28E+03	2.53E+04	4.81E+03	54.9%	2.55E+04	2.04E+03	2.92E+04	1.21E+03	-14.4%
C15H22O2	1.16E+05	1.90E+04	1.25E+05	1.36E+04	-8.4%	1.20E+05	1.15E+04	6.09E+04	1.07E+04	49.3%	6.94E+04	4.74E+03	7.60E+04	3.65E+03	-9.5%
C15H24O2	5.82E+05	9.11E+04	6.07E+05	5.55E+04	-4.2%	9.14E+05	1.22E+05	5.55E+05	1.16E+05	39.3%	3.20E+05	2.96E+04	3.38E+05	1.77E+04	-5.7%
C15H26O2	4.48E+05	7.17E+04	4.09E+05	4.23E+04	8.6%	6.03E+05	8.74E+04	3.19E+05	6.99E+04	47.1%	1.95E+05	2.19E+04	2.01E+05	1.17E+04	-3.3%
C15H28O2	1.53E+04	4.51E+02	1.28E+04	1.18E+03	16.1%	2.87E+04	4.23E+03	7.19E+03	1.08E+03	74.9%	4.87E+03	3.63E+02	4.76E+03	2.61E+02	2.3%
C15H30O2	4.71E+02	4.29E+01	3.82E+02	2.53E+01	19.0%	9.13E+02	1.07E+02	2.00E+02	3.48E+01	78.1%	1.51E+02	1.07E+01	1.42E+02	3.18E+00	5.9%
C16H20O2	1.73E+05	2.63E+04	1.77E+05	1.83E+04	-2.5%	1.86E+05	1.93E+04	8.47E+04	1.70E+04	54.5%	8.71E+04	8.48E+03	1.04E+05	4.48E+03	-19.1%
C16H22O2	7.78E+04	1.09E+04	7.78E+04	8.32E+03	0.0%	8.38E+04	8.58E+03	3.71E+04	7.24E+03	55.8%	4.14E+04	2.27E+03	4.40E+04	2.34E+03	-6.3%
C16H24O2	1.19E+05	1.81E+04	1.14E+05	9.47E+03	3.8%	1.34E+05	1.39E+04	6.39E+04	1.21E+04	52.4%	7.62E+04	7.11E+03	8.21E+04	4.08E+03	-7.7%
C16H26O2	3.31E+05	5.07E+04	2.88E+05	2.92E+04	12.9%	5.07E+05	7.52E+04	2.65E+05	5.72E+04	47.8%	1.76E+05	1.67E+04	1.80E+05	9.61E+03	-2.1%
C16H28O2	5.27E+04	2.46E+03	4.41E+04	4.54E+03	16.4%	1.12E+05	1.44E+04	2.97E+04	4.66E+03	73.5%	2.13E+04	1.69E+03	2.14E+04	1.28E+03	-0.3%
C16H30O2	4.90E+03	2.79E+02	3.52E+03	3.85E+02	28.2%	9.92E+03	1.28E+03	2.23E+03	3.92E+02	77.5%	1.58E+03	1.19E+02	1.47E+03	8.89E+01	7.2%
C17H22O2	1.93E+05	2.78E+04	1.85E+05	1.88E+04	4.3%	2.39E+05	2.37E+04	1.07E+05	2.22E+04	55.1%	1.11E+05	8.95E+03	1.24E+05	7.22E+03	-11.7%
C17H24O2	8.42E+04	1.21E+04	7.86E+04	7.42E+03	6.7%	9.26E+04	9.22E+03	4.01E+04	8.33E+03	56.7%	4.34E+04	3.35E+03	4.49E+04	2.10E+03	-3.4%
C17H26O2	6.51E+04	9.59E+03	5.45E+04	5.90E+03	16.2%	7.78E+04	7.67E+03	3.35E+04	6.81E+03	56.9%	3.82E+04	2.90E+03	3.74E+04	2.25E+03	2.2%
C17H28O2	2.59E+04	1.06E+03	2.02E+04	2.33E+03	21.8%	6.35E+04	7.71E+03	1.76E+04	2.72E+03	72.3%	1.24E+04	1.01E+03	1.27E+04	8.11E+02	-2.7%
C17H30O2	9.28E+03	8.92E+02	5.97E+03	6.80E+02	35.6%	2.05E+04	2.17E+03	4.53E+03	8.03E+02	77.9%	3.37E+03	2.77E+02	3.08E+03	1.88E+02	8.8%
C17H32O2	7.81E+02	1.07E+02	4.37E+02	4.06E+01	44.0%	1.81E+03	1.65E+02	3.39E+02	7.01E+01	81.3%	2.74E+02	1.72E+01	2.24E+02	8.88E+00	18.4%
C18H24O2	1.69E+05	2.54E+04	1.52E+05	1.30E+04	10.2%	2.01E+05	2.10E+04	8.68E+04	1.78E+04	56.8%	9.16E+04	8.56E+03	9.98E+04	5.23E+03	-8.9%
C18H26O2	6.39E+04	9.43E+03	5.40E+04	5.55E+03	15.5%	7.23E+04	7.16E+03	2.96E+04	6.48E+03	59.1%	3.11E+04	2.23E+03	3.04E+04	1.77E+03	2.1%
C18H28O2	6.92E+03	4.06E+02	5.34E+03	5.75E+02	22.9%	1.74E+04	2.10E+03	5.05E+03	7.88E+02	71.0%	3.53E+03	2.37E+02	3.50E+03	2.06E+02	0.9%
C18H30O2	3.94E+03	4.04E+02	2.60E+03	2.70E+02	34.0%	1.05E+04	7.80E+02	2.53E+03	4.19E+02	75.8%	1.94E+03	1.63E+02	1.76E+03	9.94E+01	9.1%
C18H32O2	9.72E+02	1.52E+02	5.70E+02	6.28E+01	41.4%	2.69E+03	1.44E+02	5.00E+02	8.57E+01	81.4%	4.12E+02	3.90E+01	3.33E+02	1.23E+01	19.3%

	2018					2019A					2019B				
ng/sample	Forebay	SE	Final Deep Pool	SE	E_C (%)	Forebay	SE	Final Deep Pool	SE	E_C (%)	Forebay	SE	Final Deep Pool	SE	E_C (%)
C19H26O2	9.54E+04	1.46E+04	7.64E+04	8.55E+03	19.9%	1.12E+05	1.12E+04	4.66E+04	1.01E+04	58.2%	4.44E+04	3.10E+03	4.57E+04	2.45E+03	-2.8%
C19H28O2	8.28E+03	3.29E+02	7.06E+03	8.17E+02	14.7%	1.98E+04	2.27E+03	5.59E+03	9.31E+02	71.8%	3.62E+03	2.07E+02	3.60E+03	1.78E+02	0.6%
C19H30O2	1.57E+03	1.43E+02	1.11E+03	1.17E+02	29.0%	3.95E+03	3.16E+02	1.04E+03	2.00E+02	73.6%	7.45E+02	4.80E+01	6.77E+02	2.89E+01	9.2%
C19H32O2	5.80E+02	7.65E+01	3.24E+02	3.78E+01	44.0%	1.61E+03	8.84E+01	3.65E+02	6.47E+01	77.3%	3.84E+02	2.69E+01	2.71E+02	7.97E+00	29.3%
	7.36E+01		3.08E+01		58.2%										
C19H34O2	(54.2-92.9)	9.25E+00	(0-61.5)	5.65E+00	(34-100)	3.37E+02	3.16E+01	7.12E+01	1.72E+01	78.9%	1.07E+02	1.07E+01	6.35E+01	7.20E+00	40.4%
C20H28O2	3.18E+04	4.51E+03	2.45E+04	4.33E+03	23.0%	3.70E+04	3.49E+03	1.56E+04	3.51E+03	57.9%	1.57E+04	9.82E+02	1.54E+04	1.03E+03	2.3%
C20H30O2	2.37E+03	2.89E+02	1.62E+03	2.21E+02	31.5%	5.40E+03	4.07E+02	1.29E+03	2.60E+02	76.1%	9.02E+02	5.12E+01	7.83E+02	5.57E+01	13.3%
	1.56E+02				14.6%										
C20H32O2	(134-177)	4.73E+01	1.33E+02	3.13E+01	(1-25)	4.93E+02	4.10E+01	1.07E+02	3.88E+01	78.2%	1.44E+02	1.04E+01	9.78E+01	4.30E+00	32.1%
	5.99E+01		3.83E+01		36.0%										
C20H34O2	(34-85)	2.16E+01	(19-58)	9.52E+00	(32-45)	1.73E+02	1.25E+01	6.65E+01	3.19E+00	61.6%	7.14E+01	3.63E+00	4.47E+01	2.77E+00	37.4%
C21H30O2	2.33E+03	2.47E+02	1.57E+03	1.92E+02	32.5%	4.72E+03	2.83E+02	1.26E+03	2.19E+02	73.3%	8.34E+02	5.04E+01	7.54E+02	3.46E+01	9.7%
C21H32O2	2.39E+02	2.51E+01	1.33E+02	1.55E+01	44.3%	4.78E+02	1.16E+01	1.06E+02	2.46E+01	77.9%	1.05E+02	7.36E+00	7.41E+01	3.20E+00	29.2%
						3.22E+01		7.50E+00		76.7%			1.11E+01		53.6%
C21H34O2	--	--	--	--	--	(15-49)	7.17E+00	(2.8-12.1)	9.26E-01	(75-82)	2.38E+01	1.69E+00	(9-13)	2.49E+00	(45-62)
			9.80E+00		59.9%										
C21H36O2	2.45E+01	2.43E+00	(7.7-12)	2.57E+00	(51-69)	3.00E+01	2.16E+00	1.19E+01	1.38E+00	60.4%	2.46E+01	1.37E+00	1.38E+01	1.01E+00	43.7%

Appendix D: Chapter 5 Supplementary Information

Table D.1: Log K_{OW}, molecular weight, aqueous solubility, Henry's law constant, half-life in water, and log K_{OC} of select PAHs used for model inputs

COMPOUND	log K_{OW} untiless	MW g/mol	$S_{aq.}$ mg/L (25 deg-C)	H Pa.m3/mol	$t_{1/2}$ days	log K_{OC} L/kg
1-Methylchrysene	6.07	242.32	0.013	0.192	132	5.27
1-Methylnaphthalene	3.87	142.20	25	52.1	8.89	3.36
1-Methylphenanthrene	5.08	192.26	0.17	5.00	23.9	4.41
1,2,6-Trimethylphenanthrene	5.99	220.32	0.021	5.07	61.2	5.20
1,7-Dimethylphenanthrene	5.44	202.29	0.071	2.98	38.3	4.72
1,8-Dimethylphenanthrene	5.44	202.29	0.071	2.98	38.3	4.72
2-Methylnaphthalene	3.86	142.20	24.6	52.5	8.89	3.35
2-Methylphenanthrene	5.15	192.26	0.26	2.78	23.9	4.22
2,3,5-Trimethylnaphthalene	4.81	170.26	4.8	46.2	22.7	4.17
2,3,6-Trimethylnaphthalene	4.73	170.26	5.6	46.2	22.7	4.11
2,4-Dimethyldibenzothiophene	5.39	212.31	0.074	1.35	46.8	4.48
2,6-Dimethylnaphthalene	4.37	156.23	15	43.1	14.2	3.74
2,6-Dimethylphenanthrene	5.44	206.29	0.071	2.98	38.3	4.71
2/3-Methyldibenzothiophenes	4.71	198.28	0.33	3.12	44.2	4.09
3-Methylfluoranthene/Benzo[a]fluorene	5.48	216.28	0.058	0.912	73.5	4.76
3-Methylphenanthrene	5.15	192.26	0.28	3.29	23.9	4.22
5,9-Dimethylchrysene	6.62	256.35	0.0038	0.206	235	5.75
5/6-Methylchrysene	6.07	242.32	0.065	0.192	132	5.27
7-Methylbenzo[a]pyrene	6.66	266.35	0.0008	0.0507	162	5.78
9/4-Methylphenanthrene	4.89	192.26	0.25	2.78	23.9	4.24
Acenaphthene	3.92	154.21	3.9	18.6	18.8	3.40
Anthracene	4.45	178.24	0.043	5.63	123	3.86
Benzo[b]fluoranthene	5.78	252.32	0.021	0.0666	285	5.02
Benzo[e]pyrene	6.44	252.32	0.0056	0.0304	422	5.59
Biphenyl	4.01	154.21	6.9	31.2	31,0	3.48
Chrysene	5.81	228.30	0.026	0.53	344	5.04
Fluoranthene	5.16	202.26	0.26	0.898	191	4.80
Fluorene	4.18	166.22	1.3	9.75	15.1	3.70
Phenanthrene	4.46	178.24	0.68	4.29	15.0	3.87
Pyrene	4.88	202.26	0.22	1.21	60.0	4.90
Retene	6.35	234.34	0.0085	6.37	56.0	5.51

Table D.2: Z, number of double bond equivalents (DBE), molecular weight, Henry's law constant, log D, and half-life in water for O2-NAs used for model input.

Chemical	z	DBE	MW (g/mol)	H (Pa/mol.m3)	log D (pH=7)	t1/2 water (d)
C12H18O2	-6	4	194	1.77E-03	0.706	117
C12H20O2	-4	3	196	6.70E-03	1.12	103
C12H22O2	-2	2	198	2.92E-02	1.79	50.4
C12H24O2	0	1	200	2.60E-01	2.70	23.6
C13H20O2	-6	4	208	3.04E-03	1.09	143
C13H22O2	-4	3	210	8.79E-03	1.62	64.2
C13H24O2	-2	2	212	3.69E-02	2.31	37.4
C13H26O2	0	1	214	3.10E-01	3.21	29.0
C14H20O2	-8	5	220	3.13E-04	0.86	82.5
C14H22O2	-6	4	222	8.69E-04	1.47	102
C14H24O2	-4	3	224	7.11E-03	1.99	71.7
C14H26O2	-2	2	226	4.06E-02	2.82	28.8
C14H28O2	0	1	228	3.70E-01	3.72	20.7
C15H18O2	-12	7	230	5.49E-05	2.94	68.9
C15H20O2	-10	6	232	5.49E-05	0.76	47.1
C15H22O2	-8	5	234	5.29E-04	1.57	57.5
C15H24O2	-6	4	236	1.17E-03	1.87	72.4
C15H26O2	-4	3	238	8.81E-03	2.50	41.9
C15H28O2	-2	2	240	4.98E-02	3.33	18.4
C15H30O2	0	1	242	4.40E-01	4.22	16.3
C16H20O2	-12	7	244	6.76E-05	1.15	49.4
C16H22O2	-10	6	246	6.76E-05	1.15	38.6
C16H24O2	-8	5	248	9.00E-04	3.34	41.1
C16H26O2	-6	4	250	9.39E-04	2.24	37.9
C16H28O2	-4	3	252	9.24E-03	3.04	19.3
C16H30O2	-2	2	254	6.01E-02	3.82	15.4
C16H32O2	0	1	256	5.10E-01	4.72	13.0
C17H22O2	-12	7	258	1.40E-05	1.12	39.6
C17H24O2	-10	6	260	5.47E-05	1.53	33.3
C17H26O2	-8	5	262	7.29E-04	2.32	28.0
C17H28O2	-6	4	264	1.17E-03	2.72	19.4
C17H30O2	-4	3	266	1.13E-02	3.55	14.3
C17H32O2	-2	2	268	7.00E-02	4.32	11.8
C17H34O2	0	1	270	5.80E-01	5.22	13.0
C18H24O2	-12	7	272	1.17E-05	1.54	33.7
C18H26O2	-10	6	274	1.51E-04	2.42	26.9
C18H28O2	-8	5	276	2.03E-04	2.75	19.3
C18H30O2	-6	4	278	1.22E-03	3.63	15.1
C18H32O2	-4	3	280	1.21E-02	4.06	12.0
C18H34O2	-2	2	282	8.78E-02	4.82	12.0
C18H36O2	0	1	284	6.60E-01	5.71	12.0
C19H26O2	-12	7	286	8.82E-06	1.92	27.3
C19H28O2	-10	6	288	2.61E-04	3.20	20.4
C19H30O2	-8	5	290	2.79E-04	3.15	16.4
C19H32O2	-6	4	292	1.44E-03	3.76	12.1
C19H34O2	-4	3	294	1.44E-02	4.56	9.9
C19H36O2	-2	2	296	1.00E-01	5.32	10.0
C19H38O2	0	1	298	7.50E-01	6.19	10.0
C20H28O2	-12	7	300	1.10E-05	2.40	25.3
C20H30O2	-10	6	302	3.07E-05	2.94	14.9

Chemical	z	DBE	MW (g/mol)	H (Pa/mol.m3)	log D (pH=7)	t1/2 water (d)
C20H32O2	-8	5	304	2.18E-04	3.51	14.1
C20H34O2	-6	4	306	1.55E-03	4.26	15.6
C20H36O2	-4	3	308	1.70E-02	5.04	8.0
C20H38O2	-2	2	310	1.10E-01	5.80	9.0
C21H30O2	-12	7	314	9.77E-06	2.78	16.0
C21H32O2	-10	6	316	4.11E-05	3.34	11.9
C21H34O2	-8	5	318	2.58E-04	3.99	8.7
C21H36O2	-6	4	320	1.81E-03	4.76	12.1
C21H38O2	-4	3	322	1.94E-02	5.54	7.0
C21H40O2	-2	2	324	1.30E-01	6.30	8.0

Table D.3: Model parameterization for the Kearl Treatment Wetland

System Characteristics and Design	Symbol	Forebay	Shallow Area 1	Deep Pool 1	Shallow Area 2	Shallow Area 3	Final Deep Pool
Surface area of wetland cell (m^2)	SAw	496.8	4412	545	695	1001	455
Vegetation cover (%)	Vegcover	10%	39%	10%	22%	51%	10%
Surface area of catchment area (m^2)	SAcatchment	960	8528	1053	1343	1935	880
Average water depth (m)	Dw	1.7	0.4	1.7	0.4	0.4	1.7
pH of water	pH	7	7	7	7	7	7
Water temperature (avg. - degC)	Tw	10.97	10.97	10.97	10.97	10.97	10.97
Water inflow (L/day)	F	432000	430003	412275	410086.	407293	403271
Concentration of particles in water (kg/L)	Cpw	4.23E-06	4.23E-06	4.23E-06	4.23E-06	4.23E-06	4.23E-06
Concentration of DOC in water (kg/L)	Cdoc	0.00002	0.00002	0.00002	0.00002	0.00002	0.00002
Concentration of solids in rooting medium (kg/L)	Css	0.18	0.18	0.18	0.18	0.18	0.18
Rooting medium surface area (m^2)	Sas	496.8	4412.08	545	695	1001	455
Depth of rooting medium (m)	Ds	0.5	0.5	0.5	0.5	0.5	0.5
Number of emergent plants per m^2 (1/m^2)	NumberofPlants	1	53	1	26	76	1
Water content of vegetation (g/g)	Wp	0.8	0.8	0.8	0.8	0.8	0.8
Weight of rhizomes of one plant (kg/plant)	WeightRhizomes	1	1	1	1	1	1
Weight of submerged part of one plant (kg/plant)	WeightSubmerged	1	1	1	1	1	1
Weight of emerged part of one plant (kg/plant)	WeightEmerged	3	3	3	3	3	3
Surface area-volume ratio for submerged vegetation (m^2/m^3)	AreaVolSV	400	400	400	400	400	400
Surface area-volume ratio for emergent vegetation (m^2/m^3)	AreaVolEV	800	800	800	800	800	800
Density of suspended solids (kg/L)	dpw	1.5	1.5	1.5	1.5	1.5	1.5
Density of rooting medium solids (kg/L)	dss	1.85	1.85	1.85	1.85	1.85	1.85
Density of vegetation (kg/L)	dv	0.85	0.85	0.85	0.85	0.85	0.85
Density of organic carbon (kg/L)	doc	1	1	1	1	1	1
Organic carbon content of suspended solids (unitless)	OCpw	0.05	0.05	0.05	0.05	0.05	0.05
Organic carbon content of rooting medium solids (unitless)	OCss	0.382	0.382	0.382	0.382	0.382	0.382
Organic carbon content of vegetation (fraction; unitless)	OCv	0.005	0.005	0.005	0.005	0.005	0.005
Gamma	gamma	1	1	1	1	1	1
Oxidation-Reduction Potential	ORP	1	1	1	1	1	1
Water transport in xylem per plant (L/day)	Qwx	0.0928	0.0928	0.0928	0.0928	0.0928	0.0928
Average annual precipitation (mm)	Qp	0.0	0.0	0.0	0.0	0.0	0.0

System Characteristics and Design	Symbol	Forebay	Shallow Area 1	Deep Pool 1	Shallow Area 2	Shallow Area 3	Final Deep Pool
Total annual average potential evapotranspiration (mm)	Qe	1467.6	1467.6	1467.6	1467.6	1467.6	1467.6
Solids settling velocity (m/day)	vsolidsinwater	0.005	0.005	0.005	0.005	0.005	0.005
Sediment burial rate (m/day)	vaccretion	0	0	0	0	0	0
Water-side evaporation mass transfer coefficient (m/day)	vTew	0.05	0.05	0.05	0.05	0.05	0.05
Air-side evaporation mass transfer coefficient (m/day)	vTea	0.05	0.05	0.05	0.05	0.05	0.05
Water-to-sediment diffusion mass transfer coefficient (m/day)	vd	0.1	0.1	0.1	0.1	0.1	0.1
Plant-side transpiration mass transfer coefficient (m/day)	vTplantside	0.05	0.05	0.05	0.05	0.05	0.05
Air-side transpiration mass transfer coefficient (m/day)	vTairside	0.05	0.05	0.05	0.05	0.05	0.05
Water-side submerged vegetation-water mass transfer coefficient (m/day)	vTwater	0.0001	0.0001	0.0001	0.0001	0.0001	0.0001
Plant-side submerged vegetation-water mass transfer coefficient (m/day)	vTsv	0.0001	0.0001	0.0001	0.0001	0.0001	0.0001
Temperature correction factor (unitless)	omega	0.96	0.96	0.96	0.96	0.96	0.96
Growth submerged vegetation (1/day)	kgsv	0	0	0	0	0	0
Growth emergent vegetation (1/day)	kgev	0	0	0	0	0	0

Table D.4: Model variables, symbols, and equations. Rate constants for FWS processes that are illustrated in Fig. 5-1.

Variable	Symbol	Calculation
Octanol-water partition coefficient (unitless)	Kow	=10^logKow
Organic carbon-water partition coefficient (L/Kg)	Koc	=SOCOW*Kow
Air-Water Distribution Coefficient (L/L)	Kaw	=H/(8.314*(273+Tw))
Suspended Solids Water Distribution Coefficient (L/kg dw)	Kpw	=OCpw*SOCOW*Kow
Rooting medium Solids-water partition coefficient (L/kg dw)	Kps	=OCss*SOCOW*Kow
Dissolved Organic Matter Water Partition Coefficient	Kdom	=adoc*Kow
Vegetation to air partition coefficient(L/kg)	Kvegair	=Kvegwater/Kaw
Vegetation-water partition coefficient (L/kg)	Kvegwater	=(Wp+(OCv*Kow^VOCOW))*(dv/1)
Plant organic carbon-water partition coefficient	Kocveg	=VOCOW*Kow
Transpiration stream concentration factor #1	TSCF1	=IF((0.784*EXP(-((logKow-1.78)^2)/2.44))>(0.7*EXP(-((logKow-3.07)^2)/2.78)),(0.784*EXP(-((logKow-1.78)^2)/2.44)),(0.7*EXP(-((logKow-3.07)^2)/2.78)))
Total external loading (g/day)	L	=F*Cin
Water out-flow (L/day)	Fout	=(F+((Qp/1000/365.25)*Sas*1000)-((Qe/1000/365.25)*Sas*1000)))
Solids settling rate (kg/day)	vss	=Cpw*vsolidsinwater*SAw*1000
Sediment burial rate (kg/day)	vb	=Css*vaccretion*Sas*1000
Solids resuspension rate (kg/day)	vrs	=vss-vb
Settling of suspended solids flux (kg/day)	SetFlux	=vss*SAw
Burial flux of sediment solids (kg/day)	BurFlux	=vb*Sas
Volatilization mass transfer coefficient (m/day)	ve	=IF(Kaw="na",0,1/((1/vTew)+1/(Kaw*vTea)))
Fraction of freely dissolved contaminant in water (unitless)	fDW	=1/(1+(Cpw*Kpw)+(Cdoc*adoc*Kow))
Fraction of particle bound contaminant in water (unitless)	fPW	=IF(Kdom="na",(Kps*Cpw)/(1+(Kps*Cpw)),(Kps*Cpw)/(1+(Kps*Cpw)+(Kdom*Cdoc)))
Fraction of DOC bound contaminant in water (unitless)	fDOCW	=IF(Kdom="na",0,(Kdom*Cdoc)/(1+(Kps*Cpw)+(Kdom*Cdoc)))
Fraction of (freely dissolved) contaminant in water of vegetated rooting medium (unitless)	fDS	=(Vsw/Vs)/((Vsw/Vs)+(Kps*dss*Vsss/Vs)+(Kvegwater*Vrv/Vs))
Fraction in solids of vegetated rooting medium	fSS	=(Kps*dss)*(Vsss/Vs)/((Vsw/Vs)+(Kps*dss*Vsss/Vs)+(Kvegwater*Vrv/Vs))
Fraction in vegetation of vegetated rooting medium	fVS	=(Kvegwater*dv)*(Vrv/Vs)/((Vsw/Vs)+(Kps*dss*Vsss/Vs)+(Kvegwater*Vrv/Vs))
Sediment solids mass balance and resuspension flux (kg/day)	ResFlux	=SetFlux-BurFlux
Water transport in plant xylem (L/day/plant)	Qwx	=(Qe/1000/365)*SUM(C5:M5)/((NumberofPlants*SAw)+(E20*E5)+(G20*G5)+(I20*I5)+(K20*K5)+(M20*M5))*1000

Variable	Symbol	Calculation
Volume of water at t=0 (m^3)	Vw	=(SAw*Dw)
Volume of vegetated rooting medium (m^3)	Vs	=(Sas*Ds)+Vrv
Volume of rooting medium (m^3)	Vrm	=(Sas*Ds)
Volume of solids in vegetated rooting medium (m^3)	Vsss	=(Css/dss)*Vrm
Volume of water in vegetated rooting medium (m^3)	Vsw	=Vrm-Vsss
Volume of emergent vegetation (m^3)	Vev	=WeightEmerged*NumberofPlants*Sas/1000*dv
Volume of submerged vegetation (m^3)	Vsv	=WeightSubmerged*NumberofPlants*Sas/1000*dv
Volume of rhizomes (m^3)	Vrv	=WeightRhizomes*NumberofPlants*Sas/1000*dv
Submerged vegetation surface area (m^2)	Ssv	=NumberofPlants*WeightSubmerged*SAw*AreaVolSV/(dv*1000)
Emergent vegetation surface area (m^2)	Sev	=NumberofPlants*WeightEmerged*SAw*AreaVolEV/(dv*1000)
Bioavailable solute fraction (unitless)	sigma	=fDW
Concentration of particulate organic carbon (kg/L)	Xpoc	=Cpw*OCpw
Contaminant fraction in water of vegetation	fWVeg	=(1-OCv)/((1-OCv)+Kocveg*OCv)
Contaminant fraction in organic carbon of vegetation	fOCVeg	=1-fWVeg
Transpiration mass transfer coefficient (m/day)	vT	=IF(Kvegair="na","na",1/((1/vTplantside)+1/(vTairside/Kvegair)))
Water to submerged vegetation diffusion mass transfer coefficient (m/d)	vWaterVeg	=1/((1/vTwater)+1/(Kow*vTsv))
	Rate constants	
Outflow (/day)	ko	=Fout/(1000*Vw)
Volatilization (/day)	kv	=(SAw*(1-(Vegcover))*fDW*ve/Vw)*(omega^(Tw-C124))
Overall water-to-sediment transport (/day)	kws	=_kws1+_kws2
Overall sediment-to-water transport (/day)	ksw	=_ksw1+_ksw2
Solids settling (/day)	_kws1	=(vss*fDW*Kpw/(dss*1000*Vw))*(omega^(Tw-C124))
Water-to-sediment diffusion (/day)	_kws2	=(Sas*vd*fDW/Vw)*(omega^(Tw-C124))
Solids resuspension (/day)	_ksw1	=(vrs*fSS/(Vs*1000*dss))*(omega^(Tw-C124))
Sediment-to-water diffusion (/day)	_ksw2	=(Sas*vd*fDS/Vs)*(omega^(Tw-C124))
Burial (/day)	kB	=(vb*Sas*fSS/(dss*1000*Vs))*(1.02^(Tw-C124))
Rhizome vegetation to submerged vegetation	krvsv	=(fDS*Qwx*TSCF1/Vrv)*(omega^(Tw-C124))
Water-to-submerged vegetation diffusion (/day)	kwsv	=(Ssv*fDW*vWaterVeg/Vw)*(omega^(Tw-C124))
Submerged vegetation to water diffusion (/day)	ksvw	=(kwsv/(Kvegwater))*(omega^(Tw-C124))
Submerged vegetation to emergent vegetation transport (/day)	ksvev	=(fWVeg*Qwx/WeightSubmerged/dv)*(omega^(Tw-C124))
Emergent vegetation to air transport (/day)	kevair	=(Sev*fWVeg*vT/(Vev*Kvegair))*(omega^(Tw-C124))
Transformation in water (/day)	kwr	=(0.693/(hlw)*(C143^((Tw-C124)/C124))*gamma^(ORP-C123))
Transformation in vegetated rooting medium (/day)	ksr	=(0.693/(hls)*(C143^((Tw-C124)/C124))*gamma^(ORP-C123))
Transformation in submerged vegetation (/day)	ksvr	=((0.693/hlsubmerged)*(C143^((Tw-C124)/C124)))*(gamma^(ORP-C123))
Transformation in emergent vegetation (/day)	kevr	=(0.693/hlemerged)*(C143^((Tw-C124)/C124))*(gamma^(ORP-C123))
Rooting medium depuration (1/day)	RMD	=ksw+krvsv+ksr+kB

Variable	Symbol	Calculation
Water medium depuration (1/day)	WMD	=kws+kwsv+kv+ko+kwr
Submerged vegetation depuration (1/day)	SVD	=ksvw+ksvev+ksvr+kgsv
Emergent plant depuration (1/day)	EVD	=kevair+kevr+kgev
	Steady State Solution	
Total mass of contaminant in water (g)	Mw	=-(L*RMD*SVD)/(RMD*ksvw*kwsv - RMD*SVD*WMD + SVD*ksw*kws + krvsv*ksvw*kws)
Total mass of contaminant in vegetated rooting medium (g)	Ms	=-(L*SVD*kws)/(RMD*ksvw*kwsv - RMD*SVD*WMD + SVD*ksw*kws + krvsv*ksvw*kws)
Total mass of contaminant in submerged vegetation (g)	Msv	=-(L*(RMD*kwsv + krvsv*kws))/(RMD*ksvw*kwsv - RMD*SVD*WMD + SVD*ksw*kws + krvsv*ksvw*kws)
Total mass of contaminant in emergent vegetation (g)	Mev	=-(L*ksvev*(RMD*kwsv + krvsv*kws))/(EVD*(RMD*ksvw*kwsv - RMD*SVD*WMD + SVD*ksw*kws + krvsv*ksvw*kws))
Total mass of contaminant in rhizomes (g)	Mrva	=Ms*fVS
Concentrations		
Freely dissolved concentration of contaminant in water (g/L)	Cwdo	=Cw*fDW
Concentration of contaminant in water (g/L)	Cw	=Mw/(Vw*1000)
Concentration of contaminant in vegetated rooting medium (g/kg dry)	Cs	=(Ms/Vs)/1000
Concentration of contaminant in solids of vegetated rooting medium (g/kg dry)	Cssolids	=Ms*fSS/(1000*Vsss*dss)
Concentration of contaminant in water of vegetated rooting medium (g/L)	Cswater	=Ms*fDS/(1000*Vsw)
Concentration of contaminant in vegetation of vegetated rooting medium (g/kg dry)	Csveg	=Ms*fVS/(1000*Vrv*dv)
Concentration of contaminant in solids of rooting medium normalized to organic carbon (g/kg OC)	Csoc	=Cssolids/OCss
Concentration of contaminant in vegetation of rooting medium normalized to organic carbon (g/kg OC)	Csvegoc	=Csveg/OCv
Concentration of contaminant in submerged vegetation (g/kg)	Csv	=Msv/(1000*Vsv*dv)
Concentration of contaminant in emergent vegetation (g/kg)	Cev	=Mev/(1000*Vev*dv)
	Fluxes	
Inflow (g/day)		=L
Outflow (g/day)		=ko*Mw
Volatilization (g/day)		=kv*Mw
Overall water-to-rooting medium transport (g/day)		=kws*Mw
Overall rooting medium-to-water transport (g/day)		=ksw*Ms
Burial (g/day)		=kB*Ms
Rhizome vegetation to submerged vegetation		=krvsv*Ms
Water-to-submerged vegetation diffusion (g/day)		=kwsv*Mw

Variable	Symbol	Calculation
Submerged vegetation to water diffusion (g/day)		=ksvw*Msv
Submerged vegetation to emergent vegetation transport (g/day)		=ksvev*Msv
Emergent vegetation to air transport (g/day)		=kevair*Mev
Transformation in water (g/day)		=kwr*Mw
Transformation in vegetated rooting medium (g/day)		=ksr*Ms
Transformation in submerged vegetation (g/day)		=ksvr*Msv
Transformation in emergent vegetation (g/day)		=kevr*Mev
Growth dilution submerged vegetation (g/day)		=kgsv*Msv
Growth dilution emergent vegetation (g/day)		=kgev*Mev

Table D.5: Parameterization of Penman-Monteith equation used to estimate evapotranspiration (ET) from the Kearl Treatment Wetland. Temperature, relative humidity, and wind speed was obtained from meteorological records of the Kearl Lake weather station.

Description	Symbol	Units	Formula or value
Penman-Monteith, evapotranspiration	ET	m/day	$ET = \frac{1}{\rho_w \lambda} \cdot \frac{\Delta(R_n - G) + \rho_a c_p (\frac{e_s - e_a}{r_a})}{(\Delta + \gamma\left(1 + \frac{r_s}{r_a}\right))}$
Gradient of the saturated vapour pressure vs temperature curve	Δ	kPa/C	$\Delta = \frac{4098\left[0.6108 \exp\left(\frac{17.27T}{T + 237.3}\right)\right]}{(T + 237.3)^2}$ T = average air temperature (deg-C)
Net radiation	R_n	MJ/m²d	$R_n = S_n + L_n$ $S_n = (1 - \alpha)\left[a_s + b_s \frac{n}{N}\right]\left[\frac{1440}{\pi} G_{sc} d_r (\omega_s \sin\phi \sin\delta + \cos\phi \cos\delta \sin\omega_s)\right]$ $L_n = -\sigma\left(\frac{T^4_{\max,K} + T^4_{\min,K}}{2}\right)(0.34 - 0.14\sqrt{e_a})\left(1.35\frac{R_s}{R_{s0}} - 0.35\right)$
Density of moist air	**ρ**a	kg/m³	$\rho_a = 3.450 \frac{p}{T + 273}$
Saturation vapour pressure	e_s	kPa at T_{avg}	$e_s(T) = 0.6108 \exp\left[\frac{17.27T}{T + 237.3}\right]$
Ambient vapour pressure	e_a	kPa	$e_a = \frac{e_s(T_{\max})\frac{RH_{\max}}{100} + e_s(T_{\min})\frac{RH_{\min}}{100}}{2}$
Aerodynamic resistance to vapour and heat diffusion	r_a	d/m	$r_a = \frac{\ln\left[\frac{z_m - d}{z_{0m}}\right]\ln\left[\frac{z_h - d}{z_{0h}}\right]}{k^2 u_z}$
Bulk surface resistance	r_s	d/m	$r_s = \frac{r_l}{LAI_{active}}$
the inverse relative distance between the earth and the sun	d_r	unitless	$d_r = 1 + 0.033 \cos\left(\frac{2\pi}{365} J\right)$
sunset-hour angle	ω_s	radians	$\omega_s = \cos^{-1}[-\tan\phi \tan\delta]$
solar declination	δ	radians	$\delta = 0.4093 \sin\left(\frac{2\pi}{365} J - 1.405\right)$
Density of water	**ρ**w	kg/m³	998.2
Latent heat of vaporization of water	**λ**	MJ/kg	2.45
Specific heat of moist air (1.013)	c_p	MJ/(kg·C)	0.001
Psychrometric constant	***γ***	kPa/C	0.0675
Latitude	φ	degrees radians	57.4 1.0016
Crop height	h	m	1.5

Description	Symbol	Units	Formula or value
n is the number of bright-sunshine hours per day (h), N is the total number of daylight hours in the day (h)	n/N	unitless	0.69
Height of wind measurements	z_m	m	2
Height of air temperature (T) and relative humidity (RH) measurements	z_h	m	2
Albedo or canopy reflection coefficient	α	unitless	0.2
Zero-plane displacement height	d	m	= 2h/3 = 1
Roughness length governing momentum transfer	z_{0m}	m	= 0.123*h = 0.185
Roughness height governing heat and vapour transfer	z_{0h}	m	= $\alpha * z_{0m}$ = 0.0369
Leaf-area-index (sunlit)	LAI_{active}	unitless	3.054
Bulk stomatal resistance of well-illuminated leaf	r_l	s/m	100
Fraction of extraterrestrial radiation reaching earth on overcast days (n = 0)	a_s	unitless	0.25
Fraction of extraterrestrial radiation reaching earth on clear days	b_s	unitless	0.50
Solar constant	G_{sc}	MJ/m^2d	0.082
Stefan–Boltzmann constant	σ	MJ/m^2K^4d	$4.903x10^{-9}$
Clear-sky solar radiation	R_{s0}	$MJ/m^2 \cdot d$	0.75
Total incoming solar radiation	R_s	$MJ/m^2 \cdot d$	0.595
Soil heat flux	G	MJ/m^2d	$G = 0.4R_n$
Pressure	p	kPa	101.325
Von Karman constant	k	unitless	0.41
Temperature	T	K	Variable (data obtained from historical climate records)
Relative humidity	RH	%	Variable (data obtained from historical climate records)
Wind speed measured at height z_m	u_z	m/d	Variable (data obtained from historical climate records)
Julian day	J	day	Variable (data obtained from historical climate records)

Table D.5: Model estimated time to reach 95% of steady-state (t_{95}; days) for PAHs in rooting medium (RM), water (W), submerged vegetation (SV), and emergent vegetation (EV).

Chemical	RM	W	SV	EV
1,2,6-Trimethylphenanthrene	265	5.8	2246	2647
1,7-Dimethylphenanthrene	165	5.6	1191	1656
1,8-Dimethylphenanthrene	165	5.6	1191	1656
1-Methylchrysene	570	5.8	4322	5712
1-Methylnaphthalene	37.9	5.5	105.5	212.5
1-Methylphenanthrene	103	5.6	667.6	1034
2,3,5-Trimethylnaphthalene	97.9	5.6	502.0	799.9
2,3,6-Trimethylnaphthalene	97.8	5.6	458.4	771.7
2,4-Dimethyldibenzothiophene	202	5.6	1319	2026
2,6-Dimethylnaphthalene	61.0	5.5	239.7	463.0
2,6-Dimethylphenanthrene	165	5.6	1191	1656
2/3-Methyldibenzothiophenes	189	5.6	574.8	1909
2-Methylnaphthalene	37.8	5.5	104.1	209.3
2-Methylphenanthrene	103	5.6	704.2	1036
3-Methylfluoranthene/Benzo[a]fluorene	317	5.7	1887	3180
3-Methylphenanthrene	103	5.6	704.2	1035
5,9-Dimethylchrysene	1016	5.9	8746	10170
5/6-Methylchrysene	570	5.8	4322	5712
7-Methylbenzo[a]pyrene	700	5.9	6355	7006
9/4-Methylphenanthrene	103	5.6	561	1034
Acenaphthene	78.8	5.5	133.2	674.8
Anthracene	503	5.5	428.4	5111
Benzo[b]fluoranthene	1225	5.7	5259	12325
Benzo[e]pyrene	1821	5.8	12662	18251
Biphenyl	129	5.5	165.6	749.6
Chrysene	1477	5.7	5916	14881
Fluoranthene	822	5.6	1769	8283
Fluorene	65	5.5	188.5	637.9
Phenanthrene	64.3	5.5	274.4	646.1
Phenanthrene	64.3	5.5	274.4	646.1
Pyrene	259	5.6	820.2	2597
Retene	242	5.8	2262	2424

Table D.6: Model estimated time to reach 95% of steady-state (t_{95}; days) for NAs in rooting medium (RM), water (W), submerged vegetation (SV), and emergent vegetation (EV).

Chemical	RM	W	SV	EV
C12H18O2	14.5	5.3	54.8	50842
C12H20O2	14.2	5.3	55.0	44866
C12H22O2	15.0	5.3	56.3	21825
C12H24O2	19.2	5.3	68.0	10169
C13H20O2	14.4	5.3	55.0	61810
C13H22O2	14.7	5.3	55.8	27811
C13H24O2	17.6	5.3	60.1	16202
C13H26O2	24.6	5.3	98.6	12506
C14H20O2	14.2	5.3	54.8	35728
C14H22O2	14.6	5.3	55.5	44192
C14H24O2	16.3	5.3	57.3	31019
C14H26O2	20.7	5.3	72.5	12451
C14H28O2	29.4	5.3	193.5	8921
C15H18O2	24.1	5.3	78.2	29836
C15H20O2	13.9	5.3	54.7	20404
C15H22O2	14.4	5.3	55.6	24880
C15H24O2	15.7	5.3	56.7	31361
C15H26O2	19.6	5.3	63.2	18146
C15H28O2	23.3	5.3	112.3	7967
C15H30O2	34.6	5.3	474.5	7041
C16H20O2	13.8	5.3	55.0	21406
C16H22O2	13.5	5.3	54.9	16688
C16H24O2	28.0	5.3	114.5	17807
C16H26O2	17.1	5.3	59.2	16404
C16H28O2	20.8	5.3	84.0	8371
C16H30O2	27.7	5.3	227.9	6646
C16H32O2	37.3	5.4	1168.4	5625
C17H22O2	13.5	5.3	54.9	17153
C17H24O2	13.8	5.3	55.4	14436
C17H26O2	17.1	5.3	60.2	12113
C17H28O2	18.6	5.3	68.7	8378
C17H30O2	23.7	5.3	148.5	6172
C17H32O2	30.4	5.3	560.7	5121
C17H34O2	42.9	5.4	2483.7	5626
C18H24O2	13.8	5.3	55.5	14608
C18H26O2	17.8	5.3	61.6	11625
C18H28O2	18.7	5.3	69.4	8366
C18H30O2	25.1	5.3	166.4	6523
C18H32O2	27.5	5.3	342.3	5187
C18H34O2	36.4	5.4	1363.5	5194
C18H36O2	44.1	5.6	3719.2	5194
C19H26O2	14.7	5.3	56.7	11803
C19H28O2	22.6	5.3	97.5	8814
C19H30O2	20.8	5.3	92.0	7111
C19H32O2	24.2	5.3	202.7	5231
C19H34O2	29.4	5.4	840.2	4281

Chemical	RM	W	SV	EV
C19H36O2	35.5	5.5	2426.6	4329
C19H38O2	39.6	5.7	3890.5	4328
C20H28O2	17.5	5.3	61.3	10955
C20H30O2	18.7	5.3	77.8	6453
C20H32O2	23.1	5.3	139.7	6088
C20H34O2	34.5	5.3	512.5	6736
C20H36O2	28.2	5.4	1607.0	3463
C20H38O2	34.7	5.6	3134.8	3896
C21H30O2	18.1	5.3	70.5	6945
C21H32O2	20.2	5.3	112.7	5168
C21H34O2	22.4	5.3	295.1	3778
C21H36O2	35.9	5.4	1230.3	5219
C21H38O2	27.0	5.5	2264.3	3030
C21H40O2	32.4	5.7	3232.3	3463

Table D.7: Mean (μ*) and standard deviation (σ) of the elementary effects of model parameters on treatment efficiency.

Parameter	μ^*	σ
Water inflow (L/day)	29.77%	34.03%
Surface area of wetland cell (m^2)	24.64%	21.12%
log Kow or log D (unitless)	24.26%	34.73%
Number of emergent plants per m^2 (1/m^2)	21.33%	34.33%
Water temperature (avg. - degC)	18.76%	29.27%
Transformation half-life time in submerged vegetation (day)	18.51%	40.24%
Weight of submerged part of one plant (kg/plant)	17.39%	39.10%
Vegetation organic carbon to octanol equivalency factor	16.09%	35.89%
Solids settling velocity (m/day)	16.06%	39.15%
Temperature correction factor, θ (unitless)	12.45%	21.05%
Concentration of particles in water (kg/L)	12.23%	29.13%
Water-side submerged vegetation-water mass transfer coeff. (m/day)	12.12%	32.06%
Density of vegetation (kg/L)	11.70%	18.83%
Concentration of DOC in water (kg/L)	10.29%	23.78%
Surface area of catchment area (m^2)	9.53%	11.90%
Average water depth (m)	9.47%	17.93%
Average annual precipitation (mm)	6.52%	11.52%
Rooting medium surface area (m^2)	5.56%	14.33%
Surface area-volume ratio for submerged vegetation (m^2/m^3)	5.41%	12.82%
Growth submerged vegetation (1/day)	5.39%	12.11%
Water-to-sediment diffusion mass transfer coefficient (m/day)	4.75%	9.80%
Q_5	3.96%	10.27%
Solids organic carbon to octanol equivalency factor	3.71%	8.14%
Density of rooting medium solids (kg/L)	3.63%	7.91%
Transformation half life in sediment (day)	3.44%	6.80%
Total annual average potential evapotranspiration (mm)	3.38%	9.15%
Organic carbon content of vegetation (unitless)	3.33%	6.16%
Water content of vegetation (g/g)	3.14%	8.15%
Concentration of solids in rooting medium (kg/L)	2.53%	7.97%
DOC-octanol proportionality constant (unitless)	2.23%	4.62%
Plant-side submerged vegetation-water mass transfer coeff. (m/day)	2.23%	6.24%
Weight of rhizomes of one plant (kg/plant)	1.92%	5.10%
Organic carbon content of suspended solids (unitless)	1.31%	2.99%
Depth of rooting medium (m)	0.24%	0.46%
Organic carbon content of rooting medium solids (unitless)	0.18%	0.57%
Henry's Law Constant (Pa.m3/mol)	0.02%	0.04%
Air-side evaporation mass transfer coefficient (m/day)	0.02%	0.04%
Vegetation cover (%)	0.01%	0.02%
Water-side evaporation mass transfer coefficient (m/day)	0.00%	0.00%
Sediment burial rate (m/day)	0.00%	0.00%
Transformation half life time in water (day)	0.00%	0.00%
Initial concentration of chemical in water (g/L)	0.00%	0.00%

Parameter	μ^*	σ
Air-side transpiration mass transfer coefficient (m/day)	0.00%	0.00%
Density of organic carbon (kg/L)	0.00%	0.00%
Density of pure contaminant (kg/L)	0.00%	0.00%
Density of suspended solids (kg/L)	0.00%	0.00%
Growth emergent vegetation (1/day)	0.00%	0.00%
Molecular weight (g/mol)	0.00%	0.00%
pH of water	0.00%	0.00%
Plant-side transpiration mass transfer coefficient (m/day)	0.00%	0.00%
Surface area-volume ratio for emergent vegetation (m^2/m^3)	0.00%	0.00%
T-[X]	0.00%	0.00%
Transformation half-life time in emergent vegetation (day)	0.00%	0.00%
Water solubility of contaminant (g/L)	0.00%	0.00%
Weight of emerged part of one plant (kg/plant)	0.00%	0.00%

Table D.8: Mean model bias and 95% confidence intervals for uncalibrated and calibrated treatment wetland model concentration estimates for contaminants in water.

Data grouping	MB (95% CI) Uncalibrated	MB (95% CI) Calibrated
Total (all concentration estimates, PAHs + NAs)	0.889 (0.184 – 4.298)	1.030 (0.233 – 4.559)
Total steady-state (PAHs, Deployments 1 and 2)	1.069 (0.166 – 6.867)	0.981 (0.198 – 4.858)
Total time-dependent (PAHs and NAs)	0.884 (0.185 – 4.231)	1.031 (0.234 – 4.551)
PES time-dependent (PAHs only)	0.268 (0.037 – 1.958)	1.044 (0.281 – 3.876)
POCIS time-dependent (NAs only)	0.510 (0.201 – 1.289)	0.954 (0.616 – 1.478)
C_{aq} Time-dependent (PAHs only)	1.075 (0.155 – 7.467)	1.079 (0.156 – 7.463)
C_{aq} Time-dependent (NAs only)	0.879 (0.354 – 2.181)	1.006 (0.435 – 2.325)
All PAH concentration estimates	1.018 (0.137 – 7.544)	1.071 (0.161 – 7.110)
All NA concentration estimates	0.788 (0.276 – 2.250)	0.995 (0.440 – 2.249)

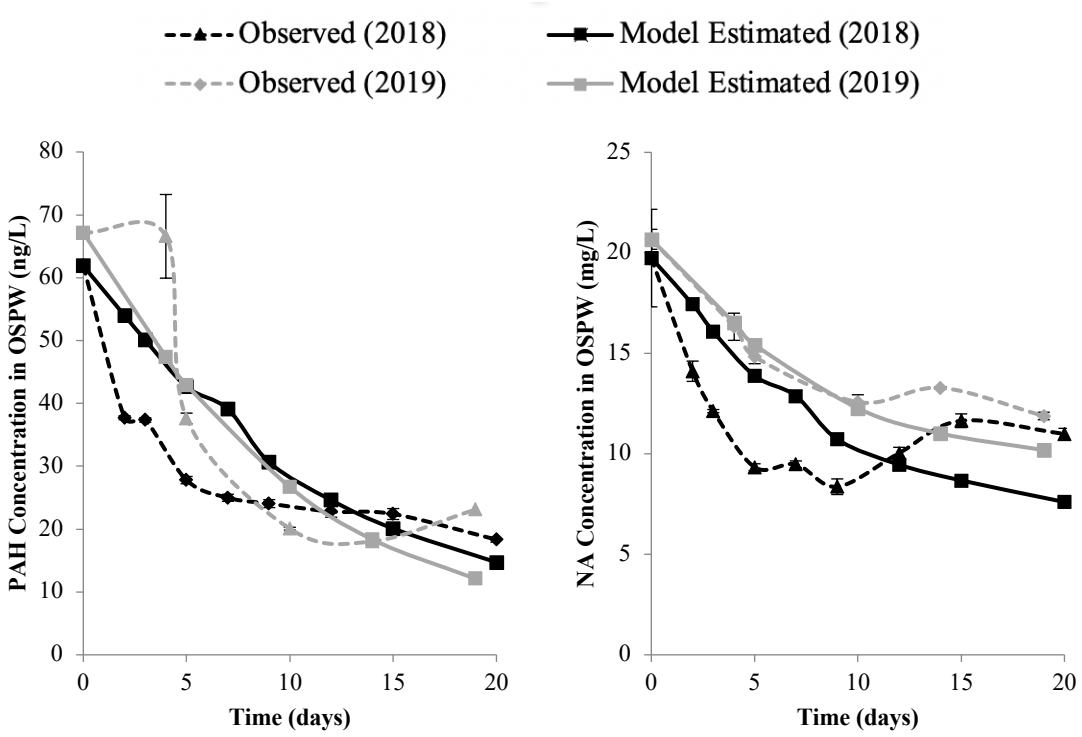

Fig. D.1: Measured and model estimated total concentrations of PAHs (left) and NAs (right) in OSPW over time in the Kearl Treatment Wetland.

Figure D.1 illustrates the model-estimated and measured total concentration of PAHs (n = 46) and NAs (n = 53) over time in the wetland. The change in chemical concentrations appears to follow first-order kinetics. The removal of PAHs from OSPW in 2019 shows a lag-effect for chemical degradation resulting from an early start to the 2019 field work (May) compared to 2018 (August). The later start to the 2019 field study allowed for maturation of the microbial community which swiftly began degrading OSPW contaminants. In 2019, this microbial community was not fully established and therefore degradation was delayed, resulting in little change in total PAH concentration from days 0 to 4. The total concentration of NAs, we do not see this same lag-effect in 2019 data, but we do observe a slower initial reduction in total NA concentrations compared to 2018. If we compare the linear slope of concentration over time from days 0 to 5, slower chemical removal is observed in 2019 (-1.15 mg/L/day) than 2018 (-2.08 mg/L/day).